Short to Medium Range Aircraft with Zero Emission Taxi

AE3200 Design Synthesis Exercise: Final Report

Group 26

Delft University of Technology

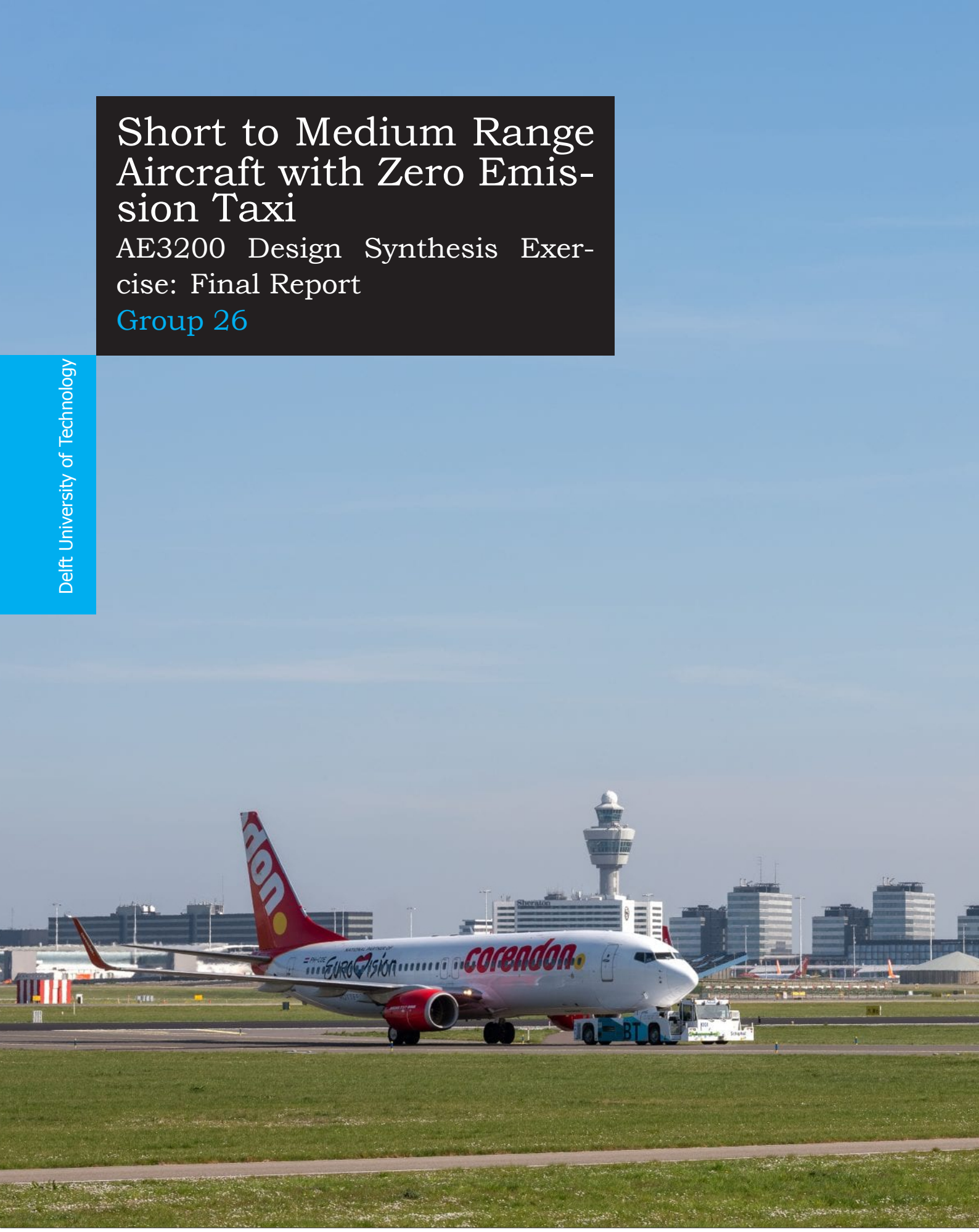

TU Delft Delft University of Technology

Challenge the future

This page was intentionally left blank

Short to Medium Range Aircraft with Zero Emission Taxi

AE3200 Design Synthesis Exercise: Final Report

by

Group 26

Name	Student Number
N.J. van Amstel	4666895
S. de Boer	4652673
S. Brunia	4549643
W.G.E. Dekeyser	4673921
J.J.A. van 't Hooft	4665953
N.M. Jahjah	4653351
K.Y.T.Y. de Lange	4560213
M.N.X.Y. Pellé	4650077
G. Salem	4555821
R.A. Vos	4588304

Tutor:	Ir. P.C. Roling	TU Delft
Coach:	Dr.ir. D.M.J. Peeters	TU Delft
Coach:	N.K. Rajan MSc	TU Delft

Version Number	What	Date
1.0	Initial Draft	June 22, 2020
1.1	Final Version	June 29, 2020

June 29, 2020

Cover Image was adapted from Roger Cremers https://airport-world.com/sustainable-aircraft-taxiing-trial-launched-at-schiphol/

TU Delft

Preface

The contents of this report are a continuation of the design ideas presented in the Midterm Report, the project strategy and design ambition presented in the Project Plan and the Baseline Report [1–3]. Moreover, this report is the cumulation of 11 weeks of work by a design team consisting of 10 students. The Team would like to thank the PM/SE TAs, and the members of the OSCC, as without their help this project would not have been possible. Special thanks go out to our tutor Paul Roling, and the project coaches Navi Rajan, and Daniël Peeters, as they have been extremely helpful during the whole project, and provided useful insights during the weekly meetings.

DSE Group 26
June 29, 2020, Europe

Executive Overview

In current society, climate change can no longer be ignored. For the aerospace industry, this means that new technology will primarily focus on more fuel-efficient designs resulting in a reduction of emissions such as carbon dioxide. Although new aircraft designs tend to be more fuel-efficient once airborne, as much as 6% of the total fuel per flight could be saved on existing aircraft by switching from engine based taxiing to a wheel based alternative [4, p. 1] [5]. During this design project, a team of ten aerospace students will elaborate on this idea by designing 'Reduced Emission Taxi System' (RETS). The mission statement will therefore be:

"Reduce the total emissions of an aircraft through lowering emissions during taxiing from gate to runway and vice versa."

In the baseline report [3], design options for a RETS system were identified and narrowed down. This led to three different designs that were further researched in the midterm report. These three designs were the Wheel Based Engine, Towbarless Tractor and Differential Drive Shaft Vehicle. The Wheel Based Engine is a concept in which motors are added to the main landing gear, these are electrically powered by an external vehicle that has batteries and is connected to the aircraft. The Towbarless Tractor consists of three external vehicles that each lift one of the landing gears. When these are all lifted, the aircraft is moved to the runway. The Differential Drive Shaft concept has two external vehicles attached to the main landing gear by a shaft that mechanically transfers the power to the main landing gears. A trade-off was preformed on the concept to select the one that would be researched in the final design phase. However, the trade-off did not provide a satisfying outcome, as none of the concepts were sufficiently optimal with respect to the requirements. This led to a new hybrid design concept, which was a combination of the Wheel based engine and Towbarless Tractor. This new design was tested in a second trade-off, in which it clearly scored better than the other concepts.

The hybrid design consists of an aircraft tug-like external vehicle at the nose wheel gear, which is based on the concept of the Towbarless Tractor. This is then combined with powered main landing gear wheels, which is based on the Wheel Based Engine concept. The two components both provide a forward force, and drive the aircraft to the desired spot, while the pilot is in control. The external vehicle will house the batteries used for powering the main landing gear. The power from these batteries can also be used for aircraft procedures like engine pre-heating. The remainder of this executive overview will summarise the most important points and conclusions of this report.

Resource and Budget Allocation

Before entering the final design phase, a budget and resource allocation was conducted. This was done to know, before designing, how many resources were available for the design. Firstly, the budget limitations had to be found. These came from three requirements stated by the stakeholders, and provided limitations on the mass added to the aircraft and the external vehicle mass. Next to this, a limitation on the operational cost came from these requirements. The on-aircraft mass budget limit is 940 kg and the external vehicle mass limit is 22 000 kg. In the later design phases, the required resources usually tend to increase, so for this reason the budget limit for mass was taken to be 80% of the actual limit. This way there is some room for the design to overshoot the budget limits, without violating the requirements. The set budgets were divided into budgets for various components.

For the cost, the limitation stems from the fact that the client must make a profit out of the RETS within five years. This means that in five years, the savings on the operational cost of the product compared to current taxi operations must be higher than the price paid for the RETS. Hence, the limit on the operational cost is 123 USD per cycle, which consists of one taxi-in and taxi-out.

Operational Analysis

First, a market analysis was performed. The customers of the vehicle are airports or ground-handlers. For the internal component, the customer can be the aircraft manufacturer or the airlines. Based on data set [6], the five airports with most departing A321 have been found as well as the flight range percentages, with 70% of flights having a range of 1806 km or less. Some already-existing infrastructure could potentially be used for coupling or decoupling, such as parallel taxiways, emergency pads, and de-icing pads. The infrastructure of three airport out of the five airports found, Tan Son Nhat, Dallas, and Atlanta airport are analysed to identify potential coupling and decoupling locations. Both Tan Son Nhat and Atlanta have few large areas for potential coupling or decoupling compared to Dallas. Both Dallas and Atlanta have many entrances and exits for each runways. Next, recommendations for airport are to add large areas and runways entrances and exits, have an area for the charging station and consider the extra personnel needed.

Furthermore, research was done on how to eliminate emissions during RETS-taxiing. Electricity can be supplied by the external vehicle, but some other systems need the engines running. Examples are the air-conditioning and pneumatic system, but also engine start-up that now should be done during taxiing. These require either active APU or engine support. Furthermore, in order to be able to do engine start-up as close as possible to take-off, the engines need to be warmed up. All systems were researched, however air-conditioning and engine start-up systems were deemed unfeasible to directly integrate. They can be provided as options to the system, where they are trailer based and hooked onto the external vehicle. An engine pre-heat system however was implemented, sized and integrated into the engines. It can lead up to an estimated 1 min engine run time reduction. This significantly increases RETS fuel savings.

Another part of the operational analysis was to evaluate how RETS can be implemented within current operations. In order to evaluate this, a taxi performance model was made. Various taxi routes were analysed, both for inbound and outbound taxiing. An example of a simulation is shown in Figure 1.

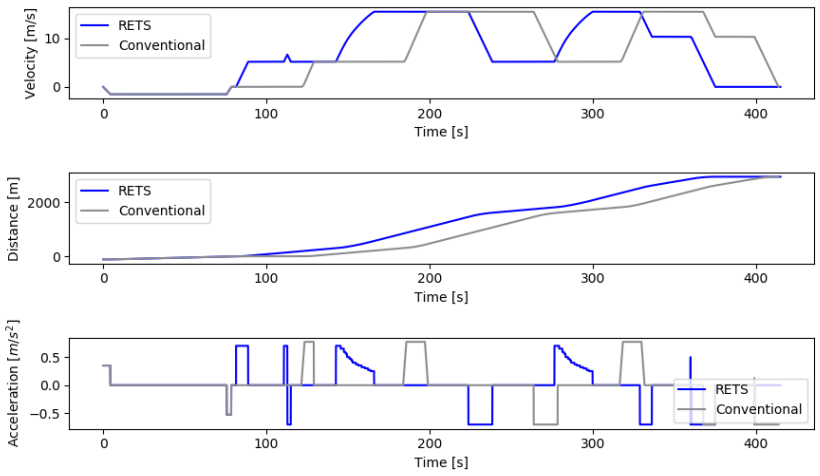

Figure 1: Outbound taxi comparison for an average taxi route (Schiphol, Gate D14-Runway 36C). The taxi characteristics for RETS-taxiing as well as conventional taxiing are modelled.

As can be seen in Figure 1, both methods start with pushback, but where conventional taxiing has to de-couple from the pushback vehicle, RETS can immediately continue to taxi to the runway. However, RETS de-couples at or close to the runway entry, so the difference in taxi time is barely noticeable. De-coupling at or near the runway does not necessarily lead to traffic congestion, especially when queues are already existing at the runway entry. During landing however, conventional taxiing does not need coupling to an external vehicle, whereas RETS has to couple. When there are many runway exits or parallel taxiways, coupling procedures can happen without too much effect on the airport capacity. The models were used to validate if RETS will meet the specified

requirements on operational compatibility. This seemed to be the case, with sufficient contingency margins left. However, the effects of (de-)coupling near the runway should be further investigated for specific airports in order to get a better insight.

Lastly, a fuel reduction simulation was made to evaluate the total fuel savings of the RETS for a conventional taxi route. The implementation of RETS will result in fuel savings for phase 1, 2 and 8 of the mission profile. For the other phases, RETS will induce extra fuel burn by adding weight to the aircraft. In the end, the final fuel saving per mission profile will be between 208 kg for a range of 3856 km and 240 kg for a range of 1806 km. Here, the range is a indication of the coverage of the A321 flights, where a range of 1806 km and 3856 km will cover up to 70% and 98% of all A321 flight routes respectively.

Power and Electronics

The power subsystem consists of landing gear-mounted electrical motors, batteries on the external towing vehicle, and a diesel engine to drive the vehicle. This diesel-electric hybrid design allowed for the necessary components of the system to be powered. The RETS has two modes of operation, namely vehicle-powered and APU-powered operation. APU-powered operation enables pushback and slow taxiing when the towing vehicle is not available, though at reduced performance. Therefore, a connection is made to the APU distribution bus. Moreover, an engine heating component is implemented such that the aircraft is ready to take off as soon at the taxi phase is completed.

Engine preheating

To supplement the taxiing system, an engine preheating system is implemented, as doing so through conventional means also consumes fuel. For this, a conduction heating is designed, using Joule heating. The total energy required to sufficiently heat the engines is determined to be 293 MJ, which is transferred through a wire mesh. For this mesh, molybdenum disilicide, nichrome V, and silicon carbide were considered as a material; nichrome V was ultimately chosen as it resulted in the lowest weight.

MLG motors

One motor is placed on each landing gear, using a direct drive configuration and several gears to reach the desired torque levels. The type of motor chosen was an axial flux permanent magnet motor due to their increased efficiencies and reduced size and mass compared to radial flux motors and other electrical motor types [1]. The motors were sized based on the required peak and continuous torque and power to achieve the desired acceleration profile, leading to the EMRAX 268 being chosen as a motor model. The EMRAX 268 offers a peak toque and power of 500 Nm and 200 kW respectively, has a mass of only 20.3 kg.

Batteries

Batteries are housed on the towing vehicle to power the various system components. A battery type was chosen with a trade-off between four common battery types in aerospace applications: nickel-cadmium, lead-acid, lithium-ion, and nickel-metal hydride. Lithium-ion batteries were selected mainly due to their high specific power and specific energy and recyclability characteristics, but other benefits such as low discharge rates and low maintenance exist. Disposal of these batteries are taken into account, opting for lithium-iron-phosphate batteries to minimise potential environmental contamination risks. To size the battery mass needed, the newest ”100 kW h” battery of the Tesla Model S 100 D are used as a reference; the system uses 6 of these battery packs.

[1] https://www.powerelectronics.com/markets/automotive/article/21864194/axialflux-motors-and-generators-shrink-size-weight [cited 20 June 2020]

Diesel engine

The purpose of the diesel engine is to power the towing vehicle itself. To achieve the high power demands by the vehicle, the MAN D2862 was chosen, rated to produce between 588 and 816 kW [2]. This engine provide power to the vehicle wheels through an all-wheel drive hydrostaic system.

Subsystem performance

During vehicle-powered operation, the system is capable of a maximum acceleration of 0.7 m s^{-2}, a top speed of 30 kts, and a 0 to 30 kts time of 31 s. During APU-powered operation, 62 kW is available from the APU to power the motors, allowing a pushback speed of 3 kts to be reached in 15 s. For the limit case, a taxi in and out of the Polderbaan, 5.64 cycles are possible on one charge or refuel. For an average baseline taxi route, 18.12 cycles are possible, if no traffic is present. When traffic is present, 15.33 baseline cycles are possible.

Structures

As has been described previously, RETS is a hybrid system which consists of two main components. The components describe two separate systems which work together to form RETS. The systems are, an External Vehicle, and a Wheel-Based Engine System. The total system is shown in Figure 2.

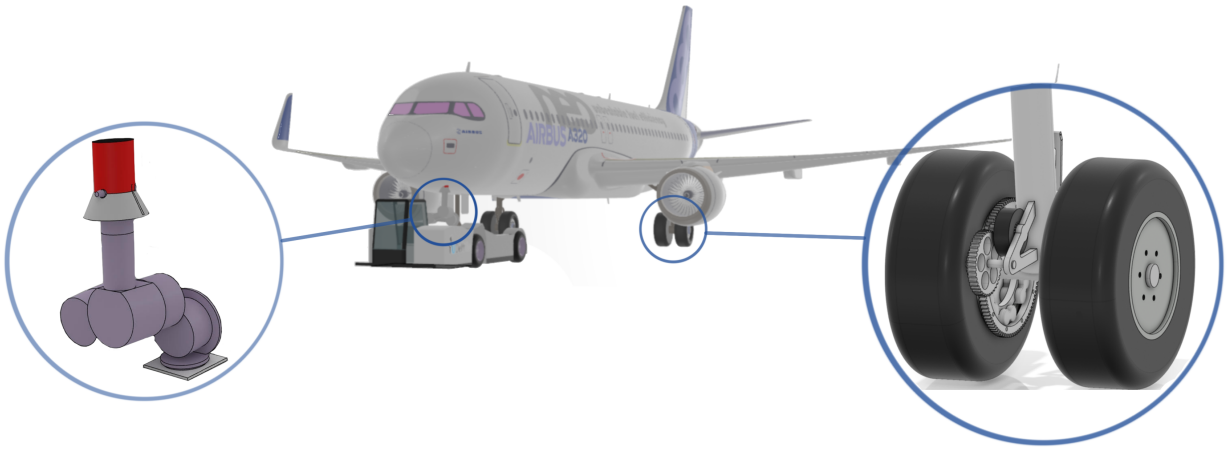

Figure 2: RETS overview

Load Analysis

Since the aircraft nose gear will be subjected to large horizontal forces for an extended period of time, which currently isn't the primary focus of landing gear manufacturers, a load analysis had to be performed. Given the lack of advanced modelling software, the load analysis of the nose gear had to be performed on a simplified structure. Following the analysis it was found that the loads did not cause excessive stress in the nose gear, and did not decrease the fatigue life.

In the case of the main landing gear, the analysis was performed on the additional structure which will be supporting the motor and gears of the internal system. This is due to the large decelerations upon landing impact. From the analysis, a steel 4340 structure, weighing 15.59 kg, was selected. The main landing gear itself is already designed to sustain these loads and thus no further analysis was performed on it.

External Vehicle

The External Vehicle is based on the Goldhofer "Phoenix" AST-2X. For RETS to function as intended, several modifications had to be performed. The modifications included the addition of a power

[2]https://www.engines.man.eu/global/en/off-road/agicultural-machinery/in-focus/D2862-Tier-4-Final.html [cited on 23 June 2020]

connection, and the placement of a power source to power the Wheel-Based Engine System, and the reduction of the width of the External Vehicle. To comply with highway requirements, the vehicle can not exceed a total mass of 22 t [7].

Power Connection

The Power Connection between the External Vehicle and the Aircraft will consist of a robotic arm, inspired by the European Robotic Arm, and a set of coil connector wires. When the power connection, has been established, the robotic arm dumps the hydraulic pressure on the hydraulic stepping motors and actuator, with the set arm positions remaining in place. The robotic arms are moved around their joints using hydraulic stepping motors, and the extendable arm is moved using a hydraulically powered linear actuator. The dumping of the hydraulic pressure allows the arm to rotate freely around its base, which makes it possible for the power connection to remain in place when RETS takes a turn. The robotic arm consists of three arms, one of which is extendable, a plug and a rotating base. The base is connected to the External Vehicle. The power connection on the aircraft is placed to the left of the centreline, just in front of the Nose Landing Gear Bay.

Power Generation

The power needed to operate the RETS will come from two sources. A diesel motor on the External Vehicle, which is used to generate all the power required, to power the External Vehicle, and a battery pack, which is used to provide the required energy to the Wheel-Based Engine System. The battery pack is created from separate cells and placed in such a way that the available space is optimised.

Width

The width of the External Vehicle is reduced by 700 mm, from 3.5 m to 2.8 m. This means that the external vehicle now also complies with highway lane width restrictions [7]. The width of the vehicle can be reduced this drastically, as the width of the lifting cradle only needs to be wide enough to function with the Airbus A321, as the Goldhofer "Phoenix" AST-2X, has originally been designed to perform pushback, on Narrow-Body and Wide-Body airliners, such as the Embraer E-Jets and the Boeing 777 [3]. Even though the External Vehicle, has been optimised for the A321, its dimensions and lifting capacity still allow the External Vehicle to work with Narrow body Airliners comparable to the A321

Wheel-Based Engine

The electrical motor to provide the torque and RPM needed to turn the outer main landing gear (MLG) wheel will be positioned behind the MLG strut. The main reason for this is the better protection from FOD and that a smaller supporting structure is needed. To transfer the torque to the outer wheel, gears will be used. In total four gears will be used of which the last one is mounted on the wheel rim. The other three gears have been positioned in the gear analysis.

This gear analysis takes into account the chosen gearing ratio of 19. Also the motor torque is used as input for this analysis. In the gear design process, all gears have been subjected to a load analysis. Specifically this will be a load analysis on the most critical component: the gear teeth. These structural elements have been checked for their bending strength and their surface durability.

During this gear analysis, it has been found that two or three single gears would not satisfy the set structural load checks. Therefore the decision has been made to use four gears where the two middle ones are connected to each other via a short shaft. In this way, the RPM and torque is transferred while the gear sizes are allowed to differ. This has led to the design of two gear sets with a gearing ratio of 4 and 4.75. An overview of the respective location of the gears is shown in Figure 3. As the design must be fail-safe. The gears must be able to couple and decouple. This

[3] https://www.goldhofer.com/fileadmin//downloads/airport_technology/DS_PHOENIX_AST-2P-X_EN-met_A4.pdf [accessed 8 June 2020]

will be done by implementing a spring cylinder into the supporting structure. The most suitable material to manufacture the gears has been found to be the steel alloy SNC815. With this material, the gears show a combined mass of 59.8 kg per MLG.

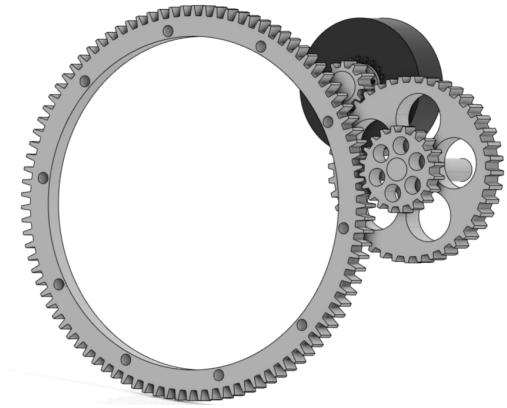

Figure 3: Overview of the final gear design (including motor)

Control and Stability

The control and stability for the RETS is built up out of three topics. The control and stability of the aircraft in flight and on the ground, the steering system of the RETS, and the communication and data handling.

The stability and controllability of the aircraft in flight and on the ground must be re-evaluated. The centre of gravity is changed due to the weight that has been added to the aircraft. A change in centre of gravity influences multiple things. Firstly, the tip-over acceleration, which is the maximum acceleration during taxiing. Secondly, the tip-back angle, which verifies if the tail will hit the ground during landing. Thirdly, the ground equilibrium, which checks if there is enough force on the nose wheel to be able to steer during taxiing. Lastly, the longitudinal in flight stability, which is influenced by the location for the centre of gravity with respect to the aerodynamic centre. The components added to the aircraft induce a horizontal and vertical centre of gravity change of less than a centimetre. The values are so small that none of the above mentioned parameters changes enough to compromise the stability and controllability of the aircraft.

RETS uses a combination of two steering techniques, which are differential steering and nose wheel steering. The procedure is as follows: the pilot inputs a desired steering angle on the tiller in the cockpit. When the external vehicle is attached, this input gets directed to the external vehicle steering system, instead of the nose wheel steering system. This input goes through the cockpit taxi computer, which calculates the needed power difference on the main landing gear. This way the differential steering and nose wheel steering together induce a turn with the same angular velocity. The advantage of using differential steering is that shorter turns can be performed compared to regular taxi steering operations.

The communication architecture of the system contains five entities that communicate with each other. These are the pilot, the external vehicle driver, the air traffic control, the ground crew and the ground control centre. The pilot has direct contact with the air traffic control, this link is used as is currently done to communicate taxi clearance and route. Next to this, the pilot also has a link to the driver of the external vehicle, with whom he communicates to see if the system is coupled or decoupled. The driver has two more communication links, one with the ground control centre and one with the ground crew. These are mainly used during pushback and when driving the external vehicle without the aircraft. Next to these communication lines, there are a lot of other connections in the system, most of which transfer data. These connections connect the two computers used with each other and with all the sensors and hardware located on the system.

Sensitivity Analysis

In order to check how robust the calculations are, and how solid the design parameters hold up to potential changes in the following design phase, a sensitivity analysis has been performed. In this analysis the fuel savings of the system were evaluated and reported plenty of contingency. The system taxi performance was also evaluated. The acceleration is not a sensitive parameter, however the top-speed is both very important and sensitive and should therefor be optimised.

Sustainability

The sustainability of the different departments is first summarised. Afterwards, the way RETS should be used for a sustainable usage is explained, the most important being that the operator should be trained. Next, the way RETS improves airport surroundings is explained. As it reduces emissions produced, the surroundings are less polluted which improves the life quality of the people living around airports. Next, the disposal of RETS is detailed. The removal of the system is offered with the purchase of RETS. When the customer does it by himself, the correct procedures can be explained such that the impact on the environment is minimised. Finally, the main components of engine exhaust are CO_2, NOx, and CO. Compared to classic engine-based taxiing, RETS saves approximately 52% of emissions. Looking at the emissions for the entire mission profile, RETS reduces emissions by approximately 2.6% for a flight range of 1806 km. Compared to all the emissions produced at Dallas Fort Worth Airport, RETS would reduce the emissions by approximately 0.5%.

Final Design Analysis

With the Final Design Characteristics having been described in the previous sections, several design aspects had to be investigated. The aspects were an analysis on the Reliability, Availability, Maintainability and Safety (RAMS) Characteristics, an analysis on the Final Resource allocation and the analysis of the technical risks present in the design.

Reliability, Availability, Maintainability and Safety (RAMS) Characteristics

The RETS has been designed to be highly reliable, safe and easy to maintain. For reliability, the focus was laid on the safety-critical aspects of RETS. The aspects are Power Connection Failure, Drive Motor Failure and the Engine Heating System Failure. By analysing the safety-critical aspects, it has been concluded that the reliability requirements have been met. Aspects which have been determined to influence the availability of the system are, maintenance, the Weather and the recharging Time. By analysing these aspects, it was concluded that the availability of the RETS complies with the stated requirements. To be able to ensure the safety and reliability, of RETS, the system will be equipped, with state of the art sensors which will ensure the smooth operation of RETS.

Final Resource

The final resource and budget allocation is performed after the different departments have made the design decisions, and performed the needed calculation. Knowing this, the final mass values for the different components located in the aircraft and on the external vehicle were known. It could therefore be concluded that the two requirements for the mass were met, as the total values were below the set budget limit.

Knowing the fuel needed for a cycle using the RETS, the operational costs for the system for one cycle could be calculated. This was calculated to be 40 USD below the budget limit for operational costs per cycle. This means the requirement on profitability is met.

Future Outlook

To be able to bring RETS to the market, several steps have to be performed. The main phases which have been determined, that need to be performed after the DSE, are the detailed design,

the production of prototypes, certification, production, and finally entry into service. The total development and production time is expected to take seven years. The detailed design phase is expected to take 2 years. After the detailed design phase, the prototypes are produced. This is expected to take a maximum of six months. During the detailed design phase, and the prototype phase, the certification is already started. This is done to speed up the whole certification process, as the certification process is expected to take up to 4.5 years. The initial production run is expected to take 1 year, with the expected entry into service in July 2027.

Conclusion & Recommendations

The design of RETS has led to several Conclusions and Recommendations, which are presented below.

Conclusion

The goal of this project was to design a system, which allows for the reduction of the emissions, produced during the taxi from the gate to the runway, and vice versa. The design process, which started during the baseline phase, and continued throughout the midterm and final phase of the DSE, resulted in RETS [1, 3].

RETS has achieved its goal, with the addition of approximately 315 kg to the aircraft. The use of RETS will reduce the fuel consumed during a flight with at least 204 kg for 98% of all A321 flight, and at least 240 kg for 70% of all A321 flights.

Recommendations

Besides some minor recommendations on the specific design of RETS, such as the extra investigation, which is needed for the specific motor used, the location of the power connection on the aircraft, and the (de)coupling of the aircraft and the tug, a major recommendation which can be done, is the investigation into the use of RETS on other aircraft types. RETS has been designed to work with the whole Airbus A320 Family, but its use on the Boeing 737 will unfortunately be limited, as full-RETS integration requires aircraft which are equipped with Steer-by-Wire.

An aircraft for which research into the use of RETS can be beneficial is the Boeing New Midsize Airplane (NMA) [4]. If this aircraft will be equipped with a Steer-by-Wire system, and be more electrical than the Boeing 737, then RETS will be highly beneficial to the NMA. In the end, it can be concluded that RETS will be highly beneficial for new short to medium range aircraft. These aircraft will be running primarily on electrical systems and equipped with Steer-by-Wire systems. This means that the APU or other generator will not have to run during taxiing as the external vehicle is able to provide electricity. Further research into the use of RETS is recommended for this new generation of aircraft.

[4] https://airlinegeeks.com/2020/05/01/boeing-developing-plan-for-new-nma-planes-dubbed-757-plus-767-x/ [accessed 29 June 2020]

Contents

Nomenclature

Acronyms

APM	Aircraft Performance Model	
APU	Auxiliary Power Unit	
ASU	Air Start-up Unit	
BADA	Base of Aircraft Data	
CG	Centre of Gravity	
CM	Circular Mil	
Dm	Motor displacement	$cm^3\,rev^{-1}$
Dp	Pump displacement	$cm^3\,rev^{-1}$
FDR	Final Drive Ratio	
FOD	Foreign Object Debris	
IDR	Input drive ratio between pump and engine	
LR	Loaded Radius	m
LVNL	Luchtverkeersleiding Nederland	
MAI	Manufacturing, Assembly and Integration	
MLG, mlg, MG	Main Landing Gear	
MTOM	Maximum Take-Off Mass	kg
Ne	Full load governed engine speed	RPM
NLG, nlg, NG	Nose Landing Gear	
Nm	Motor Speed	RPM
n	Efficiency	
OEM	Original Equipment Manufacturer	
OEW	Operational Empty Weight	
PCA	Preconditioned Air Unit	
Pi	Rated input power	kW
P	System Pressure	bar
SFC	Specific Fuel Consumption	$lb\,lbf^{-1}\,h^{-1}$
Te	Tractive effort	N
Tp	Pump input torque	Nm
Tw	Wheel Torque	Nm
VD	Voltage Drop	V

Greek Symbols

α	Nose Wheel Steering Angle	°
β	Landing Pitch Angle	°
Δt	Time Difference	s
$\Delta T, \delta T$	Heat Difference	°C
Δx	Material Length	m
ω	Rotational Velocity	$rad\,s^{-1}$
ρ	Specific Material Resistance	$\Omega\,m$
σ	Stress	Pa

Roman Symbols

A	Cross-Sectional Area	m^2
A	Effective Aspect Ratio	
a	Acceleration	$m\,s^{-2}$
C_D	Drag Coefficient	
c_f	Consequence of failure	
C_L	Lift Coefficient	
C_p	Specific Heat	$kJ\,kg^{-1}\,°C^{-1}$
C_{D_0}	Parasite Drag Coefficient	
D	Drag	N
d	Diameter	m
E	Energy	J
e	Oswald Span Efficiency Factor	
F	Force	N
g	Gravitational Constant	$m\,s^{-2}$
h	Wheelbase Length	m
I	Current	A
I	Moment of Inertia	m^4
k	Material Conductivity	$W\,m^{-1}\,°C^{-1}$
L	Lift	N
L, l	Wire Length	m
M	Moment	Nm
P	Power	W
p_f	Probability of failure	
Q	Heat Inserted	W
R	Range	km
R	Turn Radius	m
r	Radius	m
T	Torque	Nm
t	Time	s
V	Potential Difference, Voltage	V
V, v	Velocity	$m\,s^{-1}$
W	Weight	N
w	Width	m
y	Distance from Neutral Axis	m

Subscripts

b	Back
ev	External Vehicle
ff	Fuel Fraction
fric	Friction
f	Front
L, l	Left
mit	Mitigated
NW	Nose Wheel
R, r	Right
roll	Rolling
tot	Total
TO	Take-Off

1 Introduction

"'It is our duty to protect the planet from the disastrous impacts of climate change'" [5], these are the words of Alexandre de Juniac, the current International Air Transport Association (IATA) Director General and CEO. In order to fulfil such a duty, the IATA set out a goal for the reduction in carbon dioxide emission [6]. This has placed a focus on finding novel technologies for a greener and more sustainable aviation industry. However, it has become apparent that little attention has been given to the possible reduction in emissions of the ground segment of flights. The goal of this project is therefore to design a system which allows for a reduction in emissions during the ground phase of a short to medium range passenger aircraft's mission profile, in order to lower its total flight emissions.

The goal of this report is to present the design procedure which lead to the solution of the problem stated above. The approach, along with the solution itself and the further steps required to fully complete the design phase, are discussed in this report. In prior phases, the project objectives and planning, as well as the group structure, were laid out. Following this, the requirements were defined, after which designs were thought out and a trade-off was performed, which lead to the selection of the final concept discussed in this report.

To start off, a brief summary of the trade-off will first be presented to describe how the final design idea was obtained. Next it was possible to start designing the system starting from a resource and budget allocation. This was done to set the mass and cost to certain limits. As seen in the previous reports, sustainability and risk analysis are very important parts of the design process and are now linked with the final technical design. The team was divided into four subsystems: operations, power, control and stability, and structures. The design philosophy and methodology are presented within this report. This was first initiated from requirements and a functional analysis. Each section then dives into the details of their design including specific focus on sustainability and risk analysis. The verification and validation plan drafted in the midterm report was applied to the design tools used in each subsystems. A compliance matrix concludes each subsystem's section in order to clearly present if requirements are satisfied or not. The final parts of the report focus on more general aspects of the design and the next step the team will take towards the design, this includes updated resource and budget allocations, competitor analysis, RAMS (Reliability, Availability, Maintainability, and Safety) characteristics, a production plan and an additional requirement and risk analysis.

[5] https://www.iata.org/en/pressroom/speeches/2019-06-02-01/ [cited 26 June 2020]
[6] https://www.iata.org/en/programs/environment/climate-change/ [cited 26 June 2020]

2 Trade-off Summary

In this chapter a summary of the trade-off process conducted in the midterm phase will be provided. First the different design options that came out of the baseline report [3] will be stated, then the trade-off criteria and the trade-off results are discussed. Lastly the final design will be elaborated on.

2.1 Top-level requirements

Firstly the top-level requirements will be stated, as they were used throughout the project. The driving requirements are shown in green, the key requirements are shown in orange and the killer requirements are shown in red.

- **[RETS-SH-TLREQ-01]**: RETS taxi time shall be no more than 1 minute longer than engine based taxiing.*(Performance)*
- **[RETS-SH-TLREQ-02]**: RETS shall not lead to a reduction in aircraft payload. *(Performance)*
- **[RETS-SH-TLREQ-03]**: RETS shall induce a maximum increase of 2% in operational empty weight of the aircraft. *(Performance)*
- **[RETS-SH-TLREQ-04]**: RETS shall have a probability of catastrophic failure of less than 10^{-6} per year. *(Reliability)*
- **[RETS-SH-TLREQ-05]**: RETS shall have an availability per system of at least 95% per taxi in and taxi out. *(Availability)*
- **[RETS-SH-TLREQ-06]**: RETS shall not increase total energy consumption from gate to gate with respect to engine based taxiing. *(Sustainability)*
- **[RETS-SH-TLREQ-07]**: RETS shall only use recyclable materials. *(Sustainability)*
- **[RETS-SH-TLREQ-07N**: RETS shall use recyclable materials. *(Sustainability)*
- **[RETS-SH-TLREQ-08]**: RETS shall be fail-safe to prevent damage in case a take-off is attempted while the system is engaged. *(Safety)*
- **[RETS-SH-TLREQ-09]**: RETS shall have a positive net present value after five years based on average fuel prices before 2020.

2.2 Design Concepts

Previously, a concept selection was performed [3], which led to three different design concepts that were taken along in the trade-off. These three concepts will shortly be discussed.

- **Wheel-based engine**: This solution was inspired by systems like WheelTug and EGTS [8, 9]. The system drives the main landing wheels by means of electrical engines that are mounted to the main landing gears. The power transfer is therefore done electrically. For this system an external vehicle is used to provide the needed power as it will carry the batteries. This vehicle would attach itself autonomously to the back of the aircraft.
- **Towbarless tractor**: This solution was inspired by the taxiing system Taxibot. The system consists of three external vehicles that all lift one of the gears. When all gears are lifted the system will drive to the runway to decouple again. This system therefore transfers the power kinetically.
- **Differential drive shaft power vehicle**: This is a system that consists of two external vehicles which are connected to the main landing gear. The connection is done via a drive shaft that is connected to the landing gear axle. The drive shaft is powered by an engine inside the external vehicle, this turning motion is then translated to the turning of the landing gears. The power is transferred mechanically by means of a differential in this concept.

2.3 Trade-off Criteria

To perform a trade-off, the trade-off criteria and their weights need to be established. This was done by looking at the design requirements that were most critical. Those were the top level user requirements and the key, killer and driving requirements. On the basis of these requirements 6 main criteria were chosen, which all consisted of multiple sub-criteria. The main criteria are as follows. Firstly, the weight, this means weight added to the aircraft and the weight of a external vehicle. Secondly, the sustainability, which takes into account if the total energy consumption from gate to gate is reduced. Next is operations, this concerns the operational complexity and compatibility of the design. Also a criterion is the performance, the system is tested if it is comparable with existing taxi operations when looking at the performance of the system. Next to these there is the cost, concerns if the investment will be profitable for the customers. Finally, design complexity, the risks and technology readiness level are assessed. These are summarised in Table 2.1.

The weights for these criteria were established by linking the key, driving, killer and top-level requirements to one of the criteria. This resulted in the systematic scores shown in Table 2.1. Next to these systematic scores, all group members scored the criteria resulting in group scores. These scores were then by logic combined to a final criterion score.

Table 2.1: The weights for each criteria.

	Related requirements	**Systematic score**	**Group score**	**Final score**
Weight	25	0.16	0.20	0.20
Sustainability	8	0.05	0.17	0.13
Operations	45	0.30	0.21	0.25
Performance	20	0.13	0.18	0.15
Cost	28	0.18	0.13	0.13
Design complexity	27	0.18	0.11	0.14

2.4 Trade-off Results

The scoring of the trade-off criteria was done by giving all sub-criteria a grade between zero and ten. Some of these grades were established using a numerical approach, this was for example done for taxi time and the weights. Other sub-criteria were scored by the group. For these criteria the group members all gave a score and the average score was taken for the trade-off. This was done for criteria of which there was no numerical test available in that design phase. This together resulted in the trade-off scores that are shown in Table 2.2. The legend for this table can be found in Table 2.3.

Table 2.2: Trade-Off Results

	WBE	**TT**	**DS**		**WBE**	**TT**	**DS**
textbfWeight (0.2)	**8.13**	**9.50**	**8.77**	**Cost (0.126)**	**6.52**	**5.91**	**6.70**
Weight on A/C (0.144)	8.08	9.97	9.47	Development (0.072)	6.20	5.70	6.60
External weight (0.056)	8.26	8.28	6.98	Operating cost (0.023)	7.20	6.20	6.60
Sustainability (0.13)	**7.00**	**6.80**	**6.98**	Manufacturing (0.031)	6.70	6.20	7.00
Total energy consumption (0.098)	6.90	6.80	7.00	**Design Complexity (0.141)**	**6.63**	**6.27**	**6.64**
Recyclability (0.032)	7.30	6.80	6.90	Risk (0.021)	5.80	7.00	7.00
Operation ability (0.253)	**6.70**	**5.72**	**5.68**	TRL (0.021)	6.20	4.90	6.00
Compatibility (0.124)	6.40	6.90	5.70	Design Safety (0.099)	6.90	6.40	6.70
Operation complexity (0.067)	6.50	3.10	4.90	**Final Score (1.0)**	**7.19**	**7.23**	**7.02**
Operational Safety (0.062)	7.50	6.20	6.50				
Performance (0.15)	**8.00**	**9.15**	**7.60**				
Time (0.083)	8.34	10.00	8.67				
Maneuverability (0.067)	7.60	8.10	6.30				

Table 2.3: Trade-Off Score Legend

Legend	1	2	3	4	5	6	7	8	9	10
	Unfeasible			Not meeting requirements, but correctable			Meeting Requirements			Exceeding Requirements

It can be seen that all three designs, and especially the Wheel Based Engine (WBE) and the Towbarless Tractor (TT), have a very similar final score. The Towbarless Tractor design has the highest final score, however, there is a large variation in the given scores of the different main criteria, as can be seen in Table 2.2. Several of the scores are under a 7, where a 7 is seen as meeting the requirements. The Wheel Based Engine has a final score that is very similar to the Towbarless Tractor, but the different criteria scores are more consistent for the Wheel Based Engine. But this concept also does not score a 7 for most of the criteria. The difference in final score for the Drive Shaft Power Vehicle (DS) is significantly lower, although its final score is still above the 7. Next to all this is the fact that none of the three designs has a score which suggests that it meets the requirements for operational ability, however, this is the most important criterion as it has the highest weight.

From this trade-off it is clear that none of these designs are performing as desired. However, there are some aspects of especially the Wheel Based Engine and the Towbarless Tractor that could be interesting to combine. It was therefore decided that a hybrid of these two concepts would be designed, this would then be taken along in a second trade-off.

2.5 Final Design

The hybrid design consists of an aircraft tug-like external vehicle at the nose wheel, which is based on the previously discussed Towbarless Tractor. This is then combined with powered main landing gear wheels, which is based on the Wheel Based Engine concept. The biggest advantages of this concept, compared to the previous concepts, is that there is only one external vehicle present per airplane, and that the on-aircraft part of the system can be downsized, resulting in a lower on aircraft weight. The external vehicle also provides a pulling force which is lower compared to other designs such as WheelTug and also provides better traction. The nose wheel vehicle will house the batteries used for powering the main landing gear. The power from these batteries can also be used for aircraft procedures like engine pre-heating, which is researched further in this report. However, a major disadvantage compared to all other designs is the need to modify the aircraft as well as requiring new ground equipment. This concept was taken along in a second trade-off which was scored using the same scoring procedure as in the first trade-off. The results can be seen in Table 2.4.

Table 2.4: Updated Trade-off Summary Table

	Weight (0.200)	**Sustainability (0.130)**	**Operation Ability (0.253)**	**Performance (0.150)**	**Cost (0.126)**	**Design Complexity (0.141)**	**Final Score**
Wheel-Based Engine	8.13	7	6.7	8	6.52	6.63	7.19
Towbarless Tractor	9.5	6.8	5.72	9.15	5.91	6.27	7.23
Differential Drive Shaft Vehicle	8.77	6.98	5.68	7.6	6.7	6.64	7.02
Final	8.15	7.2	7.15	8.94	6.94	7.32	7.62

It can be seen in Table 2.4 that the new hybrid design scores considerably better compared to the previous three concepts. Especially the operational ability and design complexity are scored better. This is mostly due to the established nose gear coupling mechanism. Nose wheel lifting as a way to couple to the aircraft is already proven, therefore it has a higher technology readiness level, and a more certain coupling time. This resulted in higher scores for those criteria. It is also good to note that all criteria score well beyond a 7 or very close to a 7 for cost. This means that the hybrid design is deemed to meet the requirements for almost all criteria.

To validate the decision for this new design, a sensitivity analysis was performed on the trade-off scoring and method. First for the trade-off scoring. Since some criteria are determined by the judgement of the group, a variation in scores from different group members exists. Therefore the final scores were calculated by taking the highest and lowest given scores per criterion. This results in the final scores as shown in Figure 2.1. It can be seen that the new hybrid design has the smallest range of given scores, it also is the only design that has a minimum given score above the 7 threshold.

Next to this a sensitivity was performed on the trade-off method. This is done by looking at the group scoring and systematic scoring on it own, and by changing some important criteria to simulate a change in customer needs. This results in the scores shown in Table 2.5. The new value for the changed criteria weight is shown in between brackets. It can be seen that the new hybrid design is the highest scoring design in all situations. Therefore it was concluded that this hybrid design will be taken along in the final design phase of the project.

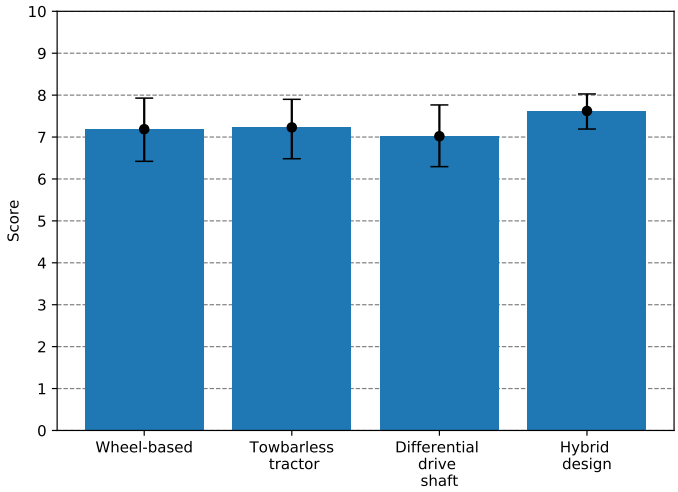

Figure 2.1: Sensitivity analysis results

Table 2.5: Results of Sensitivity Analysis

Changes	Wheel-Based Engine	Towbarless Tractor	Differential Drive Shaft Vehicle	Hybrid	
Original Scoring	7.19	7.23	7.02	7.59	**Legend**
Group Scoring	7.25	7.37	7.11	7.65	1 (Best)
Systematic Scoring	7.07	6.97	6.86	7.52	2
Increase Sustainability (0.206); Decrease Cost (0.05)	7.22	7.3	7.04	7.61	3
Increase Design Complexity (0.194); Decrease Operation Ability (0.2)	7.18	7.26	7.07	7.63	4 (Worst)
Increase Performance (0.176); Decrease Cost (0.1)	7.23	7.31	7.04	7.64	
Increase Cost (0.152); Decrease Performance (0.124)	7.15	7.15	7	7.54	
Increase Weight (0.26); Decrease Sustainability (0.07)	7.26	7.39	7.13	7.64	

3 Resource and Budget Allocation

Before going into the final design phase, a budget allocation of the technical resources will be established. These resources tend to grow undesirably during the design phase, so for this reason a limit and a margin will be set at the start. This will be checked and taken into account all throughout this design iteration to make sure the product does not go over the set budgets.

3.1 Budget Limitations

When looking at the requirements set [3], three main limitations on the technical resources can be identified. These flow from the following three requirements: **[RETS-SH-TLREQ-03]**, **[RETS-SH-TLREQ-09]**, **[RETS-F-GEN-08]**. The limit on weight added to the aircraft is 2% of the operational empty weight, this means a maximum of 940 kg can be added to the aircraft. Also for the external vehicles a weight limit has been set to ensure compatibility with current airport service roads. This comes down to a maximum axle load of 11 000 kg [1], so 22 000 kg for the 2-axle vehicle planned. The last budget limit comes from the fact that the product must be profitable within 5 years for the buying party. A limit for the cost budget will be calculated in section 3.3. These limitations will be analysed and constructed into budgets in the next two sections.

3.2 Mass Budget

Two different mass budgets will be established, one for the on-aircraft mass and one for the external vehicle mass.

3.2.1 On-aircraft Mass

A strict mass budget for the on-aircraft weight is important to comply with **[RETS-SH-TLREQ-03]**. Mass added to the aircraft needs to be carried on board for every flight. This will increase the emissions of the flight phase and it should therefore be minimised.

The mass added to the aircraft can be divided in five different categories. These are the motors, gears, cables, engine pre-heating system and other hardware. All these components together can weigh a maximum of 940 kg. Since the masses usually increase when designing, the current preliminary mass budget will be made for 80% of this maximum. In this way there is room to overshoot the estimations without violating the requirement. This results in a maximum mass of 752 kg. For the motors, gears and cables, a mass estimation has been made in the previous design phase [1]. As the cables will be longer than assumed in the previous design phase, the estimated cable mass will be doubled. The mass of the engine pre-heating system and the needed hardware components was not estimated, so it will be assumed that they take up 80% and 20% respectively of the left over mass budget. This assumption is made by doing preliminary research in engine pre-heating. All this results in the budget masses and percentages shown in Figure 3.1.

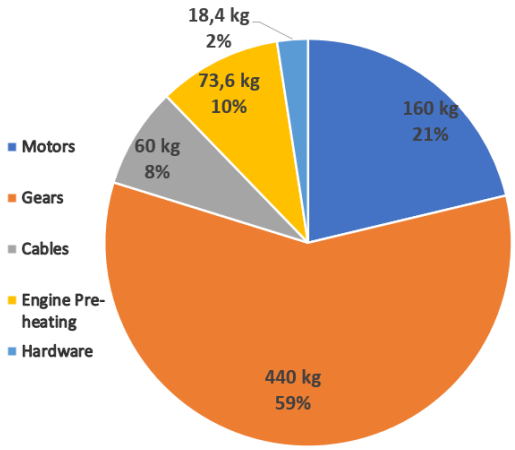

Figure 3.1: On-aircraft mass Budget

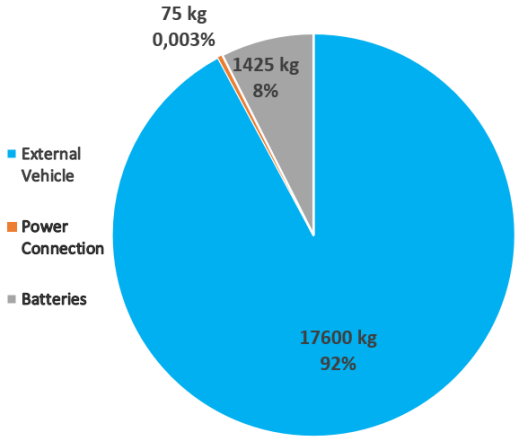

Figure 3.2: Nose wheel vehicle mass budget

3.2.2 External vehicle mass

The mass of the external vehicle is limited by the fact that it needs to be able to use the service roads when the vehicle is not attached. This means a maximum mass of 22 000 kg [7][3]. Just as with the on-aircraft mass, the mass budget will consist of 80% of this mass, which results in 17 600 kg. This budget needs to be divided over the following components: the external vehicle itself, the batteries and the power connection between the vehicle and the aircraft. The external vehicle will be designed using an existing pushback tug as a baseline. The mass estimate for the vehicle will therefore be the mass of this tug, which is 16 100 kg [3]. Of the leftover mass in the budget, it is estimated that 95% of it will go to the batteries and 5% will go to the vehicle-aircraft power connection. This results in the masses and percentages shown in Figure 3.2.

With these mass budget values and the values from the on-aircraft mass budget, a requirement is set for every subsystem on their mass budget. These can be found in the various requirement section in the next chapters.

3.3 Cost Budget

The limiting budget factor for the cost budget is the fact that the RETS must be profitable within five years after the product has been purchased. This results in a limit on both the operational costs per cycle and on the price of the product. As previously researched [3], the target price for a solution that is incorporated on the aircraft is around 1 million USD. In subsection 4.9.2, it will be discussed that an average taxi cycle, so taxi-out and taxi-in for an A321, costs around 330 kg of jet fuel. With an average jet fuel price over the last five years of around 0.61 USD per kg [7], and around 7 flights per day on average with the A321 [8], the current taxi operations costs an airliner 2,571,608 USD in 5 years. This means that using a price of 1 million USD, the total operational costs of RETS must be lower than 1,571,608 USD in 5 years, when performing 7 cycles per day. This will be a max operational cost of 123 USD per cycle.

In this situation, the maximum value for the production and development costs will be such that with a price of a million USD, the project will still be profitable for the developing party. The maximum cycle operational costs is then 123 USD. It will be taken into account that these two limits are interchangeable. When the operational costs turns out lower, there will be more budget for the development cost and production cost. Similarly, a lower development cost can result in a lower price which can compensate for a higher operational costs.

[7] https://www.indexmundi.com/commodities/?commodity=jet-fuel&months=60 [accessed 19 June 2020]
[8] https://www.flightera.net/en/airline/IndiGo/model/A21N [accessed 18 June 2020]

4 Operational Analysis

In this chapter, the operations and logistics of RETS is analysed. First, the flow diagrams of RETS are displayed. Both the functional flow diagrams and the functional breakdown structure are shown. After that, in section 4.3, the requirements related to the operations of the system are listed. After that the related risks are identified. The market analysis comes after, where the infrastructures of airports are analysed in detailed. Furthermore in section 4.6, a system research is done discussing about ways to eliminate engines and APU running while taxiing with RETS. In section 4.7 the level of automation. After the system research, the Taxi Performance Simulation is discussed in section 4.8. Moreover, the fuel reduction simulation is explained in section 4.9. Verification and validation of the developed models is treated in section 4.10. The chapter ends with the new operational risks identified, a sustainability analysis and the compliance matrix in section 4.11, section 4.12 section 4.13.

4.1 Functional flow diagrams

Below, the functional flow diagram (FFD) for the taxi-out phase and the taxi-in phase can be found, as well as the general operations FFD. The taxi-out phase and the taxi-in phase flow diagrams are based on the ”Ground Operations Logistics” (Figure 9.1) in the Midterm Report [1]. This will also be used to expand on the logistics and maintenance of the system in section 9.4. The general operations FFD is based on the ”Detailed functional flow diagram of the operations of the RETS system.” (Figure 4.4) in the Baseline Report [3]. A legend for the different elements present in the flow diagrams is displayed below.

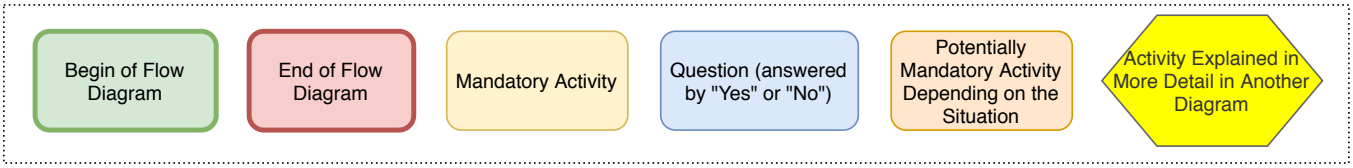

Figure 4.1: Legend for the Flow Diagrams in Operations

4.2 Functional Breakdown Structure

The general functional breakdown structure is identical to the ”Functional breakdown structure of the RETS system.” (Figure 4.1) in the Baseline Report [3]. Only the operational branch was adapted from the ”Detailed functional breakdown diagram of the operations of the RETS system.” (Figure 4.2) in the Baseline Report [3] based on the adapted functional flow diagrams.

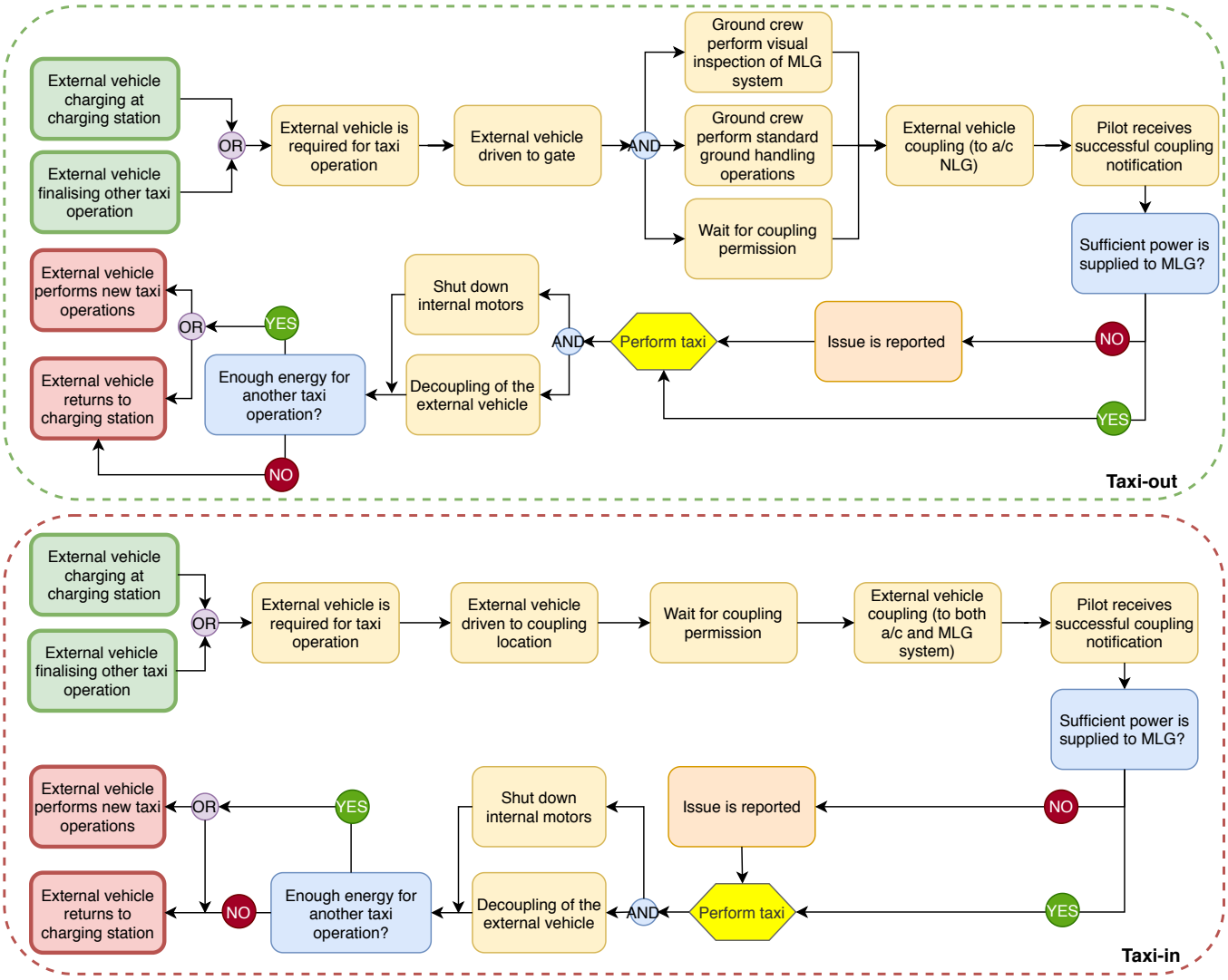

Figure 4.2: Taxi-in & Taxi-out Functional Flow Diagrams based on [1]

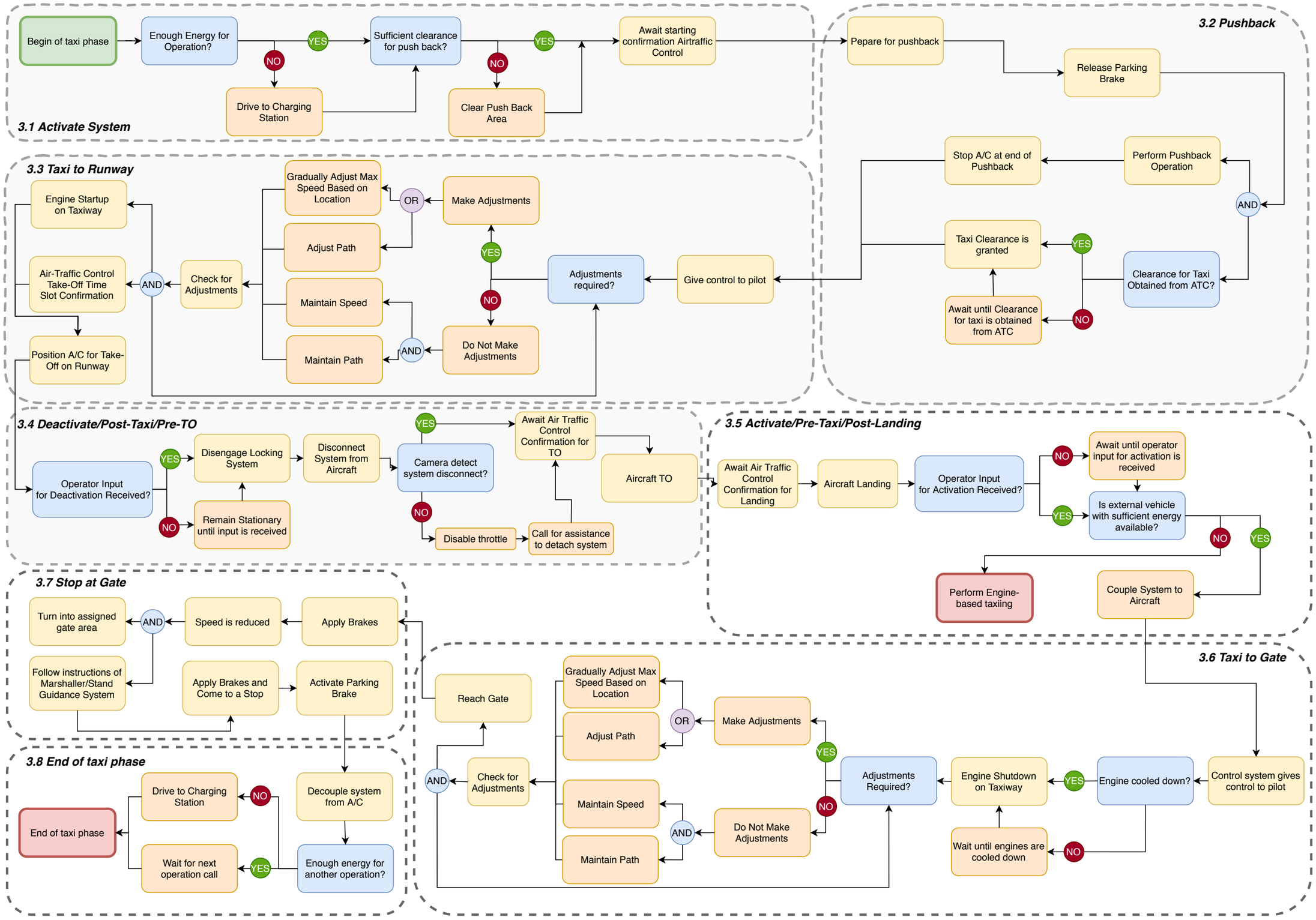

Figure 4.3: General functional flow diagram

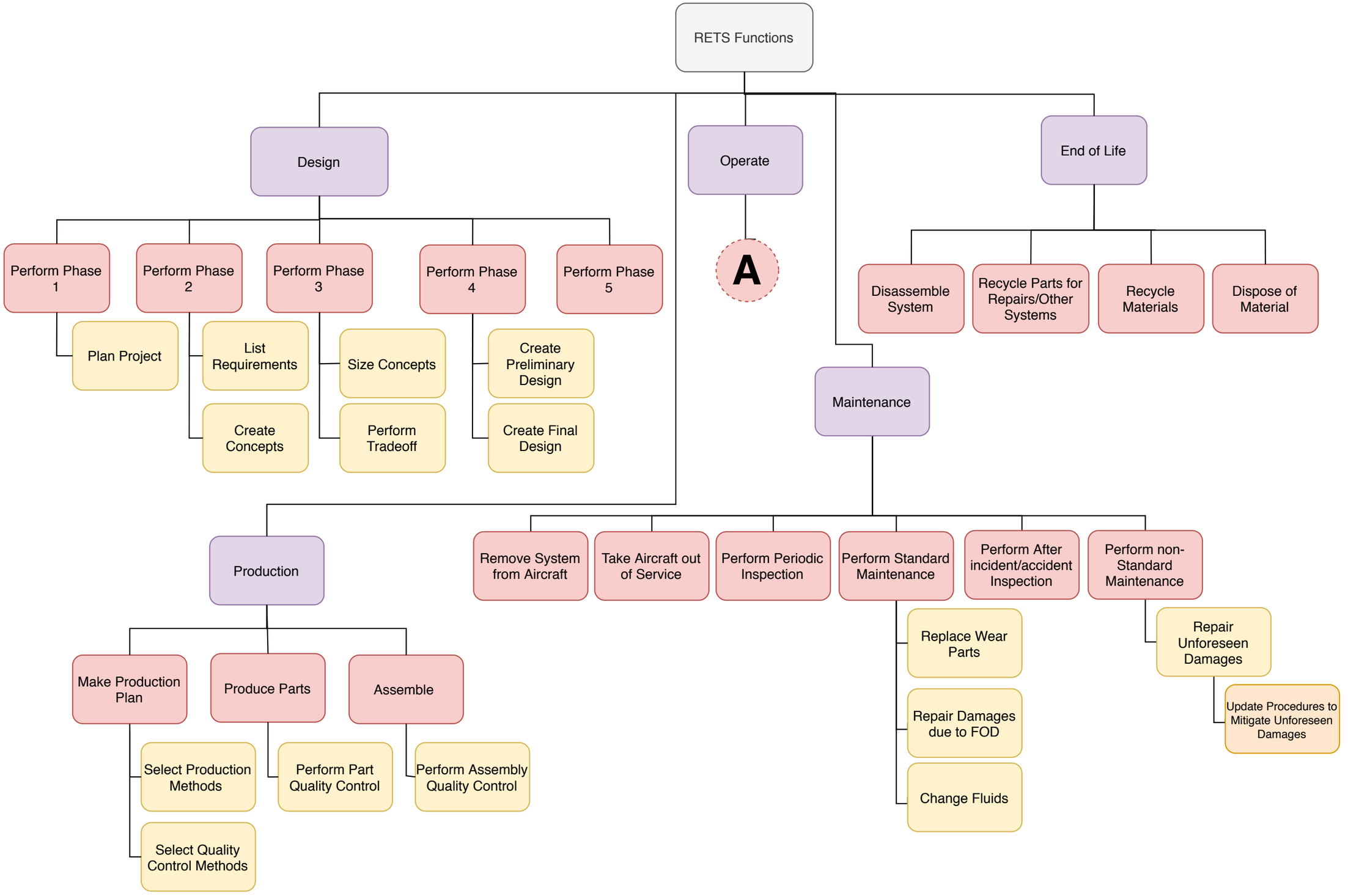

Figure 4.4: General functional breakdown structure taken from Baseline Report [3]

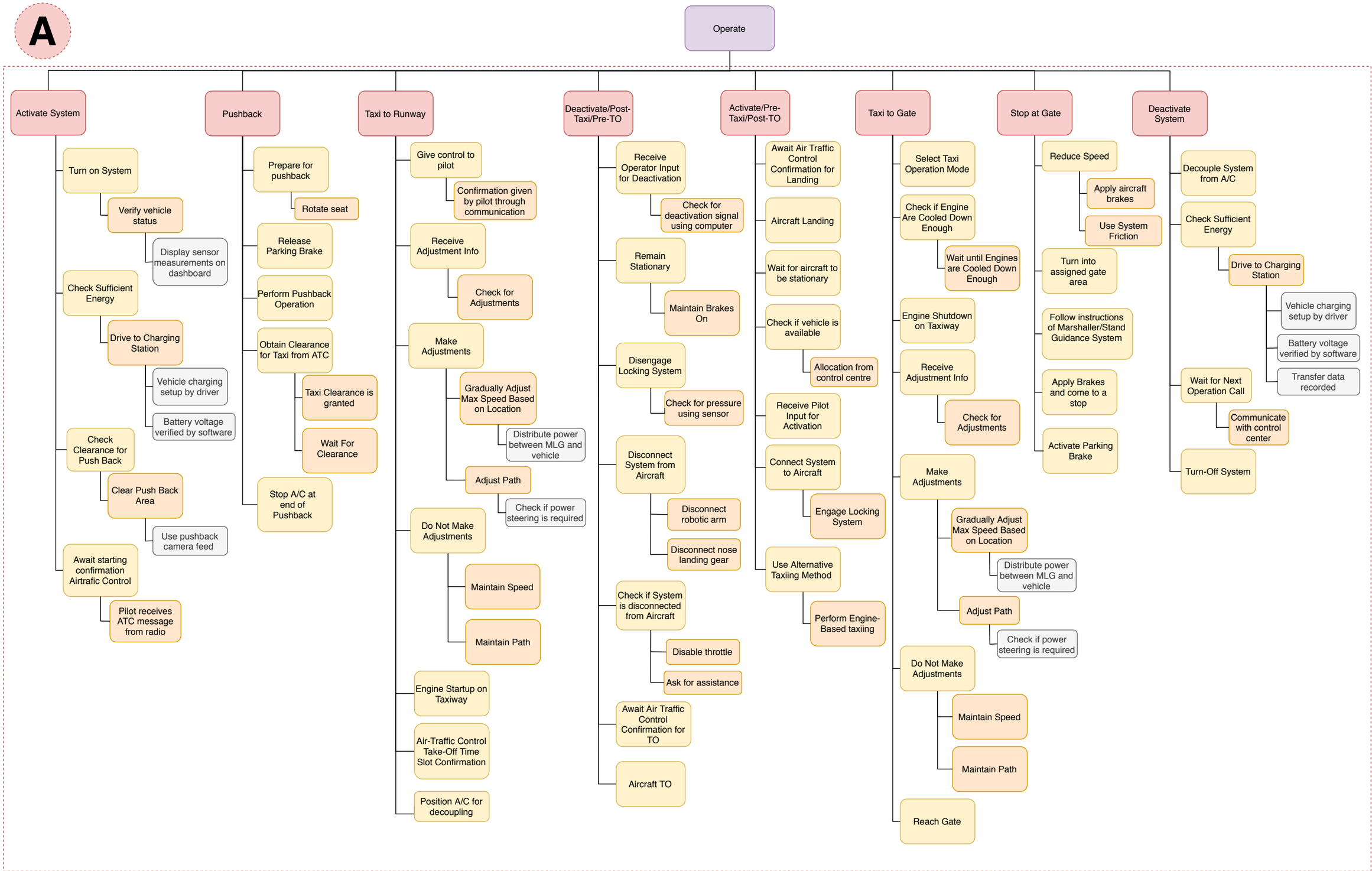

Figure 4.5: Operate branch functional breakdown structure [3]

4.3 Risk Analysis

Next to the functional analysis, a closer look at the risks will also provide useful input into the specific subsystem design. In the midterm phase [1] relevant risks for the operations of the RETS have already been identified. Table 4.3 shows these identified risks together with the cause, consequence, mitigation and the pre- and post-mitigation probability of failure p_f and consequence of failure c_f. Note that the pre- and post-values are separated by '/' and that both could be effected by the mitigation strategy. The estimated scores for p_f and c_f are based on the scales in Table 4.1 and 4.2.

Table 4.1: Scale for probability of occurrence between 1 and 5, where p is the actual probability of occurrence [2, p. 8]

Numerical rating	Explanation
1	Highly unlikely; $p_f \approx 0$
2	Low, improbable; $0 < p_f < 0.2$
3	Low-to-medium; $0.2 < p_f < 0.5$
4	High-to-medium; $0.5 < p_f < 0.8$
5	High, frequent; $0.8 < p_f < 1.0$

Table 4.2: Scale for consequence on mission by risk occurrence between 1 and 5, where c_f is the actual consequence of failure

Rating	Consequence	Explanation	C_f range
1	Negligible	Quick fix; reset	$0 < C_f < 0.2$
2	Marginal	Small damage to RETS system; maintenance of max 1 day required	$0.2 < C_f < 0.4$
3	Moderate	Damage to RETS system; maintenance of several days required	$0.4 < C_f < 0.6$
4	Critical	Damage to the aircraft and/or RETS system; extensive maintenance required	$0.6 < C_f < 0.8$
5	Catastrophic	Failure to satisfy mission goal; product will not be launched on the market; failure project	$0.8 < C_f < 1.0$

For the subsystem design especially the risk mitigation strategy listed in Table 4.3 could be of great importance, since some risks can only be mitigated with a certain design aspect. Therefore, the risk mitigation strategies will be taken into account in the coming sections explaining the detailed design of the operational subsystem. For example, a Fuel Reduction Simulation is made to make sure that total emissions will be reduced. Moreover, a Taxi Performance Model is made to examine if the RETS system will have adverse effects on normal operations. However, for some risks, this is not possible as they require more detailed information not yet available in this early design stage.

Table 4.3: Previously identified risks related to operations

ID	Risk	Risk Cause	Risk Consequence	Mitigation	p_f/ $p_{f_{\text{mit}}}$	c_f/ $p_{f_{\text{mit}}}$
T.O.1	RETS cannot be used for its intended purpose	RETS does not comply with aircraft and airport regulations and restrictions	Mission need statement not fulfilled	Designate operations officer during project; systems engineer must ensure proper design communication	3/1	5
T.O.2	Product support risk	Spare parts for mainte-nance/repair operations are not available	RETS system (component) down time; potential flight delays	Maintain proper spare part overview; document spare parts in maintenance plan	3/2	3/2
T.O.3	Damaged parts cannot be identified during inspection	Cracks, fatigue, etc. cannot be identified	Can lead to failure of RETS; potential flight delays	Design for inspection; document critical components	2/1	3
T.O.4	Total emissions will not be reduced	Wheel based engines too heavy	Primary mission objective not achieved	Quality control should allow for analysis of all flight phases	2/1	5
T.O.5	RETS system has adverse effects on normal operations	System takes up too much room; system is too slow; system does not work for most weather conditions; turn radius too big	Primary mission objective not achieved	Designate an operations officer during project; systems engineer must ensure proper design communication	4/2	5

4.4 Requirement Analysis

The last analysis to be done for every subsystem will be the requirement analysis. Similarly to the risk mitigation these requirements set boundaries for the actual subsystem design. It should be noted that some requirements have immediately flowed down from a certain risk mitigation strategy. All relevant requirements for the operational subsystem are listed below. The requirements set in orange are key requirements and therefore essential to the customer. The green requirement is a driving requirement, it drives the design above average. The requirements related to operations are listed below. They have been taken from the Baseline Report [3]. The compliance matrix, presented in section 4.13, shows if all requirements have been met.

- **[RETS-SH-TLREQ-01]**: RETS taxi time shall be up to 1 minute longer than engine based taxiing.*(Performance)*
- **[RETS-SH-TLREQ-02]**: RETS shall not lead to a reduction in aircraft payload. *(Performance)*
- **[RETS-SH-TLREQ-06]**: RETS shall not increase total energy consumption from gate to gate with respect to engine based taxiing. *(Sustainability)*
- **[RETS-SH-REQ-01]**: Current pushback and taxi methods shall still be effective on an airport/aircraft equipped with the RETS.
- **[RETS-SH-REQ-02]**: During the final concept design stage of the RETS, a study concerning the feasibility of the RETS with other CS25 commercial passenger aircraft shall be conducted. *(Technical)*
- **[RETS-SH-REQ-04]**: The weather conditions under which the RETS can operate will be clearly documented. *(Technical)*
- **[RETS-SH-REQ-05]**: The RETS shall be able to withstand the demanding working environ-

ment, specified in the operating manual, that is present on the apron for 8 years without significant loss of performance. *(Performance)*
- **[RETS-SH-PBC-01]**: The operation of the RETS by a ground crew member shall be clear and straightforward after an educational programme of 8 hours is followed. *(Technical)*
- **[RETS-SH-INV-02]**: The RETS shall uphold to the highest industry standards with regards to safety, professionalism, quality and respect *(Legal)*
- **[RETS-SH-GOV-01]**: The RETS shall adhere to the legislation set-out by the local government *(Legal)*
- **[RETS-SH-ASA-01]**: The RETS shall adhere to the legislation set-out by the aircraft safety agency *(Legal)*
- **[RETS-SH-APC-01]**: The RETS shall abide by the relevant airport legislation *(Legal)*
- **[RETS-SH-APC-02]**: The RETS shall not drastically hinder other operations on the apron causing additional delays by delaying those activities. *(Operations)*
- **[RETS-SH-APC-03]**: In case of a failure that immobilises the aircraft on a taxiway, that taxiway shall be cleared in 10 minutes. *(Operations)*
- **[RETS-SH-EMS-01]**:The RETS shall not hinder emergency service operations in a major way such that the success of the operation is affected. (Technical)
- **[RETS-SH-EMS-02]**: If necessary, a document specifying the hazards shall be available for the emergency services. (Legal)
- **[RETS-SH-RES-01]**: The noise level around the airport shall not increase due to operations of the RETS. *(Environmental)*
- **[RETS-SH-OAO-01]**: Depending on the outcome of the study conducted for [RETS-SH-REQ-01], the RETS shall be redesigned/sized upon request for one of the studied aircraft within 26 weeks. *(Time)*
- **[RETS-F-GEN-05]** RETS shall be compatible with an A321.
- **[RETS-F-GEN-08]** RETS shall be compatible with existing airport infrastructure.
- **[RETS-F-OPR-01]** RETS shall have a taxi mode.
- **[RETS-F-OPR-02]** RETS shall have a pushback mode.
- **[RETS-F-OPR-03]** RETS shall be able to warm-up the engines.
- **[RETS-F-OPR-04]** A system failure shall not prevent normal taxiing operations.
- **[RETS-F-OPR-08]** Operator training shall take a maximum of 2 days.
- **[RETS-F-PE-15]** RETS shall reduce the operational engine warm-up time by 15%.

4.5 Market Analysis

In this section, the different important aspects for RETS to succeed that are not directly related to designing is explained. First, the potential customers of RETS are identified. Following, the market analysis of the airlines using the A321 is explained. Next, the airports with most A321 movements are listed and an analysis of the infrastructure of those airports is performed. Also, recommendations for airport with regards to their infrastructure are given. Finally, the baseline taxi route used is explained.

4.5.1 Customers

RETS will have two different types of customers, the internal and external parts will be sold to two different entities. First, the most obvious is for the vehicle. As it stays in airports and won't be used for a particular airline nor for a particular aircraft manufacturer, the airport or ground handler is purchasing them. Also, airlines pay airports for using the facilities and thus it is the most logical for the airport to own the vehicles. For the internal part, as it is a retrofit, the customer could be the aircraft manufacturer or the airline. Airlines that do not have the required technicians might prefer the aircraft manufacturer to place the system on the aircraft. However, some bigger airlines that have the required resources to do it, might have a preference for doing it themselves. The second option (selling to airlines) allows the system to be put on aircraft that are already in use, assuming the aircraft manufacturer does not propose that option. However, when installed by the

airline, getting it certified can be an issue, requiring it to be approved by multiple entities.

4.5.2 Airlines Market Analysis

A detailed analysis of the airlines using the A321 [9] was explained in the baseline report [3]. Those airlines were divided in three categories [10]: low cost carriers (LCC), regional airlines (REG) and full service network carriers (FSNC). Based on the number of A321 that every airline has, it was possible to identify what airline category uses the A321 the most. The outcome was that 52% of all A321 are used by full service network carriers (FSNC), 26% by regional airlines (REG), and 22% by low cost carriers (LCC).

The system being especially useful for short range flights due to the added weight to the aircraft, its target group are mainly low cost carriers and possibly regional airlines. However, full service network carriers use the A321 for short but also medium to high ranges flights, for which the system might be not reduce emissions effectively.

4.5.3 Aircraft Model and Version Choice

The baseline aircraft used is the A321NEO. Compared to the regular A321 (CEO), it has a more efficient propulsion system and is thus more prone to be chosen by airlines that need an aircraft of the A321-family. Different versions of the A321NEO exist with different passengers capacities and thus different maximum take-off weight. The A321NEO WV072, also called the Airbus Cabin Flex version, is chosen as it is the version that has the highest passenger capacity (can fit up to 220 passengers) and has the highest maximum take-off weight. Therefore, the system can be used for all A321NEO version as the design takes into account the worst case scenario.

4.5.4 Airports with Highest A321 Movements

Data set [6] gives all the A321 flights that took place on a single day in 2018. It provides the departing airport, the arrival airport, the range, and the number of flights for that specific route. Based on this data set [6], the airports with the most departing A321 are:

1. Tan Son Nhat International Airport (SGN), Vietnam (170 departures/day)
2. Dallas Fort Worth International Airport (DFW), USA (145 departures/day)
3. Charlotte Douglas International Airport (CLT), USA (142 departures/day)
4. Istanbul Airport (IST), Turkey (138 departures/day)
5. Hartsfield–Jackson Atlanta International Airport (ATL), USA (133 departures/day)

The average taxi-in time and taxi-out time for the above mentioned airports (except SGN) according to Eurocontrol [11] is displayed in the following table:

Airport	Average Taxi-in Time (min)	Average Taxi-out Time (min)
SGN	N/A	N/A
DFW	10.1	18
CLT	7.3	20.4
IST	9.4	21.4
ATL	11.1	18.1

4.5.5 A321 ranges

Based on data set [6], it was possible to find the most common ranges of A321 flights. The results are the following:

[9] https://www.alternativeairlines.com/airbus-a321 [accessed 30 April 2020]
[10] http://airlinebasics.com/common-airline-business-models/ [accessed 4 May 2020]
[11] https://www.eurocontrol.int/publication/taxi-times-winter-2018-2019 [accessed 11 June 2020]

- 70% of A321 flights have a range equal or lower than 1806 km
- 80% of A321 flights have a range equal or lower than 2239 km
- 90% of A321 flights have a range equal or lower than 2816 km
- 95% of A321 flights have a range equal or lower than 3366 km
- 98% of A321 flights have a range equal or lower than 3856 km

4.5.6 System Compatibility with Airport Infrastructures

In this section it is analysed how existing airport infrastructures can be used to accommodate RETS. First, infrastructures present in most airports that could be used as coupling and decoupling location are presented. Next, the infrastructure of three airports is analysed. The three airports are Tan Son Nhat International Airport, Dallas Fort Worth International Airport, and Hartsfield–Jackson Atlanta International Airport. Those were taken from the ranking of airports with most A321 movements based on data set [6] in subsection 4.5.4. For these three airports, potential coupling and decoupling locations are identified. Finally, a short description of possible infrastructural changes that would be beneficial for the implementation of the system is given.

4.5.6.1 General Existing Airport Infrastructure

Areas reserved for the coupling or decoupling of an external system don't currently exist in airports. However, there are areas where it could be done but those areas are intended for other purposes. Parallel taxiways are parallel to runways. Those can be potential coupling or decoupling location. Emergency pads are available for an aircraft that requires assistance while not having additional traffic building up. Those are free most of the time. Another type of area are de-icing pads that are used as a location to de-ice an aircraft during freezing temperature times. Apart from some times in the winter when these areas would be strictly reserved for de-icing, those are free the rest of the time. Both types of areas mentioned are generally easily accessible by taking an exit while taxiing to the runway. Therefore, they are suited for coupling and decoupling, at least until infrastructures are changed to accommodate the system (if needed). Another type of area are blast pads which are located just before the start of the runway. It gets damaged by the high speed wind coming out of the engines when taking-off. However, this area is not suited for coupling and decoupling as it would block other aircraft from using the runway. Finally, in larger airports, runways have multiple entrances and exits. Some of these could be assigned for coupling and decoupling.

4.5.6.2 Airports with Highest A321 Movements Infrastructure Analysis

Tan Son Nhat International Airport

Based on the A321 data set [6], Tan Son Nhat International Airport (SGN) has the most A321 movements out of all airports in the world. It is assumed that runway 7R/25L is mainly used for departures as it is closer to the gates and thus less fuel is consumed during taxiing, and runway 7L/25R is used for arrivals. This was assumed based on sources found for DFW and ATL (next airports analysed) that explained that for those airports, usually, the runways close to the terminals are used for take-off and the further ones are used for landing.

As can be seen on Figure 4.6, to access runway 7R/25L at its beginning (at 7R), two paths are available (right after route W6). One of these paths can be used to decouple the system while the other lane is still free for aircraft to access the runway. The right lane could be used for decoupling. Although the left lane is also used to exit runway 7L/25R, by looking at aircraft movements at SGN through Flightradar24 [12], it seems like most aircraft exit the runway earlier, taking exit W4. However, at the time this was observed, only short range aircraft (A320 and A321) were landing, probably due to the COVID19 crisis. For bigger aircraft, the entire runway length might be needed in order to land. Therefore, this is not the most convenient option. It is concluded that there is not an area suited for decoupling. Only when taking off from the 25L side, the aircraft passes by two larger areas that can be used as decoupling location.

[12] https://www.flightradar24.com/10.82,106.65/15 [accessed 16 June 2020]

There are two exits for runway 7L/25R, one of them has a wider area connected to it. Both, one of the exits and the area can be used as coupling location. If the aircraft lands from the 25R side, the last exit also has a large area connected to it that can be used as coupling location.

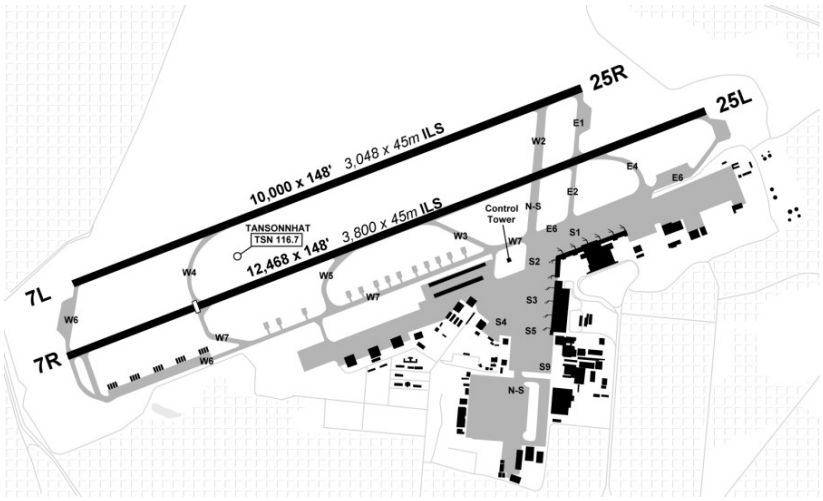

Figure 4.6: Tan Son Nhat International Airport layout [13]

Dallas Fort Worth International Airport

Dallas Fort Worth International Airport (DFW) has a very large infrastructure and is the only airport in the world that has seven runways that can be simultaneously operational (not crossing) [14]. The primary runways are the four next to the gates. The two closest are used for take-off while the two furthest are used for landing [15].

As can be seen on Figure 4.7, the airport layout is almost mirrored around the gates. Therefore, possible coupling and decoupling locations will be identified for the right side only but they also apply for the left side. To access runway 17R/35L at its beginning (at 17R), the aircraft pass by a very large area (in S-shape). This area can be used as decoupling location.

Once landed, when exiting runway 17C/35C at its end (at 35L), the aircraft again passes by a large area which can be used as coupling location. Again, in case the aircraft takes off or lands in the direction opposite to the one assumed above (for example from 35L to 17R and 35C to 17C) for wind reasons, the coupling locations become decoupling locations and vice versa.

[13] https://rzjets.net/airports/?show=2643 [accessed 12 June 2020]
[14] http://www.dfwcareerexpo.com/2016/about/fun_facts.php [accessed 15 June 2020]
[15] https://www.dfwairport.com/aircraftnoise/#:~:text=DFW%20typically%20uses%20its%20north,13L%2F31R%20in%20North%20Flow. [accessed 15 June 2020]

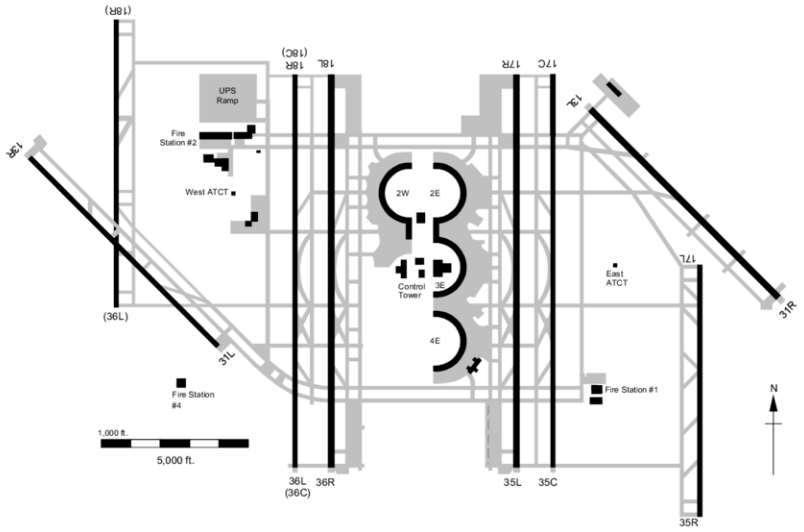

Figure 4.7: Dallas Fort Worth International Airport layout [10]

Hartsfield–Jackson Atlanta International Airport

Hartsfield–Jackson Atlanta International Airport (ATL) is the busiest airport in the world in terms of passengers movement [16]. Similar to DFW, the two runways closest to the gates are used for take-off as the taxi distance is shorter and thus, less fuel is burned during taxiing [17]. The two outside runways are mainly used for landing [18]. Compared to DFW, ATL does not have as many areas close to the runways that could be used as coupling and decoupling locations.

Aircraft landing on runway 8L/26R, exiting the runway at its end (at 26R) pass by a large area that could be used as coupling location. Another option is to use one of the two exits of runway 8L/26R as a coupling location. Runway 8R/26L has multiple entrances. The one closest to the main entrance could be used as decoupling location. However, that entrance is connected further to the runway and could thus, make the available distance for take-off too short depending on the aircraft type. The same holds for runways 9L/27R. Runway 9R/27L seems to have no potential location for coupling, apart from using another and earlier exit. However, that could make the landing distance too short depending on the aircraft type and is thus not the best option. Finally, looking at runway 10/28, to both enter (at 10) and exit (at 28), there are two paths of which one can be used as coupling (at 28) or decoupling (at 10) locations.

[16] https://edition.cnn.com/travel/article/worlds-busiest-airports-2018/index.html#:~:text=1.,according%20to%20Airports%20Council%20International. [accessed 22 June 2020]
[17] https://en.wikipedia.org/wiki/Hartsfield%E2%80%93Jackson_Atlanta_International_Airport [accessed 15 June 2020]
[18] https://www.georgiaencyclopedia.org/articles/business-economy/hartsfield-jackson-atlanta-international-airport [accessed 15 June 2020]

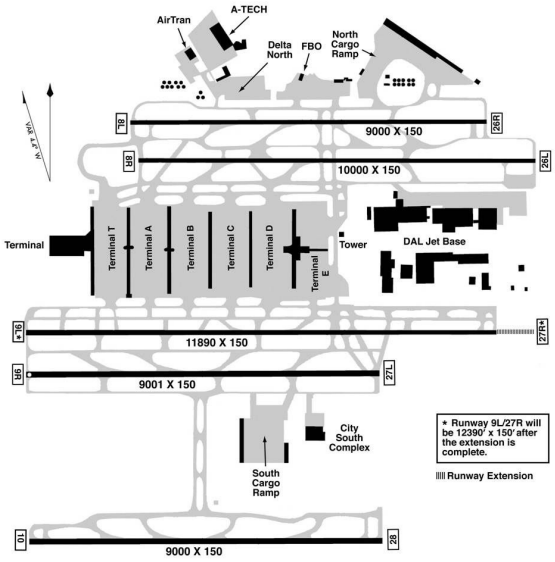

Figure 4.8: Hartsfield–Jackson Atlanta International Airport layout [19]

4.5.6.3 Recommended Infrastructure and Organisational Changes for Airports

The general recommendation for future infrastructure changes is to create areas that are close to runways, easily accessible without having to extend the taxi distance too much, and that do not create any additional traffic. If possible, they would be large enough for multiple aircraft coupling or decoupling and be easily accessible through service roads. Also, adding entrances and exits to runways can be an alternative solution that could possibly require less works on existing infrastructure. Both these possibilities require the service roads network to be rethought. The new infrastructure must also consider the possibility that other aircraft models will be equipped with the system, which means that more aircraft will have to be coupled and decoupled. Next, a charging station must be build where the vehicles would be charged.

The system requires some extra personnel. First, there are the people driving and operating the vehicles. Although the people that currently perform the pushback can get some extra training and do it, it would require additional people as it takes more time than a pushback. Second, it is required to have a group of people in charge of the logistics of the vehicles. Those can work from the control tower or from a separate place that has view on the taxi routes. Third, personnel is needed to be in charge of the charging station. Finally, some specialised mechanics are needed for maintenance but also in case of emergency.

More specifically for airports with highest A321 movements, according to an article on Bizhub [20], SGN is planning on expanding. That expansion could take into account the infrastructure changes mentioned above. DFW has the best infrastructure for the system out of the three analysed airports, with multiple large areas, and many entrances and exits per runway. Finally, ATL has many entrances and exits per runway but seemingly too few areas that could be used as coupling or decoupling location.

4.5.7 Baseline Taxi Route

The baseline taxi route is identical to the one chosen in the Midterm Report [1]. The route starts at gate D14 and ends at runway 36C, at Amsterdam Schipol Airport. The path is shown in Figure 4.9. As discussed in the Midterm Report [1], runway 36C was chosen because both runways

[19] https://www.quora.com/What-are-common-layouts-for-airports-and-their-comparative-advantages-and-disadvantages [accessed 15 June 2020]

[19] https://qph.fs.quoracdn.net/main-qimg-43c82dbe6e38bc894c479facb04ed9cc.webp [accessed 15 June 2020]

[20] http://bizhub.vn/news/tan-son-nhat-airport-must-expand_283380.html [accessed 16 June 2020]

24 (Kaagbaan) and 36R/18L (Alsmeerbaan) are too close to gate D14 for the taxi time to be close to average taxi time of Schipol. Also, runway 36L/18L (Polderbaan) is too far and the taxi time to reach it is thus also not close to average. Terminal D is the largest terminal of Schipol Airport and thus, most aircraft depart from there. Also, terminal D and especially gate D14 are located somewhere in the middle of the airport. Therefore, gate D14 was chosen as starting point. The detailed path is: D14-A8-A6-A-Q-A26-W9-36C. As mentioned in the Midterm Report [1], the distance of this taxi route was found to be 2.9 km and the taxi time was found to be approximately 12.35 minutes.

Figure 4.9: Baseline taxi route map based on map from Schipol website [21], taken from Midterm Report [1]

4.5.8 Aircraft Movements per Runway

Quantifying how busy an airport is requires multiple factors to be analysed. One of them is the number of aircraft movements per runway per day. The goal is to know what the extreme case is, for which delays during taxiing can cause additional traffic. According to this factor, a busy airport would have a lot of aeroplane movements for a small amount of active runways. Therefore, the ranking is different from airports with most aeroplane movements. It is also different from the airport's number of passengers travelling per runway as some airports could have more large aircrafts. It was found that Heathrow Airport has the largest amount of aircraft movements for the lowest number of runways, with 475 861 aircraft movements per year [22] for two runways, which is approximately 652 aeroplanes movements per day per runway. Dubai International Airport (DXB) was not far behind with 409 493 aircraft movements per year [23] for two runways, which is approximately 561 aeroplanes movements per day per runway.

4.6 Engine-off System Research

In order to make RETS effective in reducing emissions, the engines need to be turned off during the taxi phase as long as possible. However the engines (and especially the APU) have other functions besides propulsion. For example, the primary functions of the APU are aircraft's main engine start-up, providing electrical power when engines are not running and providing compressed air to operate the onboard air-conditioning.[24] Moreover, when engines are not running, the bleed

[21] https://www.schiphol.nl/en/operations/page/maps/ [accessed 12 May 2020]
[22] https://www.heathrow.com/company/investor-centre/reports/traffic-statistics [accessed 9 June 2020]
[23] https://www.flightera.net/en/airport/Dubai/OMDB/ [accessed 9 June 2020]
[24] https://www.aviationpros.com/gse/gpus-pcas-power-carts-accessories/article/10370908/the-apu-problem-a-quantified-approach [accessed on 3 June 2020]

air from the APU is used for wing and engine thermal anti-icing, hydraulic reservoirs pressurisation and water tank pressurisation.[25] Limiting APU usage has significant beneficial effects on fuel consumption, maintenance and environment.[26] The APS 3200 APU used on board of the Airbus A321 uses 148 kg h^{-1} of fuel [11, p. viii]. Moreover, the overall emissions at airports are becoming a serious problem. APU usage contributes significantly to overall emissions. This includes the emissions of nitrogen oxide, carbon monoxide and hydrocarbons, which are the main concerns regarding environmental impact. [24] In conclusion, having a design that can limit the APU usage would be beneficial and make the design more competitive and more interesting for potential customers. Therefore, the following subsections will describe potential systems that enable engine-off operation. Primarily focusing on the APU, but also taking the primary engines into account.

4.6.1 Engine start-up

As mentioned before, one of the primary functions of the APU is to provide energy for engine start-up. On the Airbus A321neo this is done by supplying the engines with high pressure bleed air. This bleed air is used to start the compressors and turbine. Aircraft jet engines can also be started electrically using the generators in the engine. This system is used in the Boeing 787 for example [12]. In order to mitigate the APU usage, both systems are analysed to see if and how this can be implemented in RETS to reduce emissions. Engine start-up will likely happen during taxiing, hence the system should be on-board the aircraft, or RETS.

4.6.1.1 Pneumatic start-up

The airbus A321neo is already equipped with a pneumatic system for engine start-up. Conventional procedures prescribe that the APU is turned on to supply bleed air for engine start-up. However, in some cases also an Air Start Unit (ASU) can be used to start the engines. This is a ground based system, either vehicle or underground-based, that can be coupled to the pneumatic system of the aircraft. The air connection points (both High and Low pressure) are on the belly of the aircraft, in the wing root fairing [13, pp. 230-231]. In order to supply the aircraft with air for engine start-up, this connection has to be moved closer to the nose gear vehicle. This would result in two pneumatic hoses from the nose to the old connection point. This is estimated to be 12 m. Given a hose weight of 1.64 kg m^{-1} [27], the extra weight added will be around 40 kg. For the sizing of the external system, it is assumed that the ASU is integrated into the external vehicle. A typical ASU weighs around 5000 kg[28]. This would compromise a very large part of the mass budget for the external vehicle. Besides that, the ASU is supplying air via a turbine, in a similar manner as the APU. It is very complex to electrify this system, both in terms of power required, mass, and to supply the high pressure air at the right temperature for start up. Therefor, a turbine equipped ASU is much more beneficial and efficient, especially compared to the marginal savings an electric ASU would offer. The idea to integrate an ASU into the RETS vehicle is hence deemed infeasible, and will only be considered on customer request or in a future iteration.

4.6.1.2 Electrical start-up

As mentioned earlier, another possibility to perform engine start-up is by electrically powering the turbine and compressor. This can be done with electricity supplied by the external vehicle. It powers the generator that functions as an electric motor when supplied with power. However, the generator in the A321neo is too weak to get the shaft up to the right spinning speed. The Boeing 787 is one of the few aircraft that can do electric start-up. It has two generators per engine for this purpose, and runs an electric system at a significantly higher voltage (235Vac)[12]. Many modifications are needed to host this. Not only do the engines require a big redesign to house two powerful generators, also the electrical system needs to be adapted to support the generators.

[25] https://www.slideshare.net/theoryce/b737-ng-air-systems [accessed on 3 June 2020]
[26] https://blog.openairlines.com/how-to-track-apu-fuel-burn-on-ground [accessed on 3 June 2020]
[27] https://www.sageparts.com/hbd-thermoid.shtm [accessed on 03 June 2020]
[28] http://www.guinault.com/wp-contenu/uploads/8753-GUINAULT-Fiche-Civile_GS.pdf [accessed on 03 June 2020]

Furthermore, the high pressure air piping can be removed for some parts, but other dependent systems such as the trim and anti ice systems might need to be changed, as was done in the Boeing 787[29]. At last, the APU should be resized to change the energy output from bleed air to electricity, as otherwise the desired emission reduction can not be fully realised. Needless to say, these modifications are very tough to realise in the already optimised design of the A321neo. The pneumatic system of the aircraft is very fundamental to the aircraft functionality, as is the electrical system. Transferring functions from one system to the other is deemed a major modification. It is hard to give a mass estimation of the modification because the extent of the modifications are not known. When changing the whole aircraft to a More Electric Aircraft (MEA)[12], weight can potentially be saved. However not all modifications might be possible, which can result in a lot of weight added. This option is therefore very uncertain and imposes more risks, hence it is decided not to develop this system.

4.6.1.3 Concluding remarks

Two possibilities have been discussed that can contribute to the emission reduction by eliminating APU powered engine start-up. It can be done either pneumatically or electrically. Pneumatically it can be done by supplying the aircraft with high pressure air, as is done with an ASU. The only aircraft modification needed is to change the position of the air connections. The downside however is that the system that supplies the high pressure air will take up a very large part of the external vehicle mass budget. The electric option however does not require the external vehicle to be much more heavy. An electrical system is already present to power the wheel based engines. However the modifications to the aircraft can be very disruptive. The engines need to be changed to house another/more powerful generator, the electric and pneumatic system need to be changed, and potentially the APU needs to be modified. The electric engine start-up system is potentially even beneficial in terms of weight, but it requires so many changes that it is deemed infeasible at this stage. The pneumatic system can potentially be integrated into the RETS vehicle as a future option in the second iteration. Service road compatibility will however likely suffer from this. It should therefor be marketed as another variant of the system. Another option is to couple an existing ASU to RETS as a trailer. This possibility requires only the installation of a towing hook, as an ASU is generally already trailer based. The possibility of adding a towing hook is only a minor modification and is therefor not worked out into more detail. Partly because the reduction of emissions is marginal as an ASU is also a turbine running on jetfuel, just like the APU. The electrification of an ASU is too complex for this design phase.

4.6.2 Engine pre-heating

As explained in the baseline report [3], aircraft manufacturers prescribe that engine warm-up is required prior to take-off. This ranges from 5 min for engines that have been turned off for more than 2 h to 3 min for engines that have shortly been turned-off[30]. Usually, engine based taxiing is sufficient for engine warm-up, however as engine based taxiing should be eliminated as much as possible, the system should provide ways to warm up the engines other than to let the engines run, as this would be very inefficient and produces emissions. In the midterm report [1] it was decided to design a system that is integrated into the engines. The most important engine parts that need to be pre-heated are the high pressure compressor, combustion chamber and the high pressure turbine. These engine components experience the most heat and the highest heat gradient due to their close position to the heat source (inside combustion chamber). Also the engine oil has to be pre-heated. Engine manufacturers have not specified what heat levels are required for the engine to be sufficiently warmed up. A few assumptions are made in order to be able to size the subsystem. The heat produced inside combustion chamber is distributed primarily to the high pressure turbine, and to a lower extent to the high pressure compressor. The A321 neo has two engine options; airlines can choose for either the Pratt & Whitney PW1100G or the CFM LEAP-1A.

[29] https://www.boeing.com/commercial/aeromagazine/articles/qtr_4_07/article_02_4.html [accessed on 03 June 2020]

[30] https://a320podcast.libsyn.com/category/NEO [accessed 7 May 2020]

Given the maximum operating temperatures in the respective data sheets[14][15], and the heat distribution of a smaller, however similar engine as shown in Figure 4.10, the minimum average component temperature for sufficient warm-up was set to be 550 °C.

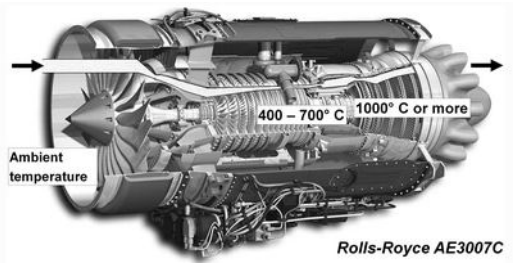

Figure 4.10: Air temperature in a geared turbofan engine [31]

In order to size the system, the energy that is required to warm the engine up to this level can be calculated with equation Equation 4.1. Where m is the mass [kg], C_p the specific heat of the material [kJ kg^{-1} °C^{-1}], and δT the difference in temperature[°C].

$$E = mC_p\delta T \tag{4.1}$$

Data on the engine and materials used for components inside the engines are not publicly available. Therefor the GMR-235 Cast Nickel Superalloy is assumed . This alloy is often used for jet engine components as it can withstand the high pressures and temperatures inside the engine, and has a specific heat value of 460 kJ kg^{-1} °C^{-1}[32]. Furthermore it is assumed that the elements to be heated (first row of turbine fan blades and combustion chamber liners) compose 15% of the engine weight (3008 kg[15]). This yields a mass of 1203.2 kg. Plugging in these numbers gives a required energy of 146.5 MJ. This is the purely theoretical number, in case the electricity is converted into heat that applies only on the parts that require warm-up. The system should try to reach an efficiency as high as possible with as low as possible weight added. The system is worked out into more detail in subsection 5.4.1

4.6.3 Air conditioning

The air conditioning system is responsible for providing temperature controlled air in the cabin. For almost all conventional aircraft, the air conditioning system uses the bleed air from the engines, APU or ground air source in the air conditioning packs [25]. Nonetheless, Boeing introduced with the B787 a new no-bleed system architecture.

4.6.3.1 Pneumatic system

To limit the usage of the APU, often Preconditioned Air Units (PCA) are used at the gates. Similarly as the ASU, the PCA is a ground based system that can be coupled to the pneumatic system of the aircraft. The PCA provides low pressure pre-cooled air to the pneumatic system of the aircraft. As described in subsection 4.6.1, the connection point is on the belly of the aircraft, in the wing root fairing.

As already mentioned at pneumatic start-up in subsection 4.6.1, a pneumatic hose needs to be implemented in the aircraft if the RETS-system needs to implement a pneumatic system for air conditioning as the mix manifold is positioned at the belly. Several companies are providing pre-conditioned air units that hang on the passenger loading bridge. It is assumed that the PCA hanging on this bridge is designed to have low weight as otherwise the loading bridge needs to be reinforced. The company Hobart developed for example the Hobart 3400 PCA series. The smallest option of this series is the PCA 130 having 2 cooling modules. This has a weight of approximately 3300 kg

[31] https://link.springer.com/article/10.1007/s11837-016-2071-2[accessed on 5 June 2020]
[32] https://www.steelgr.com/Steel-Grades/High-Alloy/gmr-235.html[accessed on 5 June 2020]

and a length of 3 m, a width of 2.23 m and a height of 1.48 m. [16, p. 4] Another company, Adelta, had similar weight, width and height for the PCA. However, the PCA designed by Adelta was even longer. [17, p. 3] Although there might be a possibility to integrate both the Pneumatic start-up system described in subsection 4.6.1 with the PCA, it still will compromise a very large part of the mass budget for the external vehicle. Moreover, these systems will have significant dimensions, therefore limiting the dimensions for other systems of the external vehicle.

4.6.3.2 Electrical systems

Another option is to use a no-bleed system architecture that Boeing introduced with the B787. Boeing states that the no-bleed system can lead to improved fuel consumption, reduced maintenance cost, improved reliability and lower overall weight therefore expanding the range [29]. Nonetheless, if a no-bleed system is implemented in the A321neo, this will lead to a significant amount of modifications. Examples of these modifications are redesigning the APU and removing parts of the pneumatic system and replacing it with electrical components.

4.6.3.3 Concluding remarks

This subsection looked at the possibility to use the external vehicle for air conditioning to reduce the APU usage. Two possibilities have been discussed, a pneumatic system or an electrical system. The pneumatic system is deemed to be too heavy and taking up too much of the available space on the external vehicle if the requirement for using the service roads must be satisfied. Implementing a no-bleed system on the A321neo is deemed to be unfeasible considering the number of extensive modifications needed. In conclusion, implementing a system for air conditioning in the first iteration of the RETS-system is not deemed feasible and beneficial. Nonetheless, if a no-bleed system will be implemented in next generation narrow bodied aircraft, it might be feasible to reserve energy for air conditioning on the external vehicle. However, if the customer wants to limit the emissions even more by eliminating APU usage, the possibility should be there to couple the Air conditioning unit as a trailer unit. Therefor, the RETS vehicle should have an option to tug the ACU along. A towing hook will therefor be installed on customer request.

4.7 Level of automation

In order to assess whether the external vehicle is autonomous or human controlled, the advantages and disadvantages of each step of the taxiing operations when autonomous is analysed. The different steps analysed are the vehicle moving to an aircraft or leaving an aircraft, the coupling/decoupling, and the taxiing.

In general, an autonomous vehicle has as advantages that it does not require any personnel operating the vehicle, there is no need to design a cabin for someone, and the chance of mistake when in operation is lower compared to a human controlled vehicle. This latter is especially important for complex manoeuvres. However, the disadvantages are the cost, the design complexity, and potentially the weight of the extra hardware. Also, a machine is not able to handle an unknown situation as a human can, which can have negative consequences. The cost includes the purchase cost but also the maintenance cost, extra energy cost, and insurance cost. As a general rule, automation is used when it allows a system to perform better.

When the vehicle is moving, there are no advantages in it being autonomous. This step is not performed better when done by a computer. Therefore, no automation is needed here. However, when coupling and decoupling, it being a complex step that requires a high precision, automation is an important advantage. The operator will drive the vehicle to certain position with respect to the landing gear and by the click of a button, the coupling is done autonomously. The decoupling is also performed by the click of a button by the operator of the vehicle. The vehicle is driven back to the charging station or the next aircraft by the operator.

Lastly, having the pilot controlling the vehicle during taxiing has the disadvantage that a training must be made available. However, it was decided that having the pilot steering the vehicle is still

the better option mainly because the pilot performs taxiing as well as a computer would do it, if not better. For example, depending on the weather condition, the pilot might decide to taxi at a lower speed which the computer would probably not be able to sense. Also, if the system is not certified to be fully reliable (or nearly fully reliable), safety reasons also play a role in the decision not to have autonomous taxiing. Only one little bug can result in catastrophic consequences. For example, if one order from the aircraft traffic control is neglected, there is a risk of collision.

4.8 Taxi Performance Model

In order to evaluate the operational performance of RETS, a taxi simulation was developed. Build on the preliminary model that was used to trade-off different designs in the mid-term report [1], a more detailed model was conceived. It included a more accurate acceleration and velocity profile, pushback, coupling, and different profiles for taxi-in and taxi-out. In order to check the operational performance of the system, an average and a limit case were modelled. The average case is the baseline taxi-route, as explained in subsection 4.5.7. The limit case in length and time is based on the route to the Polderbaan as shown in Figure 4.11.As this is one of the longest taxi routes in the world (7.8 km for this specific route), it is a good representation of a limit scenario to verify requirement TLREQ-01, and to calculate the energy required for a typical cycle. Also a very short route (Gate D28- runway 24) was analysed as the shorter limit case. This stretch was only 400 meters long.

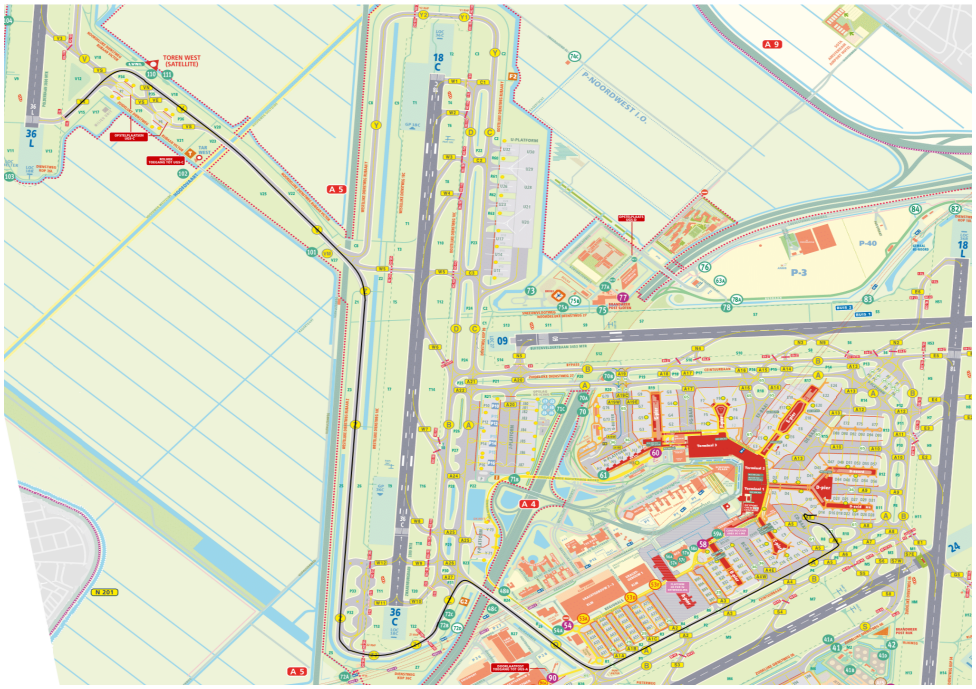

Figure 4.11: Limit taxi route at Amsterdam Airport Schiphol.[Based on [33]]

The taxi simulation also includes a model of an aircraft that is taxiing on engine power. An average acceleration of 0.7 m s^{-2} was set over the range of 0 to 30 kts. In this acceleration profile the effects of engine spool up time of approximately 8 s [34] were taken into account as well. The acceleration profile of RETS was based on the effective acceleration data as specified in subsubsection 5.4.8.1. The pushback speed was determined to be 3 kts[35]. Before showing the results of the taxi simulation, the most important assumptions made are listed in Table 4.4

[33] https://www.schiphol.nl/nl/operations/pagina/plattegronden/[cited 12 May 2020]
[34] https://eu.usatoday.com/story/travel/columnist/cox/2018/01/21/ask-captain-what-does-mean-spool-engines/1046488001[accessed on 9 June 2020]
[35] https://aviation.stackexchange.com/questions/47299/what-is-the-speed-during-push-back[accessed on 22 June 2020

Table 4.4: The primary assumptions that are of importance to interpreting the taxi simulation.

Assumption	Value	Expected influence w.r.t real world ops.	Comment
Traffic hold up	0 seconds	Energy consumption: Under-estimated	Hold ups significantly increase the time that the APU and diesel motor should run.
Traffic hold up	0 seconds	Operatinal compatability: Under-estimated	Due to hold-ups, the effect of high top-speed and de-coupling at the runway become less significant.
Top speed	30 kts	Moderate	Modelled taxi is faster as pilots do not always taxi at max speed.
Acceleration application	Maximum. Value is profile dependent	High	For segments in the taxi route that turns follow up, a pilot would never accelerate fast and brake fast due to passenger comfort. This was too complex to model
Power distribution	No regenerative braking	Energy consumption: Under-estimated	Regenerative braking can slightly reduce the energy consumption. It is however not included in the model due to a lack of data.
Coupling time	40 s	Conventional: under-estimate	Conventional push-back has coupling times that can at fastest be 40 seconds.
Speed in corners >90 degrees	10 kts	Over-estimate	This is a speed constrain set by ICAO. However pilots most certainly will drive slower for passenger comfort
Speed in corners >30 degrees	15 kts	No significant difference	In the more shallow turns, pilots can and will drive faster in order to reduce brake wear and passenger discomfort.
Speed in corners <30 degrees	20 kts	No significant difference	In very shallow turns, pilots can and will drive faster in order to reduce brake wear and passenger discomfort.

The most critical case with respect to operational implementation is the Taxi-in phase for a long taxi-route. In this case, the RETS equipped aircraft has to couple around the runway exit, while conventional taxi procedures can proceed to taxi immediately. The results are shown in Figure 4.12. As clearly visible, RETS is slower than conventional taxi operations. It arrives 46.5 seconds later at the gate. However most of the delay can be contributed to coupling. Because the time-loss is less than 60 seconds, the system is compliant with requirement TLREQ-01.

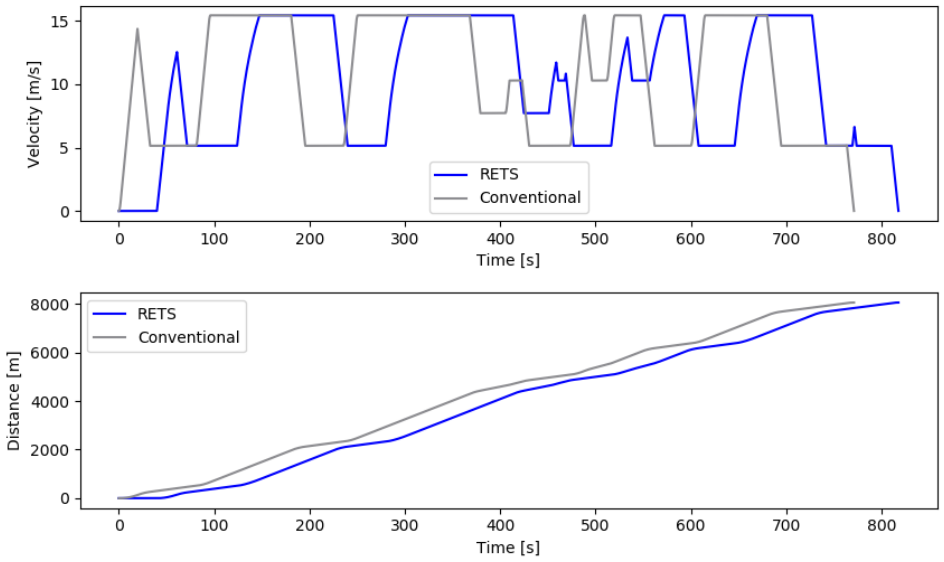

Figure 4.12: Velocity and distance profile for the taxi route Polderbaan to gate D-14.

With respect to more general operations, this case is not very representative. As explained in subsection 4.5.4, the average taxi time and distance is much lower. Therefore, to properly check operational compatibility the baseline taxi-route is analysed as shown in Figure 4.13.

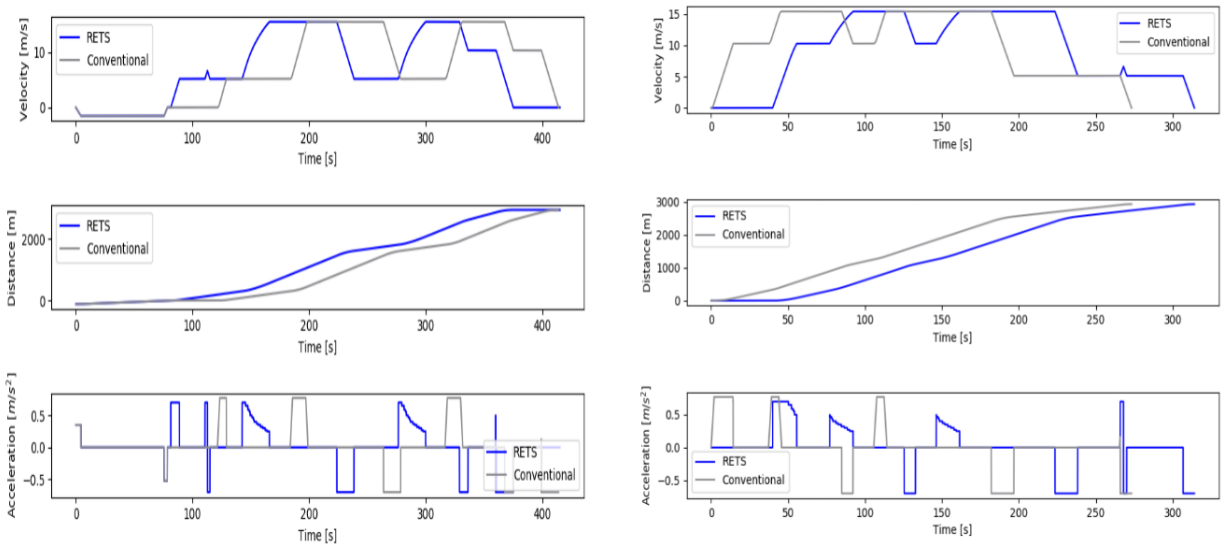

Figure 4.13: Baseline taxi-route model. Left: Taxi-out velocity, distance and acceleration diagrams. Right: Taxi-in velocity, distance and acceleration diagrams.

For taxi-out, RETS is only 1.14 seconds slower. There is a negligible operational loss. However for taxi-in, again coupling is causing a delay of 40.82 s according to the simulation. Of course, given the assumptions mentioned in Table 4.4, this value can not be interpreted with the significance it is calculated. However the general difference with respect to conventional taxiing is clear from the figures produced. What needs to be further assessed however is the effect of (de-)coupling near the runway. This takes approximately 40 seconds. This is theoretically within the departure and arrival separation intervals that are applied by air traffic controllers. The lowest wake turbulence optimisation pair is already giving a required time based separation of 100 s [36]. Given the 40 seconds (de-)coupling time the aircraft has sufficient time to decouple when it arrives at the runway. It can do so while waiting for the call to line-up. A queue at the runway helps, as it gives even more time for this process, and allows the aircraft to do engine start-up later in the taxi phase. Hence, busy airports are more beneficial for the operational implementation. When analysing landing and taxi-in, the aircraft needs to couple when it has left the runway. Again, in theory the estimated 40 seconds of coupling time should be enough to couple before the next aircraft comes in, as the same separation holds for landing aircraft. Runways usually have more than one exit, so in case coupling takes longer than anticipated, the following aircraft is likely to be marginally hindered by the RETS-equipped aircraft. However, blocking runway exits can introduce slight safety concerns for emergency situations. Especially when RETS is widely implemented, runway blocking due to coupling delays should be further investigated. This is however very airport specific. For now, because the product has not been launched, and is not expected to be introduced on a large scale from the beginning, it is not deemed necessary to research this potential safety concern in this design phase. The same holds for the airport capacity reduction, which is really dependent on the airport of application. For now, based on the model data analysis, it can be concluded that the system can be implemented without big capacity reductions. This is however only the case when the external vehicle can use the service roads to arrive or depart from the (de-)coupling point near the runway. Some airports might need to invest in this infrastructure when they implement the system.

At last, a very short route was modelled. This is a route at Schiphol airport from Gate D28 to runway 24 at only 400 meters long. For this instance, also the performance of an operation on only the internal motors powered by the APU is shown. The results look promising as can be seen in Figure 4.14. Full RETS operations arrives a second earlier at the runway. The internal motors

[36] https://www.skybrary.aero/index.php/RECAT_-_Wake_Turbulence_Re-categorisation [accessed on 19 June 2020]

operation arrives 32 s later, which still meets the requirements. The only downside however lies in the engine warm-up time. Rated at 2 min, the effective emission reducing taxi phase is only in the range of 1 min. As a result, the benefits of using the system on such short taxi routes are not weighing up to the downsides. However the simulation does show the possibilities of using the system without external vehicle.

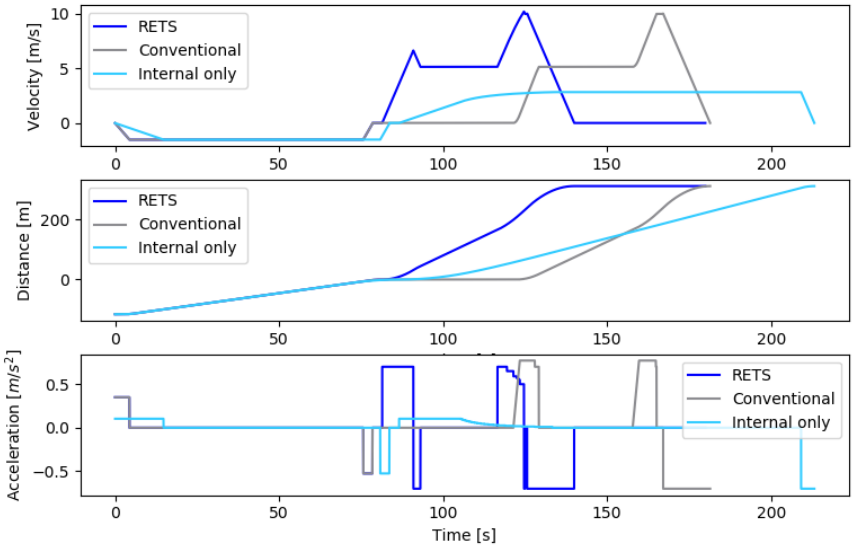

Figure 4.14: Taxi out for the short limit route (D28-runway 24). Also the performance of the internal engine operation has been included.

4.9 Fuel Reduction Simulation

The fuel reduction simulation is used to calculate the total fuel savings of the RETS-system for a conventional taxi route. This conventional/baseline taxi route is stated in subsection 4.5.7. In subsection 4.9.1, the mission profile is stated. For this mission profile, the onboard burned fuel is calculated for both conventional engine-based taxiing as well as taxiing with the RETS-system. For a specific range and an added internal weight of the RETS-system, this will result in an onboard fuel saving. The results will be presented in subsection 4.9.3. The RETS-system however also introduces savings during pushback. Moreover, the extended use of the APU brings along additional fuel consumption. Lastly and most importantly, the RETS-system itself uses diesel fuel and energy from the battery. This all will be explained in more detail in subsection 4.9.4. The final savings will be stated in subsection 4.9.5.

4.9.1 Mission Profile

In order to calculate the fuel burned, it is required to define the mission profile. The total mission consists of the following phases:

1. Engine start and warm-up
2. Outbound taxi
3. Take-off
4. Climb
5. Cruise
6. Loiter
7. Descent
8. Landing, inbound taxi and shut-down

It must be noted that in case the RETS-system is used, phase 1 and 2 will be switched. Engine start and warm-up will take place after outbound taxiing. The order has however no influence on fuel burn, as it is still before take-off.

4.9.2 Onboard Fuel Weight Estimation

The fuel weight consists out of fuel used during mission and fuel reserves required to perform the mission. In this mission profile, the fuel reserves are accounted for in the loiter phase. The mission fuel weight is estimated using the fuel-fraction method. These fuel-fractions are the ratio of the end weight to begin weight of each mission phase. Most of the fractions are determined by using statistics, although when available, using real data is preferred. [18, p. 20] Therefore it is decided to not use fuel fractions for phase 1, 2 and 8. Instead, the fuel burn is calculated using other methods. The fuel intensive flight phases, which in this mission profile are cruise and loiter, are calculated using Breguet's range and endurance equations. In the upcoming paragraphs, all fuel-fractions for both with and without RETS-system are discussed. In last paragraph, the method how to calculate the onboard fuel and the burned fuel during mission is described.

4.9.2.1 Phase 1: Engine start and warm-up

For phase 1, the engine start and warm-up, the engine start-up takes up approximately 2 min [37] and engine warm up time is between 3 and 5 min as described in subsection 4.6.2. An average warm up time of 4 min was chosen for the simulation.

Khadilkar found using Flight Recorder Data from an A321 that the Fuel Burn Index for the taxi phase was 0.12 kg s^{-1} per engine [19, p. 4]. Having two engines operable, this gives a Fuel Burn Index of 0.24 kg s^{-1}. The Fuel Burn index was validated by data of the International Civil Aviation Organization (ICAO). It is assumed that the Fuel Burn Index of phase 1 is similar to the taxi phase. This would lead to a fuel consumption during engine start and warm-up of 86 kg.

Using the engine pre-heating system of the RETS-system described in subsection 4.6.2, the engine warm-up can be partly performed electrically. It is assumed that with the pre-heating system, the engine based warm up time can be reduced by 50%, leading to an engine warm up time of 2 min. This results in a fuel saving of 29 kg.

4.9.2.2 Phase 2: Outbound taxi

For the outbound taxi, a taxi-out time of 19 min 29 s was chosen. This is the average taxi-out time of the four given taxi-out times given in subsection 4.5.4. In this taxi-out time, 6 min is accounted for pushback. A pushback time of 6 min was found to be an average pushback time for medium-sized aircraft using KLM push back time values [20, p. 21].

For the remaining 13 min 29 s, a Fuel Burn Index of 0.24 kg s^{-1} is used. This leads to an average fuel consumption for outbound taxing of 194 kg.

With the RETS-system this phase could entirely be performed electrically and therefore fuel consumption of the engines with RETS-system can be assumed to be 0 kg.

4.9.2.3 Phase 3 and 4: Take-off and Climb

For take-off and climb a fuel-fraction, $\frac{W_3}{W_2}$ and $\frac{W_4}{W_3}$, of 0.995 and 0.980 respectively is obtained from Roskam [21, p. 12].

4.9.2.4 Phase 5: Cruise

As mentioned, for the fuel intensive flight phase cruise the Breguet's range equation is used as a more analytical approach. The Breguet's range equation is given in Equation 4.2 for a jet driven aircraft.

$$R = \left(\frac{V}{g \cdot SFC}\right)_{\text{cruise}} \cdot \left(\frac{L}{D}\right)_{\text{cruise}} \cdot \ln\left(\frac{W_4}{W_5}\right) \tag{4.2}$$

[37] https://www.aeronewstv.com/en/lifestyle/how-it-works/3323-how-do-you-start-an-airliner.html#:~:text=The%20compressed%20kerosene%2Dair%20mixture,procedure%20is%20the%20most%20common. [accessed on 17 June 2020]

In order to use Equation 4.2, the performance parameters V_{cruise}; SFC_{cruise} and $\left(\frac{L}{D}\right)_{\text{cruise}}$ need to be determined. A cruise speed of 231.5 m s^{-1} and a Mach number of 0.79 was found for the A321neo. [38] The A321neo has two engine options, the CFM International's LEAP-1A and the Pratt & Whitney's PurePower PW1100G-JM. [39] The specific fuel consumption, SFC, of the LEAP-1A is during cruise between 0.53 and 0.56 lb lbf^{-1} h^{-1}. [40] The specific fuel consumption of the PurePower PW1100G-JM is not known, however the PW1431G, which is part of the same family engines, has a specific fuel consumption between 0.52 and 0.53 lb lbf^{-1} h^{-1} for cruise [22, p. 21]. The PW1100G-JM is a newer version engine and given the SFC_{cruise} between 0.53 and 0.56 lb lbf^{-1} h^{-1} for the LEAP-1A, a SFC_{cruise} of 0.54 lb lbf^{-1} h^{-1} was chosen as average for all A321neo. This responds to a specific fuel consumption of 1.53×10^{-5} kg N^{-1} s^{-1}.

For maximising range, the lift over drag ratio for cruise, $\left(\frac{L}{D}\right)_{\text{cruise}}$, can be calculated using Equation 4.3 [18, p. 39].

$$\left(\frac{L}{D}\right)_{\text{cruise}} = \frac{3}{4}\sqrt{\frac{\pi A e}{3C_{D_0}}} \tag{4.3}$$

In here, C_{D_0} is the parasite (or zero lift) drag coefficient; A is the effective wing aspect ratio and e is the Oswald span efficiency factor. The parasite (or zero lift) drag coefficient and the factor πAe during cruise are determined using Base of Aircraft DAta (BADA) of Eurocontrol Experimental Centre. This is an Aircraft Performance Model (APM) applicable for simulations of aircraft trajectory and predictions within the domain of Air Traffic Management. For the given Mach number of 0.79 during cruise, a C_{D_0} of 0.0231 and 31.68 for the factor πAe was found. Using these two values, a $\left(\frac{L}{D}\right)_{\text{cruise}}$ of 16.0 was determined.

Now the performance parameters are calculated, the fuel-fraction, $\frac{W_5}{W_4}$, can be calculated for a certain range.

4.9.2.5 Phase 6: Loiter

In this mission profile, the fuel reserves are accounted for in the loiter phase. The minimum amount of fuel reserves is specified by airworthiness regulations and consist out of alternate fuel, contingency fuel and final reserve. The International Civil Aviation Organisation (ICAO) stipulates in section 4.3.6.3 that enough alternate fuel is required to fly 15 min at holding speed at 1500 ft without a destination alternate aerodrome. This can be seen as a bare minimum. Normally, the alternate fuel is equal to the fuel needed to reach alternate. As this differs for every flight route, it was assumed for now that no destination alternate was needed and 15 min at holding speed at 1500 ft is sufficient. For contingency fuel, it is either required to have 5% trip fuel or flying 5 min at holding speed at 1500 ft. Lastly, the final reserve is accounted for by 30 min at holding speed at 1500 ft by regulations [23, p. 4-7]. Concluding the aircraft should be able to loiter 50 min at holding speed at 1500 ft.

For this fuel intensive flight phase, the Breguet's endurance equation is used as a more analytical approach. The Breguet's endurance equation for jet driven aircraft is given in Equation 4.4.

$$E = \left(\frac{1}{g \cdot SFC}\right)_{\text{loiter}} \cdot \left(\frac{L}{D}\right)_{\text{loiter}} \cdot \ln\left(\frac{W_6}{W_5}\right) \tag{4.4}$$

[38] https://www.skybrary.aero/index.php/A321 [accessed on 16 June 2020]
[39] https://www.airbus.com/aircraft/passenger-aircraft/a320-family/a321neo.html#neo [accessed on 16 June 2020]
[40] https://leehamnews.com/2015/01/19/fundamentals-of-airliner-performance-part-6-the-engine/ [accessed on 16 June 2020]

In Equation 4.4, E is the endurance in seconds. In contrary to Equation 4.2, now $\left(\frac{L}{D}\right)_{loiter}$ and SFC_{loiter} instead of $\left(\frac{L}{D}\right)_{\text{cruise}}$ and SFC_{cruise} are used. Here $\left(\frac{L}{D}\right)_{loiter}$ is the aerodynamic efficiency for maximum loiter time and can be estimated by Equation 4.5 [18, p. 41].

$$\left(\frac{L}{D}\right)_{\text{loiter}} = \left(\frac{C_L}{C_D}\right)_{\text{loiter}} = \frac{\sqrt{\pi A e C_{D_0}}}{2C_{D_0}} \tag{4.5}$$

Both the parasite drag coefficient, C_{D_0}, as well as the factor πAe are now different, because of different speed and attitude. Here again, A is the effective wing aspect ratio and e is the Oswald span efficiency factor. Loiter takes place at holding speed at 1500 ft. Holding speed can be assumed to be half the cruise velocity [24, p. 440], leading to a holding velocity of 115.8 m s^{-1}. Given the speed of sound at an altitude of 1500 ft, a Mach number of 0.34 was calculated for holding speed. Using the Aircraft Performance Model described in subsubsection 4.9.2.4, a C_{D_0} of 0.0196 and 25.94 for the factor πAe was found. Using these two values in Equation 4.5, a $\left(\frac{L}{D}\right)_{\text{loiter}}$ of 18.2 was determined.

No information could be found about the specific fuel consumption during loiter, SFC_{loiter}, for either the Leap 1A as well as the PW1100G-JM. However using Roskam, a trend of 20% decrease with respect to SFC_{cruise} was found for similar SFC_{cruise} magnitudes. Therefore a SFC_{loiter} of 0.42 lb lbf^{-1} h^{-1} was chosen.

Now the performance parameters are calculated and given the minimum of 50 min of loitering at holding speed at 1500 ft, the fuel-fraction, $\frac{W_6}{W_5}$, can be calculated using Equation 4.4. This resulted in a fuel-fraction of 0.981.

4.9.2.6 Phase 7: Descent

For phase 7, descent, a fuel fraction, $\frac{W_7}{W_6}$, of 0.990 is obtained from Roskam [21, p. 12].

4.9.2.7 Phase 8: Landing, inbound taxi and shut-down

Similarly to phase 2, the outbound taxi, it was chosen to not use a fuel fraction for this phase. Instead, a more representative fuel calculation is used. It is assumed that fuel burned during landing and inbound taxi are the main contributions to the fuel burn of this phase. The fuel burn during engine shut-down is assumed negligible. For the landing phase, a constant fuel burn of 125 kg is found for the A321 [25, p. 4]. For the inbound taxi, a taxi-in time of 9 min 29 s was chosen. Similar to the taxi-out time, this is again the average of the four given taxi-out times given in subsection 4.5.4. Of these 9 min 29 s, 3 min is reserved for engine cool down time. [41] During the 9 min 29 s, again a Fuel Burn Index of 0.24 kg s^{-1} is assumed. This results in a average fuel consumption of inbound taxiing of 136 kg. Therefore the total fuel consumption for this phase for engine-based taxiing is assumed to be 261 kg.

The fuel consumption during inbound taxiing can be reduced with the RETS-system implemented. Of the 9 min 29 s taxiing, 3 min is reserved for engine cool down time. For these 3 min, taxiing should be performed with engines on. The remaining 6 min 29 s can be performed with the engines off and using the RETS. This leads to a fuel consumption for phase 8 of 168 kg, which is a reduction of 93 kg compared to engine-based taxiing.

4.9.2.8 Onboard Fuel Weight and Fuel Consumption Mission Profile

For the onboard fuel weight estimation, first the fuel fractions will be multiplied with each other, as given in Equation 4.6.

$$M_{ff} = \frac{W_3}{W_2} \cdot \frac{W_4}{W_3} \cdot \frac{W_5}{W_4} \cdot \frac{W_6}{W_5} \cdot \frac{W_7}{W_6} \tag{4.6}$$

[41] https://blog.openairlines.com/engine-out-taxi-in-eoti [accessed on 17 June 2020]

The take-off weight, the weight after phase 2, can be determined by Equation 4.7.

$$W_{\text{TO}} = \frac{\text{OEW} + W_{\text{payload}} + W_{\text{fuel}_{\text{landing}}}}{M_{\text{ff}}} \tag{4.7}$$

Part of phase 8, namely inbound taxi and shut-down, is not taken into account for the onboard fuel calculation. This due to the reason that if no loitering or less than the 50 min loitering is required (the fuel reserve), sufficient fuel is available for inbound taxi and shutdown. In Equation 4.7, OEW is the Operational Empty Weight which is equal to 47 000 kg for the A321neo WV072 [13, p. 7-9-0]. Moreover, W_{payload} is the Payload Weight for which a Maximum Payload Weight of 28 600 kg is taken. This Maximum Payload Weight is determined by subtracting the Operational Empty Weight of the Maximum Zero Fuel Weight of the A321neo WV072 [13, p. 2-1-1]. $W_{\text{fuel}_{\text{landing}}}$ is the weight of the fuel needed for landing, which is determined to be 125 kg in subsubsection 4.9.2.7.

The onboard fuel weight at take-off can then be calculated using Equation 4.8.

$$W_{\text{fuel}_{\text{onboard}}} = (1 - M_{\text{ff}}) \cdot W_{\text{TO}} + W_{\text{fuel}_{\text{landing}}} \tag{4.8}$$

For the burned fuel during a mission profile, it is assumed that no loiter is needed. In that case, the burned fuel can be calculated using Equation 4.9.

$$W_{\text{fuel}_{\text{burned}}} = \left(1 - \frac{M_{\text{ff}}}{\frac{W_6}{W_5}}\right) \cdot W_{TO} + W_{\text{fuel}_{\text{phase},1}} + W_{\text{fuel}_{\text{phase},2}} + W_{\text{fuel}_{\text{phase},8}} \tag{4.9}$$

In Equation 4.9, $W_{\text{fuel}_{\text{phase},1}}$; $W_{\text{fuel}_{\text{phase},2}}$; $W_{\text{fuel}_{\text{phase},8}}$ are the fuel burned weight for phase 1, phase 2 and phase 8 respectively. It must be noted that the mentioned calculations are either performed using weight in N or mass in kg.

4.9.3 Onboard Fuel Savings

The use of the RETS has effect on the burned fuel for phase 1, phase 2 and phase 8. This resulted in an on board fuel saving per mission profile given in Figure 4.15. For a given added internal weight and range, this figure allows to read off the onboard fuel saving when the RETS-system is used. The reasoning about the different ranges plotted is explained in subsection 4.5.5. Summarised, the ranges represent the coverage of the A321 flights. So for example 80% of A321 flights have a range equal or lower than 2239 km. Figure 4.15 however does not take into account additional fuel savings and consumption by other systems. This will be discussed in subsection 4.9.4. The final fuel saving is presented in subsection 4.9.5.

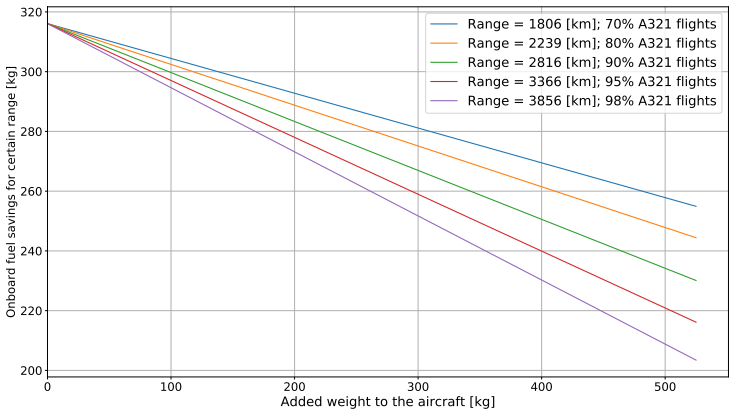

Figure 4.15: Onboard fuel saving by implementing the RETS-system for certain range and added internal weight

4.9.4 Additional Fuel Savings and Consumption

For conventional taxi operations, the aircraft is often pushed back by an external ground vehicle. A major advantage of the RETS-system is being able to perform pushback without needing the external ground vehicle. For a narrow body aircraft, the fuel consumption of conventional pushback tractors for diesel and gasoline motors is $0.231\,\mathrm{L\,BHPh^{-1}}$ and $0.337\,\mathrm{L\,BHPh^{-1}}$ respectively. Usual tractors have a brake horsepower of 175 for diesel tugs. [26] This results in a fuel consumption for conventional diesel pushback tractors of $40.43\,\mathrm{L\,h^{-1}}$. Considering the average time of 6 min that the pushback vehicle operates[42], of which 2 min are active pushback, a fuel consumption of approximately 4.0 L of diesel for conventional pushback is calculated. The energy and fuel consumption of RETS are included in the taxi simulation.

One major disadvantage of the RETS-system is the inability to supply compressed air for onboard air conditioning and engine start-up. Due to this reason, it is needed to have the APU on during the whole taxing phase. For normal taxi operations, the APU is often shut-down after engine start-up. In that case, the engines will provide the compressed air for the onboard air conditioning. The introduction of RETS will therefore lead to additional fuel burn of the APU compared to normal taxi operations. As mentioned in section 4.6, the APU has three main functions, namely providing bleed air for engine start-up; providing electrical power and providing compressed or pre-cooled air for air conditioning. During electrical taxiing, the APU only needs to supply compressed air for air conditioning and power for the internal systems. Then at the end of the outbound taxi phase, it should provide high compressed air for engine start-up. This takes generally about 2 minutes, as mentioned in subsubsection 4.9.2.1.

The A321neo has three types of APU, namely the GTCP 36-300; APS 3200 and type 131-9. Of these three types, the APS 3200 is the production standard [27, p. 21]. It is assumed that both generator and compressor are drawing around 100 kW during the taxi phase [28, p. 21]. Considering the APU-generator model made by Fabrizio for the APS 3200 [28, p. 57], this amount of APU power results in an APU fuel consumption of $0.0275\,\mathrm{kg\,s^{-1}}$. Having an outbound taxi time of 13 min 29 s, this leads to an additional fuel burn of the APU of 22.2 kg. The average inbound taxi phase takes up 9 min 29 s of which 1.5 min are reserved for engine cool down in case the engine preheating system is used. It is assumed that during engine cool down, the motors are still able to provide the compressed air and power needed. Therefore, the APU needs to be turned on for 7 min 59 s, leading to an additional fuel burn of 13.2 kg. The engine start-up will not induce extra fuel burning as the procedure is similar to conventional engine start-up. In conclusion, the usage of the RETS-system leads to an additional fuel burn of 35.4 kg.

The RETS-system itself also uses energy to complete its mission. In order to calculate the energy consumption, the taxi simulation was extended to calculate the energy consumption of the RETS-system motors and lifting mechanism to complete a single taxi cycle. Two different taxi missions have been modelled. A limit case (Gate D14-Polderbaan) which calculated the minimum energy capacity the system needed. This was used to size the batteries. This minimum cycle is a taxi-out phase (221.4 MJ), taxi-in phase (219.9 MJ), and some contingency for driving the vehicle to the pick-up point (5%). The power distribution and energy consumption for taxi-out are shown graphically in Figure 4.16. As stated in Table 4.4, the energy consumption shown here does not have reserves for when taxiing takes longer. When the batteries are sized, this should be taken into account.

[42] https://www.youtube.com/watch?v=KeG9T7Ac0e0 [accessed on 26 June 2020]

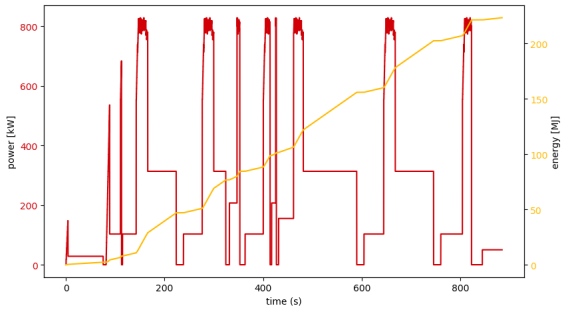

Figure 4.16: Power distribution and cumulative energy consumption for the limit scenario taxi-out.

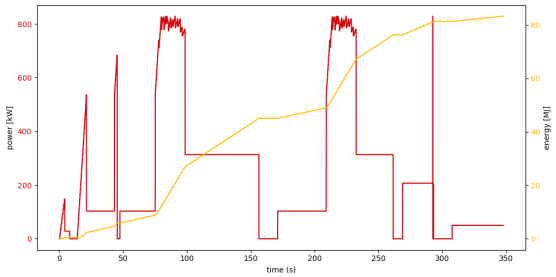

Figure 4.17: Power distribution and cumulative energy consumption for the baseline taxi-out scenario.

After battery sizing, the minimum amount of cycles was checked with the given energy consumption above, but also including the energy needed for other subsystems such as engine pre-heating, steering and sensors. It was derived that the system can do at least four cycles on battery only. The diesel engine can sustain the system for 6 cycles with a full tank, but the 4 cycles is limiting. Again, as the Polderbaan taxi route is not very representative of normal operations, the energy consumption for the baseline route taxi-out should also be included. The power distribution while driving this route, as well as the cumulative energy consumption is shown in Figure 4.17.

When adding all other systems that require power, a number of 11.4 cycles is derived before the batteries need a recharge. However, as this does not include traffic or hold ups, in practice less cycles will be possible. Therefor, the equivalent operating time is more valuable. The system is rated to operate for 126 minutes when it is performing average taxi operations. This can be stretched to almost continuous, full-day-use when the system is left attached to the aircraft at the gate. This is beneficial as the RETS-system can then charge, while also supplying the aircraft with ground power and engine pre-heating. The downside is that RETS can not be used to taxi another aircraft. This operational choice is very much depended on the situation and should be investigated by the operator.

4.9.5 Conclusion - Final Fuel Savings

The fuel saving of 4.0 L of diesel for pushback, the additional fuel burn of the APU of 35.4 kg and the fuel and electricity consumption of the RETS-system of 7.88 kg of diesel and 140.9 MJ of electricity (as calculated by the Power & Electronics department in subsection 5.4.7) are taken into account for the final fuel savings for the conventional taxi route. External vehicles used on airports will most probably work on Jet A-1 fuel. Nonetheless, the manufactures specified the specific fuel consumption for diesel. Therefore the amount of diesel used must be converted to Jet A-1 fuel. The calorific value (or specific energy) ratio of Jet A-1 over diesel is given in Equation 4.10 [43] [44].

$$\frac{\text{Calorific value Jet A-1}}{\text{Calorific value Diesel}} = \frac{43.1\text{MJ/kg}}{45.5\text{MJ/kg}} = 0.95 \tag{4.10}$$

Moreover, a calorific value of 36.9 MJ L^{-1} for diesel is used to convert the 4.0 L of diesel for pushback to kg of Jet A-1 fuel [43]. This led to a total additional fuel burn of 41.0 kg of Jet A-1. Therefore, for the final fuel saving, Figure 4.15 will be shifted by 41.0 kg downward. This led to Figure 4.18.

[43] https://www.acea.be/news/article/differences-between-diesel-and-petrol [accessed on 22 June 2020]

[44] https://www.marquard-bahls.com/en/news-info/glossary/detail/term/jet-fuel-german-kerosin.html [accessed on 22 June 2020]

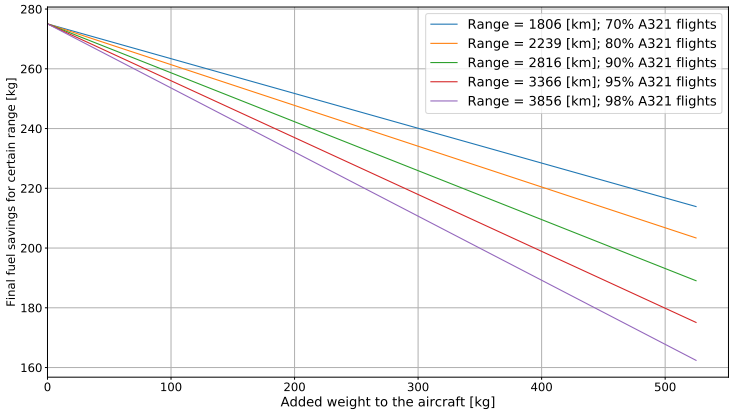

Figure 4.18: Final fuel saving by implementing the RETS-system for certain range and added internal weight

Therefore given the internal added weight of 315 kg given in subsubsection 9.1.1.1, the final saving per mission profile will be between approximately 208 kg for a range of 3856 km and 240 kg for a range of 1806 km. These ranges represent the coverage of the A321 flights, where 1806 km and 3856 km cover up to 70% and 98 % of all flight routes of the A321 respectively.

Given the airport with highest A321 movements, Tan Son Nhat International Airport (SGN), and assuming a range of 3856 km this will result in a yearly fuel saving of approximately 12 906 400 kg. This is equal to approximately 5717 flights between London Heathrow Airport (LHR) and Charles de Gaulle Airport (CDG) [29]. When a range of 1806 km is assumed (up to 70% of all A321 flights), this number will increase to approximately 6597 flights between LHR and CDG.

4.10 Verification and Validation Simulations

In this section the verification and validation of calculations made in this chapter will be discussed.

4.10.1 Verification

After carefully checking the code, calculation verification took place. To goal of this part of verification is to determine whether the numerical model does not contain any errors. For both models, the code was verified by changing data to check if the simulation behaved as expected.

For example the taxi performance model, the time step increase did not result in drastic difference, only a less refined model. Similar strategies have been executed to check the effects of different acceleration profiles, power settings and different taxi routes. The verification of the preliminary taxi model has been done in the midterm-phase, where the results were plotted to look if they made sense [1]. Moreover, the outcomes for distance, velocity and acceleration were verified by using hand calculations. For example the distance and time were compared to the average speed of the simulation.

4.10.2 Validation

4.10.2.1 Validation of Fuel Reduction Simulation

After code and calculation verification, the results must also be validated. This validation aims to match the simulated data with real-life data and explaining possible deviations. The simulation is able to calculate how much fuel needs to be taken onboard for the entire flight mission as described in subsection 4.9.1. This can be validated by looking at the Payload/Range diagram given in the A321neo manual [13, p. 3-2-1]. The A321neo WV053 has a Maximum Take-off Weight (MTOW) of 93 500 kg, Maximum Payload Weight ($M_{\text{payload,max}}$) of 26 390 kg and Operational Empty Weight (OEW) of 47 000 kg. The maximum fuel onboard for maximum payload can be calculated by

Equation 4.11.

$$M_{\text{fuel}} = \text{MTOW} - \text{OEW} - M_{\text{payload,max}} \tag{4.11}$$

This results in a maximum onboard fuel of 20 110 kg. From the Payload/Range diagram, it can be deduced that the maximum range for this payload, results in a maximum range of 4710 km. It is now possible to use this data to validate the main core of the Total Energy Reduction Simulation. Given the maximum range, OEW and $M_{\text{payload,max}}$, the simulation can calculate how much fuel needs to be taken onboard. This can be validated with the given 20 110 kg of fuel. The simulation calculated an onboard fuel of 20 382 kg, which is 1.35% off. This discrepancy can be caused by difference in performance parameters derived for each phase. It was attempted to use real data over statistics at all times. For further research, it is recommended to discard the remaining fractions that were derived using Roskam. The performance parameter $(\frac{L}{D})_{\text{cruise}}$ of 16.0 is deemed to validated by looking at the historical trend of maximum lift-to-drag ratio [30]. Moreover, the data of the Payload/Range diagram can also have some flaws. The Aircraft Characteristics & Airport and Maintenance Planning Manual is given for information only. Approved values are stated in the 'Operating Manuals' specific to the airline operating the aircraft [13, p. 3-2-1]. Therefore to increase validation accuracy, it is recommended to contact airlines flying the A321 to request more trustworthy data. Nonetheless, the 1.18% difference is deemed to be negligible and the validation data is deemed to be accurate enough for the intended use of the simulation.

In the end, the simulation was made to look at total fuel reduction possible by the designed RETS-system. For this, the largest part of the fuel reduction takes place at in and out-bound taxiing. Therefore specific attention was paid at these phases during validation. The Fuel Burn Index used for these phases was already validated by using data from ICAO. The inbound and outbound taxi-times were derived from looking at airports where most A321 fly and is also deemed to be adequate. An overall check is performed by looking at other assessment methods of fuel consumption during taxiing [4, p. 1] [5]. These sources state that aircraft taxiing takes into account up to 6% of the total fuel consumption in short-haul flights. Short-haul flights are flights that cover under 1500 km [45]. For a range of 700 km, aircraft taxiing takes into account 6.1% of total fuel consumption with the simulation. A range of 1000 km and 1500 km takes into account 5.1% and 4.1% respectively of total fuel consumption. Therefore the approximation of engine-based fuel consumption is also deemed to be validated.

4.10.2.2 Validation of taxi time simulation

After the verification of the taxi model, the model should also be validated. That is, does the calculated taxi time make sense with respect to real world operations. In order to validate the simulated times, they were compared to average taxi times [20, p. 73]. When selecting the taxi-routes for the simulation, the availability of validation data was taken into account. Unfortunately for the short taxi route Gate D28 - runway 24, no actual taxi times were found. As can be seen in Table 4.5, the simulated taxi times do show discrepancies with respect to the measured average times. However the differences can be explained, thereby validating the obtained results. The baseline taxi route shows a difference of 2.05 min, or 123 s. The difference can be explained by traffic. The measured average taxi time is taken from real-world data in which aircraft sometimes have to wait for other traffic to pass by. On the 3 km taxi distance, this can easily be in the range of 120 s of delay. This hold-up is therefore assumed to be the cause of the discrepancy. The effects of this delay are taken into account in the analysis of the outcome of the taxi model, as also explained in the assumptions (Table 4.4).

[45] https://www.caa.co.uk/Passengers/Resolving-travel-problems/Delays-cancellations/Delays/Short-haul-delays/ [accessed on 19 June 2020]

Table 4.5: Simulated taxi time versus measured average taxi time. All times are excluding pushback. [20, p. 73]

	Distance	RETS simulated time	Conventional simulated time	Measured average time
Gate D14 - 36C	2.93 km	4.53 min	4.51 min	6.58 min
Gate D14 - 36L	8.06 km	12.36 min	12.29 min	12.77 min

For the limit taxi scenario, Gate D14 to runway 36L, the taxi time difference is much less with only 0.48 min, or 29 s. This can again be related to traffic delay, however the delay is far less then compared to the two minutes delay over the shorter taxi route. A reason for this relatively small discrepancy can be related to the operational differences in taxi route to the Polderbaan, as shown in Figure 4.19. When runway 36C is in use, taxiing aircraft sometimes are directed the long north way around the runway instead of taxiing the route as shown in Figure 4.11. This route is 2.26 km longer (red route). When the runway is not in use, the aircraft can cross runway 36C resulting in a roughly 800 m shorter route (green route). This means that a lot of different routes are taken into account for the measured average taxi time. This makes the comparison of the model simulated time less representative. The last influence that can explain the difference between the model and validation data can be in the assumption that acceleration and top-speed are always maximum. In reality this is probably not the case, hence the model is slightly faster then reality. It can therefore be said that the model time is valid, as it is slightly faster than the measured time due to traffic, maximum acceleration and top-speed, and a variety of different routes that make the validation data less representative.

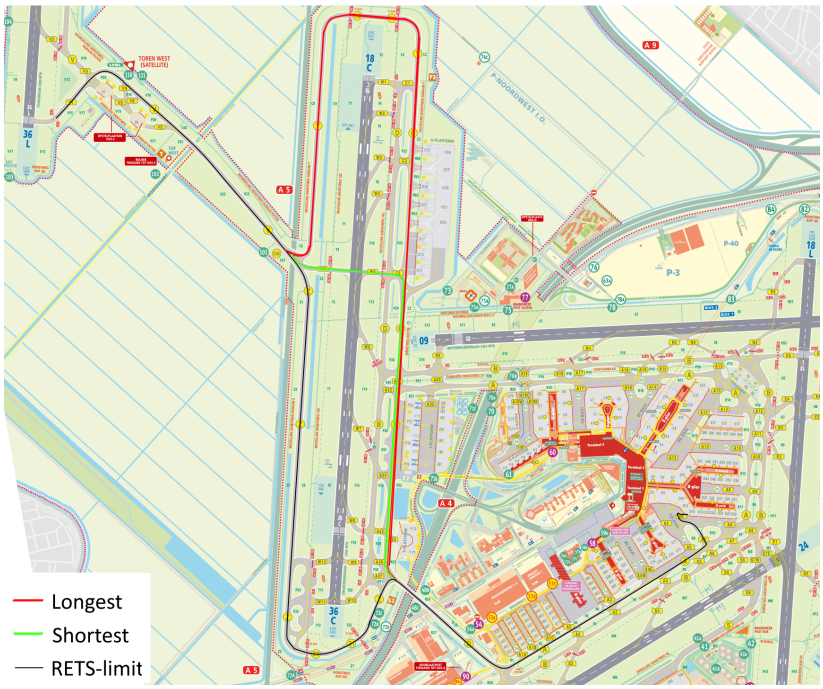

Figure 4.19: Different routes that are used to calculate average taxi time. The ratio of use-cases is not known. However it is expected that this has a considerable effect on the present discrepancy between actual taxi times and the model.

4.11 New Operational Risks

In the beginning of this chapter, several risks have already been listed in Table 4.3. As the detailed design of the operational aspects has increased the knowledge of the design specifications, new risks have been identified. These new risks will form a base for the next iteration as these must also be mitigated during the next design phase. The new operational risks are listed in Table 4.6 together with its cause, consequence and mitigation strategy. Lastly, also the pre- and post-mitigation probability of failure and consequence of failure are estimated according to Table 4.1 and 4.2.

Table 4.6: Newly identified risks related to operations

ID	Risk	Risk Cause	Risk Consequence	Mitigation	p_f/ $p_{f_{\text{mit}}}$	c_f/ $c_{f_{\text{mit}}}$
T.O.6	RETS does not reach simulated taxi times	Coupling time takes longer than 55 s	Requirement RETS-SH-TLREQ-01 not met.	Instruct operator on fast coupling procedure, optimise coupling procedure	4/3	3
T.O.7	Insufficient engine pre-heating	Temperatures too low	Higher engine temperature strain, reduced engine life	Produce better model to validate pre-heating system	3/2	4
T.O.8	RETS-vehicle can not house ASU and ACU	No space inside the vehicle or no possibility for trailer	Higher emissions as the APU has to supply bleed air	Put extra resources into this optional design	3/2	2

4.12 Sustainability

The improvement due to RETS compared to engine-based taxiing from the sustainability point of view is evident. However, using RETS in an appropriate way can make it even more sustainable. Coordinating all the external vehicles requires complicated logistics. It is important to organise the logistics in an efficient way. An external vehicle should be assigned to the closest aircraft when possible in order to avoid wasting energy because the external vehicle must travel for a long distance to reach it. For example, if an aircraft needs to be coupled or decoupled and the only vehicles available are far, while a vehicle nearby is about to finish its operation on an another aircraft, the best option is to wait the extra seconds until the closest vehicle is available. This might even be the fastest option and is the most sustainable one. Next to that, a redesign of the service roads network can be considered in order to have the vehicles covering shorter distances to aircraft. This is also beneficial to avoid delays due to the aircraft waiting for a vehicle. Ideally, the charging station for the external vehicles is located very close to the taxi routes.

4.13 Compliance Matrix

The compliance matrix, Table 4.7, shows if the requirements have been met. Within Table 4.7, three different options for the compliance with the requirements are present. They are: requirement met (✓); requirement requires more research (✱); requirement not met (✗).

Table 4.7: Compliance Matrix Operations

Requirement ID	Compliance	Reasoning
RETS-SH-TLREQ-01	✓	Using the TPM, it was found that for the most critical case with respect to operational implementation (taxi-in for long taxi route) the system will be 46.5 s slower.
RETS-SH-TLREQ-02	✓	The Maximum Take-off Mass was not exceeded for any of the represented cases in Figure 4.15. Moreover RETS will not take upon available space for payload, as the main part is incorporated on the main landing gear.
RETS-SH-TLREQ-06	✓	Given the final fuel savings given in Figure 4.18, it can be concluded that the total energy consumption from gate to gate with respect to engine based taxiing is decreased.
RETS-SH-REQ-01	✓	Given the final design, it can be concluded that current pushback and taxi methods can still be performed and are still effective.
RETS-SH-REQ-02	✱	For now, there are no signs indicating that the RETS-system cannot be implemented for other CS25 commercial passenger aircraft. For the final design stage a more extensive research will be conducted.
RETS-SH-REQ-05	✱	There are no signs indicating significant loss in performance over the years. More research is required.
RETS-SH-PBC-01	✓	There are no signs indicating that the operation of the RETS will be different than for example TaxiBot.
RETS-SH-INV-02	✓	
RETS-SH-GOV-01	✱	Local government legislation is dependent on the country in which RETS is sold. Compliance to this legislation is set for the following design phase.
RETS-SH-ASA-01	✱	Local Aviation Safety Agency (FAA/EASA/CAAC) compliance is set to be determined in the detailed design phase and certification phase.
RETS-SH-APC-01	✱	Operating airport legislation is dependent on the airport where RETS will operate. Compliance to this legislation is set for the following design phase, and for customer adaptation in the production phase.
RETS-SH-APC-02	✓	The TPM and the research done in the system compatibility with airport infrastructures (subsection 4.5.6) shows that this requirement will be met
RETS-SH-APC-03	✓	Redundancy: Multiple motors, emergency decouple.
RETS-SH-EMS-01	✓	The accessibility of the aircraft barely changed w.r.t. conventional pushback.
RETS-SH-EMS-02	✓	Hazards specified in the components data sheets (off-the shelf components).
RETS-SH-RES-01	✓	Noise level will be reduced by having the engines turned off.
RETS-SH-OAO-01	✓	Very feasible, given the past phase time planning and estimated future design phases.
RETS-F-GEN-05	✓	
RETS-F-OPR-01	✓	
RETS-F-OPR-02	✓	
RETS-F-OPR-03	✓	
RETS-F-OPR-04	✓	
RETS-F-OPR-08	✓	Pilot and pushback driver training is very straightforward. Operations are not very different compared to taxiing/pushback.
RETS-F-PE-15	✓	

5 Power and Electronics

The next aspect of the RETS to be addressed is the power subsystem, which shall provide the power necessary to operate the system's different components. The chapter begins with a functional, requirement, and risk analysis of the subsystem. Then, the design process is discussed. First the literature study concerning the battery choice, electric motor model and cable type is presented. After the design process of the entire powertrain is described. This is followed by a sustainability analysis of the design. Finally, verification and validation is discussed and a compliance matrix is shown.

5.1 Functional analysis

Before making design choices, it is necessary to identify the functions that the subsystem needs to fulfil. The power subsystem's primary function is to provide and transfer the necessary power for the system to operate, and is made up of the wheel-mounted motors, the batteries and engine on the external vehicle, as well as the interfaces between these and other components of the system. The power system will have two operation modes. Vehicle-powered operation will consist of the power source on the towing vehicle powering all on-board components. In case the vehicle is not available, the wheel-mounted motors have the option of being powered by the aircraft Auxiliary Power Unit (APU), allowing operation at reduced performance. Of the various APU available for the A321neo, the Pratt and Whitney APS 3200 is a production standard for the A321neo and will be used for this design [13]. An aircraft APU has many functions, including driving an on-board three-phase AC generator, outputting 90 kV A at 115 V [46]. The other power source is the external towing vehicle, which houses batteries that will power the on-board components, and a diesel engine that will power its own drivetrain. More specifically, the following aspects will require power:

- Wheel-mounted motors
- Engine preheating system
- External vehicle drivetrain
- Aircraft coupling mechanism
- Power attachment system
- Sensors
- Control unit

While some of these components will be described in later chapters, the power source must account for the power required to operate them. Depending on the voltage and current levels and type of current of each component, the connection from the power sources will require transformers, inverters/rectifiers, and proper cable design.

5.2 Risk Analysis

Similarly to the operational risks mentioned in section 4.11, the previously identified risks associated with power and electronics and their mitigation strategies will be listed. The proposed mitigation strategies will be implemented throughout the design process the design when possible. The effect of these mitigation strategies will be evaluated after the design, and the most critical remaining or new risks are discussed. Table 5.1 shows the pertinent risks and their associated causes, consequences, and mitigation strategies. The probability of failure p_f and consequence of failure c_f have been scored according to Table 4.1 and 4.2. The risks will be referred to by their identifier during the design section when applicable.

[46] https://www.pwc.ca/en/products-and-services/products/auxiliary-power-units

Table 5.1: Previously identified risks related to power and electronics

ID	Risk	Risk Cause	Risk Consequence	Mitigation	p_f/ $p_{f_{\text{mit}}}$	c_f/ $c_{f_{\text{mit}}}$
T.P.1	RETS is not able to move or too slowly	Engines not powerful enough	RETS will not be able to compete with existing taxi solutions; failure of mission	Account for safety factors; size engines/motors to compete with conventional taxi speeds; check with a taxi simulation to confirm performance is acceptable; look into traction	2/1	5/3
T.P.2	Fire/explosion	Overheating of internal wheel based engine or improper cables	Wheel based engine damaged or scrapped; aircraft must undergo maintenance; flight and airport delays	Ensure proper cooling of components; ensure components do not release harmful gases if burning; set high safety factors	2/1	4
T.P.3	Contamination of environment	Power source leak or contamination during disposal	Taxiway must be cleaned; environment is affected negatively	Design for anti-leak/liquid tight; consider end-of-life disposal procedures	2/1	3
T.P.4	Short circuit	Cables not isolated properly; Insufficient cable management	RETS failure or partial RETS failure; flight and airport delays	Use certified cables; design for cable insulation	2/1	3
T.P.5	Hill stand still	Provided power too low	RETS cannot continue; flight and airport delays	Evaluate performance on sloped runways; account for these using a safety factor	2/1	3
T.P.6	Battery damage due to charging faulty input	Wrong current or voltage	Batteries deteriorate faster or overheat, damage occurs to electrodes and breakdown of the electrolyte	Clear user document; Include sensors to detect faulty input and clear warnings on interface; document recommended charging voltages and currents	3/1	3
T.P.7	Inefficient use of RETS-system	Wheel-mounted motors and external system are not properly synchronised	Entire system is not used optimally	Implement a control unit that ensures the proper distribution of power to the wheel motors and external vehicle	2/1	3

5.3 Requirement Analysis

Besides the risk mitigation, the requirements will also be taken into account during the detailed design as they will set boundaries. Note that some mitigation strategies directly flow down into a requirement; for example, risk **T.P.1** directly induced **[RETS-F-PE-05]** up to and including **[RETS-F-PE-08]** and **[RETS-F-PE-10]**. All relevant requirements for the power and electronics subsystem have been listed below.

Stakeholder requirements

- **[RETS-SH-TLREQ-01]**: RETS taxi time shall be up to 1 minute longer than engine based taxiing.*(Performance)*
- **[RETS-SH-TLREQ-03]**: RETS shall induce a maximum increase of 2% in operational empty weight of the aircraft. *(Performance)*

- **[RETS-SH-TLREQ-06]**: RETS shall not increase total energy consumption from gate to gate with respect to engine based taxiing. *(Sustainability)*
- **[RETS-SH-TLREQ-07N]**: RETS shall use recyclable materials. *(Sustainability)*
- **[RETS-SH-ALC-02]**: The RETS shall be able to move the aircraft, under reasonable weather conditions defined in RETS-SH-REQ-04, with its weight ranging from OEW to MTOW. *(Operations)*

Functional requirements

- **[RETS-F-GEN-05]** RETS shall be compatible with an A321.
- **[RETS-F-OPR-03]** RETS shall be able to warm-up the engines.
- **[RETS-F-OPR-06]** RETS shall operate for a minimum time of 2 h without recharging/refuelling.
- **[RETS-F-OPR-07]** RETS shall operate for a minimum distance of 25 km without recharging/refuelling.
- **[RETS-F-PE-02]** RETS shall not move the aircraft at speeds greater than 31 kts.
- **[RETS-F-PE-03]** RETS shall be recharged/refuelled in 8 h.
- **[RETS-F-PE-05]** RETS shall not move the aircraft with an acceleration above 1 $\mathrm{m\,s^{-2}}$.
- **[RETS-F-PE-06]** RETS shall move the aircraft with a minimum average acceleration of 0.4$\mathrm{m\,s^{-2}}$.
- **[RETS-F-PE-07]** RETS shall not decelerate the aircraft over 1.5 $\mathrm{m\,s^{-2}}$.
- **[RETS-F-PE-08]** RETS shall be capable of a deceleration of at least 0.6 $\mathrm{m\,s^{-2}}$.
- **[RETS-F-PE-09-A]** The wheel motors shall not generate heat exceeding exceeding the temperature range specified in its manual.
- **[RETS-F-PE-09-B]** The diesel engine shall not generate heat exceeding the temperature range specified in its manual.
- **[RETS-F-PE-10]** RETS shall taxi the aircraft at a top speed of 30 kts.
- **[RETS-F-PE-11]**RETS electronics shall have a fail safe system in case of a voltage or current surge.
- **[RETS-F-PE-12]** RETS shall use a secondary power source in case the primary power source does not function.
- **[RETS-F-PE-13]** RETS shall have a secondary power source with a power of over 50 W.
- **[RETS-F-PE-14]** RETS' electrical interference shall not interfere with the aircraft's communication.
- **[RETS-F-PE-15]** RETS shall reduce the operational engine warm-up time by 30 s.
- **[RETS-F-PE-16]** RETS shall make use of aviation grade cables and connectors.
- **[RETS-F-PE-17]** The mass added to the aircraft due to the power and electronics department shall be limited to 293.6 kg.
- **[RETS-F-PE-18]** The mass added to the external vehicle due to the power and electronics department shall not cause the axle load of the vehicle to exceed 11 000 kg.

Non-functional requirements

- **[RETS-NF-LC-01]** Disposal of materials shall have no adverse effects on the environment
- **[RETS-NF-LC-02]** RETS shall include a manual with the correct recycling and disposing methods for materials.

5.4 Design and assumptions

With the associated requirements and risks in mind, the detailed design of the power subsystem can begin. Small trade-offs are performed when applicable to justify design choices. In this section, the design of the various components of the subsystem will be described.

5.4.1 Engine pre-heating

The need for an engine pre-heating system was explained in chapter 4. The design is now further developed for the power subsystem.

5.4.1.1 Induction heating

Inductive heating systems work on the the principle of electromagnetic induction. It generates eddy current flows against the resistance of metals. This generates heat in the metal. A coil should be wound around the metal to be heated. Supplying the coil with an alternating current rises an alternating electromagnetic field inside the coil that is counteracted by an electromagnetic field from the material. The resistance of the metal then produces heat. A schematic overview is given in Figure 5.1.

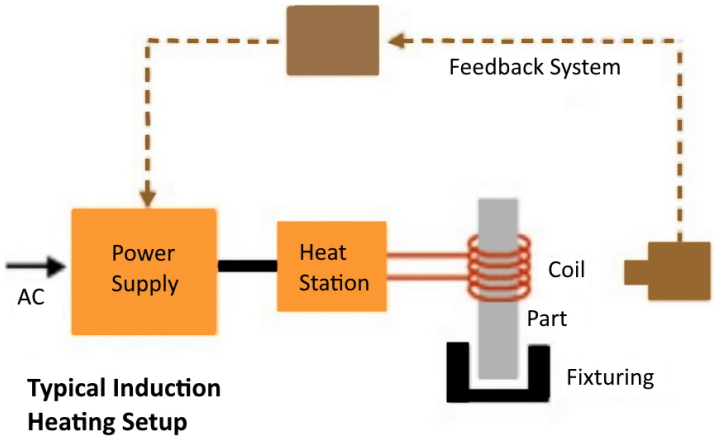

Figure 5.1: Typical Induction Heating Setup [47]

Induction heating can be applied such that the coil is twisted around the engine. The engine itself functions as the part as in Figure 5.1. The advantage is that the system does not have to be integrated into the engine itself, but in the nacelle bypass section. The nacelle is only constrained in size on the top and bottom by the wing and ground, but not on the sides, hence there is a good possibility for a retrofit. Another advantage is the fact that inductive heating can apply heat at the centre of the part. This is desirable as the centre of the engine is where the highest temperatures are reached. A downside of inductive heating is the fact that it produces an electromagnetic field. This is undesirable as it can interfere with the engine sensors and computers, as well as the aircraft sensors and computers. Furthermore, inductive heating works most efficiently in combination with ferromagnetic metals. The components of the HP compressor, combustion chamber and HP turbine are made of metal alloys that can withstand the very high temperatures and pressures, such as nickel-titanium-aluminium alloys [48]. For assumed material GMR-235 [49] contains 10% Iron and 68.4% Nickel. Both are ferromagnetic materials. However the remaining elements are non-magnetic. Hence it is uncertain if inductive heating can be properly applied. It is therefor decided not to develop the system further, but look at more conventional heating methods such as conduction heating.

5.4.1.2 Conduction heating

Conduction is the transfer of heat through solid materials. The heating is a result of internal resistance to the electrical current, known as joule heating. Conduction heating can be done by running a current through heating cables that are attached to the parts of the engine that need pre-heating. This system draws inspiration to floor heating or car-window heating. The heating cables are made of resistors that warm up when a current is run through. These can be applied on

[47] https://www.elprocus.com/induction-heating-principle-and-its-applications/ [accessed 3 June 2020]
[48] http://www.madehow.com/Volume-1/Jet-Engine.html [accessed 4 June 2020]
[49] http://www.matweb.com/search/datasheet.aspx?matguid=bbfe6976c1ec4646b98defb9157ec907 [accessed on 4 June 2020]

the engine outside, and perhaps on the inside of the combustion chamber and turbine fan blades. The first will lead to a potential nacelle redesign, while the latter most certainly leads to an engine redesign, but applies the heat closer to the more critical components. It is deemed too complicated to redesign the engine from the inside at this stage, so as a result the conductive heating elements should be retrofitted on the engine outside. The weight added is largely dependent on the resistor. Equation 5.1 and Equation 5.2 shows how the power input relates to the required resistance, where P is power in Watt[W], I is the current in amps [A], R is the resistance in Ohm [Ω] and V is the potential difference in Volts [V].

$$P = I^2 R \tag{5.1}$$

$$P = I \cdot V \tag{5.2}$$

$$P = \frac{E}{t} \tag{5.3}$$

The energy to reach the required warm up level was calculated to be 146.5 MJ. Given Equation 5.3, the power could be calculated for a specified warm-up time. With Equation 5.1 & Equation 5.2, the combinations for voltage, resistance and current could be established. The combination was chosen such that cable weight would be minimised and voltages are low. The resistor mesh is marginally insulated because it needs to transfer heat. This causes short circuit threats, so the voltage was also minimised. The potential difference was set to be 115 V, the current is 535 A and the resistivity of the wire is 0.29 Ω. The resistance has to be provided by wiring, which is optimised for transferring heat onto the engine. This means a large contact area on the engine side, and good heat insulation on the outside. The total resistance of a wire can be calculated with Equation 5.4 with ρ the specific material resistance [Ω m], l the length of the wire [m], and A the wire cross-sectional area [m^2].

$$R = \rho \frac{l}{A} \tag{5.4}$$

The length of the wiring is primarily important to create a surface area around the engine to transfer heat. For now, the sizing of the system is based on the assumption that a solid 1-D block of material is heated with a constant temperature difference on the edges. The heat transfer could be calculated with Fourier's law (Equation 5.5). Based on this heat transfer, it could be checked if the resistor does not overheat or melt with the calculated dimensions. In Equation 5.5, Q is the heat inserted [W], Δt the time over which the heat was dissipated [s], k the engine material conductivity [$W\,m^{-1}\,°C^{-1}$], A the heated surface area [m^2], ΔT the difference in temperature of the material ends [°C] and Δx the length of the material [m].

$$\frac{Q}{\Delta t} = -kA\frac{\Delta T}{\Delta x} \tag{5.5}$$

With Equation 5.5, the energy that was dissipated from the resistor could be calculated. The energy input is known, given the potential difference, current and Equation 5.2. The temperature increase of the resistor could then be calculated by Equation 4.1. This is not allowed to exceed the operating temperature of the resistor. Three different resistor materials have been evaluated that could realise the engine warm-up requirement. Many iterations were needed to arrive at the most optimal system. The final input variables are shown in Table 5.2. The system with the lowest weight is made out of Molybdenum Disilicide. The structures and materials department has checked the availability, manufacturability and sustainability of the material, with a positive outcome. However in the design of the system, many assumptions have been made. They are listed in Table 5.3

Table 5.2: Variables set for the engine pre-heating system sizing.

	Molybdenum Disilicide [50]	**Nichrome V**[51]	**Silicon Carbide** [52]
Resistivity [Ω-m]	$4 * 10^{-}8$	$1.08 * 10^{-}6$	$2.02 * 10^{-}6$
Wire radius [mm]	2.26	7.3	9.6
Density [kg/m^3]	6290	8414	4840
Operating temperature [$^{\circ}C$]	1700	1150	1600
Specific heat [J/kg$^{\circ}C$]	430	448	650
Wire length [m]	116.33	44.91	22.93
System weight [kg]	**23.48**	**126.54**	**64.27**

Table 5.3: The primary assumptions that are of importance to the sizing of the engine heating system. The overall expected effect of the assumptions is that the system is over-designed. In future iterations, weight can be reduced as well as power.

Assumption	**Value**	**Expected influence**	**Source/comment**
Definition of warm up	550 $^{\circ}C$	Uncertain	Based on turbine and compressor air temperatures Figure 4.10.
Engine elements to warm-up	15 % engine weight	Over-designed	-Based on advise by Dr. Ir. W.P.J. Visser -Combustion liners and High pressure turbine blades.
Engine warm-up time	40 min	Under-designed	-Based on turn-around times [3] - Turn-around times can be shorter. So not full benefit is obtained.
Total resistance	0.29 Ω	-	Based on system voltage
1-D solid material Fourier's Law (Δx)	HP-turbine radius 0.35 meter	Over-designed	-Based on engine dimensions [15] -More material heated then actual, as it is modelled as a solid block.
1-D solid material Fourier's Law (ΔT)	Temperature gradient at 550$^{\circ}C$	Over-designed	-The final temperature gradient is less beneficial to transfer transistor heat. This was chosen to account for the bad transfer of heat in the engine, as it was designed to not overheat.
Engine made entirely of GMR-235	- ρ 7700 kg/m^3 - C_p 460 $\frac{J}{kgC}$ - k 25 $\frac{W}{mC}$	-Uncertain -Uncertain -Under-designed	-Based on GMR-235 application and specification data [53] -The thermal conductivity is too high (under-designed) as turbine blades have heat coatings. The effect is however low as the heat can be applied below the coating.

5.4.2 Motor design

The taxi system calls for a set of electric motors to be mounted on the landing gears, to be powered by either the aircraft APU or batteries from the external vehicle, depending on the operation mode. While the specifications of these motors will be based on further requirements and calculations, some characteristics can already be explored and decided. In this subsection, decisions for the number of motors used, type of motor, and type of drive used are discussed in small trade-offs. Note that options are evaluated holistically rather than with criterion weights; this is done for simplicity, but also to account for potential design iterations.

First, a decision must be made for how many wheels in the landing gear to power; there is a possibility to have either one or two motors per landing gear as some motors also allow for motor stacking. Table 5.4 shows the advantages and disadvantages of each choice. Having one motor per landing gear poses advantages in terms of weight, complexity, structural integration, and also likely allows sufficient airflow for brake cooling. Using two motors per landing gear, while adding complexity to the system, also provides some redundancy; if one motor fails, he system can still be operational. Considering these factors, it is chosen to use one motor per landing gear.

Table 5.4: Number of motors choice

	1 motor per landing gear	2 motors per landing gear
Advantages	Less complex Less weight	Redundancy built in
Disadvantages	Single larger motor required No redundancy	Added complexity Integration problems (limited space) Added maintenance

Next, the choice between a direct drive and clutch/gearbox configuration must be made as it will effect the motor sizing process. The advantages and disadvantages of these options are explored in Table 5.5. A direct drive configuration offers a more robust, reliable, and simple solution, but may require a stronger motor. Having a gearbox and clutch will also require additional space in the landing gear structure and be inherently more complex. A direct drive configuration is therefore preferred, using gears to reach the required torque.

Table 5.5: Landing gear motor drive type [28]

	Direct drive	Drive + gearbox
Advantages	More reliable/robust No gearbox weight added	Lighter motors possible
Disadvantages	Heavier, high-torque motor needed	Added gearbox weight Integration problems in the landing gear and wheel rim. Space constraints. More complex, less reliable

The main parameters of interest for a motor type is the power and torque densities, as well as the rated peak power and peak torque. For the selection, some electric motor types commonly used in electric vehicle applications are considered, namely AC induction motors, brushless DC motors (BLDC), and permanent magnet synchronous motors (PMSM). For this application, power and flux densities are of great importance since the system should add as little weight to the aircraft as possible. As such, permanent magnet motors are considered, specifically the axial flux motor configuration. Compared to radial flux motors and other types of electric motors, axial flux motors typically exhibit increased efficiencies, reduced length/mass, and require fewer resources to manufacture [54].

5.4.3 Battery choice

For the choice of battery, four types commonly used in aerospace and electric vehicle applications are considered: nickel-cadmium, lead-acid, lithium-ion, and nickel-metal hydride batteries. These battery types are compared in multiple aspects, using reference values where available; some values will therefore change depending on the battery size and efficiency. Favourable characteristics include high specific energy and power, and the ability to be recycled efficiently. Since ranges of values for specific energy and power are possible, these are presented as a plot in Figure 5.2. For the final battery choice, risks **T.P.3** and **T.P.6** also need to be accounted for by incorporating their mitigation strategies. The comparisons of other considerations are summarised in Table 5.6, and each battery type will also be individually addressed.

[54] https://www.powerelectronics.com/markets/automotive/article/21864194/axialflux-motors-and-generators-shrink-size-weight [cited 20 June 2020

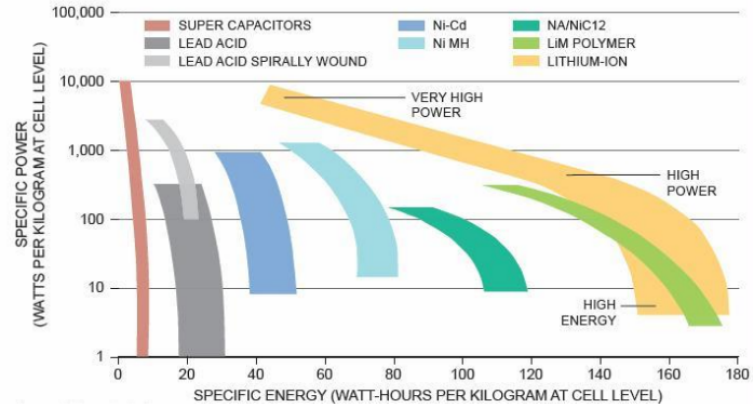

Figure 5.2: Comparison of specific energy and specific power of battery types [31]

Table 5.6: Battery characteristics [55] [32]

	Nickel cadmium	Lead acid (VRLA)	Lithium-ion	Nickel metal hydride
Charge time (hrs)	1-2	8-16	1-4	2-4
Self discharge rate (%/month)	5	17	2	30
Maintenance interval	30-60 days	3-6 months	Low maintenance; no scheduled cycling required.	60-90 days
Costs (USD, reference)	50	25	100	60
Recyclability	NiCd contains toxic metals that some countries limit the use of	The electrolyte and lead content can cause environmental damage. Restrictions on transport	Metals used (cobalt) harmful to environment. Research indicates 80% can be recycled	Only mild toxins. Profitable for recycling
Safety	Thermally stable. Fuse protection needed.	Thermally stable	Protection circuit needed to limit peak voltage while charging.	Risk of hydrogen gas forming when overcharged.
Other	Durable and forgiving. Can store at any state of charge. Has memory effect.		No memory effects. Aging effects. Different types exist.	Needs to be fully discharged in storage.

Nickel-cadmium Nickel-cadmium (NiCd) battteries are known for their robustness and performance under rigorous conditions. As such, they can operate in a wide range of temperatures and can be stored in any state. However, NiCd batteries are largely overshadowed by nickel-metal

[55] https://batteryuniversity.com/learn/archive/whats_the_best_battery [cited 11 June 2020]

hydride batteries due to the lower specific energy and energy density of NiCd batteries. This, in combination with unfavourable recycling characteristics, make NiCd batteries a sub-optimal choice for the system [55].

Lead-acid Valve-regulated lead-acid batteries (VRLA) are a type of lead-acid battery that eliminate the need to regularly check the electrolyte (typically sulphuric acid) levels. Manufacturing is simple and inexpensive. Additionally, maintenance intervals are low when using VRLA batteries. The main limitations of this type of battery include the low energy and power densities compared to the other types, and the difficulty in recycling; the contained lead and electrolyte present risks of environmental damage. Additionally, some restrictions exist on the transportation of lead-acid batteries due to the risk of spillage [55].

Lithium-ion Lithium-ion (Li-ion) batteries provide the largest specific energy and power values, making them ideal when mass is to be minimised. In addition, battery maintenance is low compared to the other battery types, not requiring any scheduled cycling. Storage is also easy, with a low self discharge rate and no memory effects. In terms of recyclability, lithium-ion cells cause minimal environmental harm, although some metals used, such as cobalt, require special attention when recycling. New recycling methods for Li-ion batteries indicate that up to 80% of the battery materials can be recycled [56]. Li-ion batteries also require protection circuits to correctly regulate the voltages it experiences. This includes limiting the peak voltage when charging as well as preventing the voltage from dropping below a specified discharge voltage [55] [33].

Nickel-metal hydride Nickel-metal hydride (NiMH) batteries are used as a replacement for nickel-cadmium batteries due to its increased energy density/capacity. However, NiMH batteries have been shown to be profitable for recycling, only containing mild toxins compared to NiCd batteries; they are therefore not regulated in terms of transportation. The main downsides of NiMH batteries lie in the maintenance and storage of them. Compared to NiCd batteries, NiMH ones suffer from a much larger self discharge rate and can degrade if stored at high temperatures. They also suffer from high maintenance; batteries must be discharged to prevent the formation of crystalline structures [55].

Battery choice Considering the comparisons made in Figure 5.2 and Table 5.6, the chosen battery type will be the lithium-ion battery, due to their favourable performance in terms of weight, maintenance, and recyclability. Lithium-ion batteries are also widely used in electric vehicles, making them a good candidate for the external vehicle. Naturally, there are different types of lithium-ion batteries that contain different metals, including cobalt, iron, and nickel [57]. Due to their use in electric vehicle applications, favourable recyclability, and availability of data, lithium iron phosphate (LiFePO4) batteries will be used. The recycling of this type of battery will be described in section 5.5, where the end-of-life procedures are discussed in reference to risk **T.P.3**. When sizing the battery further in the design, the recommended charging procedures will also be detailed, in reference to risk **T.P.6**.

5.4.4 Cable design

The design of wires and cables play a large role in the reliability and safety of the power subsystem. Improper cable selection can lead to a variety of issues, including significant voltage drops, short circuits, and electrical interference. To minimise the effect of such effects, the cable selection process takes into account the following:

[56] https://www.fortum.com/products-and-services/fortum-battery-solutions/recycling/lithium-ion-battery-recycling-solution [cited 15 May 2020]

[57] https://investingnews.com/daily/resource-investing/battery-metals-investing/lithium-investing/6-types-of-lithium-ion-batteries/[cited12June2020]

Conductor material The most common conductor materials include copper and aluminium. Copper has a higher conductivity than aluminium, but can be more expensive and heavier. Aluminium conductors can therefore desirable for long distance connections [32]. When considering copper wires, a plating material must also be chosen; this is due to bare copper developing a surface coating on its own, reducing the conductivity of the overall wire. Common plating materials include tin, silver, and nickel, each with their respective operational temperature limits [32]. While the cable lengths needed to power the necessary subsystem are not particularly long, the choice of conductor material will have an effect on both the total mass and cost of the cable. The choice will therefore be made per cable needed, prioritising cable mass over cost. Mass should be prioritised as the mass of cables are too large to be neglected, and may therefore have non-negligible effects on aircraft stability and the fuel savings.

Wire size There exists limits on the allowable voltage drop for aircraft systems; this voltage drop can be calculated with Equation 5.6. Evident from the equation, a stricter allowable voltage drop results in a thicker, and thus heavier, cable to reduce the resistance. The effect of the required cable length is also governed by Equation 5.6: the longer a cable is required to be, the higher the voltage drop becomes. From [32], the allowable voltage drop from a 115 V system is 4 V, or around 3 %. The cable sizing procedure will take this 3 % drop in voltage into account.

$$VD(Volts) = R_m(\Omega/meter) * L(meter) * I(Ampere) \tag{5.6}$$

Voltage and current When designing the cable connections within the subsystem, there is a possibility to use transformers to achieve different voltage-current combinations. Exploring these combinations can help optimise cable mass, as higher currents require thicker cables. However, wires or cables that carry very high currents require proper insulation to avoid interference [58]. Voltage levels that start requiring significant amounts of insulation begin at around 2 kV. These combinations are compared using various common transformer voltages, and are also done on a case-by-case basis.

Insulation The cables used must have sufficient shielding to prevent electromagnetic interference with other systems, especially with the increasing number of electronic devices installed on aircraft [32]. This involves covering the wire with a metallic coating. Insulation deals with two properties: insulation resistance and dielectric strength, which refer to the resistance of the insulation material to current leakages and potential differences, respectively [32]. Common insulation materials types include plastics, rubbers, and fluoropolymers [59]. The insulation needed to carry the voltage and current of each cable needs to be taken into account, but insulation also helps to mitigate certain risks such as heat and moisture damage. Another factor to take into account is the recyclability of the insulating material; plastic and rubber based materials are far easier to recycle than polymer-based ones, and since only small amounts of insulation are expected due to the low voltages present in the system, recyclability can be prioritised to a degree. In Table 5.7, three common insulator materials are compared: polyvinylchloride (PVC), high-density polyethylene (HDPE), and cross-linked polyethylene (XLPE). HDPE is chosen as the insulation material as it offers the best balance between performance, recyclability, and safety in case of failure. In terms of performance, HDPE has a low mass density, allowing for lighter insulation layers, but also the lowest dielectric loss factor, yielding a higher cable efficiency. HDPE is non-biodegradable, but is one of the easiest plastic polymers to recycle. Typically, after HDPE is disposed of, it is refined through a shredding and melting process to be formed into pellets for reuse. In fact, recycling HDPE is also economical, as it is cheaper to produce using recycled HDPE than with new HDPE due to the fossil fuels needed to produce it [60]. Additionally, in case of failure in the form of a fire,

[58] https://www.anixter.com/en_us/resources/literature/wire-wisdom/insulation-levels.html
[59] https://www.awcwire.com/insulation-materials [cited 17 June 2020]
[60] https://www.azocleantech.com/article.aspx?ArticleID=255 [cited 18 June 2020]

no harmful gases are released by the material. These characteristics make HDPE a logical choice compared to the others presented in Table 5.7. The sustainability aspects of this material is further discussed in section 5.5.

Table 5.7: Comparison of common insulator materials [61] [62] [63] [64] [34]

	PVC	HDPE	XLPE
Density [g/cm^3]	1.35-1.5	0.94 - 0.98	0.92
Dielectric loss factor (tan \delta)	1 x 10^-1	3 x 10^-4	2 x 10^-3
Weather resistance	Moderate	Moderate	Good
Corrosive gases in case of fire	Hydrogen chloride	None	None
Recycling	Chlorine content is potentially hazardous. Mechanical and chemical processes exist.	Easy to recycle and can be done more than 10 times. Is more economical to use recycled HDPE.	Cannot be melted down or moulded; impossible to retrieve the material for reuse. Usually only burned as fuel.

Selection process Once the required voltage and current of a component is known and the required cable length is determined, a cable can be selected. First, different voltage-current combinations are considered; the cable size needed for a three-phase circuit can be determined by Equation 5.7 [65], where the cable size, in circular mils, depends on the conductor resistivity, ρ, the current, I, and the allowable voltage drop, VD, in %. Once this is known, an existing cable of this size is found to determine a mass and cost per meter to allow for an estimate for the total mass and cost using the cable length. The plating and insulation is checked on these wires and modified if necessary. Because of the low mass density of HDPE and that the voltages in the system are far below 2 kV, little insulation is required; the mass of this is therefore considered negligible compared to that of the rest of the cable.

$$CM = \frac{2\sqrt{3}\rho IL}{VD} \tag{5.7}$$

The cables that need to be installed on the aircraft will be sized so that the effect of the added mass on stability can be evaluated. Smaller cables that are in the towing vehicle are considered less critical because of this, and are assumed to be included in the reference mass of the towing vehicle. Cable lengths are approximated graphically based on Figure 5.3. The major cables added to the aircraft to be sized are as follows:

- From the APU generator to the MLG motors for APU-powered operation. Estimated 18 m.
- From the towing vehicle to the engine heating system for engine pre heating. Estimated 17 m.

[61] https://www.azocleantech.com/article.aspx?ArticleID=255 [cited 18 June 2020]
[62] https://www.bioenergyconsult.com/tag/pvc-recycling-methods/ [cited 18 June 2020]
[63] https://www.generalkinematics.com/blog/different-types-plastics-recycled/ [cited 18 June 2020]
[64] https://myelectrical.com/notes/entryid/178/cable-insulation-properties [cited 18 June 2020]
[65] https://www.electricaltechnology.org/2014/04/electrical-wire-cable-size-calculator.html [cited 11 June 2020]

- From the towing vehicle to the MLG motors for vehicle-powered operation. Estimated 17 m.

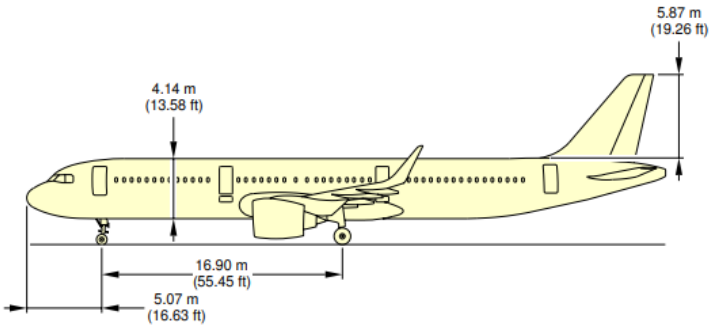

Figure 5.3: Diagram used for cable length approximation

These cable lengths are slightly over-approximated to account for cable routing issues. With these estimated lengths, Equation 5.7 can be used to determine the cable size needed to carry the necessary currents. Multiple smaller cables can be used when a single large cable is not cannot carry the required current. The cable sizes, in the American Wire Gauge (AWG) system, are used to estimate the cable mass and costs, using a mass and cost per meter of reference off-the-shelf cables [66]. The results will be shown in Table 5.11. The conductor material used is copper, and the insulator is HDPE, as described previously.

Grounding In accordance with safety requirements and risks such as **T.P.4**, electrical grounding must be considered in the system. Typically, in vehicles and aircraft, low-voltage electrical equipment are grounded to the chassis as a way to disperse any current surges or leakages. For high-voltage electrical vehicles, this method is not possible as the currents are not easily dispersed; instead, the high-voltage batteries are isolated from the chassis as a floating voltage and the current are regulated through a distribution bus, shunted by capacitors [35]. With this in mind, the low-voltage components, such as the sensors, are grounded to the chassis, but the high-voltage battery packs are isolated to prevent damage to the chassis or the operator.

5.4.5 Powertrain and Energy Source

Now, the design process and final design of the power and energy system will be discussed. More precisely, preliminary engine suggestions and energy sources will be presented together with establishing their performance.

Concept As mentioned in the midterm report [1], the RETS will have two modes, vehicle powered and APU powered, as visualised in 5.4. The philosophy behind the former is that a truck carrying the power sources pulls the plane and provides to certain on board systems like the electric motors that power the main landing gear wheels. This allows for higher performance for less weight added to the aircraft. The latter uses available power of the OEM APU to power the MLG electric motors and is used when no external vehicle is available, or at smaller airports that have not yet adopted the system.

[66] `https://www.wireandcableyourway.com` [cited 15 June 2020]

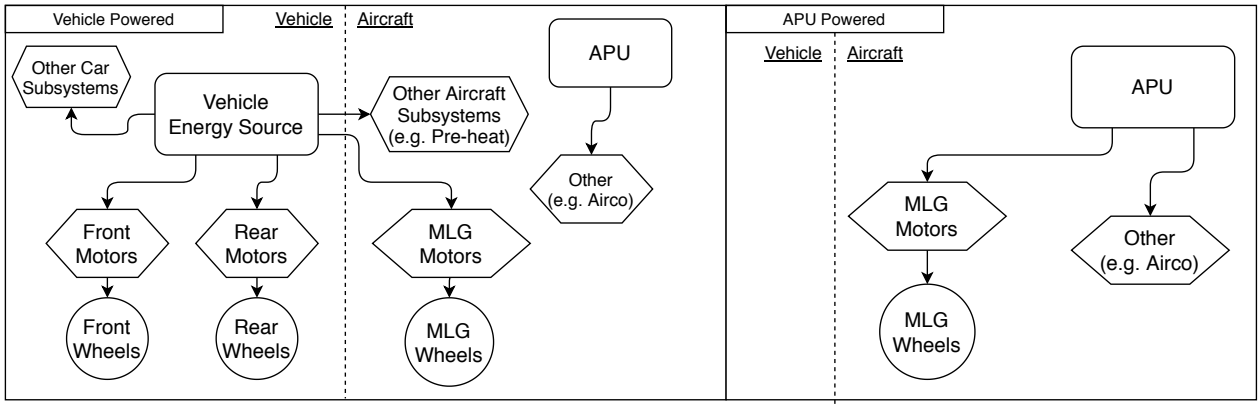

Figure 5.4: Basic top level power and energy layout. Note: transformers and computer systems are left out for clarity.

Set-up The mechanics behind the performance are shown in 5.5. The total force, mainly dominated by the tractive force which is determined by the torque put on the wheels, will establish the acceleration of the system. It should be noted that due to the low speeds, aerodynamic drag is neglected.

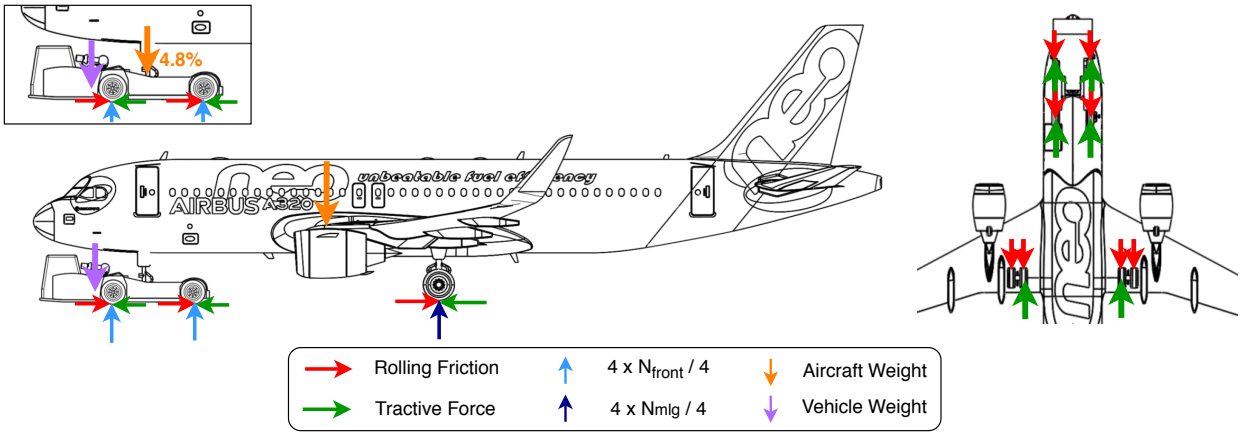

Figure 5.5: Free body diagram used for motor sizing

This leads to the force equation given by Equation 5.8; in this equation, the torque of each powered wheel is divided by the respective outer diameter of that wheel, then summed, resulting in the tractive force provided by that wheel. On the car, the required pulling force is divided evenly over all four wheels, meaning that when the tire sizes are the same for all wheels, the torque will be as well. The difference in torque between the vehicle tires and plane tires will be determined by the power ratio [67] between the two. The rolling friction is then subtracted.

$$F_{\text{tot}} = \sum \frac{T}{r} - F_{\text{fric}_{\text{roll}}} \tag{5.8}$$

If one simply combines this with the power equation, Equation 5.9, and applies newtons third law, a relation between engine power and acceleration can be established. Note the T is the torque that the engine needs to deliver and ω is the rotational speed of the shaft. This equation will be at the core of the designing and sizing process for the motors. Furthermore, to get the required torque needed to keep rolling, the left hand side should simply be set to 0.

$$P = T \cdot \omega \tag{5.9}$$

[67] For more info refer to 5.4.6

However, some physical phenomena and properties demand special attention:

- **Internal Forces**: At this stage, most of the internal forces are neglected, however the limit load of the NLG is not. In fact, the maximum allowable force will be a starting point for the power ratio between the MLG engines and Vehicle engines and may never be exceeded. This is expanded upon in subsection 6.4.1.
- **Internal Forces**: The static friction may never be exceeded, otherwise the powered wheels will start slipping and a lot of the traction force gets lost.
- **Initial acceleration**: To start rolling, the initial force needs to be 2 to 2.5 times the rolling friction [68].

5.4.6 Sizing and Design Decisions

In this subsection, the used approach, used tools and the main design decisions are detailed.

5.4.6.1 Approach

A python program that produces all the provided graphs was made in parallel with the design process in order to simplify it and speed up the iteration process. The different graphs proved to be very helpful as they allowed for a quick visualisation of the effects a certain parameter change had to the overall performance and whether or not the set-up was (still) feasible.

Due to extra freedom that vehicle offers, in terms of what size and weight your energy and power systems may have, it was decided to put the focus initially on performance. From a performance point of view the top speed and to a lesser extend the acceleration profile were deemed most important. In particular [RETS-SH-TLREQ-01] was checked with the taxi performance model (section 4.8). Hence an initial power calculation was conducted for a chosen acceleration profile that could reach the predefined 30 kts top speed, including the appropriate checks with regards to static friction and initial force brought up in the previous paragraph. The results of this are shown in Figure 5.11 and Figure 5.12. For good measure the power consumption needed to keep the velocity constant or coast, seen in Figure 5.13, was also already implemented. Then, the focus shifted to implementing the on-aircraft motors, together with the mechanism that transfers the power of motor onto the wheels, where the mechanical limits of the gears are also taken into account. To simplify this the graph seen in Figure 5.6 was created and used to quickly visualise and assess the effect of parameter changes. Next, the attention was turned to the the vehicle power source that drives the towbarless truck wheels. The decision of what this source would exactly entail was made with energy source selection in mind, which would be the final element that would be considered in this stage of the design process. Once that decision, based upon research into the different possible power source energy source combination , was made, an off the shelve example that met the criteria was integrated in the design. Lastly, the energy source was designed.

It should be noted that, for every design addition or iteration, all previously chosen and derived values were updated and checked; that is, checking if all previously met conditions are still met in the new iteration. If conditions were not satisfied anymore, adjustments were made until all conditions are met, such that that iteration could be further investigated.

5.4.6.2 Motors

As mentioned, the MLG motors were first sized based upon the acceleration profile (peak torque profile) and power ratio. This was first done using just Figure 5.11 and Figure 5.12. Then, after an initial acceleration profile was established, the different models of the EMRAX of axial flux motors with a permanent magnet were researched and tested using Figure 5.6. For later stages in the design process, these three graphs were still used and updated to double check that the performance of the RETS and the engine were still adequate.

[68] https://www.plantengineering.com/articles/calculating-proper-rolling-resistance-a-safer-move-for-material-handling/ [cited on 17 June 2020]

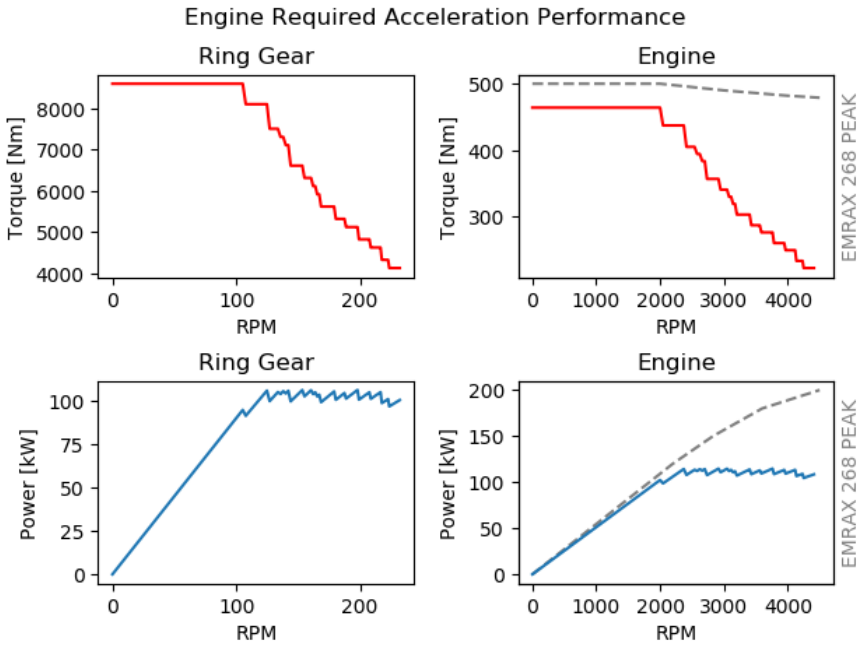

Figure 5.6: Graphs used to determine the power ratio between the vehicle and MLG motors, determine the gear ratio, determine acceleration profile and set maximum acceleration.

The diesel engine was chosen in the end of the design process together with the design of the energy source(s). To make an informed choice, research was done in the MAN gamma for truck and off-road engines, and an engine with correct power requirements was picked. Its size and mass were then checked with the structural capabilities of the vehicle to see if a lower power ratio, which results in more powerful MLG engines, was necessary; it was deemed not necessary.

5.4.6.3 Energy sources

As mentioned in the approach the energy source was chosen together with the power source of the vehicle. To substantiate that choice the total peak power, weight and a rough estimate of the total energy were looked into.

A battery only set-up was rejected, due to their low specific energy density. One would already need several battery packs just to meet the peak power required and then multiples of that set would be needed to increase the operation time. With a battery array weighing 625 kg Not including cooling and the vehicle weight limited to 22 000 kg due to the per axle weight limit of 11 000 kg this operation time was low and the recharging time high. There were also some sustainability concerns, these can be found in subsubsection 8.1.1.2. However, with battery technology being heavily researched at the moment due to the EV revolution in the automotive industry a future design could have an all battery powered vehicle.

A diesel only set-up, be it just one bigger diesel engine or diesel engine in combination with a diesel generator, was also rejected. For the first option no engine used for any type of vehicles could be found that was powerful enough to comfortably reach the peak power required. The second option was rejected because of the nature of the power demand. Generators are generally used to provide a constant supply of power, however in this application the required power would quickly shift from 0-178 kW, needed when coasting, to 322 kW needed when accelerating.

Hence a hybrid design was chosen, where diesel would be used as energy source of the truck and battery arrays would serve a capacitor-like role for the on-aircraft subsystems. To size it, the 22 vehicle weight limit was used. The energy usage per Polderbaan taxi cycle was calculated using a simulation, described in section 4.8. Using this result, the optimum ratio of diesel and battery power was determined and the weight required for one cycle was determined. Then, the amount

of cycles possible on one charge or refuel was increased unit the energy source weight reached the per axle limit

5.4.7 Final System

After several iterations, the design converged to one that meets all requirements. Nonetheless, the design needs to be further investigated for reasons mentioned in subsubsection 5.4.8.4. The proposed preliminary powertrain of the vehicle-powered scenario is presented in Figure 5.7.

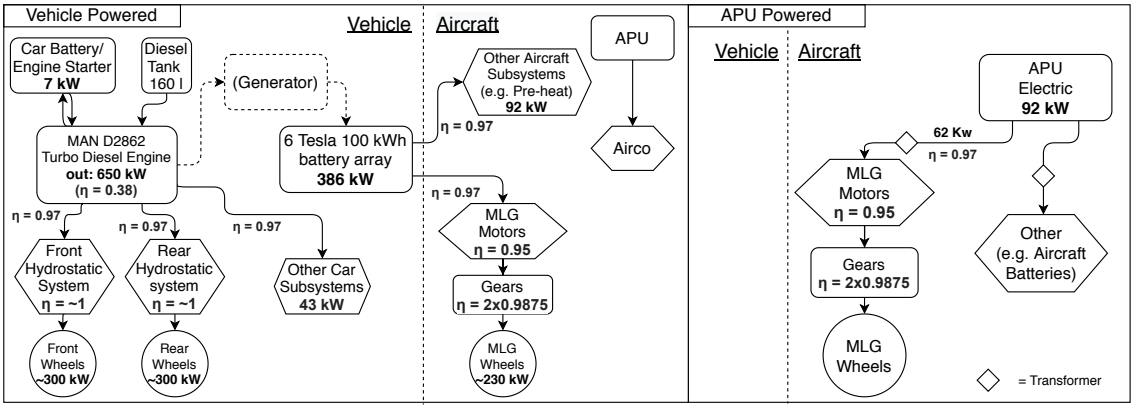

Figure 5.7: Powertrain, including efficiencies and peak power required of the RETS when it is vehicle powered and APU powered

The diesel engine starter is specified by the producer of the engine [36]. The 6 ”100 kW h” battery arrays are split into two sets of three arrays. Each set will be responsible for powering one side of the aircraft; one set will power the electric motor on the right MLG and provide the power for the preheating of the righthand jet engine, the other set does the same thing for the left side. An in-depth explanation of the hydrostatic system is given in subsubsection 6.5.1.2. The peak power in the two scenarios are shown in Figure 5.8. The generator shown in the vehicle powered scenario is still just a mere suggestion. As the diesel engine would be greatly overpowered to drive the vehicle when it is not towing the aircraft. It would be efficient if some of that power could be used to recharge the batteries between towing cycles.

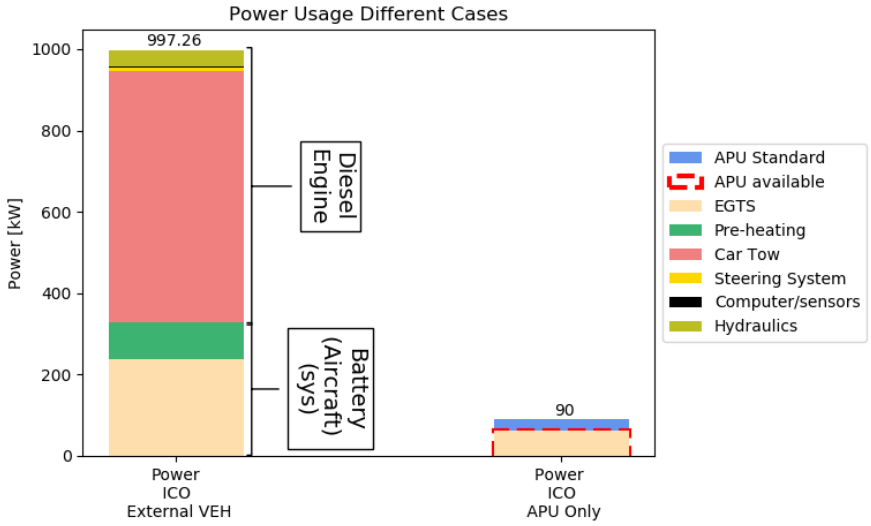

Figure 5.8: Breakdown of (peak) power consumed by RETS

It is evident that most of the power is needed to power the motors that create the torque to move the aircraft, with those on the external vehicle requiring the most due to the power ratio of

0.7383. Other notable power intensive systems are the engine preheating system, which was to be expected, and the car hydraulics system. The others are considered negligible.

Motors For the motors powering the main landing gear, the EMRAX 268 [37] was chosen as an example of an axial flux motor with a permanent magnet. Its most important specifications, found in the manual [37], are shown in Table 5.8. The manual also sheds light on the exact efficiencies under different operating conditions and how the engine should be cooled.

Table 5.8: Most important specifications of the EMRAX 268.

EMRAX 268			
Weight	20.3 kg	Peak Power	200 kW
Diameter ø / width	268/91 mm	Peak Torque	500 N m
Efficiency $(used)$	0.92 - 0.98 (0.95)	Continuous Power*	67 - 107 kW
Models	High, Medium, Low Voltage (800 V, 650 V, 250 V)	Continuous Torque*	200 - 250 N m
	Liquid, Air, Combination Cooled	Maximum RPM	4500

*Depending on the motor type and cooling method

Some concerns about the feasibility of this motor are made in subsubsection 5.4.8.4. The power of these engines is then translated to the wheels via gears with a gearing ratio of 19 and an efficiency of 98.75%, more information can be found in subsubsection 6.6.3.1.

For the diesel engine powering the car subsystems, the MAN D2862 was chosen [36]. These engines are tuned for their purpose by MAN and are stated to produce between 588 and 816 kW. The manufacturer specifies that this range is divided into and 588, 650, 750 and 816 kW [69], however no specific data for these models was found, so the general data in the off-road engine brochure [36] was used. Its most important specifications are shown in Table 5.9.

Table 5.9: Most important specifications of the MAN D2862

MAN D2862			
Weight	1885 kg	Power $(used)$	588 - 816 kW (650 kW)
Dimensions	1600x1460x1430 mm	Troque	3750 - 5000 N m
Efficiency $(calculated)$	0.38	Other	One-stage, 12 Cylinder
Specific Energy Consumption	205-210 g/kWh		1 exhaust gas turbocharger
			Integrated Engine Control

This power is applied to the wheels through a hydrostatic system. In order to make the car all-wheel drive, the following suggestion, shown in Figure 5.9, is made, and is used in demining machines.[38] A preliminary sizing and characteristics of such a system can be found under sub-subsection 6.5.1.2.

Energy Sources As mentioned, the vehicle will be powered diesel and the power of the aircraft will come from batteries. For the battery array the newest ”100 kW h” battery of the Tesla Model S 100 D [70] will be used. Currently, this battery technology sits at the top of the line. However, due the

[69] https://www.engines.man.eu/global/en/off-road/agricultural-machinery/in-focus/D2862-Tier-4-Final.html [cited on 53 June 2020]

[70] https://iaspub.epa.gov/otaqpub/display_file.jsp?docid=39834&flag=1 [accessed 20 June 2020]

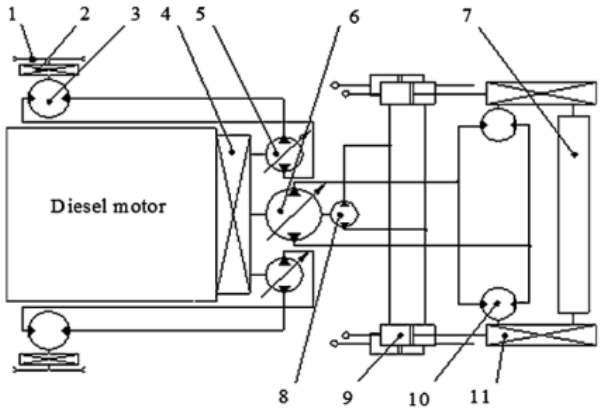

Figure 5.9: Hydraulic scheme of a demining machine (MV-4) 1 drive chain wheel, 2 planetary reduction gear, 3 track hydromotor, 4 gearbox multiplicator, 5 drive hydropump, 6 flail hydropump, 7 flail rotor, 8 hydropump for telescope flail arm, 9 hydrocylinders for telescope flail arm, 10 flail hydromotor, 11 chain [38]

electrification of the automotive world a lot of research and development is poured into batteries and electric motors. Hence, it is reasonable to assume that this battery model will become the norm or even obsolete in just few years. For example there are already rumours of Teslas battery manufacturer CATL having developed a million mile battery[71]. Hence, upgrading the batteries is something that should be looked into during the whole design of the system or when redesigning the external vehicle after this hybrid design is concluded. The performance of the energy sources are presented in Table 5.10[72] [73] [74].

Table 5.10: Energy Sources in vehicle powered scenario

VEHICLE ENERGY SOURCES			
Diesel		**Battery**	
Active Towing Time on Baseline Route	3.33 h	Including Traffic	7.4 h
Diesel Fuel	160 L	Power per Battery Pack	193 kW
Fuel Weight	175.7 kg	Battery Weight	0.498 m s^{-2}
Corresponding Fuel Energy	640.72 kW h	Total Battery Energy	600 kW h
Total Energy Used for Baseline	218.94 MJ	Complete Cycles (w traffic)	18 (15)
Baseline Route Cycles	18.12 (16.84)	Baseline Route Cycles	33.47 (15.33)
Fuel Burned for Baseline	7.318 kg (7.875 kg)	Battery Energy Used for Baseline Route	64.5 MJ (3%) (140.91 MJ (6.5%))
Total Energy Used for Polderbaan	590.51 MJ	Complete Cycles	5.5
Polderbaan Route Cycles	5.64	Polderbaan Route Cycles	11.82
Fuel Burned for Polderbaan	23.51 kg	Battery Energy Used for Polderbaan	182.72 MJ (8.5%)
Refueling time	5 - 15 min	Recharging Time	Super Charger: 40 min (10–80%) Type 2: 7 h

Looking at Table 5.10, there are some important facts to point out. The main one being that the active towing time with no traffic is considerably shorter than the time with traffic. The amount

[71] https://www.bbc.com/news/technology-52966178 [cited on 20 June 2020]
[72] http://www.aboutrving.com/rv-topics/fueling-up-at-truck-pumps/ [accesed on 20 June 2020]
[73] https://ev-database.nl/auto/1088/Tesla-Model-S-100D [accessed 20 June 2020]
[74] https://iaspub.epa.gov/otaqpub/display_file.jsp?docid=39834&flag=1 [accessed 20 June 2020]

of cycles that can be completed must also be considered as what the limiting factor is. Naturally, in the case without traffic, more cycles can be completed, increasing from 15 to 18. Looking more closely, in the case without traffic, the amount of diesel in the diesel tank is limiting and contrarily the battery capacity is limiting when traffic is included in the design. This is due to the high continuous energy consumption of the jet engine pre-heating system, hence the energy for it still needs to be supplied when the plane is standing still and waiting in traffic. However, this is something that was accounted as in the case traffic is included the system lasts roughly a full shift. Whereas in cases when the diesel consumption limits the design, the towing time is a few hours short of a full shift. However, this less of problem as refuelling the truck takes a matter of minutes, something that cannot be said about recharging the batteries. If the earlier suggested generator makes it way into a future design iteration, the performance with traffic will greatly increase. For the structural aspects concerning the energy sources one is referred to subsubsection 6.5.1.3

Electric Cables Using the method described previously, the cables to be added to the aircraft are sized and summarised below in Table 5.11. Of note, the MLG motors will run at 250 V DC; the 115 V AC from the APU is therefore rectified and transformed through an Auto-Transformer Rectifier Unit (ATRU) to the required 250 V DC. For this connection, one cable is used for each landing gear motor. As the engine heating system requires a large amount of power, the power is transported at 240 V, 190 A through 2 cables to reduce cable weight. Similarly, the power for the MLG motors from the vehicle is transported through 2 cables per motor to reduce cable weight. The electrical set-up of the system is further described in subsection 5.4.8 in an electrical block diagram. The size is shown in terms of the American Wire Gauge (AWG) system, which corresponds to a cable diameter and rated ampacity. As stated previously, existing reference cables are used to estimate mass and cost using per-meter mass and cost values.

Table 5.11: Sizing of cables added to aircraft

Cable	Number of cables	Length [m]	Voltage [V]	Current [A]	Size needed [AWG]	Total mass [kg]	Total cost [USD]
APU to MLG	2	18	250	72	4 AWG	8.89	88.58
Vehicle to engines	2	17	240	191	3/0 AWG	30.51	223.10
Vehicle to MLG	4	17	250	230	4/0 AWG	20.16	200.79
Total						59.56	512.47

5.4.8 Electrical block diagram

With the system architecture established, the relationships between electronic components can be summarised in Figure 5.10. The control unit both determines which power source will be used to power the main landing gear motors and translates the pilot input to the input required by the motors; this process is further explored in chapter 7. The two power sources are visible: the electrical power from the APU is used when the towing vehicle is not available, and the Li-ion batteries housed in the towing vehicle are used during nominal operation. When the APU is used as a power source, the 115 V AC provided by the APU generator must be transformed and rectified into the 650 V DC power used by the motors; this is done with an Auto-Transformer Rectifier Unit (ATRU), similar to the EGTS system [75]. On the external towing vehicle, a 24 V car battery is used for start-up, and the on-board 400 V DC Li-ion batteries power the necessary subsystems and processes through a power distribution bus, similar to those that distribute the power from the

[75] https://www.aviationtoday.com/2019/05/01/electric-taxiing-systems-past-present-possible-future/ [accessed 30 April 2020]

aircraft APU [32]. Included in this bus are a surge protector and circuit breaker to protect the system from surges in voltage and current, respectively. As stated previously, the motors require 650 V. Additionally, the engine preheating system requires 121 V, and the sensors, which are described in chapter 7, require 24 V.

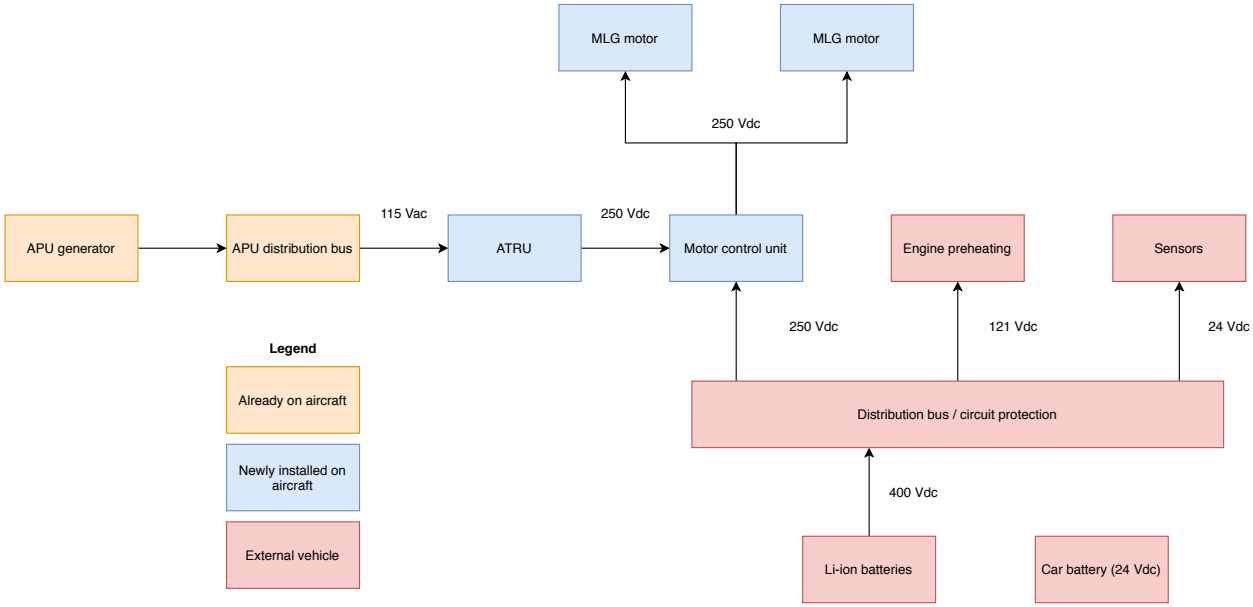

Figure 5.10: Electrical block diagram

5.4.8.1 Performance of Full System

As explained at the beginning of subsection 5.4.5, the performance of the RETS with the external vehicle is intended to be the primary operation scenario. The power is supplied by batteries and a turbo diesel engine, both located on the external vehicle, as presented in Figure 5.7. The performance of this set-up is shown in Figure 5.11 and Figure 5.12. The velocity and acceleration plots show the performance of the overall system, with the orange coloured dotted line in the acceleration plot showing the contribution of the respective motors to the total acceleration, which goes hand in hand with total force. The lower diagrams show the power required per powered wheel and of the diesel engine in case of the vehicle performance plot. It should be noted that the power presented in these graphs represents only the power needed to power the wheels; the diesel engine plot includes the 41 kW needed for other car subsystems. Nonetheless, for a complete overview of the total power, refer to Figure 5.8.

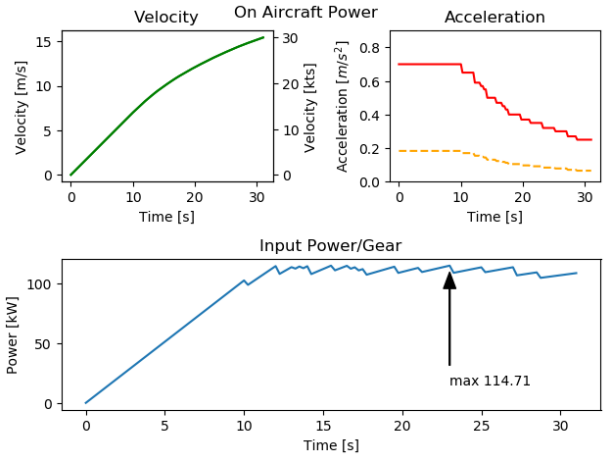

Figure 5.11: Performance of the MLG motors of the RETS system when the external vehicle supplies power.

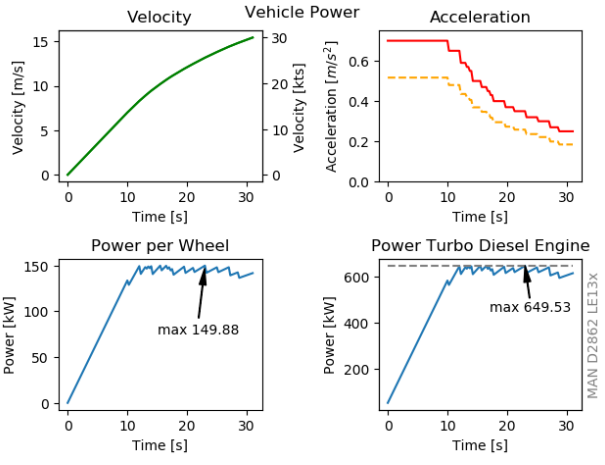

Figure 5.12: Performance of the car wheels and engine of the RETs systems external vehicle.

Looking at both figures, a distinctive sawtooth profile is visible. This profile originates from the designing method described previously under the approach in subsection 5.4.6. For fitting the acceleration profile to match the maximum torque and power limits of the both engines, discrete acceleration intervals were established to speed up the design process. Hence, this effect is a product of that discretisation. When the design is further finalised, effort can be put into smoothing out this acceleration profile. A straightforward way to do this would be taking the approach that is already followed to determine the APU-powered performance that is starting the from the available engine performance. However, this requires the engines and power sources to be picked.

One can also see which factors limit the performance of the vehicle by looking at the individual performance curves provided in this subsection together with Figure 5.6. Note Figure 5.6 corresponds to the set-up, with the EMRAX 268, described earlier in subsubsection 5.4.8.1 and the acceleration profile in Figure 5.11 and Figure 5.12. Looking at that plot, the engine power and the peak torque of the MLG engines are visible. This limits the maximum acceleration for the first 10 s, after which the acceleration is lowered to limit the power required by the system which is constricted by the vehicle motor characteristics. Another reason for lowering the acceleration at higher velocities is the fact that there is less demand for high acceleration at increasingly higher speeds.

Next to the acceleration performance of RETS shown in Figure 5.11 and Figure 5.12, it should also be able to keep its velocity constant. As stated under set-up at the beginning of subsection 5.4.5, the RETS should only compensate the deceleration caused by friction. The required power for the different engines to keep this equilibrium is shown in Figure 5.13.

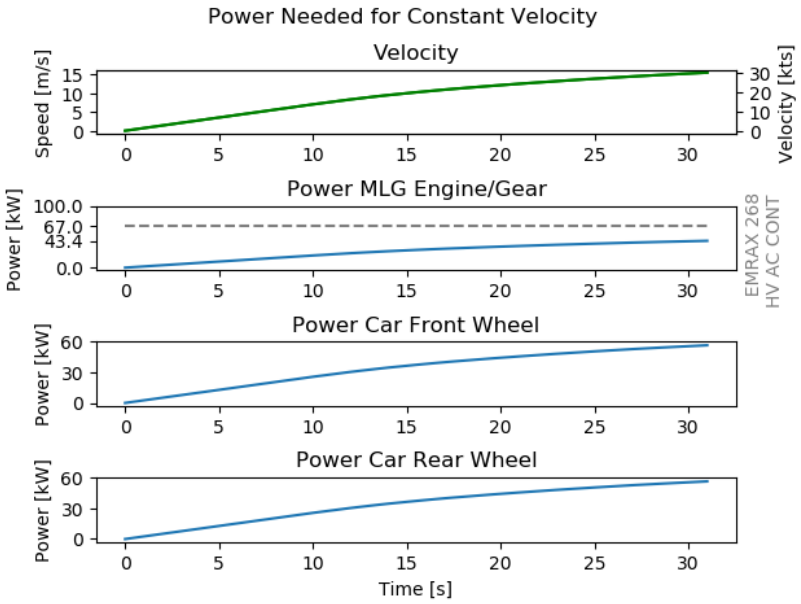

Figure 5.13: Power required by the different engines of the RETS to keep the taxi speed constant.

Logically, the power increases with speed as the required torque remains constant and the rotational velocity of the wheels increases with speed. This could have been anticipated by looking at Equation 5.9 at the beginning of subsection 5.4.5. Although the peak power for all the EMRAX engines is the same, continuous power differs. The indicated engine for the MLG continuous power required is the high voltage (HV), aircooled (AC) version of the EMRAX 268. This version provides the lowest amount of continuous power. [37] However the required power lies far below it, meaning that it is not limiting to the design. This is of course assuming that the engine is properly air-cooled. A remark about the cooling of the electric motors can be found under subsubsection 5.4.8.4.

Some notable parameters of the set-up are provided below in Table 5.12.

Table 5.12: Vehicle Powered performance characteristics

VEHICLE POWERED PERFORMANCE			
Force Ratio Vehicle - MLG	0.7383	Max Acceleration	$0.7\,m\,s^{-2}$
Max Force	107.02 kN	Average Acceleration	$0.498\,m\,s^{-2}$
MLG Peak Torque at Wheel per Engine	8598.43 N m	Min Acceleration Required for Speed	$0.02\,m\,s^{-2}$
Gear MLG Ratio	19	Top Speed	30 kts
Vehicle Required Peak Torque per Powered Wheel	10 255.61 N m	0 to 30 kts	31 s

5.4.8.2 Performance of System without External Vehicle

As explained at the beginning of subsection 5.4.5, the performance of the RETS without external vehicle is fully defined by the available power provided by the APU. This instance of the system is illustrated in Figure 5.7. The performance of this set-up for both situations wherein it is used, i.e. pushback without tow-truck and slow taxi/maintenance movements, are shown in Figure 5.14. It is clear that this performance is limited by the available power and peak torque in both occasions. However, it is deemed adequate as it can reach the 3 kts, prescribed in section 4.8, in 15 s. For the slow taxi, no requirements were stated as this is rather an extra feature of the RETS as under normal operations, an aircraft would use its main engines to taxi in case the vehicle is not available.

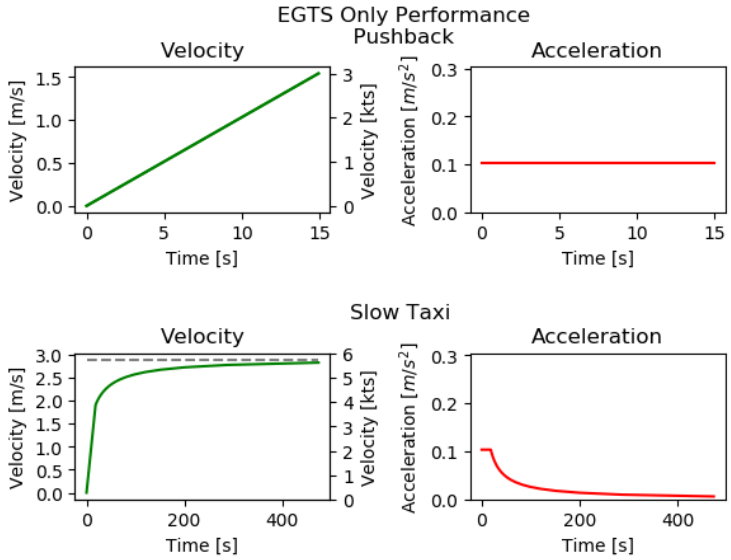

Figure 5.14: Performance of the RETS when only APU power is available.

As mentioned before, the performance is limited by torque and power, more precisely for the first part, which conveniently roughly corresponds to the pushback time interval and corresponding acceleration profile; the acceleration is limited by the peak torque the motors can deliver. Once the acceleration starts decreasing, the performance is limited by the available power. Some notable parameters of the set-up are provided below in Table 5.13.

5.4.8.3 Performance of System with just External Vehicle

Although, the RETS is designed to use both vehicle and on-board motors, it also possible to use just the towbarless truck as a standalone system. In this case the performance drops with 26.7%.

Table 5.13: APU Powered performance characteristics

APU POWERED PERFORMANCE			
Power	62 kW	Max Acceleration	0.103 m s^{-2}
Max Torque per Engine	500 N m	Top Speed	2.88 m s^{-1}
Max Force	10.1 kN	0 to 3 kts	15.43 s

5.4.8.4 Comments

In this subsection, the considerations with regards to the power and energy system are given for the future design phases.

Electrical Motors In the specification sheet of the EMRAX 268 [37] it is not clearly stated for what period of time the engine can provide peak torque. It mentions that it is only for a couple of seconds, which could turn out problematic as the engine should be capable of delivering peak torque for more than 10 s in order to achieve the 0 to 30 kts performance described in subsection 5.4.7. A simple solution would be to use a larger model, the EMRAX 348 [37], which has a peak torque of 1000 N m and a continuous torque of 500 N m. This would easily resolve the peak torque worries, however it would also most notably increase the on-aircraft weight (from 20.3 kg to 42 kg) and demand a redesign of the gears and energy system amongst other aspects.

Engine cooling is another import factor that determines the engine performance and, more specifically, the continuous power and acceleration intervals it can deliver. In the technical specifications of the EMRAX 268 & 348 [37], three cooling methods are specified: air cooled, water cooled and combination. It is only the last option that provides the maximum continuous power. However, it would add additional weight to the aircraft. An option also exists to use the landing gear leg as a radiator or heat sink in combination with one of these systems. The technicalities of cooling the engine are also provided in the manual under chapter 13 motor cooling [37].

The motors need to be powered by different energy sources in the different scenarios. This is something that also has not been looked into yet at this phase of the design. In a future phase one should look if a simple switch is adequate or if something with a higher complexity should be considered.

Diesel Engine Charging Batteries It would also be wise to research the probability of charging the batteries during operations with the diesel engine when it is not running at peak power and torque as hinted in subsection 5.4.7. It could result in a possible weight reduction for the truck and decrease the difference in power that the engine needs to provide. Furthermore it could also improve the active operation time of the truck as that is currently limited by energy stored in the battery arrays. However, it would come at the cost of a more complex design. A starting point would be to look at normal diesel trucks where the car battery is also charged when the motor is running. Note that, such a (smaller) car battery, which is mainly used to start the engine and power the electronics on the car,is already included into the current design. Thus one could begin by looking to combine that battery together with the battery packs in one or connect the small battery to the battery arrays with a distribution unit.

Battery Cooling Batteries have specified operating temperature ranges. Since the vehicle will need to be able to operate during winters at airports situated at high latitudes but also in desert climates like for instance Dubai, an adequate cooling/heating should be developed. This needs to be done in a later phase and attention should be paid to the added weight and energy consumption of such a system.

5.5 Risk and sustainability

Most of the sustainable aspects and risks of a design stem from its power generation and energy storage. Hence the sustainability aspects of the design were taken into consideration from the beginning of the designing and trade-off processes and the risks were noted down meticulously during the design. A summary of the main sustainability factors is provided in this section together with a discussion of the newly encountered risks.

5.5.1 Sustainability

The truck uses a hybrid design for its powertrain as explained in subsection 5.4.7, on the one hand it uses battery arrays to power the on-aircraft systems and on the other hand it uses a turbo diesel engine to power forth the car and its systems. From a sustainability point of view the battery recyclability is the biggest factor concerning the battery arrays this will be discussed in subsubsection 5.5.1.1. A closer look at the sustainability of the electric motor and power cables is provided in subsubsection 5.5.1.2. Lastly, the sustainability aspects of the turbo diesel engine and its fuel are discussed in subsubsection 5.5.1.3.

5.5.1.1 Battery recycling

With the battery type chosen, it is important to address the requirements regarding recyclability. Recycling LiFePO4 batteries is not as economically interesting as recycling other types of Li-ion batteries due to a relatively low content of valuable materials. However, proper recycling procedures are still necessary as, despite their low toxicity levels compared to other batteries, improper procedures can cause harm to the environment [33]. For this, the current methods of recycling LiFePO4 batteries will be discussed; an overview of the entire process is also given in Figure 5.15.

When Li-ion batteries reach their end-of-life (EOL), the first step to recycling them is to discharge and dismantle the battery. As stated previously, Li-ion batteries contain a protection circuit to regulate the discharge voltage. As a result, there exists some residual capacity that needs to be fully discharged. To do so, one can either use dedicated discharging equipment, or submerge the batteries in saltwater to cause an intentional short circuit, thus discharging the battery[33]. The various components can then be retrieved during a dismantling phase; these include circuit boards, such at the one to regulate voltages, cables, and casings. From here, the different components can be reused or further recycled, depending on the component. This phase is then followed by the separation and mechanical treatment of the components through shredding and crushing, as well as chemical and thermal treatments. Two options then exist for the LiFePO4 active material, a metal recovery through a hydrometallurgical method, and a regeneration process [33].

With the metal recovery option, a hydrometallurgical method is used, consisting of a leaching step and a separation step. During the leaching step, the desired element to be recovered is dissolved; for LiFePO4, sulphuric acid (H2SO4) is often used, though other, newer methods also exist. The lithium can then be retrieved through the separation step, using techniques such as precipitation and solvent extraction [33]. The other option is to instead aim to regenerate the active material. Several methods exist for this, including solid-state and liquid-state regeneration, and heat-treatment methods. These methods are expanded upon in [33], and current recycling methods indicate that 80% of Li-ion batteries can be recycled [76].

5.5.1.2 Electric Motor and Power Cables

Conductor material The copper in the cables can be used as scrap metal and remelted. Recycling copper is also very economical as less energy is spent in doing so than in primary production, reducing energy by approximately 85% and 40 million tonnes of CO2 per year [77].

[76] https://www.fortum.com/products-and-services/fortum-battery-solutions/recycling/lithium-ion-battery-recycling-solution [cited 15 May 2020]
[77] https://copperalliance.eu/benefits-of-copper/recycling/ [cited 29 June 2020]

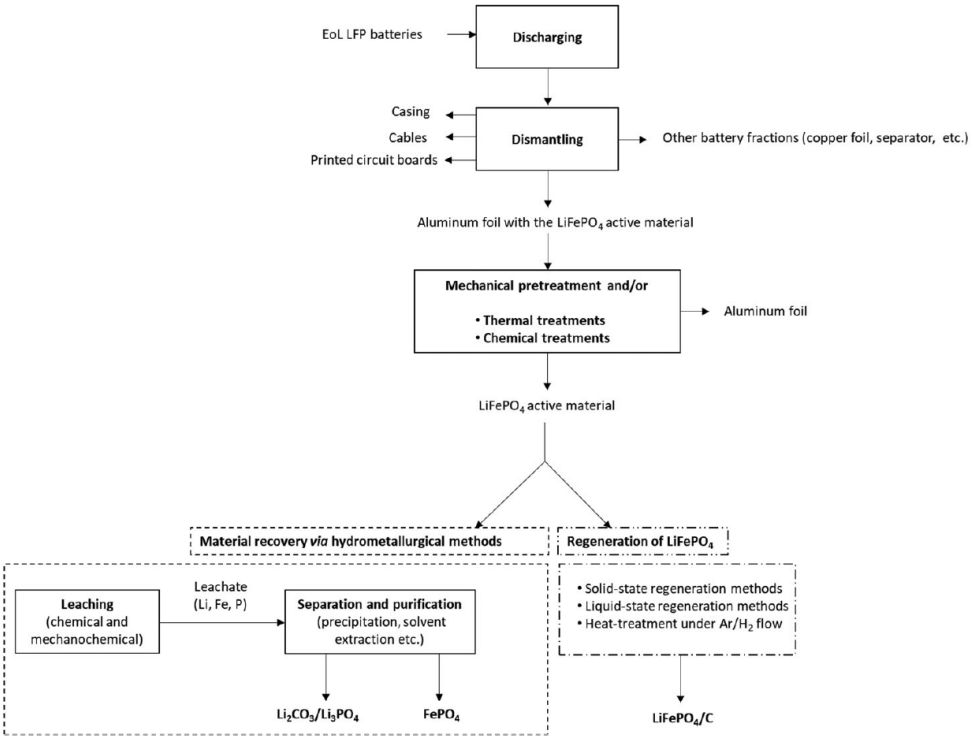

Figure 5.15: Overview of End-of-Life procedures for LiFePO4 batteries [33]

Insulator material While the recycling of the copper conductor is fairly straightforward, sustainability was taken into account when choosing the insulator material. As stated previously, HDPE is an easy and economical plastic to recycle. A typical recycling process involves the sorting and cleaning of the discarded plastic, such that the plastic is isolated from debris and other materials. The plastic is then shredded and melted into a refined polymer, then cooled and formed into pellets. Also stated previously, using recycled HDPE benefits manufacturers as it is cheaper to use than manufactured HDPE; 1.75 kg of oil is needed to create each kilogram of HDPE. Furthermore, HDPE products, depending on the application, have a service life of approximately 10-20 years, and can be recycled over 10 times [78].

5.5.1.3 Turbo Diesel Engine

Besides the reasons provided in subsubsection 5.4.8.4, there are also multiple sustainability reasons that support the choice for a combustion engine. This choice might seem odd at a first glance as combustion engines have come under scrutiny in recent years, especially diesel after the worldwide Volkswagen "Dieselgate" scandal . However, it should be noted that, partly due to "Dieselgate", combustion engine emissions are now more thoroughly inspected and the efficiency of them has ever been improving meaning that combustion engines are cleaner than ever.

Why not use all batteries? Apart from the structural aspects that would be a problem in case of a car that is fully powered by batteries, there are also some sustainability issues. To meet the peak power requirement the vehicle would need more than double the amount of 100 kW h Lithium-ion batteries. Hence, the dependence of the design on rare earth materials such as Lithium increases and makes the design more susceptible to battery shortages and price spikes of these materials, especially with the electrification of the automotive industry. Although, with the particular choice for Lithium iron phosphate batteries this dependence is greatly reduced. Another one could be the reliability of the battery arrays, as theoretically a higher amount of individual cells could increase the chance of failure. However, this something that needs to be looked into. A similar argument can be

[78] https://www.azocleantech.com/article.aspx?ArticleID=255 [cited 18 June 2020]
[78] https://www.bbc.com/news/business-34324772[cited 21 June 2020]

made when talking about battery lifespan. As the Tesla 100 kW h is a relatively new technology, it is unclear as of now what the actual lifespan of them is when operated on EVs, thus this is something that should be looked into at a later stage in the design. It should be noted that the choice for the diesel engine mainly stems from the low energy density of battery arrays.

The Chosen Engine: MAN D2862 The suggested engine, the MAN D2862, is a turbo-charged V12 diesel engine. Diesel was chosen over gasoline because of the high torque required and its higher efficiency. Next to that they also require less maintenance and depreciate less than their gasoline counterparts. Even though diesel cars generally emit less CO_2 than gasoline cars they do emit nitrous oxides, hydrocarbons and particulates.[79] However, the chosen engine complies with ”emission standard Tier 4 final” and ”EU Stage V” which are the strictest regulations for off-road vehicle emissions and limits the emissions.[80] The diesel engine also allows for the use of biodiesel, but this is something that needs to be looked into further.

Exhaust In order to achieve this high of an emission standard, MAN uses SRC technology which is a compact and flexible modular exhaust gas after-treatment system. SRC Or Selective Catalic Reduction is a process in which is a liquid-reductant agent, NH3, is mixed together with the exhaust fumes of the diesel engine with help of a catalyst. It transforms NOx into harmless N_2, water and tiny amounts of CO_2 [81]. The fact that the engine meets the strictest regulations and has SRC technology does not mean that further improvements can be made by looking into filtering more of the exhaust gases. Unfortunately MAN specifies that the engine can or is only equipped with SRC[36], hence a cleaner (road) engine must also be looked into. This is something that needs to be done in the following design phase.

5.5.2 New Power & Electrical Risks

Again for this subsystem, new knowledge has been gained which resulted in the identification of new relevant risks for the power and electronics subsystem. These new risks are listed in Table 5.14. The risk cause, consequence and mitigation have also been identified for these new risks as well as the estimated probability of failure and consequence of failure before and after mitigation according to Table 4.1 and 4.2.

5.6 Verification and validation

To ensure a valid result from the code used to size the various aspects of the power subsystem, the code needs the be verified and validated. Testing is performed in the form of unit and system tests; unit testing was done with the python ”unittest” module. Next to this, inputs were changed by the programmer as a form of dynamic testing to check if the results respond in a logical manner. In this section, the unit and system tests performed are described and their outcomes are shown.

5.6.1 Unit testing

Unit testing is done on the principle of boundary testing; if a condition is checked in the code, a test case is made for when this condition should be true, false, and on the boundary of these. For example, the static traction checking function in the code checks whether the static friction force is exceeded for a given torque and static friction coefficient. If the torque exceeds the specified value, the function returns ”False,” if the torque does not exceed this value, it returns ”True,” and in the case that it is equal to the value, it should also return ”True.” For this function, all three of these domain parts should be tested, and so three test cases are made. Functions that do not include conditions and only execute calculations simply have two test cases. Test cases are then calculated by hand and compared to the code output. Also note that inputs used for test

[79] https://interestingengineering.com/diesel-engine-vs-ev-which-is-better
[80] https://theicct.org/sites/default/files/publications/EU-Stage-V_policy%20update_ICCT_nov2016.pdf
[81] https://www.dieselforum.org/about-clean-diesel/what-is-scr

Table 5.14: Newly identified risks related to power and electronics

ID	Risk	Risk Cause	Risk Consequence	Mitigation	p_f/ $p_{f_{\text{mit}}}$	c_f/ $c_{f_{\text{mit}}}$
T.P.8	Electric Motors turned into generators	Due to direct link to the wheels, it could occur that the wheels drive the motor	The motor becomes a generator and an generates an output flow which could damage the electric system and batteries	Install a clutch like system in the gear arrangement and add circuit breakers in the system	3/2	3/2
T.P.9	Loss of traction	Torque applied to wheel translates to a force greater than static friction limit	Wheel goes into dynamic friction regime	Check acceleration profile on dynamic friction	3/1	2
T.P.10	Cables flammable	HDPE insulator is flammable	Operation must stop and the fire must be extinguished	Use non-flammable cable/wire jackets; investigate probability of such a failure in future design phase and take action accordingly	3/2	3

cases are not necessarily representative of realistic values for simplicity, as they serve to ensure the calculations are performed correctly. Table 5.15 shows the test cases that were made to unit test the smaller functions of the code and their results.

Table 5.15: Power subsystem unit testing results

Module	Input	Output	Expected Output
Static traction check	400, 1000, 0.5	True	True
	500, 200, 0.5	False	False
	500, 1000, 0.5	True	True
Initial acceleration check	[0.5, 0.5]	True	True
	[0.02, 0.02]	False	False
	[0.05, 0.05]	True	True
Optimal force ratio	10000, [1]	0.07	0.07001
	100000, [0.5]	1	1
Velocity array generator	[1, 1, 2, 2, 3], [0, 1, 2, 3, 4]	[0, 1, 3, 5, 8]	[0, 1, 3, 5, 8]
	[1, 0, -2, 2, 3], [0, 1, 2, 3, 4]	[0, 0, -2, 0, 3]	[0, 0, -2, 0, 3]

5.6.2 System testing

The larger modules in the power code are more difficult to test by hand as they involve large arrays and multiple calculation steps and other smaller modules. Instead, the larger modules are tested through sanity checks, where simplified inputs are used and changed to evaluate whether the code responds correctly. For example, the function that calculates the static power required to overcome rolling friction should respond accordingly to velocity arrays with constant, increasing, and decreasing values. The tests and outcomes of these system tests are shown below in Table 5.16.

5.6.3 Validation

While the unit and system tests give some validity to the results and design, they are further validated through comparison with existing products. As such, the wheel motor performance will be compared to the EGTS. It is clear that the RETS motors are much more powerful than those of the EGTS. However, this makes sense as the EGTS' two 50 kW motors accelerate an A320 to

Table 5.16: Power subsystem system tests

Module	Test	Outcome
Motor performance	Resulting acceleration, velocity, and time arrays have same length	Pass
Static power	Constant velocity gives constant power	Pass
	Increasing velocity gives increasing power	Pass
	Decreasing velocity gives decreasing power	Pass
	Zero velocity gives zero power	Pass
Car power	Power increases as velocity increases	Pass
	Higher acceleration gives higher power	Pass

20 kts, or approximately 10.3 $m\,s^{-1}$ in 90 s, resulting in an average acceleration of approximately 0.114 $m\,s^{-2}$ [82]; the RETS is capable of an average acceleration of 0.5 $m\,s^{-1}$ and uses the Emrax 268, a 200 kW motor. Since the RETS can accelerate about 4.4 times faster than EGTS, it also makes sense that the motors needed are a larger by a similar factor. Furthermore, the choice of battery (Li-ion) is backed up by the common usage of these type of battery in electric vehicles [39]. Regarding the diesel engine, the power output is approximately equal to two semi-truck engines [83] which, makes sense with the difference in mass and speeds, although a more direct comparison is more difficult.

5.7 Compliance matrix

A compliance matrix can now be made for the subsystem requirements. In Table 5.17, the compliance of the system with respect to the requirements is shown; when a requirement is met, a (✓) is used, when a requirement requires more research, a (✱) is used and when a requirement is not met, a (✗) is used.

[82] https://web.archive.org/web/20140912171731/https://aviationweek.com/commercial-aviation/electric-taxi-puts-show-paris [accessed 28 April 2020]

[83] https://www.macktrucks.com/powertrain-and-suspensions/engines/ [cited 22 June 2020]

Table 5.17: Compliance Matrix Power and Electronics

Requirement ID	Compliance	Reasoning
RETS-SH-TLREQ-01	✓	Taxi simulation indicates requirement is met
RETS-SH-TLREQ-03	✓	Mass added to aircraft by power subsystem is below the specified limit
RETS-SH-TLREQ-06	✓	Taxi simulation indicates requirement is met
RETS-SH-TLREQ-07N	✓	Materials from batteries and cables can be recycled
RETS-SH-ALC-02	✓	Performance is evaluated at MTOW at different runway conditions
RETS-F-GEN-05	✓	The power subsystem was designed for the A321neo
RETS-F-OPR-03	✓	Engine warm-up component implemented
RETS-F-OPR-06	✓	Batteries and fuel can sustain operation for more than the specified amount
RETS-F-OPR-07	✓	Batteries and fuel can sustain operation for more than the specified amount
RETS-F-PE-02	✓	Maximum taxi speed designed for 30 kts
RETS-F-PE-03	✓	Charge possible in 40 min, Table 5.10
RETS-F-PE-05	✓	Taxi simulation indicates requirement is met
RETS-F-PE-06	✓	Taxi simulation indicates requirement is met
RETS-F-PE-07	✓	Treated in chapter 4
RETS-F-PE-08	✓	Treated in chapter 4
RETS-F-PE-09-A	✱	Temperature limits are known, but further analysis in a later design phase is needed to determine if these limits are exceeded or not
RETS-F-PE-09-B	✱	Temperature limits are known, but further analysis in a later design phase is needed to determine if these limits are exceeded or not
RETS-F-PE-10	✓	Maximum taxi speed designed for 30 kts
RETS-F-PE-11	✱	Electrical system includes circuit breaker and surge protector, but needs to be further investigated in a later design phase
RETS-F-PE-12	✓	APU can be used as a secondary power source
RETS-F-PE-13	✓	APU is approximated to be able to deliver 62 kW top the motors
RETS-F-PE-14	✓	Sufficient insulation used in cables
RETS-F-PE-15	✓	Proposed engine preheating system meets warm-up time reduction
RETS-F-PE-16	✓	Reference cables used are certified and appropriately rated
RETS-F-PE-17	✓	The mass added to the aircraft is less than the requirement limit.
RETS-F-PE-18	✱	The subsystem mass limit is overestimated, however the system mass budget is still met
RETS-NF-LC-01	✓	Materials chosen with disposal and end-of-life in mind
RETS-NF-LC-02	✱	Recycling process of battery packs are described; a manual must be made in a later phase

6 Structures

Within this chapter the structural subsystem will be designed. This subsystem will make sure all subsystems will be put together in a consistent load carrying structures. To do so, first in section 6.1 the different functions of the structural subsystem will be described. The design goals and boundaries are then stated by means of relevant structural requirements and risks including mitigation in section 6.2. Next in section 6.4, the loads at the NLG and MLG will be analysed. These limits will then be taken into account for the detailed design of the modified pushback truck and the wheel-based engine structure in section 6.5 and section 6.6 respectively. section 6.7 will discuss the connection between the aircraft and the tug after which newly identified risks as well as sustainability aspects will be discussed in section 6.8. The chapter will be concluded by showing the verification and validation procedures and a compliance matrix in section 6.9 and 6.10.

6.1 Functional Analysis

Before the structural subsystem will be designed, a clear overview of the system functions must first be established. This will make sure that the focus of the structural design process will be on those parts that really are important to the system. Of course the structural subsystem will have the primary function of providing sufficient support and structural integrity to the other subsystems. However, this can be broken down into multiple structural elements. The functional analysis of these elements is divided into two main categories: structural elements of the wheel-based engine and the structural elements of the external vehicle. For both categories the materials, strength and weight are taken into account in the detailed design.

External Vehicle

Given the main outline of the design concept, four main aspects of the external vehicle can be distinguished. First of all the external vehicle must be designed itself. It serves multiple functions that largely overlap with a conventional towbarless pushback truck: lifting the NLG, accompany a driver, perform pushback, etc. To perform these functions, a conventional pushback truck will be taken as a baseline. This vehicle will then be modified with respect to the power source, steering system, electrical grounding system and drive train to fulfil the needs of the overall new taxi system.

Besides the chassis of the pushback truck, the lifting system must also be redesigned as the steering control and its input differ significantly from a conventional pushback truck. As the pilot will be in control, the steering of the vehicle with respect to the aircraft must be taken into account without damaging the nose wheel.

Next to a mechanical connection, there must also be an electrical connection from the vehicle to the aircraft to provide power to the engines mounted on the MLG. In this case as well, turning will be critical as the connection must not damage the aircraft or the vehicle itself.

Lastly, the safety function of the external vehicle must be designed in more detail. The system is active during a long part of the taxi phase while attached to the aircraft, extra safety measures must be taken in order to guarantee a safe operation.

Wheel-based Engine

The wheel-based engine is positioned on the MLG of the aircraft. The first function of this element will be to provide sufficient power, torque and rpm to one of the MLG wheels. While designing, it must be taken into account that the brakes will still have sufficient air flow to cool down with the presence of the wheel-based engine and accompanying gears.

Although the focus will be on the gear design, the attachment of the wheel-based engine and

the gears must also be taken into account with respect to load paths. Conventional operations or a rough landing should not lead to a failure of either the landing gear structure and/or the new wheel-based engine system. Besides, in case of a failure of the RETS, the design must make sure for proper maintainability by means of removal and replacement of components.

6.2 Risk Analysis

Table 6.1 shows the identified risks relevant for the structural and material design of the RETS. The risk mitigation strategy will, if possible, be implemented during the detailed design later discussed in this chapter. Besides the risk itself, also the cause and the consequence as well as the probability of failure p_f and the consequence of failure c_f are given according to Table 4.1 and Table 4.2. Also note that some mitigation strategies directly induce a specific requirement.

Table 6.1: Previously identified risks related to structures

ID	Risk	Risk cause	Risk consequence	Mitigation	p_f/ $p_{f_{\text{mit}}}$	c_f/ $c_{f_{\text{mit}}}$
T.S.1	RETS primary structure failure	Load limit exceeded due to wrong load determination; fatigue loads; poor design	RETS must undergo maintenance; RETS (component) is scrapped; aircraft may be damaged; airport operation delays	Thoroughly analyse and identify maximum load limits and clearly document in operating manual	3/1	4
T.S.2	RETS secondary structure failure	Load limits exceeded; fatigue loads; poor design	RETS must undergo (simple) maintenance; potential airport operation delays; flight delay(s)	Thoroughly analyse and identify load limits; clearly document in operating manual; have backup RETS on stand-by; Make sure normal A/C operations can be performed without RETS	3/2	3
T.S.3A	Main landing gear loads exceeded	Poor design; wrong RETS-A/C attachment	Aircraft severely damaged; RETS potentially damaged; flight delay/cancellation	Analyse induced loads on main landing gear; find documentation on maximum aircraft loads; design system such that (small and easily replaceable) RETS component will break before the aircraft would be damaged	2/1	4/3
T.S.3B	Nose landing gear loads exceeded	Poor design; wrong RETS-A/C coupling	Nose landing gear severely damaged; RETS potentially damaged; flight delay/cancellation	Use of sensors to measure loads	3/2	4
T.S.4	Aircraft tyre puncture	Sharp edges on RETS	Aircraft and potentially RETS must undergo maintenance; flight delay	Check on pointy parts during design phase and on finished products; trim edges; design RETS structure such that A/C tyre failure can be dealt with	2/1	4/3
T.S.5	RETS tyre puncture	FOD; inconsistent maintenance; aircraft weight too high	RETS must undergo (extra) maintenance; potential airport delays; flight delay	Specify design aircraft weights and maintenance procedures in operations/maintenance manual; have backup RETS on stand-by; make tyres of RETS easily replaceable	2/1	3

Continued on next page

Table 6.1 – continued from previous page

ID	Risk	Risk cause	Risk consequence	Mitigation	p_f/ $p_{f_{\text{mit}}}$	c_f/ $c_{f_{\text{mit}}}$
T.S.6	Improper cooling of brakes	Wheel based engine restricting airflow for cool down	Overheating of brakes; increase of wear	Design for proper cooling, minimise components near brakes	3/2	4
T.S.7	Main landing gears cannot be retracted	Wheel based engine does not fit in main landing gear bay	RETS system will not be used	Chief Structures and Materials must restrict dimensions for Power and Electronics department	2/1	5
T.M.1	Assembly not possible	Designed accuracies not feasible in manufacturing; poor manufacturing quality control	RETS parts should be adapted or scrapped	Check manufacturing procedures during design; have active quality control in manufacturing	3/2	3
T.M.2	Batch disposal (parts)	Material not meeting standards	Delay in delivery; extra manufacturing and material costs	Check supplier documentation	3/2	3
T.M.3	Manufacturer cannot meet requirements of wheel based engine	Desired performance is unfeasible	Failure of the RETS mission	Quality control of manufacturer, research on feasibility	2/1	5

6.3 Requirement Analysis

In this section, the requirements which are specific to the structures and materials subsystem, are shown. These requirements have been determined, during the Baseline and Midterm phase of the DSE [1, 3]. The meaning of the colours in the requirements can be seen in section 4.3. The requirements are split into three groups. These groups are the Stakeholder Requirements, Functional Requirements, and the Non-Functional Requirements. The compliance matrix, presented in section 6.10, shows that all requirements have been met for the listed relevant structural subsystem requirements.

Stakeholder Requirements:

- **[RETS-SH-TLREQ-07N]**: RETS shall use recyclable materials. *(Sustainability)*
- **[RETS-SH-TLREQ-03]**: The RETS installation shall be reversible, allowing the aircraft to operate in the same way as it would before the RETS.(Technical)
- **[RETS-SH-MAN-01]**: The RETS shall only use recognised and proven manufacturing techniques *(Technical)*
- **[RETS-SH-MAN-02]**: The materials used in the RETS shall be tailored to the manufacturing method. *(Technical)*
- **[RETS-SH-ABS-01]**: RETS shall limit the number of components on the aircraft. *(Technical)*
- **[RETS-SH-PAX-01**]: The RETS taxi shall not cause additional disturbances, specifically with regards to vibrations & noise, in comparison to current pushback and taxi methods. (Technical)
- **[RETS-SH-MTC-03]**: The RETS' non-critical components shall be replaceable. *(Technical)*
- **[RETS-SH-INS-01]**: The RETS' critical failure scenarios shall be clearly defined such that they are insurable. *(Legal)*

Functional Requirements:

- **[RETS-F-GEN-07]**: RETS shall include an emergency braking system

- **[RETS-F-SAF-03]** Incorrect (de)activation of RETS shall cause no severe damage to aircraft.
- **[RETS-F-SAF-04]** Incorrect (de)activation of RETS shall cause no severe damage to the system.
- **[RETS-F-SM-01]** RETS shall be able to safely sustain limit loads during its lifetime.
- **[RETS-F-SM-02]** A safety factor of at least 1.5, complying with regulations, shall be used for the determination of the maximum loads on the primary structure.
- **[RETS-F-SM-03]** A safety factor of at least 1.2, complying with regulations, shall be used for the determination of the maximum loads on the secondary structure.
- **[RETS-F-SM-04]** RETS shall be accessible for maintenance.
- **[RETS-F-SM-05]** RETS performance shall not be affected by corrosion.
- **[RETS-F-SM-06]** RETS shall protect the critical inner components against liquid damage.
- **[RETS-F-SM-07]** RETS structure shall provide easy access for assembly/disassembly.
- **[RETS-F-SM-08]** RETS shall withstand the complete operational temperature range of −40 °C to 60 °C.
- **[RETS-F-SM-09]** 70% of RETS parts shall be recyclable at End of Life.
- **[RETS-F-SM-10]** The RETS power source shall be enclosed in non-flammable material.
- **[RETS-F-SM-11]** The mass added to the aircraft due to the structures department will be limited to 440 kg.
- **[RETS-F-SM-12]** The mass added to the external vehicle due to the structures department will be limited to 17 675 kg.

Non-functional Requirements:

- **[RETS-NF-MAN-01]** The manufacturing processes shall apply Lean manufacturing methods.
- **[RETS-NF-MAN-02]** The materials shall have no harmful effects to the manufacturer when using appropriate PPE.
- **[RETS-NF-MAN-03]** The time constraints set for the manufacturer shall be 30 days.
- **[RETS-NF-LC-01]** Disposal of materials shall have no adverse effects on the environment
- **[RETS-NF-LC-02]** RETS shall include a manual with the correct recycling and disposing methods for materials.

6.4 Load Analysis

In this section the load analysis will be performed. The purpose of the load analysis is to determine the additional stress the system applies to the aircraft, and whether it can cope with this additional stress, but also to determine the type of loads the internal system will have to sustain. This is directly related to the mitigation of risks T.S.3A and T.S.3B shown in Table 6.1.

6.4.1 Nose Landing Gear

One important factor in the design of the external system is the loads it exerts on the nose landing gear. Landing gear structures are designed to carry the heavy loads of the aircraft, often multiplied by large load factors during landing. However, these are only vertical forces, and the horizontal forces experienced are often much lower. Nevertheless, both the maximum stress and the fatigue life of the landing gear must still be analysed with respect to these horizontal forces.

Currently, the most significant horizontal forces applied to the nose landing gear are during push-back. In the case of this design, the aircraft will also be pulled from gate to runway at higher accelerations and speeds. Hence, the pulling force will likely be higher and in turn, the fatigue on the nose wheel will also be greater.

As explained in chapter 5, the maximum acceleration will be partially generated by applying a 79 kN horizontal force on the nose landing gear. This will cause both an increase in the normal stress, due to bending, and in the shear stress, due to the horizontal load. Landing gears are very complex systems, and modelling them effectively requires advance software the team does not have access

to. Hence, the landing gear was modelled in two different methods. These are somewhat limiting methods, hence the actual loading case will be somewhere in between. However, by proving that the loading is acceptable in both cases, it is safe to assume that, in reality, it is likely to also be acceptable. The first model assumes the landing gear strut carries the entire load, and that, when locked, the root acts as though it were clamped. From this it is easy to get an approximation of the stresses in the landing gear. A free body diagram of this loading case strut can be found in Figure 6.1. The diameter of the strut is 170 mm (at and above the shock absorber), and the length of the compressed strut is 1486 mm [13]. In the free body diagram F_P and F_N represent the pulling force and the normal force experienced by the nose gear, respectively. The blue arrows represent the reaction forces and moments.
The second loading case assumes that the strut only carries the vertical load, so the appropriate weight percentage of the aircraft, and that the simplified locking mechanism carries the full horizontal load.

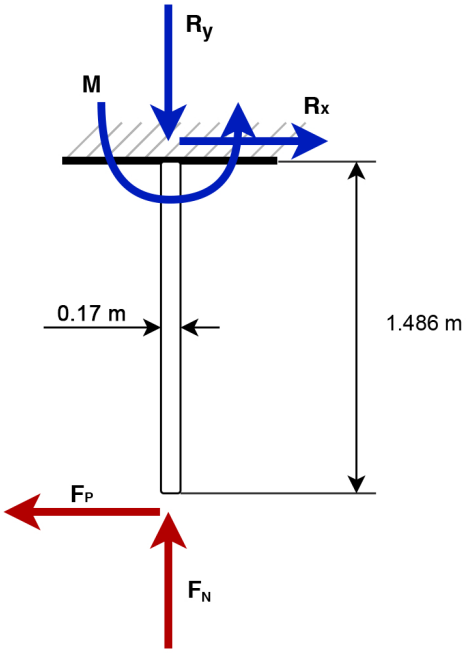

Figure 6.1: Free body diagram of the simplified strut during acceleration.

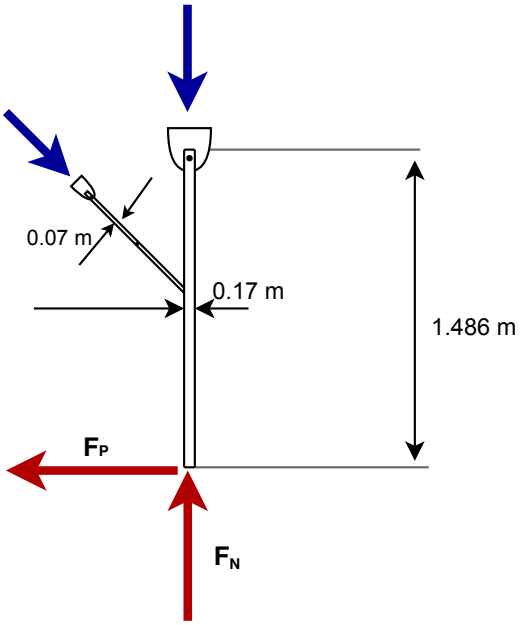

Figure 6.2: Simplified free body diagram of the simplified strut along with locking mechanism.

As, during operation, the nose gear must remain in place with respect to the aircraft, this amounts to a static problem. In the case described in Figure 6.1, by calculating the reaction forces and moments at the root due to the weight and the pulling force, in Figure 6.1, it can be found that:

$$R_x = 45\,863.712\,\text{N} \tag{6.1}$$

$$R_y = 79\,000\,\text{N} \tag{6.2}$$

$$M = 1.486 \cdot 79000 = 117\,394\,\text{Nm} \tag{6.3}$$

Given that the forces are applied at the free end of the strut, and that these are effectively point loads, the maximum bending moment will be at the root. Therefore, this is where the highest normal stress will occur, since the normal stress is given by Equation 6.4, where y is the distance from the neutral axis, I is the area moment of inertia, and A the cross-sectional area [40].

$$\sigma_{max} = \frac{M \cdot y}{I} + \frac{F_N}{A} = 245\,\text{MPa} \tag{6.4}$$

The maximum shear stress can be found from Equation 6.5, where Q is the multiplication of the

area above the neutral axis by its centroid ($\bar{y}' \cdot A'$) and t is the thickness, in this case the diameter, given that the maximum shear stress occurs at the neutral axis [40].

$$\tau_{max} = \frac{F_P \cdot Q}{I \cdot t} = 4.6\,\text{MPa} \tag{6.5}$$

However, this is well below σ_{max}. By constructing Mohr's circles to analyse the plane stress at different points on the circumference of the strut, it can be found that the highest shear stress occurs at the point where the direct stress is maximum. This absolute maximum shear stress is equal to half the maximum axial stress [40]. Furthermore, at this point, the shear stress due to the shear force itself is equal to zero (as Q in Equation 6.5 is equal to zero), and given that the normal stress is only present in one direction, the principal stress is equal to the calculated σ_{max} [40]. To summarise, the absolute maximum shear stress is 123 MPa and the principal stress is 245 MPa.

In the case of the loading shown in Figure 6.2, the strut carries the entire load until the connection, where it is assumed that the horizontal load is transferred into the locking mechanism. Using the same equations as previously it is found that the maximum normal stress is about half (the length is essentially halved) in the strut, at the connection point. In the rest of the strut, above the connection, only a portion of the normal stress is present, as there is no bending, and the vertical component of the force now in the locking mechanism also reduces the normal force. Finally, in the locking mechanism itself, given that it is assumed to carry the full horizontal pulling force, the force it experiences will be 136 782 N, since it is angled with respect to the horizontal. In order to prevent the landing gear from retracting, the downlock pin must also resist this force. Assuming the downlock pin has a diameter equal to that of the beams connected it to, which is equal to 7 cm, the shear stress it carries is given by Equation 6.6.

$$\tau = \frac{V \cdot Q}{I \cdot t} = 48\,\text{MPa} \tag{6.6}$$

Although, in reality the nose landing gear is a complex system of actuators, locks and struts, as can be seen Figure 6.3. Therefore the local stress at certain locks or actuators might be different than the maximum stress calculated above. For precise determination of load paths and stress distribution, simulation models of the landing gears should be used, however this will be for further development and simulation testing of the system.

Nonetheless, now that the stresses in the simplified landing gear have been determined, the material with which it is made must also be determined in order to verify whether the landing gear can support the loads. Most aircraft manufacturers outsource the design of the landing gear to third party companies, and information on the landing gears of specific aircraft are not always easy to come across. Nonetheless, it is known that high strength steel and/or titanium alloys are used [41]. In this case it will be assumed that steel 4340 alloy is used as it has the lowest yield strength [42], with a 470 MPa tensile yield strength, and a 430 MPa shear strength[85]. This clearly shows that the aircraft nose gear can sustain the loads applied, and the focus now shifts to fatigue.

To determine whether the fatigue life is affected, the current life of a landing gear must first be determined. According to Boeing, 18000 cycles (about 10 years) are performed by a landing gear before it must be replaced [86]. Based on the taxi routes discussed in chapter 4, the nose gear will be subject to an average of 8 loading cycles per taxi (acceleration/deceleration cycles). This value

[84] https://www.lavionnaire.fr/VocableLandingGear.php [accessed 28 June 2020]

[85] https://www.makeitfrom.com/material-properties/Annealed-4340-Ni-Cr-Mo-Steel [Accessed 12 June 2020]

[86] https://www.boeing.com/commercial/aeromagazine/articles/qtr_02_09/pdfs/AERO_Q209_article03.pdf [accessed 12 June 2020]

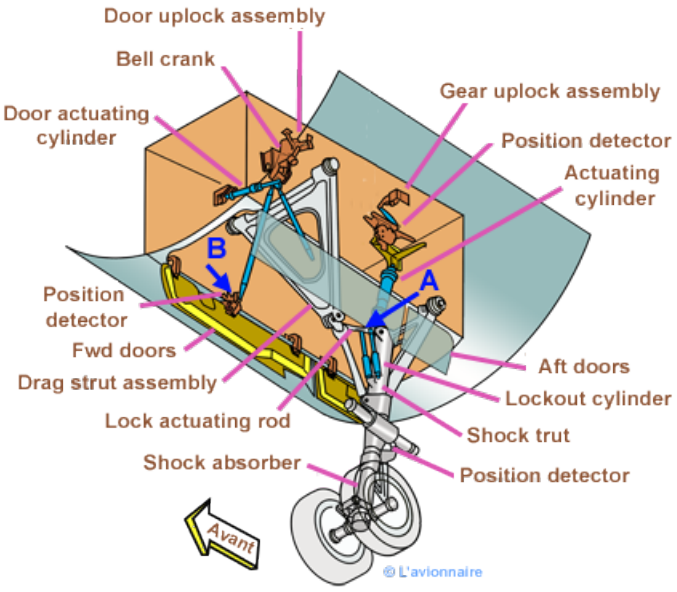

Figure 6.3: A320 nose landing gear diagram [84]

is on the higher end of the average taxi routes. This would then lead to 288 000 loading cycles over the life of the nose gear.

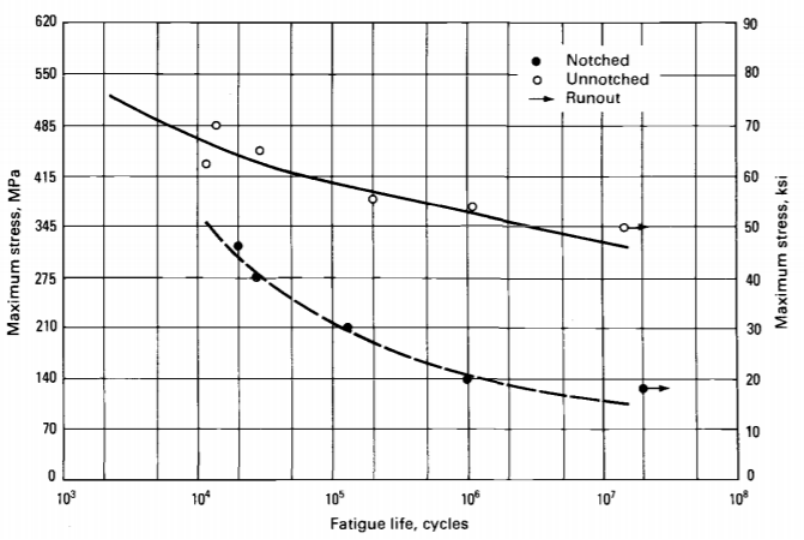

Figure 6.4: S-N curve Steel 4340 Alloy. [43]

Figure 6.4 displays the maximum stress against the number of cycles. The number of cycles the nose landing gear will be subjected to is on the lower end of the 10^5 cycle range, and, as seen in Figure 6.4, the maximum stress at this point is still above 245 MPa. Hence, whether the locking mechanism carries the entire horizontal load, or whether the strut takes the full brunt, the fatigue should not be a major concern either.

In any case, landing gears are rotable parts. This means that while a landing gear may need thorough inspection or maintenance, the aircraft can still fly with a replacement landing gear. Therefore, if issues with the nose landing gear structure are found during heavy maintenance C-checks, the landing gear can be replaced then. These C-check inspections happen every 18-24 months, which would allow for signs of fatigue to be noted and schedule more frequent inspections if necessary [87].

[87] https://www.qantasnewsroom.com.au/roo-tales/the-a-c-and-d-of-aircraft-maintenance/

6.4.2 Main Landing Gear

In the case of the main landing gear, the limiting case is different to the nose landing gear. Indeed, the wheels are powered by a motor and the force pushing the aircraft forwards is simply the reaction force due to friction between the wheel and the ground. Therefore the horizontal forces experienced by the main landing gear do not change compared to conventional taxi. The vertical forces and loads on the main landing gear are increased however. The engines which will be mounted to the landing gear will increase the load on the strut. However this should not be a problem since, according to FAA regulations (14 CFR §25.473, 2001), the aircraft should still be able to land at maximum take-off weight, and it is likely that a safety factor was added on top of this when designing the main landing gear.

The main concern stems from the internal system. Indeed, as it will be installed below the shock absorber it will experience a large deceleration, in the range of 4g. This is due to the fact that, below the shock absorber, the plane decelerates almost instantly. According to FAA regulations (14 CFR §25.473, 2001), the maximum landing sink rate is $10\,\mathrm{ft\,s^{-1}}$, which is the equivalent of $3.05\,\mathrm{m\,s^{-1}}$.

Applying basic dynamics equations can be done to determine the deceleration rate, assuming it is constant. These equations are Equation 6.7 and Equation 6.8, where x_0 and v_0 are the initial displacement and velocity, and x and v the final displacement and velocity, respectively. The a and t represent acceleration and time, which are unknown.

$$x = x_0 + v_0 \cdot t + \frac{1}{2} \cdot a \cdot t^2 \tag{6.7}$$

$$v = v_0 + a \cdot t \tag{6.8}$$

However, by rearranging these equations into Equation 6.9 and Equation 6.10, the time required to decelerate completely can be found. Once this is known, the deceleration can also be found. The total displacement is equal to the allowable deflection of the tyre, which is 32% [44]. Given that the diameter of the tyre is 49" and that the rim is 20", it can be found that the maximum deflection is $0.32 \cdot \frac{49-20}{2} = 4.64$", which is equivalent to 117.86 mm [88]. The initial speed is the sink rate mentioned previously, while the final speed is zero.

$$t = \frac{x - x_0}{\frac{v+v_0}{2}} = 0.077\,\mathrm{s} \tag{6.9}$$

$$a = \frac{v - v_0}{t} = 39.4\,\mathrm{m\,s^{-2}} \tag{6.10}$$

From Equation 6.10 it can then be found that the internal system will be subjected to a 4.02g deceleration. This case is the extreme dynamic loading case on the system, and should be added to the static load experienced by the system (in this case its own weight). Hence, when designing the attachment between the internal system and the landing gear, this must be taken into account.

6.5 External Vehicle

For the external vehicle, the decision has been made to start with an existing towbarless pushback truck instead of designing a whole new vehicle. The use of a baseline vehicle does require the need to modify the vehicle. However, it was decided that the use of an existing towbarless tractor was more beneficial to the whole design process, as it eliminated the need to design the aircraft

[88] https://www.jupitor.co.jp/pdf/michelin_aircraft.pdf

lifting system. The modified external vehicle will still have to comply with the requirements stated in section 6.2 and the Baseline Report [3, pp. 28-33].

The towbarless tractor selected as the baseline vehicle is the Goldhofer "Phoenix" AST-2X. The vehicle can be seen in Figure 6.5.

Figure 6.5: Goldhofer "Phoenix" AST-2X [89]

Figure 6.6: Goldhofer Phoenix AST-2X Lifting Cradle [89]

The Goldhofer "Phoenix" AST-2X was selected, as it is a towbarless aircraft tug which is designed to pushback and pull the A321, among other aircraft [3]. The use of this pushback tug will take away the need to design an aircraft nose gear (NG) lifting system and therefore also partially mitigates risk T.S.4 (see Table 6.1). The AST-2X has a width of 3.49 m and a length of 7.85 m, without the optional GPU [3]. The tug uses a hydrostatic drive system, which powers all four wheels and can provide a maximum tractive force of 120 kN [3]. The deadweight of the towbarless aircraft tug is 16.1 t [3].

6.5.1 Modifications to Goldhofer "Phoenix" AST-2X

It was decided that modifications done to the aircraft tug were not going to be done on the primary structure. Hence, changes to the design such as the addition of a third axle will not be performed, but modifications such as an upgrade to the drive train system will be done if necessary. As the system will have to be able to drive over the airport service roads, the weight per axle needs to be below 11 t to stay within the highway regulations [7]. This means that the total external vehicle weight can not be more than 22 t. The width of the external vehicle also needs to be less than 3.5 m to comply with the regulations [7].

The modifications to the Goldhofer "Phoenix" AST-2X which are deemed necessary, are the addition of a power connection between the tug and the aircraft, the placement of an additional power source, and a reduction in the width of the vehicle by reducing the width of the side panels. The width of the aircraft tug can also be reduced by reducing the total vehicle width, as the width of the lifting cradle can be reduced to the width of the nose landing gear (NLG) of the A321. The lifting cradle is the section of the towbarless tractor, where the aircraft NLG is locked to the tractor, and lifted by the tractor. The non-modified lifting cradle can be seen in Figure 6.6.

The total width of the NLG of the A321 was found to be 720 mm [13]. Based on manufacturer data on the Goldhofer AST-2X, and a CAD model which has been created, the cradle width was found to be 1.8 m [3]. As the external vehicle, is being designed to work with the A321, the decision has been taken to reduce the cradle width, and hence, the total vehicle width, by 700 mm. This resulted in a vehicle width reduction from 3.5 m to 2.8 m. Hence, the vehicle now complies with the highway lane width requirements [7]. The cradle width reduction of 700 mm resulted in a new cradle width of 1.1 m, which means that the NLG has 0.2 m available to each side when placed in the middle.

[89] https://www.goldhofer.com/en/towbarless-tractors-ast-2p-x-phoenix [accessed 8 June 2020]

This space allows for the non-perfect placing of the NLG into the aircraft tug. Even though the external vehicle has been modified to fit the Airbus A321, the width reduction does not influence its capability to tow comparable narrow-body airliners. Hence, the external vehicle can be used, to tow, Boeing 737s and Embraer E-Jets.

6.5.1.1 Power Connection

The power connection system will consist of two parts. An arm which is inspired by the European Robotic Arm (ERA) [45] and a set of connector wires with a connector inspired by the coil connector system used on lorries. The ERA is shown in Figure 6.7, and a coil connector system is shown in Figure 6.8.

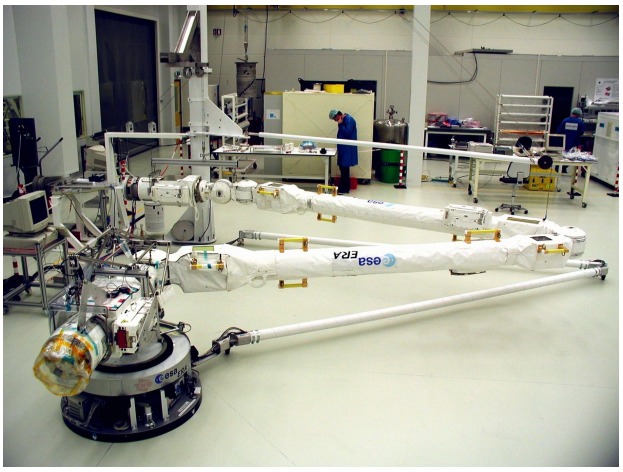

Figure 6.7: European Robotic Arm [90]

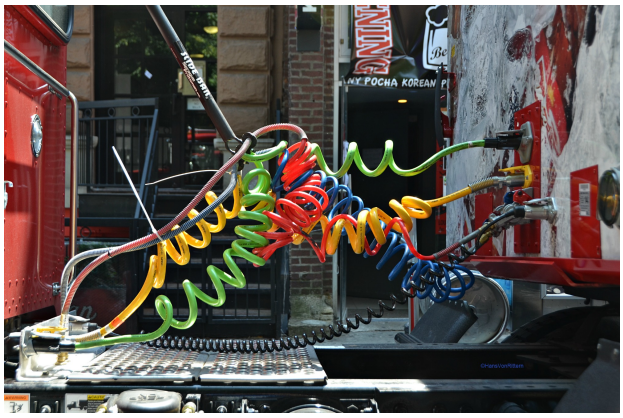

Figure 6.8: Coil Connector [91]

The arm is used to place and remove the power connector from the aircraft. When the system is not connected to the aircraft, the arm is stowed.. The stowed power connection arm can be seen in Figure 6.9. How the arm is stowed on the pushback tug, can be seen in Figure 6.10.

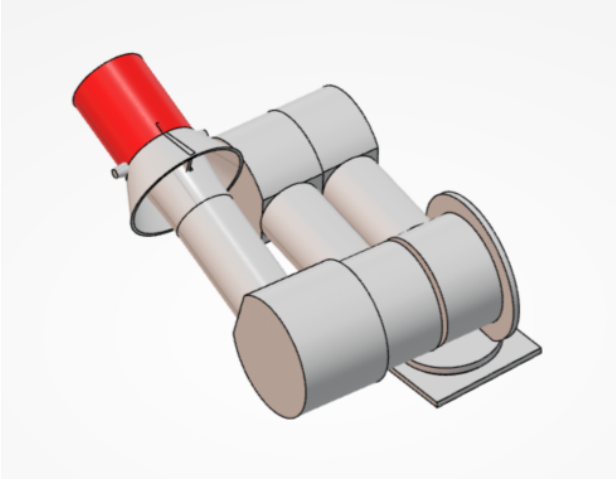

Figure 6.9: Stowed Power Connection Arm

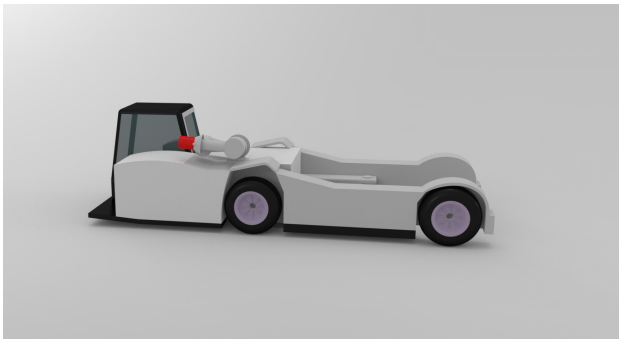

Figure 6.10: Stowed Power Connection Arm on Aircraft Tug

The 3D model of the Goldhofer "Phoenix" AST-2X, seen in Figure 6.10, has been made in CATIA V6, based on manufacturer documentation [3] and pictures, which are freely available online. This model was made, to help with the visualisation of the available space inside the aircraft tug, and to find locations where the required modifications could be placed.

[90] https://twitter.com/esa/status/1131558955052916736 [accessed 8 June 2020]
[91] https://newyorkcityinthewitofaneye.com/tag/truck-wires/ [accessed 8 June 2020]

The power connection arm, shown in Figure 6.9, will consist of three arms connected to a rotating base. The material used for the robotic arms will be Al-7075 T6, which is a readily available aerospace grade material, which can withstand the expected loads on the arm [92]. The rotating base will be connected, to the AST-2X. The middle arm will be extendable through a sliding mechanism placed inside the arm. A detailed look at how this mechanism will look can be seen, in Figure 6.11. The sliding mechanism will be operated using a hydraulic linear actuator. The rotational movement of the robotic arm, will be done using hydraulic motors which are placed in the joints (elbows) of the robotic arms [93]. The hydraulic motors will function as stepping motors that move the arm to the required position. When the power connection has been established, the hydraulic pressure in the arm is released, allowing the arm to move freely. The arm needs to move freely during taxi operations for RETS to be able to perform turning manoeuvres. To make sure that the power remains connected, the arm is only allowed to rotate around its base. The position of the arms is locked in place using the hydraulic stepping motors [93]. The power connection arm is shown in its extended position in Figure 6.12.

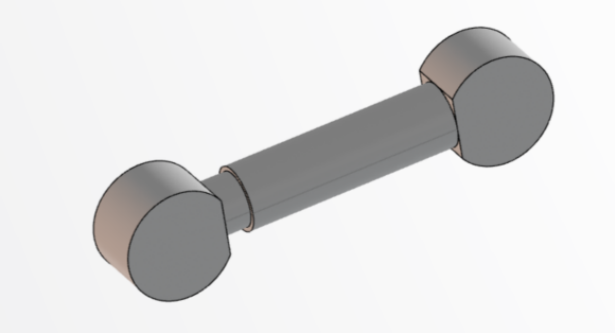

Figure 6.11: Extendable Arm in retracted position

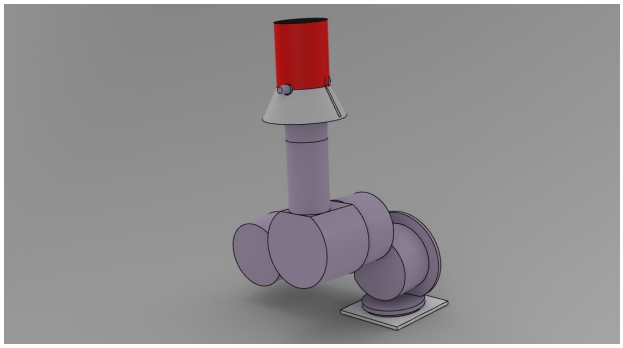

Figure 6.12: Power Connection Arm in extended Position

6.5.1.2 Drivetrain

The Goldhofer "Phoenix" AST-2X has a maximum speed of 32 km h^{-1} [3]. Following from the 30 kts, equivalent to 55.56 km h^{-1}, maximum speed requirement set in section 9.2, it can be concluded that the drivetrain of the aircraft tug needs to be modified. Following from the power and traction calculations done in chapter 5, it was found that the traction which could be provided by the aircraft tug was limiting. Hence, it was decided to install a 4-wheel drive system. This can be done relatively easily by using the same wheels, wheel hub gearing and hydro-static drive motor for the rear wheel as for the front wheels. A hydrostatic drive system, as used on the AST-2X, is a drive system which uses hydraulic fluid to drive a transmission and motor system [94]. A hydrostatic drive system can deliver a continuous power curve, and the system can also increase the torque delivered without the need to shift gears [94]. The use of this modification does require the use of a larger motor to get the required flow to power the wheels. The speed set in chapter 4 is 1.73 times greater than the original maximum speed of the AST-2X. It was decided to not modify the existing wheel hub gear ratios. This means that the hydraulic motor placed at each wheel has to spin 1.73 times faster. Based on the information provided by the motor manufacturer this is possible [95], but the system pressure and flow needs to be increased.

To increase the system pressure and the flow of the hydraulic oil through the system, a larger hydraulic pump will be needed. Besides the larger pump, the pump RPM also needs to be increased. To achieve a higher pump RPM, the engine power is increased.

[92] http://asm.matweb.com/search/SpecificMaterial.asp?bassnum=MA7075T6 [accessed 15 June 2020

[93] http://www.hydraulic-pump.info/hydraulic-engineering/electro-hydraulic-stepping-motors.html [accessed 25 June 2020]

[94] https://www.machinedesign.com/motors-drives/article/21831634/hydrostatic-drives [accessed 19 June 2020]

[95] https://www.kessler-axles.de/en/products/axles/steer-drive-axles/ [accessed 9 June 2020]

To be able to get an idea of the order of magnitude of the system pressures, engine and pump rpm needed, a set of basic hydro-static drive system sizing calculations will have to be performed. For this, the following equations will be used [46]:

$$\mathrm{Tp} = \frac{9549.3 \cdot \mathrm{Pi}}{\mathrm{Ne} \cdot \mathrm{IDR}} \tag{6.11}$$

$$P = \frac{\mathrm{Tp} \cdot 20\pi \cdot 0.95}{\mathrm{Dp}} \tag{6.12}$$

$$\mathrm{Tw} = \frac{\mathrm{Te}}{\mathrm{LR}} \tag{6.13}$$

$$\mathrm{Tm} = \frac{0.95 \cdot \mathrm{Dm} \cdot P}{20\pi} \tag{6.14}$$

$$\mathrm{FDR} = \frac{\mathrm{Tw}}{\mathrm{Tm} \cdot n} \tag{6.15}$$

$$\mathrm{Nm} = \frac{\mathrm{Vs} \cdot \mathrm{FDR} \cdot 2.65}{\mathrm{LR}} \tag{6.16}$$

Table 6.2: Input and Output Values for Hydrostatic Drive Sizing for a single wheel

Parameter	Value	Unit
Pi	149.88	kW
Ne	2250	RPM
IDR	1.3	-
Dp	127.8	$cm^3\,rev^{-1}$
Te	30×10^3	N
LR	0.584	m
Dm	89.16	$cm^3\,rev^{-1}$
n	0.92	-
Tp	489.32	Nm
P	229.3	bar
Tw	5.14×10^4	Nm
Tm	309.1	Nm
FDR	181	-
Nm	3.8×10^4	RPM

The design parameters used to design the hydro-static drive system for a single wheel can be seen in Table 6.2. The power needed for a single wheel (Pi) has been calculated in chapter 5. Based on comparable engines used in existing aircraft tugs [96], an engine with an engine RPM (Ne) of 2250 RPM was selected. The Input drive ratio (IDR) was set to 1.3, as this was in accordance to manufacturer specifications, and given design examples [46]. The Motor Displacement (Dm) and Pump Displacement (Dp) has also been based on the pumps and motors produced by Eaton [46]. The loaded radius of each wheel is the wheel radius. This has been determined from the data on the Goldhofer "Phoenix" AST-2X [3]. The total system efficiency (n) was set to 0.92. This is in correspondence with comparable systems [97] [46].

Using the previously mentioned input parameters, the following system parameters have been calculated. The pump input torque (Tp), system pressure (P), wheel torque (Tw), motor torque (Tm), Final Drive Ratio (FDR) and the maximum rated motor speed (Nm). These parameters are

[96] https://www.cummins.com/g-drive-engines/diesel-qsl9-series [accessed 9 June 2020]

[97] http://www.hydraulic-pump.info/hydraulic-engineering/hydrostatic-transmissions-advantages.html [accessed 10 June 2020]

also presented in Table 6.2. The values presented in Table 6.2 are for a single wheel. The total engine power, which is needed to drive the system is $149.88 \cdot 4 = 599.52$ kW. To provide the required hydraulic pressure and flow to power the wheel, 4 separate hydrostatic systems will be used. A hydrostatic system consists of a pump and motor. A more detailed layout of the proposed hydrostatic system can be found in Figure 5.9.

6.5.1.3 Power Generation

The exact layout and sizing of the power generation of the system has already been explained in depth in subsection 5.4.6. However there are certain important structural aspects with respect to the external vehicle that need to be taken into consideration, in particular if there is sufficient free space on the truck and the added weight. For the power generation a hybrid system, consisting out of a battery array and a turbo diesel engine, will be used.

As can be seen in subsection 5.4.7, six 100 kW h Tesla battery packs will be used to power the on-aircraft systems. The batteries will take up a total volume of 2.4 m^3 [98]. With 3.2 m^3 of space available inside the external vehicles, it can be concluded that the battery pack will fit inside the external vehicle. However, it can be concluded that the battery pack will not fit inside the external vehicle in their original form, hence, a new housing for the battery cells will have to be designed to make optimal use of the available space inside the external vehicle, and not influence the weight distribution of the external vehicle. The original Cummins QSL9-G7, a 4 cylinder, inline, turbo charged, air-cooled engine, takes up 3.794 m^3.[47] Its replacement, the MAN D2862 a turbo charged V12 engine [36], is in fact smaller. It is 497 mm shorter lengthwise and 132 mm shorter heightwise but 334 mm wider. These differences in dimension translate to a total volume of 3.466 m^3 or a 0.328 m^3 reduction on the truck. However, the more powerful D2862 will need a beefier cooling system amongst other supporting system that need to be bigger, which will compensate the reduction in volume. In subsection 5.4.7 it is mentioned that 160 L of diesel is needed, hence it should be double checked that the existing fuel tank is large enough. Unfortunately, Goldhofer has not made the volume of the fuel tank of the "Phoenix" public, but only states that it has enough for an entire shift. However a similar towbarless truck from a competitor called Aerospecialities, the TLD TPX-200, boasts a 155 L tank [99]. By combining the expected size of the fuel tank, and the required volume for the battery packs, it is save to assume that the 3.2 m^3 available inside the external vehicle is enough to accommodate the energy storage and power generators.

Due to the 11 t per axle weight limit set by the service roads, the truck can only weigh up to 22 t. As explained in subsection 6.5.1 the original weight of 16.1 t is taken as a starting point to size the entire energy power generation system. With the six Tesla battery arrays, weighing 625 kg[98] each, a heavier V12 turbo diesel weighing 1885 kg [36] and 136 L of diesel the final weight of the refurbished truck was estimated to be 20 798 kg. This leaves margin to include the weight of additional or components that are not accounted for upon till this point at a later stage in the design. The bigger oil reservoir, engine cooling system, vehicle battery (engine starter) are good examples of such non-included components in the weight analysis.

6.6 Wheel-Based Engine

This subsection will describe the necessary modifications to the MLG structure. First the general structure of the MLG will be discussed, specifically how the electrical motor and the accompanying gears will be placed. Next, the gears will be sized and its relative location to the MLG strut will be determined. Lastly, the loads on the structural element connecting the gears and electrical engine with the MLG structure will be analysed.

[98] https://iaspub.epa.gov/otaqpub/display_file.jsp?docid=39834flag=1 [accessed 20 June 2020]

[99] https://www.aerospecialties.com/aviation-ground-support-equipment-gse-products/tld-ground-support-equipment/tld-tpx-200-towbarless-aircraft-pushback-tractor/ [accessed 20 June 2020]

6.6.1 MLG Structure

In order to properly size and position the components needed for the taxi system, a proper understanding of the current MLG structure must first be established. The loads that the main strut and the axle will experience will most likely be very high. Interfering with these load paths by changing or modifying these primary structures would therefore be an intensive redesign task. As the taxi system is designed as an additional (retrofit) system, the decision has been made to only add the needed components to the already existing parts.

The most important aspect of the structure is the 3D spacing of all components. This is due to the limited availability of space for the new system components as the gear must be able to retract in the same retraction bay. To visualise this space, a 3D CAD model of the MLG has been created in CATIA software (v6). The main dimensions of the landing gear structure have been specified in the Airport Planning Manual [13, pp 92]. However, these sketches do not include the detailed information necessary for the system to be properly sized and positioned. The braking system located in every wheel is of especially great importance as the taxi system must not interfere with this critical component. Therefore, the 3D model has been fitted with a braking system with dimensions estimated on available images [48]. Note that the CAD model does not include the wiring and tubing as these will be easier to relocate when the motor is placed.

6.6.2 Motor and Gear Placement

As discussed in section 5.4, an electric motor will be used to create part of the torque required to set the aircraft in motion. On each MLG strut, the motor will be placed on the rear side of the MLG strut. The main reason for this is to keep sufficient air flow for the cooling of the brakes and therefore the mitigation of risk T.S.6 (see Table 6.1). Besides, the motor including the gearing system will then be better protected from FOD coming from the front of the aircraft and/or runway. The physical connection to the motor will for now be designed as an extension of the existing MLG strut. This will make sure all added elements will be able to be removed and replaced for maintenance purposes. It should be noted that further analysis should be done to design this structural element to be detachable for retrofit purposes and to maintain proper load paths.

The part that is connecting the electric motor to the MLG strut can be extended to also serve as a connecting element of the gears that will be designed. With this approach, weight could be saved with respect to two separate connections. Note that the focus in this design iteration is on the gear sizing and therefore the supporting strut will only be subject to a simple preliminary load analysis. Depending on the number of gears, the location of each gear will be chosen based on the required alignment with other gears and the proximity to the strut and MLG wheel. In this way, the air flow needed for brake cooling will be taken into account. The goal will be to position the gears as much to the rear as possible to ensure proper air flow from the front. Besides, the engine must also not be positioned too far from the strut as this will require a larger and longer connection which will add more weight to the on board system.

Eventually the torque from the electric motor must be transferred to one or two MLG wheels. Since the electric motor only has an axle on one side, the decision has been made to only power one of the MLG wheels as two powered wheels would require a very complicated and therefore heavier differential gear design. In section 7.5 it will be discussed that a powered outer wheel will have slight advantages over a powered inner wheel. Therefore, the outer wheel will be used. As it is desired to keep the current structure intact as much as possible, it has been decided that the best way to transfer the torque to the wheel is via a gear mounted on the wheel rim. This will make sure that the current axle configuration is kept and assures that the aircraft brakes can still be applied in the exact same way as is done without the taxi system. It will also not restrict the air flow for brake cooling too much as the gear will be ring shaped. The gear will be mounted on the rim of the wheel with ten small supporting struts, yet to be designed in a later design phase. Therefore, the only major adaptation of the MLG will be the change of two MLG wheels in total while the rest of the MLG structure will remain the same.

The exact dimensions of the rim have not been specified. Therefore, it is estimated that the rim extends 62 mm towards the centre of the wheel. The brakes have been modelled inside the wheel rim. However, for adequate margins, the wheel gear will have a slightly larger inner radius than the rim of 329 mm. A consequence of this relatively large inner radius is that this will influence the behaviour in case of a flat tyre. Given a double flat tyre of the MLG, the margin is just over 205 mm [13, pp 138]. This would mean that the wheel gear would touch the ground in case of this double flat tyre. Because of a fail-safe design of the wheel gear supporting struts to to the wheel rim, the gear would then break off the wheel rim such that 'normal' flat tyre behaviour is experienced. Consequently, besides the gear, also the wheel needs to be replaced. Since it seems that a double flat tyre is quite rare, a relatively large inner gear radius is accepted. The behaviour of a single flat tyre is not discussed in the A321 Airport Planning Manual [13]. Similarly for this scenario, it is expected that occurrence will be low and consequences will also be lower than a double flat tyre.

6.6.3 Gear Analysis

Besides the existing MLG strut, also the implemented gears will be subject to a load analysis to mitigate the identified risk T.S.1 (see Table 6.1). The most critical element of the gear will be the teeth. This element will be checked for bending strength and surface durability which are deemed the most critical loading cases of the gear teeth [49, pp 28]. For the bending strength, Equation 6.17 and 6.18 will be used [100]. Equation 6.17 calculates the actual bending stress σ_F that is experienced by a tooth when it is in contact with another gears' tooth. The main variables are the tangential force F_t, the gear module m_n and the facewidth b. The tangential force is simply calculated by a division of the applied torque by the effective gear radius. The torque is multiplied from one gear to another by the gearing ratio. However, for spur gears, an efficiency of 98% must also be taken into account [101]. The gear module is a specific number that represents the size of the gear. For two connecting gears, this module must be equal for proper working as this makes sure the dimensions of the teeth and locking places are equivalent for both gears. The gear module can be calculated by dividing the reference diameter by the number of teeth. Facewidth is the width of each tooth.

Besides these three main variables, eight other coefficients are taken into account. These are all dependent on different aspects of the gear and are listed in Table 6.3. The values of each coefficient used in the calculation are also indicated in that same table. Note that the determination of these values is very detailed and therefore left out of this report. These variables are also present in Equation 6.18 to calculate the limiting tangential force with the help of a limiting stress σ_{Flim} originating from a chosen material. The material with the highest σ_{Flim} is a structural alloy steel. The alloy SNC815 has a limiting stress of 491 MPa [100]. Although this alloy is expected to have a relatively high density with respect to other metals it is still being considered. This is due to the fact that the strength is found to be more important than weight for this specific structural element as failure would be catastrophic for the mission objective.

$$\sigma_F = F_t \frac{Y_F Y_\epsilon Y_\beta K_V K_O}{m_n b K_L K_{FX}} S_F \tag{6.17}$$

$$F_{tlim} = \sigma_{Flim} \frac{m_n b K_L K_{FX}}{Y_F Y_\epsilon Y_\beta K_V K_O S_F} \tag{6.18}$$

[100] https://khkgears.net/new/gear_knowledge/gear_technical_reference/bending-strength-of-spur-and-helical-gears.html [cited 10 June 2020]

[101] https://khkgears.net/new/gear_knowledge/abcs_of_gears-b/gear_types_and_characteristics.html [cited 17 June 2020]

Table 6.3: Coefficients for the bending stress calculation of the gear teeth.

Coefficient	Dependency	Value
Tooth Profile Factor Y_F	Number of teeth and its shape	2.45
Load Sharing Factor Y_ϵ	Gear diameter and gearing ratio	0.592
Helix Angle Factor Y_β	Helix angle	1.0
Life Factor K_L	Cyclic repetitions	1.2
Root Stress Size Factor K_{FX}	Independent, always 1.0	1.0
Dynamic Load Factor K_V	Tangential speed, tooth shape	1.5
Overload Factor K_O	Load impact	1.25
Safety Factor S_H	Independent, 1.2 minimal	1.2

Equation 6.17 and Equation 6.18 can now be used to obtain an actual stress σ_F and a limiting tangential force F_{tlim} of a gear tooth. A gear is designed with the correct parameters if the limiting tangential force F_{tlim} is higher than the actual tangential force F_t. Similarly, the limiting stress σ_{Flim} should be larger than the actual stress σ_F that is experienced in the tooth.

To determine the limiting values for a proper surface durability, the same approach will be followed. However, now Equation 6.19 and Equation 6.20 [102] will be used with the coefficients provided in Table 6.4. The main objective will now also be to find a limiting tangential force F_{tlim} and a limiting (Hertz) stress σ_{Hlim}. Again the facewidth b is used as well as the reference diameter d. The gearing ratio is also taken into account as variable i. For the same structural steel allow SNC815, the limiting Hertz stress will be 1.57 GPa.

$$\sigma_H = \sqrt{\frac{F_t}{db}\frac{i+1}{i}}\frac{Z_H Z_M Z_\epsilon Z_\beta}{K_{HL} Z_L Z_R Z_V Z_W K_{HX}} S_P \sqrt{K_{H\beta} K_V K_O} \tag{6.19}$$

$$F_{tlim} = db\frac{i}{i+1}\left(\frac{K_{HL} Z_L Z_R Z_V Z_W K_{HX}}{Z_H Z_M Z_\epsilon Z_\beta}\sigma_{Hlim}\right)^2 \frac{1}{K_{H\beta} K_V K_O {S_P}^2} \tag{6.20}$$

Table 6.4: Coefficients for the surface durability calculation of the gear teeth.

Coefficient	Dependency	Value
Zone Factor Z_H	Helix angle	2.495
Material Factor Z_M	Gear material	189805
Contact Ratio Factor Z_ϵ	Independent, always 1.0	1.0
Helix Angle Factor Z_β	Independent, assumed 1.0	1.0
Life Factor $K_H L$	Cyclic repetitions	1.4
Lubricant Factor Z_L	Lubrication	1.0
Surface Roughness Factor Z_R	Average material roughness	0.9
Lubrication Speed Factor Z_V	Tangential speed	0.97
Hardness Ratio Factor Z_W	Gear material hardness	1.05
Size Factor K_{HX}	Independent, assumed 1.0	1.0
Longitudinal Load Distribution Factor $K_{H\beta}$	Tooth contact loading	1.1
Safety Factor for Pitting S_P	Advised 1.15 minimal	1.15

[102] https://khkgears.net/new/gear_knowledge/gear_technical_reference/surface-durability-of-spur-and-helical-gears.html [cited 10 June 2020]

6.6.3.1 Final Gear Design

As discussed in subsection 5.4.7, the EMRAX268 electric motor will be used to provide the torque to the MLG wheel. The specifications of this motor together with the maximum MLG wheel RPM have been used as input for the final gear design. The gears have been sized for the maximum torque required for the accelerations as stated in subsection 5.4.6. Therefore, a maximum motor torque of 0.5 kN m and a maximum RPM of 4500 have been used as fixed starting values. Another parameter that will be fixed during the gear design is the diameter of the gear fitted on the wheel rim. This diameter is found to be 750 mm. Therefore the dimension of the gear is exceeding the flat tyre clearing discussed in subsection 6.6.2. Also the diameter of the first possible gear, pinion gear, is set to a fixed value. This is the minimum diameter possible within the boundaries of equations 6.17, 6.18, 6.19 and 6.20. The minimum diameter, regardless of the number of teeth, is found to be 88 mm.

The next step will be to decide on the gearing ratio. As discussed in subsection 5.4.6, the gearing ratio to be used will be 19. This mainly comes from the boundaries set by the power subsystem. From a structural perspective, the maximum gearing ratio that could have been achieved is 22. This is based on the equations discussed in the beginning of this subsection used with the described fixed parameters. From the same equations it can also be concluded that the simplest form of gear design, only two adjacent gears, will fail at the most critical element when using the final gearing ratio of 19. Moreover, this design would not result in two gears with the same module.

Given this failure, a different gear design has been chosen. Adding one extra gear would not solve the problem as this would not change the number of teeth of the first and last gear for the given gear ratio and thus similar failure as using two gears would occur. To achieve the chosen gearing ratio, four gears will be used in the final design. This will consist of two times two corresponding gears with the same gear module. The two intermediate gears will then be connected by a shaft to transfer the torque from the first set of gears to the second as shown in Figure 6.13b. The main advantage of this design is the extra design space that is available with respect to only having multiple gears connected to each other. With the boundaries set by Equation 6.17 through 6.20 one final design with the lowest gear diameters possible has been chosen as the final gear design. This final gear design including the electrical motor is shown by Figure 6.13a.

With the given coefficients in Table 6.3 and Table 6.4, the bending and the surface durability have been checked for this final gear design. For a facewidth of 40 mm for the ring gear combination and 50 mm for the pinion gear combination, this resulted in lower forces and stresses than the limiting forces and stresses as can be seen in Table 6.5. Besides these parameters, the gear diameter, number of teeth, torque and RPM are also indicated. Lastly also the weight has been given for the chosen SNC815 steel alloy with a density of 7700 kg m^{-3} [103]. The price of this steel alloy is found to be 2 USD kg^{-1} [104]. The total material cost for two sets of gears would then be 239.17 USD.

[103] https://www.steelgr.com/Steel-Grades/Carbon-Steel/snc815.html [cited 17 June 2020]

[104] https://wuxihuihengjia.en.made-in-china.com/product/TsenGjbUCMcV/China-JIS-Snc815-Steel-Bar-12crni3-Steel-Price-Per-Kg-of-Alloy-Steel-Rod.html [cited 17 June 2020]

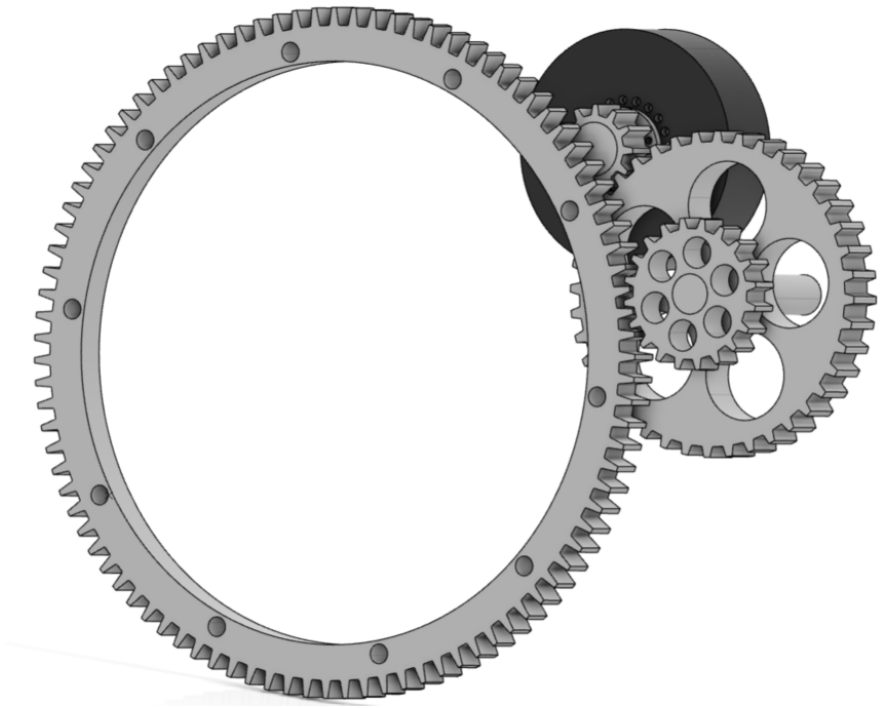

(a) A complete overview of the final gear design including electric motor

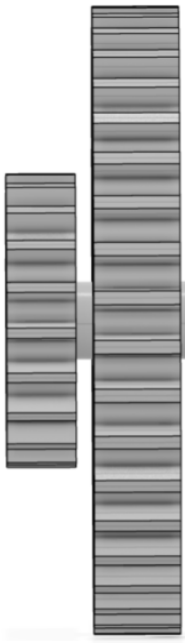

(b) The two intermediate gears connected by a shaft

Figure 6.13: Graphical overviews of the final gear design

Table 6.5: Final gear design parameters. (Bold indicates fixed value)

Design Parameter	**Ring Gear**	**Intermediate 2**	**Intermediate 1**	**Pinion Gear**
Torque $[kNm]$	9.12	1.96	1.96	**0.5**
RPM [-]	**232**	1102	1102	4408
Teeth	95	20	40	10
Diameter $[mm]$	750	157.9	352	**88**
Facewidth b $[mm]$	40	40	50	50
Weight $[kg]$	30.84	3.54	24.31	1.10
Tangential Force F_t $[kN]$	24.3	24.8	11.1	22.7
Actual Stress σ_f $[MPa]$	209	214	98.8	140
Actual Hertz Stress σ_H $[MPa]$	604	1329	542	1549
Limiting Tangential Force F_{tlim} $[kN]$	57.0	34.6	79.4	23.3
Limiting Stress σ_{flim} $[MPa]$		491		
Limiting Hertz Stress σ_{Hlim} $[GPa]$		1.57		

With all the discussed parameters, the final gear design has been modelled into the CAD model. This final gear design on the MLG can bee seen in Figure 6.14. However it should be noted that this gear design only takes into account the described bending stress and the surface durability of the teeth. Therefore a more detailed analysis must be done in future design iterations. One of the aspects to look at is the effect of the holes created in the gears. These holes have been designed for weight saving purposes, however the effect on the load carrying capacity has not been analysed yet.

Related to the gears is also the fact that all gears are exposed to the environment. This has an effect on for example the corrosion and wear of the gears. These exposing effects must be investigated further to see if a different material might be better or a special coating should be applied. Also for the motor it holds that the effects of rain and other environmental conditions must be analysed.

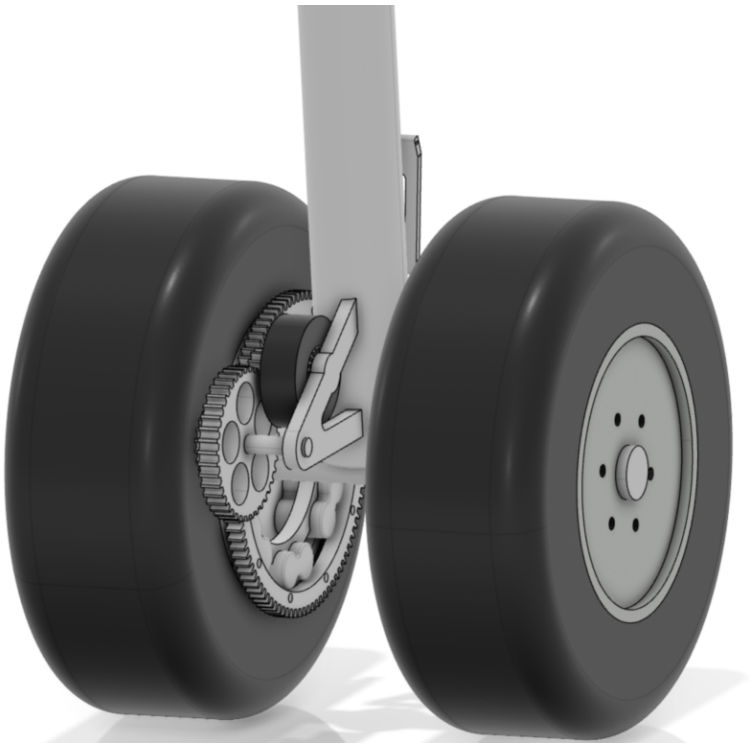

Figure 6.14: Final gear design located on the left MLG

6.6.3.2 Fail-Safe Design

Due to **[RETS-SH-TLREQ-08]**, the complete RETS must be designed fail-safe. The above described gear design is not yet fail-safe as the gears will be coupled at all times. Particularly during landing and take-off, high wheel RPM and thus high gear RPM is expected. This has also been identified in section 5.5 as an electrical risk **T.P.8**. However, the gears have also not been designed to sustain loads above a taxi speed of 30 kts. To achieve the desired fail-safe design, a spring cylinder is considered. A sketch of such a cylinder can be found in Figure 6.15. If the cylinder is activated, pressure will be applied to one side of the cylinder which will force the spring to be pushed. This will then couple the gears. When deactivated, the pressure will drop and therefore the spring will force the gears to decouple again, making it safe for take-off and landing wheel RPM. Within the operations of the RETS, the activation and deactivation can be linked to the physical coupling of the pushback truck and the airplane as described in subsubsection 6.5.1.1. The placement of the spring cylinder can be incorporated in the supporting strut design. This will also result in a limited estimated added mass of 3 kg.

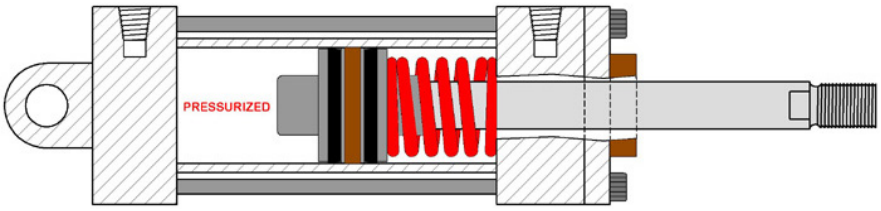

Figure 6.15: Sketch of a spring cylinder [105]

6.6.4 Analysis of Supporting Structure

As discussed in section 6.4, the internal system will be subjected to a large deceleration. A strong supporting structure is therefore required. The load that the structure must support is given in Equation 6.21, where the total load is the sum of the dynamic load, due to deceleration, and static

[105] https://www.peninsularcylinders.com/HH_Links/HH_LH_NFPA_Cylinders/HH_LH_NFPA_Spring%20Extend%20and%20Return.htm [Cited 26 June 2020]

load, which is simply the weight of the system components. The components in question are the pinion gear and the two intermediate gears, as well as the internal motor.

$$F_{total} = F_{dynamic} + F_{static} = 49.45 * 4 * 9.81 + 49.45 * 9.81 = 2433.9\,\text{N} \tag{6.21}$$

The supporting structure is one triangular shaped member attached to the main landing gear. Although the structure is one rigid member, it was analysed as two separate members. Furthermore, to insure a large enough safety margin, each member was analysed under the assumption that each member would carry the full load, as shown in Figure 6.16.

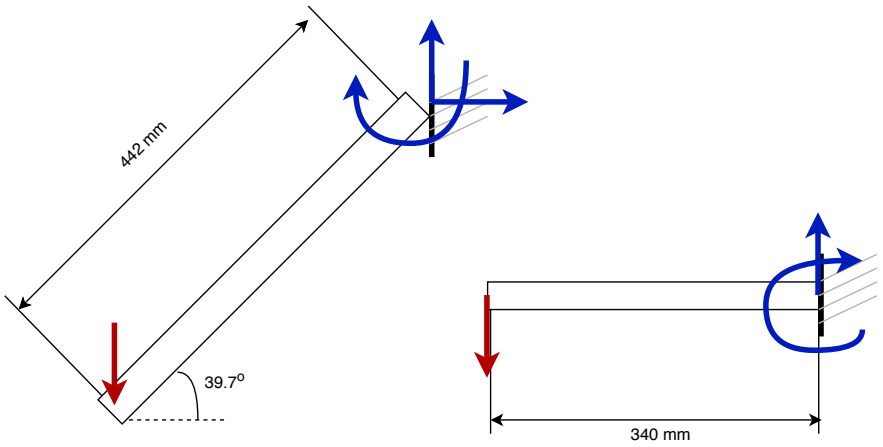

Figure 6.16: Free body diagram of split internal design support.

In the case of the horizontal member, it would be subject to bending and shear. Assuming that all the weight is applied as a point load at the end of the member, the reaction moment would be equal to 827.5 N m. Given the selected width and height of the cross-section, 35 mm and 65 mm, the maximum normal stress was found to be 33.57 MPa.

$$\sigma_{max} = \frac{M \cdot y}{I} = 33.57\,\text{MPa} \tag{6.22}$$

With regards to the shear stress, the equation is as shown in Equation 6.23, where the shear force is the full 2433.9 N. This leads to a shear stress of 3.2 MPa, however this is a much lower value than the normal stress, hence the actual experienced shear stress would be half the normal stress, or 16.785 MPa.

$$\tau_{max} = \frac{V \cdot Q}{I \cdot t} = 3.2\,\text{MPa} \tag{6.23}$$

By performing the same calculations on the angled member, it can be seen that it has a normal force component as well as the shear and bending load. The angled member has the same width as the horizontal member, but has a slightly larger height of 70 mm. The larger height leads to a larger area and moment of inertia, and ultimately lower stresses. Indeed, from Equation 6.24, where F is the axial component of the load, it can be seen that the maximum normal stress is 29.6 MPa, and therefore the maximum shear stress 14.8 MPa.

$$\sigma_{max} = \frac{M \cdot y}{I} + \frac{F}{A} = 29.6\,\text{MPa} \tag{6.24}$$

The stresses calculated above are over-estimations, but they show that the system will not fail under the loads of a hard landing. Indeed, the support will be made of the same material as the

main landing gear, assumed to be a Steel 4340 Alloy. These overestimated stresses are only around 7% of the yield stresses, and will not cause significant fatigue.

It is worth noting that the support bears more resemblance to a truss. Calculations were also performed this way, and the stresses found did not amount to more than 2 MPa. This is due to the fact that in truss members only the normal force is considered, whereas in reality shear and bending would add extra stress. The stresses would therefore have been slightly underestimated.

Given the overestimation at this point, in an iteration to come, the connection should be designed in a more detailed way. As the weight of this element would be 15.59 kg for the given alloy, weight reductions will be possible to achieve when downsizing this structural element. The cost of the current supporting structure will be 54.99 USD kg^{-1}

6.7 Aircraft and Tug Connection

Within this section the connection between the Aircraft and Tug is discussed. The power connection is discussed in subsection 6.7.1. The general coupling and safety features are discussed in sections 6.7.2 and 6.7.3 respectively.

6.7.1 Power Connection on Aircraft

To be able to provide energy to power the Wheel-Based Engine, described in section 6.6, a receptacle for the power connection arm, described in subsubsection 6.5.1.1, needs to be placed inside the aircraft. It has been decided, to place the receptacle in front of the nose landing gear bay, and slightly to the left of the aircraft centreline when looking in flight direction. In Figure 6.17, the extended power connection arm can be seen plugged into the aircraft. When the power connection is established, the power connection arm retracts itself, leaving the plug in place. Using coil connector cabling the aircraft is powered.

To make sure that the power connection on the aircraft does not influence the aerodynamics of the aircraft, and is protected from the elements, a cover, has been designed, which can be seen in Figure 6.18. The cover consists of a door which is connected to the aircraft skin using hinges and a locking mechanism (coloured black in Figure 6.18), which is used to make sure that the door remains closed during flight. As the plug is connected, to the power connection arm, the plug is always in the correct position to be connected. Hence, a pin is added to the side of the plug, which unlocks the locking mechanism. When the door is unlocked, the plug is used to push against the door and open it. The door has a maximum opening limit. Hence, it can be used to guide the plug into the correct position. When the plug is retracted, the door falls close using gravity, and when it has fallen shut, the locking mechanism engages itself. Gravity can be used to close the door, as the maximum opening angle is limited such that the centre of gravity of the door is on the inside of the hole in the fuselage, hence, when the plug is retracted the door will fall shut. In case the plug is retracted to slow for gravity to engage the locking mechanism, a spring inside the hinge will make sure that the required force to engage the locking mechanism is applied in all cases.

The whole aircraft and aircraft tug combination is shown in Figure 6.19.

Figure 6.17: Power Connection between Tug and Aircraft

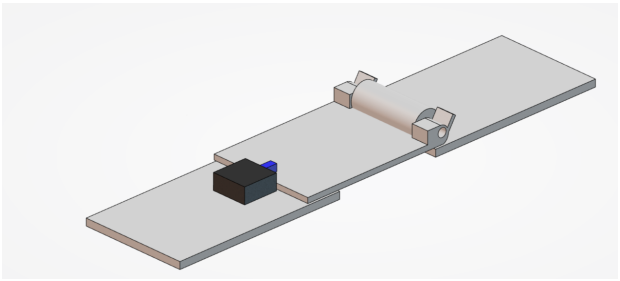

Figure 6.18: Aircraft Power Connection Protector

Figure 6.19: Airbus A320 Family and Aircraft Tug

6.7.2 General Coupling

The connection between the aircraft and the towbarless tractor is mechanical. It consists of a lifting cradle and a set of doors which lock the NLG into place. When the tug wants to attach itself to the aircraft, it drives towards the NLG, stops at the NLG, and closes the doors. When the doors are closed, the lifting mechanism is activated, and the NLG is lifted from the ground.

6.7.3 Safety Features

To make sure that the system will have no adverse effects during emergencies, The emergency decoupling of the aircraft and the power connection, and the grounding of the system will be discussed in the following sections.

6.7.3.1 Aircraft Decoupling

As the Goldhofer "Phoenix" AST-2X, is being used as a baseline towbarless tractor, it is safe to assume that the safety features present on this vehicle, will also be present on the modified vehicle which is used in the design. This means that emergency decoupling can be performed in the same way as the Goldhofer "Phoenix" AST-2X. Emergency decoupling is performed by quickly lowering

the lifting cradle, and opening the locking doors. According to manufacturer data, this emergency release procedure can be done in less than 30 s [3].

6.7.3.2 Power Connection Decoupling

In an emergency, it may also be necessary for the power connection to decouple. To prevent unnecessary delays in an emergency, the power connection needs to be able to decouple itself in less or equal time that it takes for the towbarless tractor to decouple itself from the aircraft. Hence, during an emergency, the power plug can be removed by pulling it out of the receptacle on the aircraft, without the need for the robotic arm to connect. This unplugging will be done using a metallic wire, that is connected to a spool, which can apply enough force to remove the plug.

6.7.3.3 Grounding

To make sure that a short circuit within the system does not influence the safety of the system, and the passengers, a grounding system will have to be present on the RETS. When the external vehicle is connected, the grounding will be done through a grounding cable present in the power connection, and the external vehicle. When the external vehicle is not connected, the grounding will be done through the landing gears. However, the detailed grounding design will have to be performed during the detailed design.

6.8 Risk and Sustainability

6.8.1 New Structural Risks

With the detailed design within the structural subsystem, new knowledge has been gained on the risks of the RETS. This new knowledge also came with the identification of new structural risks which can be found in Table 6.6. In this table, the cause, consequence and mitigation of these new risks are also listed. The probability of failure p_f and the consequence of failure c_f after mitigation have been estimated in accordance with Table 4.1 and Table 4.2.

Table 6.6: Newly identified risks related to structures

ID	Risk	Risk Cause	Risk Consequence	Mitigation	p_f/ $p_{f_{\text{mit}}}$	c_f/ $c_{f_{\text{mit}}}$
T.S.8	External Vehicle Drive System Failure	Hydraulic leak; Failure of Gearboxes	Delays in Taxi; Holdups on taxiways due to stationary aircraft; External vehicle must undergo extensive maintenance	Monitor Hydraulic System and gearboxes; Make sure adequate warning is given in case of possible system failure; Perform maintenance on the whole system after a set amount of cycles/hours	3/2	4
T.S.9	Failure of Power connection System	Robotic Arm Structural Failure; Robotic Arm Drive System Failure: Failure of the Plug	Power cannot be transferred from tug to aircraft, hence, system on aircraft cannot function; Taxi Performance Reduced; Power connection system must undergo maintenance	Allow for use of the External Vehicle as a pushback tug only; Perform pushback and continue on engine taxi	2	3/2
T.S.10	External vehicle exceeds service road limits	Materials /structure used too heavy; structure used not optimised for weight and strength	External vehicle must drive over taxiways, creating extra congestion	Optimise for weight and strength/stiffness; Use lighter materials and structures	3/2	4/3
T.M.4	External vehicle engine performance cannot be met	Desired Performance is Unfeasible	Failure of RETS mission	Design for existing engines; Perform market research on available components	2/1	5
T.M.5	Material used cannot meet recycling requirements	Sustainability not considered well enough during material selection	At EOL, system cannot be recycled in desired ways	Analyse recyclability and sustainability of selected materials; Analyse recycling methods	2/1	4

6.8.2 Sustainability

The design of the structure and the selection of the materials also plays a role in sustainability. The main aspects of sustainability are the production and recyclability of the materials used in the design.

In the case of the internal, wheel-based part of the system, the entirety of the components, with the exception of the motors, are made of steel alloys. As explained in the Midterm Report, the recycling of metals is already a fairly well developed process which will likely get more efficient in the future. Furthermore, compared to other metals, the energy required to recycle steel alloys is lower. Indeed, the remelting and refining process for steel alloys stands at around $1.5\,\mathrm{GJ\,t^{-1}}$, whereas for aluminium it is more in the range of $7.6\,\mathrm{GJ\,t^{-1}}$ [1].

The external vehicle, just like any other vehicle, can be recycled for parts. Like most vehicles in the commercial automotive industry, it is likely predominantly made of high-strength steel [50]. Therefore, the same recycling processes apply to the most part of the external vehicle chassis as to the internal system. This is not the only part of the vehicle that can be recycled, indeed lots of the parts used in the engine are metals which can just as easily be recycled. Batteries and tyre rubber

are also among commonly recycled parts of automotive vehicles [106]. A more detailed recyclability analysis of the batteries is provided in subsubsection 5.5.1.1.

With regards to production, using recycled materials to build the system would also prove to be more sustainable. Firstly, by doing so, the team would be actively contributing to the reduction of global waste. Furthermore, the energy costs of recycling metals are much lower than primary production of metals. Indeed, the total energy required for primary production of steel amount to around 79 GJ of energy, which translated to around 5.3 t of CO_2. In comparison, the numbers for the total production process of recycled steel are closer to 26 GJ and 1.6 t of CO_2 [51]. Similar reductions can also be observed for other metals as well, such as aluminium [1].

To summarise, the main sustainability aspects related to structures and materials are recyclability and production. From a recyclability point of view, the vast majority of the system can be recycled. Most non-recyclable materials are likely to be composite structures of the vehicle and/or polymer laminate parts [1]. Furthermore, using recycled steel to produce the required steel parts will lead to a 70% decrease in CO_2 emissions when compared to primary production.

6.9 Verification & Validation

Calculations for the structural aspects of the design were performed using Excel. Although the Excel sheet is relatively small and not very complicated, verification and validation has been performed. Two verification tests and two validation tests have been performed for each pair of gear equations (6.17-6.18 & 6.19-6.20). For the bending strength, first the input variable σ_{Flim} has been set to zero. When looking at Equation 6.18, the limiting tangential force should then also be equal to zero. If all variables in the formula have been set to unity, the value of the tangential force and the experienced stress should be exactly the same for both Equation 6.17 and Equation 6.18. Validation has been performed with respect to an example that has been given alongside the explanation of the equations [100]. From the four performed tests and its results shown by Table 6.7, it can be concluded that the bending strength calculations are valid to use.

Two similar verification tests have also been performed on the surface durability calculations. Both are null tests which match the expected output of zero. However for the two validation tests performed based on a given example [102], the output differs slightly. This is remarkable as the performed calculation is rather easy. Given that two separate calculations gave exactly the same answer, it is expected that either the input values of the example or the answer of the example have not been documented correctly. Therefore, the surface durability calculations are assumed to be valid as well.

Table 6.7: Verification and validation results for the bending strength and surface durability of gears

Verification or Validation	Input	Output	Expected Output
		Bending Strength	
Verification	σ_{Flim} = 0	F_{tlim} = 0	$F_t lim$ = 0
Verification	All variables 1.0	F_t=σ_F and F_{tlim}=σ_{Flim}	F_t=σ_F and F_{tlim}=σ_{Flim}
Validation	Example set 1	594.14	594.1
Validation	Example set 2	601.88	601.9
		Surface Durability	
Verification	σ_{Hlim} = 0	F_{tlim} = 0	F_{tlim} = 0
Verification	σ_H = 0	F_t = 0	F_t = 0
Validation	Example set 1	235.19	233.8
Validation	Example set 2	235.19	233.8

[106] https://www.epa.gov/sites/production/files/2015-09/documents/2013_advncng_smm_fs.pdf

6.10 Compliance Matrix

The compliance matrix, Table 6.8, shows if the requirements have been met. Within Table 6.8, three different options for the compliance with the requirements are present. They are: requirement met (✓); requirement requires more research (✱); requirement not met (✗).

Table 6.8: Compliance Matrix Structures and Materials

Requirement ID	Compliance	Reasoning
RETS-SH-TLREQ-07N	✓	Recyclable materials have been used
RETS-SH-TLREQ-03	✓	Installation Procedure has been designed to be reversible
RETS-SH-MAN-01	✱	Further research into manufacturing necessary
RETS-SH-MAN-02	✱	Further research into manufacturing necessary
RETS-SH-ABS-01	✓	Only six major components on MLG strut
RETS-SH-PAX-01	✓	System has been designed to minimise vibrations and noise
RETS-SH-MTC-03	✓	Non-critical components are replaceable
RETS-SH-INS-01	✱	Failures other than flat tyres should be documented
RETS-F-SAF-03	✓	Fail-safe design of gears including teeth
RETS-F-SAF-04	✓	Fail-safe design of External Vehicle
RETS-F-GEN-07	✱	Emergency Braking System using Aircraft Brakes has been investigated. Detailed implementation needed during future design phases
RETS-F-SM-01	✓	NLG fatigue taken into account
RETS-F-SM-02	✓	Safety Factor of 1.5 used
RETS-F-SM-03	✓	Safety Factor of 1.2 used on gear design, 1.5 on structure
RETS-F-SM-04	✓	Wheel-based engine components easily removable
RETS-F-SM-05	✓	Structure has been designed to prevent corrosion
RETS-F-SM-06	✓	Structure has been designed to prevent liquid damage
RETS-F-SM-07	✓	Wheel-based engine components accessible on MLG
RETS-F-SM-08	✱	Futher research into effects of temperature on RETS necessary
RETS-F-SM-09	✓	Recyclable materials have been used
RETS-F-SM-10	✱	Flammability yet to be implemented
RETS-F-SM-11	✓	The mass added to the aicraft is less than the requirement limit.
RETS-F-SM-12	✓	The mass added to the external vehicle is less than the requirement limit.
RETS-NF-MAN-01	✱	Further research into manufacturing necessary
RETS-NF-MAN-02	✱	Further research into manufacturing necessary
RETS-NF-MAN-03	✱	Further research into manufacturing necessary
RETS-NF-LC-01	✱	Metal components recyclable, partially met
RETS-NF-LC-02	✱	Manual will need to be created during a later phase

7 Control and Stability

This chapter discusses the control and stability functions of the RETS. The discussed subjects are aircraft stability, steering during taxiing, communication, sensors and data handling.

7.1 Functional Analysis

The first step in designing the control and stability systems of the RETS will be to make a functional analysis for this subsystem. This will consist of a clear overview of what functions the system needs to execute.

Firstly, the stability of the aircraft will need to be re-evaluated. Weight will be added to the aircraft which will change the location of the centre of gravity. Research must be done into the stability parameters that change due to this new weight distribution. These parameters will be with respect to in-flight stability, as well as with the on the ground stability and controllability.

A second function, that is connected to the controllability of the RETS, is the steering mechanism. This should be designed such that all the steering requirements are met. Extra attention with respect to the three different propelling components of the system will be needed when looking at the steering, as all three parts need to correctly move with respect to each other to avoid unnecessary stresses.

The functions with respect to the communication and data handling are also placed under the control and stability department. The communication is the information flow between the different persons working with a system. The data handling consists of a network of sensors that measures all needed data, which will then be recorded on the system.

Finally, a fail safe operational approach will be designed. This is needed to make sure that the aircraft can not start to take-off procedures with the RETS attached. This would result in severe damage to both the aircraft and the RETS and must be avoided at all times.

7.2 Risk Analysis

For the control and stability subsystem the boundaries and goals will also partially be set by means of identifying the relevant risks. Table 7.1 summarises the identified risks in the midterm phase [1] for the control and stability subsystem. Similarly to the previous subsystems, the risk mitigation strategy will, where possible, be taken into account in the detailed design of the RETS.

Table 7.1: Previously identified risks related to control and stability

ID	Risk	Risk Cause	Risk Consequence	Mitigation	p_f/ $p_{f_{\text{mit}}}$	c_f/ $p_{f_{\text{mit}}}$
T.C.1	Stability reduction of aircraft (ground & in-flight)	RETS components in aircraft structure are (too) heavy/have large moment arm	Aircraft certification might be cumbersome; aircraft documentation needs to be adapted	Limit RETS components on aircraft	3	4/3
T.C.2	Aircraft-RETS (de)-attachment is not done correctly	Malfunctioning RETS control system	Aircraft is delayed; RETS must maintained; aircraft could be damaged	Fail-safe control system design; extra sensors to check proper movements	3/2	4/2
T.C.3	RETS does not respond to user input	Loss of connection; software malfunction	Flight delay; potential airport delays; RETS reset or maintenance	Fail-safe control system design; signal checking system	2/1	3/2
T.C.4	Sudden control input	Software malfunction; 'enthusiastic' operator	Sudden RETS movement; RETS or aircraft loads exceeded (T.S.1, T.S.2, T.S.3)	Control system should gradually increase input instead of sudden peak input	2/1	4
T.C.5	RETS incorrectly measures/reports data	Defunct sensor, software bug, factors affecting measurements	Incorrect statistics, lifetime and mission predictions might be offset	Test equipment and setup. Use larger safety margins for lifetime/reliability. Reset certain parameters during maintenance	3/1	3/2

7.3 Requirement Analysis

The following requirements were previously set as requirements for the control and stability of this design [3]. All these requirements are set on stability, steering, data recording and sensors, which are all discussed in the upcoming sections. In section 7.10, the compliance matrix for these requirements is shown, it can be seen whether or not the requirements are all met. Note that some risk mitigation strategies have directly flowed down into a specific requirement. For example, **[RETS-F-CS-01]** and **[RETS-F-CS-02]** directly links to risk **T.C.1**.

- **[RETS-SH-TLREQ-08]**: RETS shall be fail-safe to prevent damage in case a take-off is attempted while the system is engaged. *(Safety)*
- **[RETS-SH-ALC-03]**: The effects that the RETS has on the stability and control of the aircraft shall be documented. *(Operations)*
- **[RETS-SH-ATC-01]**: The RETS shall be able to follow the ATC directions, be it via direct input or through the pilot *(Operations)*
- **[RETS-SH-ATC-02]**: Ongoing RETS operations shall be clearly distinguishable for ATC. *(Operations)*
- **[RETS-F-SAF-02]** RETS shall have an emergency stop/override.
- **[RETS-F-CS-01]** RETS shall keep the aircraft longitudinally stable at all times when attached.
- **[RETS-F-CS-02]** RETS shall keep the aircraft laterally stable at all times when attached.
- **[RETS-F-CS-03]** RETS shall have a maximum steering angle of 75 °.
- **[RETS-F-CS-04]** RETS shall record data on its energy output.
- **[RETS-F-CS-05]** RETS shall record data on the distance it travels.
- **[RETS-F-CS-06]** RETS shall record data on its speed.

- **[RETS-F-CS-07]** RETS shall be able to use differential braking as a secondary steering technique.
- **[RETS-F-CS-08]** RETS sensors shall be resettable.
- **[RETS-F-CS-09]** RETS sensors shall allow for recalibration.
- **[RETS-F-CS-10]** RETS shall be able to perform turns larger than 90° at a maximum speed of 5.14 $m\,s^{-2}$ (10 kts).
- **[RETS-F-CS-11]** The mass added to the aircraft due to the control department will be limited to 18.4 kg.
- **[RETS-NF-REG-02]** RETS shall comply with airport lighting regulations.
- **[RETS-NF-REG-03]** RETS shall be provided with a clear and complete user manual.

7.4 Aircraft Stability

There are several components added to the aircraft, which are taken along in the flight. These components add weight to the aircraft and change the location of the centre of gravity (CG). This induces changes in the stability of the aircraft for the in-flight phase as well as the on the ground phase, which both need to be re-evaluated.

7.4.1 Centre of Gravity

In this section the new horizontal and vertical centre of gravity will be calculated. These new locations are calculated using Equation 7.1. In this equation, all coordinates will be measured from the tip of the aircraft for the horizontal CG, and from the ground for the vertical CG. The components and their locations can be found in Table 7.2. The aircraft weight used will be the operational empty weight, as this is the lowest possible weight so using this will result in the larger change in CG.

$$CG = \frac{\sum_{n=1}^{N} m_n \cdot CG_n}{m_{tot}} \tag{7.1}$$

Table 7.2: Component masses and locations

Component	**Mass *[kg]***	**Horizontal location *[m]***	**Vertical location *[m]***
Motor	40.6	23.24	0.9
Gears	156.76	23.28	0.7
Cables	59.56	13.52	2.5
Power plug cover	2.0	5.07	1.84
Cockpit hardware	5.2	2.0	4.3
Engine pre-heating	23.48	18.03	1.71
Wheel hardware	14.90	22.97	0.9
Total	**311.00**	**20.72**	**1.19**

7.4.1.1 Longitudinal Centre of Gravity

The components that influence the horizontal centre of gravity the most will be the motors and the gears, as these have a high mass and are located most aft. When applying Equation 7.1 to the values, the change in centre of gravity can be seen in Table 7.3. The change in horizontal centre of gravity is less than a centimetre in all 3 configurations.

Table 7.3: Change in centre of gravity due to added weight

Centre of gravity	Old location *[m]*	New location *[m]*
Most forward CG	20.362	20.362
Most aft CG	21.242	21.240
OEW CG	20.684	20.683
Vertical CG	1.870	1.868

7.4.1.2 Vertical Centre of Gravity

The current vertical centre of gravity was estimated to lay at one third of the fuselage height, as mentioned in the midterm report [1]. Using the values given in Table 7.2 and Equation 7.1 the vertical centre of gravity was calculated and shown in Table 7.3.

7.4.2 Stability Conditions

The position of the aircraft's centre of gravity is constrained in a number of cases, depending on which operational phase (taxiing, take-off, flight, landing) the aircraft is in. It is therefore important to check all conditions in order to verify that the modifications on the aircraft do not alter its stability in a drastic manner. All following equations in this subsection have been derived and checked with [52].

7.4.2.1 Taxiing Tip-over Acceleration

The first condition that was checked was the maximum possible acceleration that could be applied at the nose landing gear without the aircraft tipping over backwards. This is especially important if the centre of gravity moves backwards and the nose landing gear sustains a high acceleration. Equation 7.2 can therefore be used to constrain the maximum acceleration that will be applied to the nose landing gear. x represents a distance along the body axis of the aircraft and z along the normal as shown in Figure 7.1. Note that the most aft centre of gravity is used here as it is the limiting case. The limiting acceleration was found to be 2.21 m s^{-2}. This is much higher than he maximum acceleration of the RETS system as stated in chapter 4.

$$a_{limit} = g \cdot \frac{x_{mlg} - x_{cg}}{z_{cg}} \tag{7.2}$$

7.4.2.2 Tip-back Angle

When the aircraft pitches upwards, there is a risk that the tail hits the ground in case the centre of gravity is too far aft. The angle (β) between the main landing gear contact point and the centre of gravity therefore needs to be larger than the tip-back angle (θ) of 11° [107]. This is shown in Figure 7.1. The following equation therefore verifies that tail strike is not an issue. With the addition of the new mass, the landing pitch angle increased by 0.055° from 12.618° to 12.673°. This is a very minor change, it complies with the stability condition and even provides a greater pitch rotation margin to the aircraft.

$$\beta = \arctan\left(\frac{x_{mlg} - x_{cg}}{z_{cg}}\right) > 11\,\text{deg} \tag{7.3}$$

https://www.goshawk.aero/our-portfolio/[accessed on 26 June 2020]

[107] https://assets.publishing.service.gov.uk/media/5422f72240f0b613420005d3/dft_avsafety_pdf_507757.pdf[accessed on 10 June 2020]

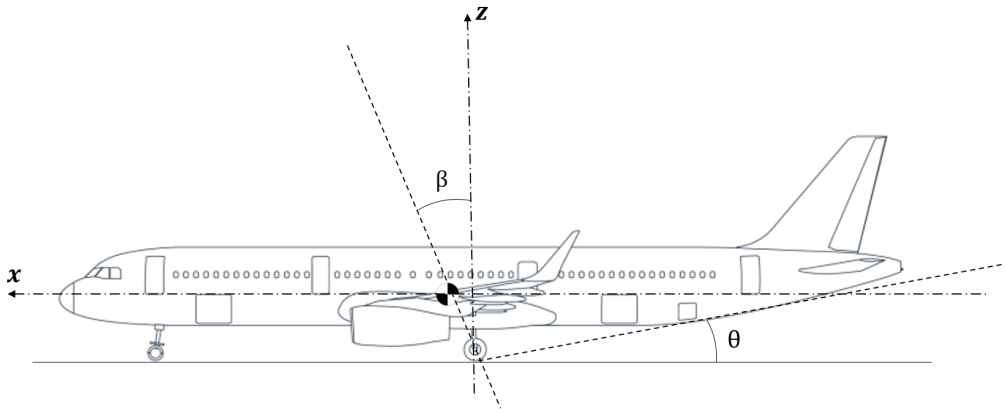

Figure 7.1: Aircraft coordinate system and tip-back [108]

7.4.2.3 Ground Equilibrium

The weight of the aircraft needs to be appropriately distributed between the main and nose landing gears. There cannot be too much load on the nose landing gear because of structural restrictions. However there needs to be enough load on the nose landing gear in order to properly steer the aircraft. It is estimated there should be between 8% to 15% of the total aircraft weight on the nose landing gear [53]. This can therefore be checked with the help of Equation 7.4, using the most forward centre of gravity to check for the structural restriction and the most aft centre of gravity to check for the steering restriction. Note that this equation was simply obtained from moment and force equilibrium. The values obtained for the nose landing gear weight fraction were found between 4.32% and 9.51%. There was very little variation due to the addition of the new mass. In fact the values for the aircraft without modifications where also found to be outside the limits previously mentioned. It is believed that this will only be an issue in case of wet or icy surfaces as the aircraft will loose steering capacity. As part of the RETS system, the external vehicle offers a solution to this by holding the nose landing gear in position and providing enough traction to steer the aircraft in wet or slippery conditions.

$$\frac{F_{nlg}}{W} = \left(\frac{x_{mlg} - x_{cg}}{x_{mlg} - x_{nlg}} \right) \tag{7.4}$$

7.4.2.4 In-flight Stability

The in-flight stability of an aircraft is dependent on a lot of different factors. Fortunately, the only real factor that is influenced by the centre of gravity is the longitudinal stability. To be longitudinal stable, the centre of gravity must be in front of the aerodynamic centre of the aircraft. This is the case because this way the aircraft will counteract any increase in pitching moment by the moment of its own weight around the aerodynamic centre.

As the changes in horizontal centre of gravity are almost non-existent, as can be seen in Table 7.3, the assumption can be made that the longitudinal stability is not changed due to the implementation of the RETS on the A321 neo.

In conclusion, very minor shifts in cg were observed, leading to negligible effects on the stability of the aircraft. It is safe to assume that the aircraft's control and stability characteristics will remain close to the original version of the aircraft. Nevertheless, the changes to some of the centre of gravity and stability limits will be documented and communicated to the pilots.

7.5 Steering System

During current taxi operations the aircraft is steered purely by means of nose wheel steering. The nose wheel will be lifted onto the external vehicle as shown in section 6.5, a new way of steering

needs to be established. This is described in detail in the following section.

7.5.1 Steering Technique

Two different steering systems were considered to be implemented on the RETS. The first being steering the aircraft purely by steering the nose wheel vehicle. This technique is most similar to the one used in current taxi operations, in which the pilot provides an input on the tiller of the A321, which by means of actuators get transferred to the nose wheel. This system used is a steer-by-wire system, which means there is no mechanical link between the tiller and the nose wheel steering system [54]. Since the nose wheel will be lifted, the external vehicle needs to steer when using this nose wheel steering technique. The change made to the present-day system would be to reroute the tiller input, when the nose wheel vehicle is attached to the external vehicle steering system. This way the nose wheel will not get an input, so it will stay stationary while the external vehicle will get the inputs and therefore take over the steering.

The second steering technique to be considered is that of differential steering. The differential steering technique uses a difference in the motor torque applied on both vehicle sides [55]. This can be done by applying more power to one of the wheels, or by braking on one of the wheels. The wheels will therefore reach a different speed, which results in a turn. This way of steering became an option since both main landing gears are equipped with an internal motor capable of providing a precise power. An advantage of this technique, is the dynamic characteristics of differential steering which are very high in both normal weather and more extreme weather conditions [55].

After analysing the possibilities offered by both systems, it was decided to combine both steering techniques to allow more manoeuvrability freedom. It was decided to place the motors on the outside wheels of the main landing gear. The wheels are not far apart from each other, but this small distance creates a longer turn radius for the most outside powered wheel when turning, while creating a smaller turn radius for the inner power wheel. It was found that 13% smaller turn radii could be achieved for the same power difference.

7.5.2 Steering Relations

The principle of differential steering is simple, a difference in motor torque has to be applied. The more challenging thing is to make sure that the vehicle steering and differential steering implement the same angular velocity. This is needed to not induce any extra loads on the nose wheel gear structure. The procedure will be as follows: the pilot will turn using the tiller at all times. When the external vehicle is attached, the input will go through the computer located in the cockpit which will then calculate what power difference is required over the wheels, and at what velocity the nose wheel vehicle should drive.

For the computer to calculate these values, a relation between the nose steering angle and the required speed for each wheel is needed. Furthermore, a relation between the nose steering angle and the speed of the external vehicle's wheels is also required.

Power Steering

To find a relation between the speed of the three landing gears and the steering angle of the nose wheel vehicle, the turning radius of the nose wheel vehicle needs to be found. This is done using Equation 7.5 [56] and the geometry of the aircraft, shown in Figure 7.2. Note that here α represents the nose wheel steering angle which is measured relative to the tangent of the circle of the turn.

$$R = d_{nlg} \cdot \tan\left(\frac{\pi}{2} - \alpha\right) \tag{7.5}$$

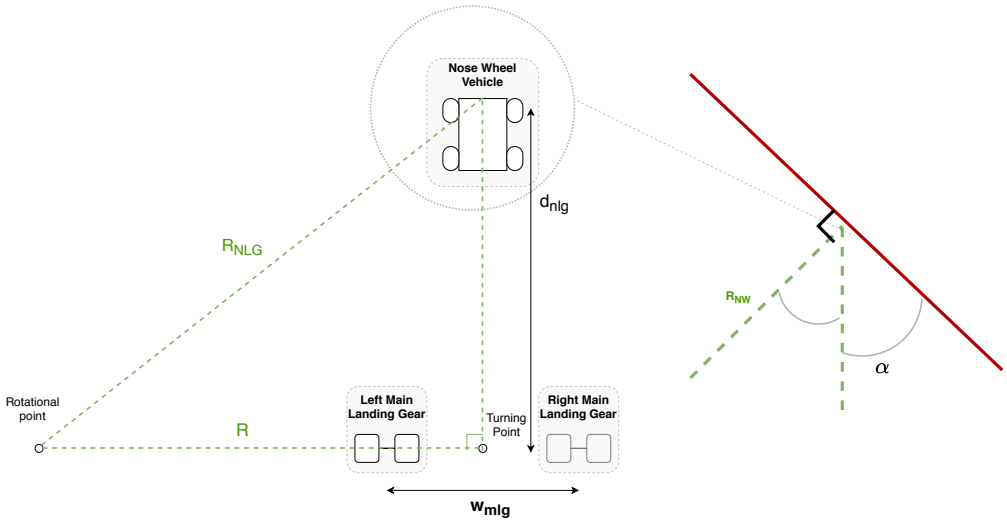

Figure 7.2: RETS Top View Geometry and steering dimensions

Equation 7.5 calculates the turning radius ($R\ [m]$) of the turning point in between the main landing gears. Using the width between the main landing gears ($w_{mlg}\ [m]$), the velocity of the left landing gear ($V_L\ [m/s]$) and the velocity of the right landing gear ($V_R\ [m/s]$) can be computed with Equation 7.6 and Equation 7.7 respectively. The turning radius for the nose wheel vehicle ($R_{\mathrm{NW}}\ [m]$) can be calculated using Pythagoras' theorem and then used to obtain the nose wheel velocity ($V_{\mathrm{NW}}\ [m]$) with Equation 7.8. In all three equations, $\omega\ [rad/s]$ is identical and gives the aircraft performance on turns, or more specifically the amount of rotation the aircraft can perform in a certain time. This is however controlled by the pilot with the help of the tiller for the steering angle and the power lever for the speed. Here, $\omega = V/R$ is used with V as the indicated ground speed of the entire aircraft, represented at the centre of gravity. Once the velocities are obtained by the computer, they can be converted to the wheel revolutions and subsequently the motor rpm, making it possible to determine the necessary power the motor requires. In addition, brakes can also be used to allow for greater steering capability, although this is redundant it is still an available option. The steering relations are similar to power steering and the method is commonly applied in taxiing especially for smaller aircraft.

$$V_L = \omega \cdot \left(R - \frac{w_{mlg}}{2}\right) \tag{7.6}$$

$$V_R = \omega \cdot \left(R + \frac{w_{mlg}}{2}\right) \tag{7.7}$$

$$V_{\mathrm{NW}} = \omega \cdot \left(\sqrt{R^2 + d_{nlg}^2}\right) \tag{7.8}$$

Nose Wheel Steering

As discussed in the previous section, the nose wheel vehicle will need to be steered when differential steering is used. This steering system will work as follows. When the pilot inputs a certain amount of power on the wheels as well as a certain deflection on the tiller, this will result in a specific velocity for all three wheels. Via this velocity, the power required by each motor and the external vehicle can be calculated. The nose landing gear will remain in line with the external vehicle at all times. This was chosen over making the nose wheel vehicle stay in line with the aircraft because this would make applying a pulling force with the external vehicle more complicated. This does however mean that the external vehicle will never be oriented at more than 75° relative to the aircraft, as the nose landing gear's rotation limits this. Allowing the nose landing gear to rotate more than this limit will induce higher wear and increase the complexity of the system as the nose landing gear will require to be locked back into position after the taxi phase.

To achieve higher manoeuvrability, the external vehicle requires a certain steering angle to compensate for the aircraft's limited 75° steering angle. To achieve lower turn radii, the velocity vector of the nose landing gear needs to be directed as close as possible to the tangent of the turning circle. For example to achieve a 90° turn and assuming the external vehicle is at 75°, the external vehicle would need to direct its velocity 15° relative to its axis (also the landing gear axis). As shown in Figure 7.3, the angular velocity of the external vehicle can be obtained with Equation 7.9. This can then be used with the turn radius of each wheel to obtain the velocity of each wheel as shown in Equation 7.10 to Equation 7.13. All dimensions are shown on Equation 7.9 and as taken from the AST-2X's design [3]. The subscripts r, l, b and f refer to right, left, back and front respectively. Note that the right steering angle ($\alpha_r\ [rad]$) is determined by the left steering angle ($\alpha_l\ [rad]$) as the width of the wheels is already defined. The angular velocity and hence power required to each wheel can be computed using the wheel diameter and the required speed to make the turn.

$$\omega_{\text{ev}} = \frac{V_{nlg} \cdot \cos\left(\frac{\pi}{2} - \alpha_{nlg}\right)}{d_{nlg}} \tag{7.9}$$

$$V_{lb} = \omega_{\text{ev}} \cdot \left(d_{nlg} \tan\left(\frac{\pi}{2} - \alpha_{nlg}\right) - \frac{w_b}{2}\right) \tag{7.10}$$

$$V_{rb} = \omega_{\text{ev}} \cdot \left(d_{nlg} \tan\left(\frac{\pi}{2} - \alpha_{nlg}\right) + \frac{w_b}{2}\right) \tag{7.11}$$

$$V_{lf} = \frac{\omega_{\text{ev}} \cdot h}{\cos\left(\frac{\pi}{2} - \alpha_l\right)} \tag{7.12}$$

$$V_{rf} = \omega_{\text{ev}} \cdot \left(\sqrt{h^2 + \left(w_f + h \tan\left(\frac{\pi}{2} - \alpha_l\right)\right)^2}\right) \tag{7.13}$$

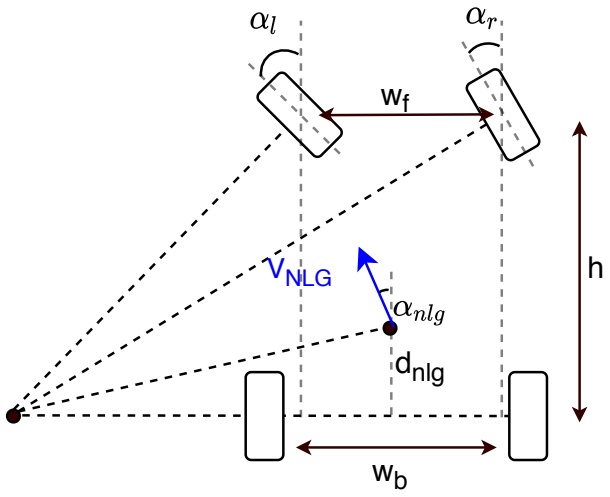

Figure 7.3: External vehicle steering geometry

It is important to realise that the steering and power inputs will have to be tuned in order for the pilot to feel comfortable with the new system. Ideally, the pilot should require as little adaptation as possible to the new taxiing system. This can be done by testing the response of a pilot to the new system and implementing his feedback for improvement. Once finalised, the new input methods used will be documented and communicated, in order for any pilot to adjust appropriately to the aircraft controls.

7.6 Communication & Hardware

This section will, with the help of the communication diagram shown in Figure 7.4, explain the most important communication flows within the operations of the RETS. Next to this, the hardware components that are added to the aircraft and external vehicle will be explained.

7.6.1 Hardware Components

This subsection will discuss the different hardware components added to the aircraft and to the external vehicle. It is important to note that the external vehicle already includes a number of components and that the list below only shows the components used for the system control that are added to the external vehicle. The hardware components are also shown in Figure 7.6.

On the aircraft:

- Cockpit taxiing computer: This computer is the centre point of the on-aircraft part on the communication architecture. It receives sensor inputs, does calculations and redirects the outputs to the needed locations. These calculations consist for example of the power and steering calculations.
- Power lever: The pilot will input his desired power on a power lever. This is then via the taxi computer transmitted to the main landing gear as well as the external vehicle.
- Cameras: These are used to check the clearance when the aircraft is in push-back mode.
- Motor controllers: These will be used to distribute the appropriate power to the internal motors.
- Sensors: These will help in detecting errors and correctly operate the system as described in subsection 7.7.1.

On the external vehicle:

- Data storage: All data that is recorded will be stored on an SD card. In this way, all the sensor data can be checked after a cycle if needed.
- External vehicle computer: This computer is the centre of the external vehicle communication. It receives all sensor inputs and transmits them to where they need to go.
- Sensors: These will help in detecting errors and correctly operate the system, as described in subsection 7.7.1.

Requirement **[RETS-NF-REG-02]**: RETS shall comply with airport lighting regulations, concerns the external vehicle of the system. As stated in section 6.5, the external vehicle will be based on the Goldhofer "Phoenix" AST-2X towbarless tractor which is certified by the German Technical Inspection Agency [109]. The modifications that will be made to the vehicle will be the upgrade of the drivetrain, the addition of a robotic arm and a slight decrease in vehicle width. The lighting system of the vehicle therefore remains unchanged and compliant with airport regulations.

7.6.2 Cockpit Communication

Communication between the pilot and external vehicle is done through the cockpit-external vehicle communication line which will be attached to the power connection arm as shown in subsubsection 6.5.1.1. This was selected as opposed to wireless communication as it does not require additional components to be added on the aircraft and the external vehicle. Additionally, as the steering and power will be communicated through this line, it is important for this component to have low risk and be reliable. Wireless communications may be subject to security issues, interference and could have delay in transmitting information. This risk is therefore included in Table 7.4.

7.6.3 External Vehicle Communication

In order to efficiently operate the system, the operator and pilot must be in direct communication. Additionally, the operator of the vehicle remains in contact with the ground control personnel by

[109] https://www.goldhofer.com/en/towbarless-tractors-ast-2p-x-phoenix [Accessed 12 June 2020]

radio. The pilot will also remain in contact with air traffic control and the external vehicle is equipped with a computer which handles the data from the sensors around the vehicle. Some sensors data, like the vehicle speed, fuel level, and charge level of the batteries, is communicated to the pilot. An overview of the communications and the information that must be transferred is provided in Figure 7.4.

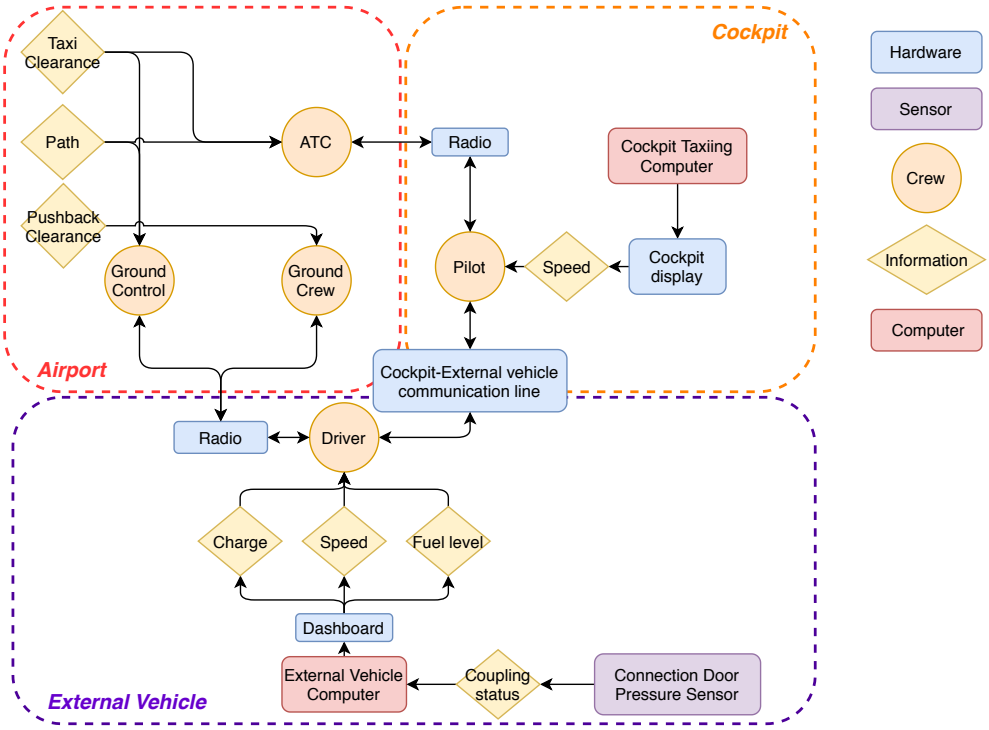

Figure 7.4: Communication diagram

7.7 Sensors & Data Handling

This section discusses the different sensors on the system, as well as the data handling processes that are taking place.

7.7.1 Sensors

In all parts of the RETS design, it is important to make use of sensors in order to receive feedback on the performance of certain components and subsequently take action if issues are detected.

7.7.1.1 Internal

A key component of the internal system is the motor assembly. In order to obtain optimal performance, the temperature and rotational speed of the motor can be monitored and adjusted according to the operating conditions. The temperature will be measured with a classic thermistor located in the motor winding and feeding back into the cockpit computer. An absolute rotary encoder is used in every motor to obtain the instantaneous rotations per minute of the motor shaft. Additionally, this measurement can also be used to obtain the aircraft's speed. This is done by dividing the motor's rotational speed by the gear ratio and multiplying by the radius of the wheels.

As previously described in subsubsection 5.4.8.2, in the case the external vehicle is not available or required for pushback, the pilot can make use of the motors on the main landing gear combined with the APU as power supply to pushback independently. However, the pilot does not have great visibility on the areas below or behind the aircraft. As stated in [13], the captain and first officer have a combined field of view of 133° from the cockpit and can see the wing tips of the aircraft if they move their head to the side. To offer a better visibility to the pilots, cameras should be installed on the belly of the aircraft and in the positions shown in Figure 7.5. Note that the dotted lines show the pilots' field of view and the grey areas the cameras' field of view. The distance is

however not representative of the cameras' resolutions. The cameras' all have a field of view of 88°. The front facing camera allows the pilots to see beneath the cockpit. The first rear facing camera displays what is beneath the aircraft and near the engines and wings. The most aft camera will help the pilot avoid any obstacles located behind the aircraft.

It is also necessary for the entire system to be fail safe. That is to prevent the aircraft from starting takeoff when the system is still attached. To achieve this, the camera system will be used. The image will be transmitted to the cockpit computer where the image can be analysed using software to detect whether any obstacles are in the way or not. If an obstacle is present, the system will prevent the throttle from giving any power to the engines. The live camera feed remains visible to the pilot and he/she can check that the issue is present.

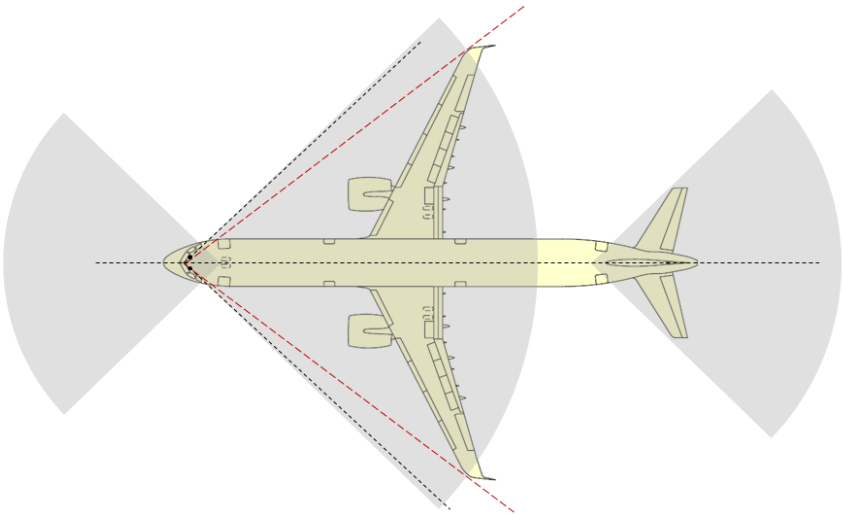

Figure 7.5: Visibility from cockpit

7.7.1.2 External

The external vehicle design and operations are identical to that of a standard pushback tractor. It is therefore assumed that the pushback truck already includes necessary sensors for pushback operations. As the truck has a hydro-static transmission, a number of pressure and temperature sensors will be present in the pumps and motors of the drivetrain. As the vehicle has been adapted for the a321, the robotic arm is placed under the aircraft in such a way that when the nose landing gear is locked into place, the position of the electrical plug on the aircraft is known and the arm can simply extend and lock itself into place. It is also assumed that the pushback truck includes sensors for other operations such as brake fluid pressure, torque or speed sensors for example.

There are a number of new components on the external vehicle that also need to be fitted with sensors. First of all, as a battery is being added, the battery's state of charge needs to be measured to inform the operators if there is a sufficient level of energy left. This can be simply estimated using a voltmeter combined with the discharge curve of the battery. Temperature also affects the voltage measurements and the battery capacity but is also a source of risk as the battery could ignite at high temperatures (see Table 5.1). It is therefore essential to include a temperature sensor to mitigate this risk and have the external vehicle computer activate a cooling system to cool down the battery.

7.7.2 Data Handling

The following two sections will introduce the components used to store and manage data throughout the system. Figure 7.6 shows the information flow and interactions between different hardware components and users. The data speed and type of information transmitted between some of the components is shown. Note that this is still a preliminary diagram and needs refining in later phases of the project. Certain aspects such as data compression, transmission rate, cable types and inter-

faces have not been investigated at this point. Figure 7.7 shows how the computers use the data received from the sensors and make the required decisions.

7.7.2.1 Internal

On the aircraft itself, a computer with storage will be fitted to the cockpit. As previously mentioned, the computer will receive the pilot's steering input from the tiller and power input from the power lever. These inputs will be used to carefully calculate speed requirements such that the system and aircraft will not undergo speed differences and induced stresses, but it also calculates the power distribution between external and internal systems and the steering angle required at the external vehicle. Once calculated, the values for the main landing gears are transferred to the motor controllers via the cockpit-landing gear communication line. The computer will also receive information from all the sensors located on the nose landing gear and some of the external vehicle sensors and display them on the cockpit's display system. Additionally, the camera system will feed back into the cockpit computer and the image will also be transmitted to the cockpit's display system.

7.7.2.2 External

Data collected from the external vehicle sensors needs to be stored and communicated to the cockpit as well. To do this the external vehicle is equipped with a computer and SD card which is the centre point of the external vehicle communication architecture. The computer will relay useful information such as battery state of charge, vehicle speed, errors detected (overheating, communication failures, limited motor torque, etc.) to the vehicle's dashboard. The driver can then decide on the urgency of the problem and act accordingly. Data will be recorded on the computer's storage space and transmitted during charging. This can then be communicated to the maintenance team to verify if maintenance is required or to detect any unusual performance related issues such as a slower external vehicle or a rapid battery discharge for example. The number of cycles the vehicle has performed will be tracked using the number of times the operator starts the coupling and decoupling procedures. The coupling and decoupling procedure is started by the vehicle driver. The computer transmits the information to the robotic arm which deploys and locks into the plug.

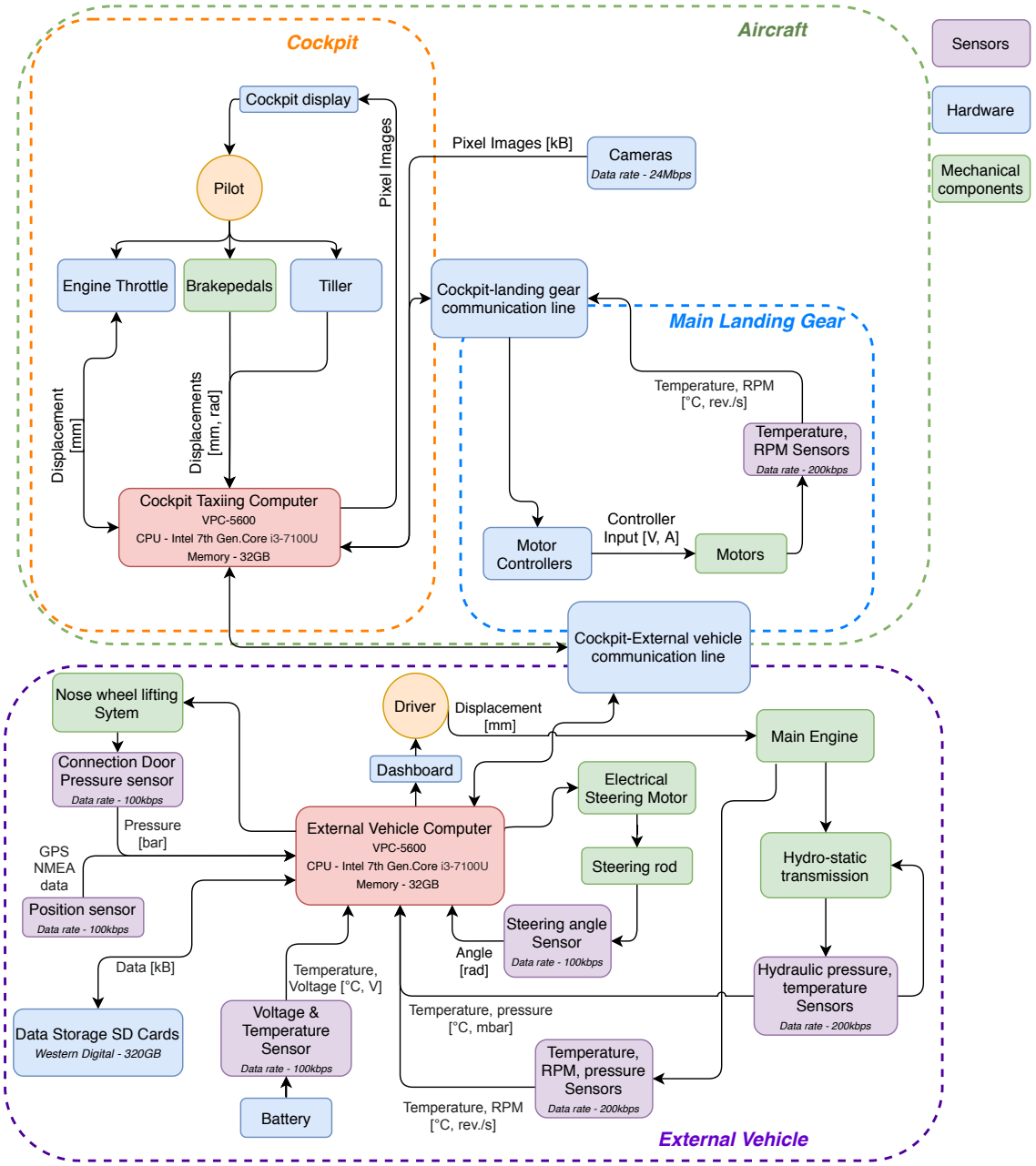

Figure 7.6: Data handling and hardware diagram

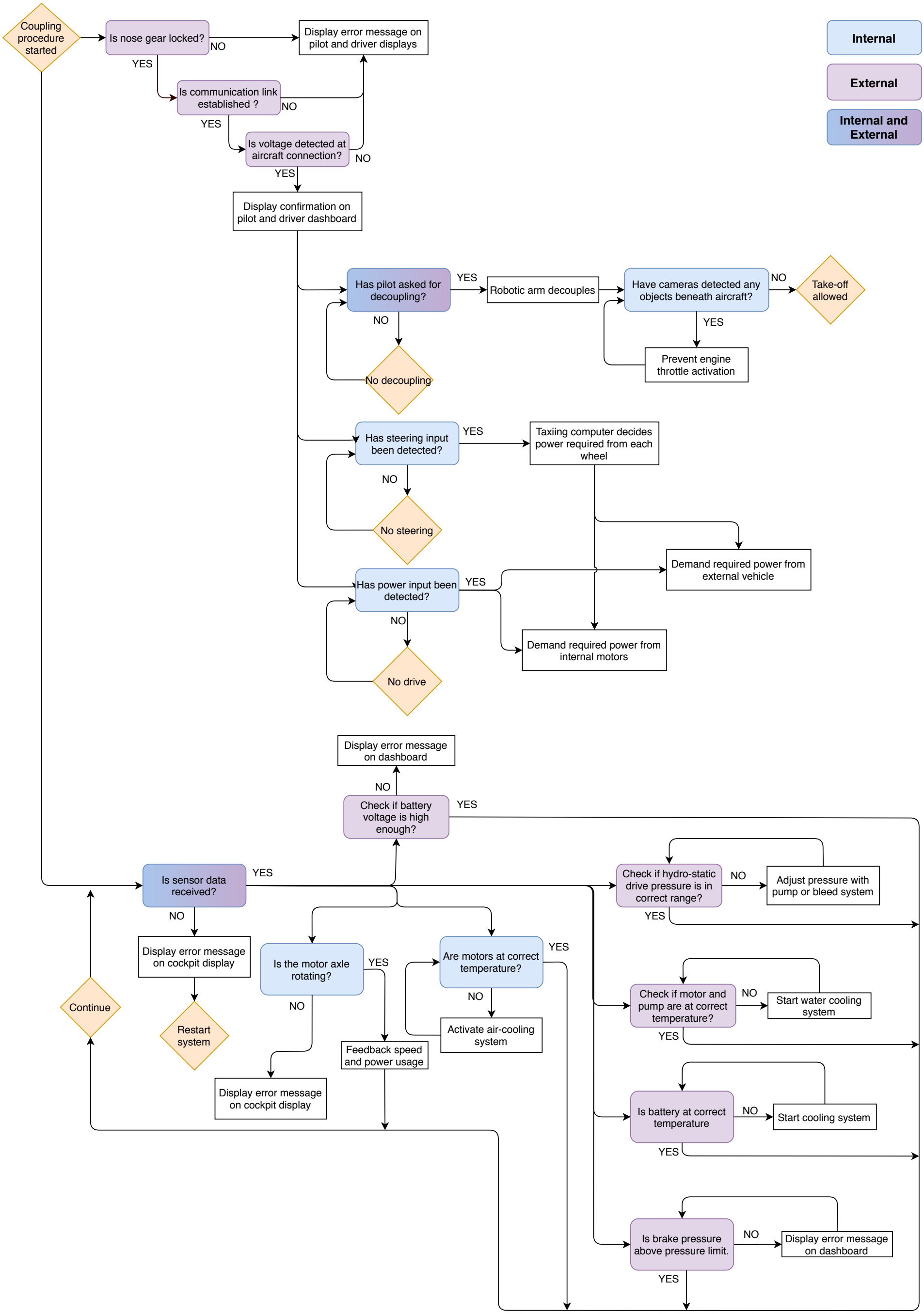

Figure 7.7: Software block diagram

7.8 Risk and sustainability

In this section the technical risk assessment and the sustainability analysis for control and stability is provided.

7.8.1 New Control & Stability Risks

In Table 7.4, newly identified risks related to control and stability have been listed. With the actual risk, also the cause, consequence and mitigation are identified. The new mitigation strategies will be incorporated in the next design operation to decrease the risk. The probability of failure and the consequence of failure are estimated according Table 4.1 and 4.2.

Table 7.4: Newly identified risks related to control and stability

ID	Risk	Risk Cause	Risk Consequence	Mitigation	p_f/ $p_{f_{\text{mit}}}$	c_f/ $c_{f_{\text{mit}}}$
T.C.6	Communication failure between external vehicle and ground control centre	Defunct communication line, non responsive ground station	External vehicle does not get input on where to go	Test equipment and setup. External vehicle driver will follow specific protocol when driving without aircraft	2/1	2
T.C.7	Power and steering relations between different landing gears are not correctly executed	Incorrect relations, incorrect sensor data	Stresses on the landing gears and external vehicle, serious damage to the aircraft and RETS	Extensive testing of the relations in simulator and in practice	3/2	2
T.C.8	Failure of hardware components	Software bug, defunct hardware	RETS will not be controllable	Extensively test equipment and setup for hardware components	2/1	2
T.C.9	Failure of communica-tion line between pilot and driver	connection loss	RETS can not safely operate	Make the communication line wired instead of wireless	2/1	1

7.8.2 Sustainability Analysis

As the control and stability is mainly composed of software and checking the aircraft stability, there are not many sustainability aspects to take into account. A number of hardware components were however selected for the communications and control systems. The main criteria for selecting these components was first of all their functions and whether they met the requirements or not. Secondly, internal components were selected to minimise the weight and therefore minimise fuel consumption. Thirdly, power consumption was also considered and minimised in such a way that the energy required from the aircraft or external vehicle is kept to a minimum. Additionally, the recyclability and materials used in each components could be further investigated in case all the previously mentioned characteristics have already been looked at.

7.9 Verification and validation

The verification and validation of the different calculations performed in this chapter will be discussed in this section. The test used are as described in the verification and validation plan presented in the midterm report [1].

7.9.1 Stability

A python code was created to check if the stability of the aircraft was maintained despite the changes brought to the aircraft. Input, sensitivity and consistency tests were mainly performed. For example, increasing the mass or position of the new added components produced a greater change of the centre of gravity of the aircraft, moving the centre of gravity of the new mass aft or up was more critical for the landing pitch angle limit, increasing the acceleration at the nose landing gear or moving the aircraft centre of gravity aft brought the tip-over acceleration close to the limit. All inputs were double checked and equations entered were checked by hand. To validate the code, the centre of gravity and mass of the airbus a321 without any modifications was used as input. It was obtained that the aircraft does not violate any of the stability requirements checked.

7.9.2 Steering Relations

In section 7.5 two relations were found that are used to calculate the external vehicle steering angle and velocity, when knowing the velocity of the main landing gears.

For the verification, both relations were tested to see if the correct units flow out of the equations. For both relations this was the case. The relations were verified by looking at the logical outcomes. When the difference in velocity of both wheels becomes larger, the aircraft will make a tighter turn. If the velocity of one wheel is kept constant and the other wheel velocity is increased, both the nose wheel vehicle velocity and steering angle should increase, to keep up with this tighter turn. The simulation shows this behaviour.

For the validation, the simulation should be compared to real world data. Since real world data and established simulations are not presently used, the simulation is validated by the few data points that are known. The first of these points is when the velocity difference over the landing gear is approaching zero. At this moment the aircraft is moving straight, so the nose wheel vehicle steering angle should approach zero, while the vehicle velocity should approach the main landing gear velocities. The second known data point is when the two main landing gears have the same velocity in opposite direction. At this moment the aircraft will make a rotation around the point between the two landing gears. This means that the steering angle for the nose wheel has to be 90 degrees, as the steering axis is tangent to the rotational circle. Both these data points are correctly calculated by the simulation.

7.10 Compliance matrix

The compliance matrix, with respect to control and stability, is shown in Table 7.5. It shows if the subsystem requirements have been met. Within Table 7.5, three different options for the compliance with the requirements are present. They are: requirement met (✓); requirement requires more research (✱); requirement not met (✗)

Table 7.5: Compliance Matrix Control and Stability

Requirement ID	Compliance	Reasoning
RETS-SH-TLREQ-08	✓	The camera system prevents throttle activation in case system is engaged
RETS-SH-ALC-03	✓	This has been done and will combined into a manual for the pilot
RETS-SH-ATC-01	✓	The external vehicle can communicate with both ATC and the pilot
RETS-SH-ATC-02	✓	ATC receives position of external vehicle and can communicate to both driver and pilot
RETS-F-SAF-02	✱	An emergency stop will be implemented later in the design
RETS-F-CS-01	✓	The change in weight is too small to change the stability of the aircraft
RETS-F-CS-02	✓	The change in weight is too small to change the stability of the aircraft
RETS-F-CS-03	✓	The steering angle can be larger than 75°
RETS-F-CS-04	✓	All sensor data is recorded on a hard drive
RETS-F-CS-05	✓	All sensor data is recorded on a hard drive
RETS-F-CS-06	✓	All sensor data is recorded on a hard drive
RETS-F-CS-07	✓	Differential braking is not affected and can still be used
RETS-F-CS-08	✓	All sensors selected can be restored to original setting
RETS-F-CS-09	✓	All selected sensors can be re-calibrated or replaced
RETS-F-CS-10	✓	This can be done, however more research will be needed in this field.
RETS-F-CS-11	✱	The subsystem mass limit is slightly overshoot, however the system mass budget is met
RETS-NF-REG-02	✓	Vehicle is already certified for airport use.
RETS-NF-REG-03	✱	Content needs to be determined after testing is performed.

8 Sustainability

In this chapter, the sustainability of RETS is analysed. The sustainability analysis has been divided between the different departments. Every department has a section where design choices are justified based on sustainability factors. First, those sections are summarised. Next, the aspects of sustainability that are not directly linked to one department are explained.

8.1 Sustainability for the different department

Here, the sustainability sections of the different departments is summarised.

8.1.1 Power and electronics

The design choices by the power and electronics department have a critical impact on the overall sustainability of the design. The main three components designed are the engines of the vehicle, the batteries carried by the vehicle, and the cables.

8.1.1.1 Engines

As explained in subsubsection 5.5.1.3, for the vehicle to be fully electric, it would require a large amount of batteries, making it unsustainable. Therefore, it was decided to use a diesel engine instead. Also, it is more likely for battery cells to fail than a diesel engine to fail, making the design more reliable.

Although the selected engine is a diesel engine, it complies with the strictest vehicle emission regulations of its category. Indeed, as explained in subsubsection 5.5.1.3, the exhaust system manages to reduce the harmful NOX particles it emits in favour of N_2, water and low amounts of CO_2. There is however the possibility of performing further research into additional exhaust filters, the use of biodiesel, or even cleaner engines in later design phases.

8.1.1.2 Battery choice

One of the criteria when choosing a battery type was recyclability. As mentioned in subsubsection 5.5.1.1, the type of battery chosen is LiFePO4 which has a low toxicity level compared to other types of battery. However, recycling it is not very interesting from an economical perspective compared to other type of batteries as it has less valuable materials in it. More details are given in subsubsection 5.5.1.1.

8.1.1.3 Cables

As explained in subsubsection 5.5.1.2, high-density polyethylene (HPDE) was chosen as insulator material. It can be easily and cheaply recycled. Also, recycled HPDE is often used as it cheaper than new HPDE. Next, HPDE has a long operation lifetime (10-20 years) and can be recycled many times (over 10 times). More details are given in subsubsection 5.5.1.2.

8.1.2 Control and stability

It is difficult to implement sustainability in control and stability. However, when choosing hardware components, the weight, power required and recyclability were prioritised to minimise fuel consumption and emissions.

8.1.3 Structures

The structures department design decisions has a crucial impact on the sustainability level of RETS as the materials used are determined. The materials used define how sustainable the disposal of the system is.

As explained in subsection 6.8.2, the main material of RETS (both the internal part and the vehicle) is steel, which is easily recyclable and requires less energy to be recycled compared to other metals.

Also, getting steel from a recycled source requires almost a third of the energy compared to getting new steel.

8.1.4 Operations

As discussed in section 4.12, the most important for a sustainable usage of the system is to have an efficient logistics system with the least possible unnecessary travelling for the vehicles. Also, having highly trained people use the vehicles is essential for a longer operation life.

8.2 Sustainable usage of the system

The way the operator uses the RETS has an impact on its lifetime. If treated properly, the external vehicle will last longer, avoiding unnecessary repairs or even early replacement. It is important that the operator receives adequate training beforehand. The training should be extensive and include for instance how to control the vehicle but also how and where to store it, how to charge it, how to detect any dysfunctional component, etc.

8.3 Improvements on the surroundings

People living in the surroundings of the airport are important stakeholders. It is crucial that the system does not negatively affect their life quality, and in the case of RETS, it could actually improve it. The quality of life for people living in the surrounding is mainly dependent on two factors: the emissions and noise. RETS improves one, it producing less emissions compared to engine-based taxiing. It is assumed that most of the noise comes from aircraft taking-off and landing. Therefore, RETS is not solving the noise issues. However, apart from people living around the airport, RETS is beneficial for airports workers too, especially people working on the tarmac. They are directly affected by the noise level and emissions. A long exposure to high levels of noise has a serious impact on someone's health [110], so does a long exposure to a highly polluted environment [111]. From the improvements RETS offers, it is possible to satisfy the following requirement **[RETS-NF-MED-01]**: The use of RETS shall have no negative effects on the public image of the users. Additionally, should there be a further need to confirm this, a survey or presentation of the system to passengers, pilots and airport ground crews could be made.

8.4 Personnel

RETS requires some extra personnel to operate properly as mentioned in subsubsection 4.5.6.3. From the people working at the charging station to the people in charge of the logistics of the vehicles, it creates a lot of new jobs. Large airports should account for dozens of extra people needed. This is very positive for the economy.

8.5 Disposal

Although recyclability of the different materials used is discussed above, the disposal of the system concerns more than its recyclability. As almost every system, RETS will one day be obsolete and will need to be discarded. It is important that guidelines are given to the customer on how to dispose the product in the most sustainable way. A free removal of the system comes with RETS. This option is beneficial for both the customer as well as for the team. For the team it is especially economically interesting as parts can be recycled and reused. If the customer decides to discard the system by themselves, the parts that are dangerous to manipulate as well the parts that are harmful for the environment have to be clearly identifiable. For the removal of the internal system, it is a little more complicated as the aircraft has to go into maintenance. Although the internal

[110] https://www.science.org.au/curious/earth-environment/health-effects-environmental-noise-pollution#:~:text=Exposure%20to%20prolonged%20or%20excessive,cardiovascular%20disease%2C%20cognitive%20impairment%2C%20tinnitus [accessed 18 June 2020]

[111] https://www.who.int/airpollution/news-and-events/how-air-pollution-is-destroying-our-health[accessed 18 June 2020]

system can removed without having to replace the strut, replacing the system by the updated version will immobilise the aircraft for some time.

8.6 Emission reduction

The level of greenhouse gases present at and around airports is very high. However, by implementing RETS, the emissions produced can significantly be decreased. The main aircraft emission type is CO_2. It represents around 70% of the emissions of an aircraft engine [57]. Less than 1% of the emissions is made of other types of gases, mainly NOx and CO [57]. Kerosene has a specific CO_2 emission production of 3.150 kg/kg_{fuel} of CO_2, a specific NOx emission production of 0.01297 kg/kg_{fuel} of NOx, and a specific CO emission production of 0.010952 kg/kg_{fuel} of CO [58].

From section 4.9, the total fuel consumed during a classic engine-based and RETS-based taxi-in and taxi-out, for the baseline taxi route, are known. The value is found by summing the fuel needed for phase 1 (engine start and warm-up), phase 2 (outbound taxi), and phase 8 (landing, inbound taxi and shut-down). Those values are 86 kg, 194 kg, and 261 kg, respectively. Thus, the total fuel required for classic engine-based taxi-in and taxi-out is 541 kg. Fuel was saved for the phase 1 and phase 8, 29 kg and 93 kg, respectively. However, the APU consumes an additional 35.4kg. Therefore, the remaining fuel consumption during the taxi phase when using RETS is 260.4kg. From the values above, the reduction in fuel consumption for the taxi phase only is around 52%. The fuel saved can be translated into emissions reduction using the values stated at the end of the above paragraph.

From subsection 4.9.5, the total fuel saved per aircraft per mission profile by using RETS is found to be between 208 kg for a flight range of 3856 km and 240 kg for a flight range of 1806 km. Using the fuel reduction simulation, the total fuel consumption of the entire mission profile without the use of RETS for different flight ranges can also be calculated. For a flight range of 1806km, the fuel consumption is 9362.986kg. The reduction in fuel consumption for a flight range of 1806km by using RETS is around 2.6%. Again, the reduction in emissions can be found using the values given at the end of the first paragraph of this section.

According to Dallas Fort Worth International Airport (DFW) [59], the total emissions due to aircraft, also called optional emissions, amount to approximately 9.3 million metric tons of CO_2 for 2017 only. In subsection 4.5.4, the number of departures for DFW is given to be 145 departures per day. It is assumed that number of A321 departures is equal to the number of A321 arrivals. Therefore, there is approximately around 145 A321 departures and arrivals. As only the emissions at the airport is analysed, the total fuel saved for the taxiing phase only is taken, which is 280.6kg. Based on the specific CO_2 emission production of kerosene mentioned above, the total CO_2 emissions saved by using RETS on a year is 46 779 878.25 kg of CO_2. Assuming all A321 will be using RETS to taxi, the total reduction in CO_2 emissions for DFW due to aircraft is 0.5%.

The requirement related to emissions is the following, **[RETS-F-PE-01]**: The total emissions generated by using RETS shall be no more than <TBD> g cm^{-3}. This requirement has been updated to more detailed ones as found below. The numbers were taken form aircraft taxiing emissions at London Heathrow airport [60] to serve as a basis for a321 emissions during taxiing phases.

- **[RETS-F-PE-01N1]** The total NO_x emissions generated by using RETS shall be no more than 3.5 kg for a taxi-in and taxi-out.
- **[RETS-F-PE-01N2]** The total CO_2 emissions generated by using RETS shall be no more than 2.74 t for a taxi-in and taxi-out.

As previously stated, the specific emission of CO_2 and NOx are 3.150 kg/kg_{fuel} and 0.01297 kg/kg_{fuel} respectively. An aircraft taxiing with RETS will use 260.4 kg of fuel and will therefore produce 3.38 kg of NOx and 820.3 kg of CO_2. This amounts to an 3.43% decrease in NOx emissions and a 70.1% CO_2 relative to the basis set by the requirement. This clearly shows that both requirements have been met by the system.

9 Final Design Analysis

This chapter will analyse the final design in more detail. First, the mass and cost budgets will be described in section 9.1 after which a comparison with competitors will be made in section 9.2. In section 9.3 and section 9.4, a sensitivity analysis will be performed as well as a description of the reliability, availability, maintainability and safety. Lastly, the technical risks will be shown in risk tables in section 9.5.

9.1 Final Resource and Budget allocation

With the design fully established for this design iteration, the budget limitations can be checked to see if the requirements are met. This will first be done for the on-aircraft and external vehicle mass after which the cost budget is discussed.

9.1.1 Mass budget

Two requirements **[RETS-SH-TLREQ-03]** and **[RETS-F-GEN-08]** need to be met with respect to the mass budget. These lead to the two mass budget categories, on-aircraft mass and external vehicle mass. Both will be discussed in the next two subsections.

9.1.1.1 On-aircraft mass

The predicted and calculated masses for the on-aircraft components can be seen in Table 9.1, as well as the difference between them.

Table 9.1: On aircraft mass budget

Component	**Predicted Mass *[kg]***	**Calculated Mass *[kg]***	**Difference *[%]***
Motors	160	40.6	-74.6
Gears	440	156.76	-64.37
Cables	60	59.56	-0.7
Engine pre-heating	73.6	23.48	-68.1
Hardware	18.4	20.1	+9.22
Total	**752**	**315 (x1.05)**	**-56,85**

It can be seen that most of the components have a smaller calculated mass than was predicted. This is due to the fact that only preliminary research was done when making the predictions. In the final design phase, things like material choice or the type of motor were chosen, which had a large effect on the masses. In the end a 5% safety margin was put on the total weight of the on-aircraft components. The absolute limit for on aircraft weight added according to **[RETS-SH-TLREQ-03]** is 940 kg. So with the safety margin on there, this requirement is still very clearly met, as not even half of this weight will be added to the aircraft.

9.1.1.2 External vehicle mass

The predicted and calculated masses for the external vehicle components can be seen in Table 9.2.

Table 9.2: External vehicle mass budget

Component	Predicted Mass *[kg]*	Calculated Mass *[kg]*	Difference *[%]*
External vehicle	17600	16100	-8.52
Power connection	75	104.5	+39.38
Batteries	1425	3750	+163.16
Total	**19100**	**20952 (x1.05)**	**+9.70**

It can be seen that the predictions for the components within the external vehicle were quite off at some points. However, the overall weight for the external vehicle is only a bit over its prediction. This is not a problem as a margin was taken over the limit. The absolute limit for requirement **[RETS-F-GEN-08]**, for which service roads must be used to met it, is 22 000 kg. It can be seen that with the 5% safety margin, this requirement is still met.

9.1.2 Cost Budget

For the cost budget the limiting requirement (**[RETS-SH-TLREQ-09]**) is that within five years, the product must be profitable for the buyer. As discussed in section 3.3, this means that the operational cost must be below 123 USD per cycle.

The operational cost will be calculated using the power source values it takes to perform one cycle with the RETS. As shown in subsection 5.4.7, the external system uses 18.64 kg of diesel and the internal system uses 73 kWh per cycle. Next to this, using RETS leads to an additional fuel burn of 35.4 kg, as discussed in subsection 4.9.4. The average diesel price over the last 5 years is around 1.28 USD per kg [112]. The prices for energy have increased significantly over the last decade, mostly due to environmental taxes. For this reason the price for energy will be taken significantly higher to account for price increases in the future. Currently the more expensive European countries (Denmark, Germany,Belgium) pay around 0.34 USD per kWh [113]. A margin on this of 50% will be taken, resulting in a price of 0.51 USD per kWh. Next to this, the average jet fuel price over the last five years lays around 0.61 USD per kg [114]. These prices result in a cycle cost for diesel of 23.86 USD, for electricity of 37.23 and for jet fuel of 21.60 USD. So the operational costs per cycle for the RETS due to the fuel used is 82.68 USD.

This means the operational cost is on average around 33% lower when comparing the RETS with current taxi operations. It must be stated that this does not assume maintenance costs and crew costs. It is expected that the costs for the crew will be comparable, as the ground crew used for push back can be transferred to work as external vehicle crew. With respect to the maintenance costs, it is not expected that this will be more extensive than in current operations, and with the current difference in operational costs it can safely be assumed that the product will be profitable within five years, thus meeting requirement **[RETS-SH-TLREQ-09]**.

9.2 Competitor Analysis

With the design process progressing a competitor analysis can be done. In order to have a viable product the new system must be distinguishable from its market competitors with clear advantages over these other systems. However, it is also good to know the shortcomings of the new RETS product in this early design stage to identify where extra attention should be drawn to in the later design iterations. As the RETS is designed with the inspiration of Taxibot and EGTS, these systems

[112] https://www.statista.com/statistics/299552/average-price-of-diesel-in-the-united-kingdom/[accessed 19 June 2020]

[113] https://ec.europa.eu/eurostat/statistics-explained/index.php/Electricity_price_statistics[accessed 19 June 2020]

[114] https://www.indexmundi.com/commodities/?commodity=jet-fuel&months=60 [accessed 19 June 2020]

can be identified as the main competitors. Each competitor will now be compared with the new system in subsequent paragraphs. Lastly, the major positive and negative aspects that come out of these comparisons will be summarised in a SWOT diagram.

9.2.1 Taxibot

The most competitive product currently active on the market is Taxibot. Similar to the RETS it consists of a (modified) pushback truck that will tow the aircraft towards the runway while the aircraft engines are shut down. There are two major advantages of the RETS compared to Taxibot: the maximum speed and the vehicle dimensions. The most significant advantage is the higher maximum speed of the RETS of 30 kts compared to 23 kts of Taxibot [115]. Estimating that the coupling time of both systems will be very similar, the new taxi system will likely have less negative effects on the current taxi and airport operations due to its higher speed. These effects mainly originate from taxi queues that could occur due to aircraft standing still to decouple or couple.
The second main advantage of RETS over Taxibot is the reduced vehicle size. Mainly the width of the RETS vehicle is significantly smaller than conventional pushback trucks. Given this, the RETS will be more compatible with the existing service roads on airports. This has the potential to have more efficient deployment of the RETS with respect to Taxibot operations as Taxibot will only be able to drive over aircraft taxiways without investments on the service roads.

Similarly to Taxibot, fuel is saved during the taxi phases of the flight. For Taxibot, it is given that 50% to 80% fuel can be saved during taxi operations [116]. From the data given insubsection 4.9.2, RETS shows a reduction of 58.4% on the taxi phase analysed in this report. It is therefore estimated that both Taxibot and RETS will offer similar taxi fuel savings to its costumers. However, with RETS, extra fuel is burned during the flight phase due to added weight and therefore, Taxibot will be slightly more beneficial from an airline's perspective.
Although the maximum speed of the RETS is higher than Taxibot, this also brings a major disadvantage. As the higher speed is partially generated by an on-board system, the weight that is added will reduce the total energy and fuel savings. Especially the electric motor with its accompanying gears add a significant part of the weight. However, it should be noted that the aircraft modifications will make it possible for the system to be faster than Taxibot.
Moreover, the RETS having an external and internal system also induces a disadvantage of the RETS over Taxibot. Since Taxibot only consists of one system that could be made available by an airport or aircraft servicing company, RETS must have two systems for the most efficient usage. This means that the operating aircraft must be fitted with the electric motor and gears while the modified pushback vehicle must be present on an airport. This could give problems as an airline could opt to fit their aircraft with the internal system while an operating airport could choose to not purchase the external vehicle.

9.2.2 EGTS

Also for the EGTS system, the maximum speed of 20 kts [117] is lower than RETS. For the same reasoning as for Taxibot, RETS will have a big advantage on the negative influences of current airport operations. While the added weight is comparable [118], the advantage of EGTS is that no external vehicle is needed to power the electric motors on the MLG. As this is done by the aircraft APU, no coupling or decoupling is needed saving time during the taxi phase.
Since not much data is available on the fuel savings of EGTS, possibly because the system is still in a testing phase, a comparison cannot be made with RETS. However, it is estimated that the fuel savings will be similar for both systems as both electrical generators used consume fuel. Also given a similar mass, the in-flight fuel saving reduction will be similar.

[115] https://www.taxibot-international.com/concept [cited 18 June 2020]
[116] https://www.taxibot-international.com/news-c1o4v [cited 22 June 2020]
[117] https://www.ainonline.com/aviation-news/air-transport/2014-02-11/wheeltug-safran-honeywell-and-iai-offer-three-rival-solutions-airline-engine-taxiing [cited 18 June 2020]
[118] https://www.ainonline.com/aviation-news/air-transport/2013-06-18/honeywell-safran-demo-electric-taxiing-system-airlines [cited 22 June 2020]

9.2.3 SWOT Analysis

Besides the discussed advantages and disadvantages with respect to Taxibot and EGTS, other strengths, weaknesses, opportunities and threats can be identified with respect to the current market. All these SWOT parameters have been summarised in Figure 9.1. Another still undiscussed strength is the minimal effect on the aircraft stability. This mainly is the case because the extra weight is added near the MLG which is close the the CG at OEW. There are also two major opportunities for the system if further development is available. If the external vehicles can be made autonomous, there is the opportunity for ATC to control them. Also the implementation of the system on other aircraft in the A320 family has high potential as these aircraft show very high similarities.

As discussed, the airport is likely to invest in the strengthening of its service roads for a proper RETS operation. Together with the required aircraft modifications this can be seen as a major weakness of the system as it can be seen as a big investment. These investments also form a threat of the system and its implementation. The benefits could not be large enough such that an airline, aircraft manufacturer or airport might not invest in the system. Lastly, if the RETS must be slightly modified for proper operations, the system might be holding up other traffic which companies refrain from investing in the RETS.

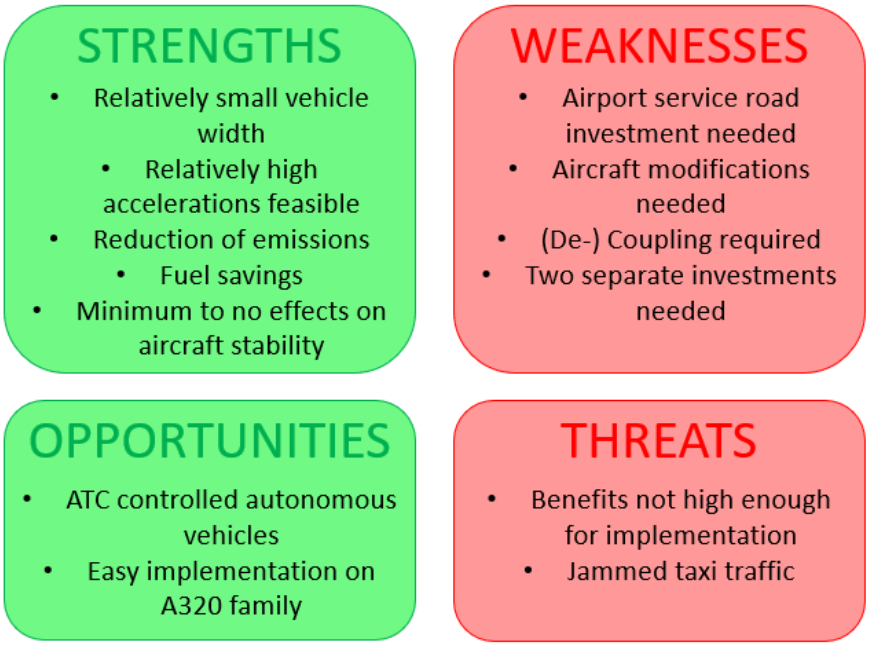

Figure 9.1: SWOT diagram of the RETS system within the current market

9.3 Sensitivity Analysis

Sensitivity of final fuel savings One of the most important results of the design is the total fuel savings that follow from the implementation of the RETS. These savings depend on and are therefore sensitive to, the amount of weight added to the aircraft. The final on-aircraft mass was found to be 324 kg, as determined in chapter 9; the effect of deviations from this value can, therefore, be analysed. As the relations are linear, the effects of deviations on the final fuel savings, are best evaluated using the slope of the different curves in Figure 4.18, presented in Table 9.3.

Table 9.3: Sensitivity of final fuel savings with respect to weight added on aircraft

Range (km)	Percentage of flights (%)	Slope [kg/kg]
1806	70	-0.116
2239	80	-0.137
2816	90	-0.164
3366	95	-0.190
3856	98	-0.215

From Table 9.3, it is clear that, depending on the desired range, the decrease in fuel savings that results from the addition of one extra kilogram of weight on the aircraft is constant. For example, when looking at 80% of A321neo flights, each additional kilogram of weight results in a decrease of 0.137 kg of fuel savings. Using the linear relation in Figure 4.18, the point at which fuel, is no longer saved can also be determined, but this point lies beyond the 2% weight increase of the aircraft empty weight (RETS-SH-TLREQ-03). As such, the sensitivity of the fuel savings with respect to weight is a linear relation, and fuel is still saved as long as the added weight stays below the limit of 940 kg added to the empty weight.

Sensitivity of acceleration and top-speed To find the acceleration sensitivity, the code was run with different acceleration profiles. The general profile was changed by a multiplication factor. These ranged from 1.5 higher to accelerations only 0.25 the magnitude of the design. The effects of higher and lower accelerations primarily apply on the taxi time and the energy consumption of the motors. The results of higher and lower accelerations are shown in Figure 9.2. For energy consumption, the limit is based on requirement RETS-SH-TLREQ-06. The savings in the least favourable situation are 233 kg of Jet A-1, as discussed in subsection 4.9.5 which yields more than 10 000 MJ. This is by far not reached in the suitable ranges of acceleration and top speed, so there is no strict limit on energy consumption. However, there are stricter limits on taxi time posed by RETS-SH-TLREQ-01. This requirement states that RETS taxi time shall be up to 1 minute longer than engine based taxiing. The limit case is used to check this requirement (Polderbaan taxi-in), as explained in section 4.8. The system is by definition slower, as the coupling time for taxi-in causes a 40 seconds delay to start with. It is questionable, that if the system would be capable to accelerate faster than average engine based taxi accelerations, that pilots would apply maximum acceleration. Engine based taxiing aircraft can accelerate faster, as the engines are designed to apply high thrust at take-off. However, due to FOD danger and passenger discomfort, these accelerations are not applied during taxiing. Would the RETS system be designed with higher than conventional acceleration capability, the pilots will unexpectedly not use this capability very often. Therefore, the lower limit is determined at 40 seconds.

As can be concluded from Figure 9.2, the acceleration of the current system is within the limits and can be changed to a large extent before it is out of limits. Acceleration can have a magnitude of 0.6 times the current acceleration before the requirement is not met. This is more than enough to leave contingency on coupling time. The lower limit is reached at an acceleration of 1.2 times the current acceleration. This shows that the current system has sufficient contingency and that the performance is not very sensitive to significant differences in acceleration profiles. For top-speed, however, the sensitivity of changing this parameter is more critical. As can be seen in Figure 9.3, the same limits in time delay hold. However, changing the top-speed of the system drastically reduces performance. The relation shown seems to be exponential. The limit is passed, at a top-speed around 13.5 $m\,s^{-1}$. As RETS is capable of reaching the same top-speed as conventional taxi, rated at 30 kts, there is some contingency left. However, attention should be paid to this in the following design phases. Of course, the prototype will differ from the estimated values during this design phase. However, top-speed is a very sensitive parameter and can quickly fail to fulfil the requirements. It is recommended that extra resources are put, into the realisation of this top-speed.

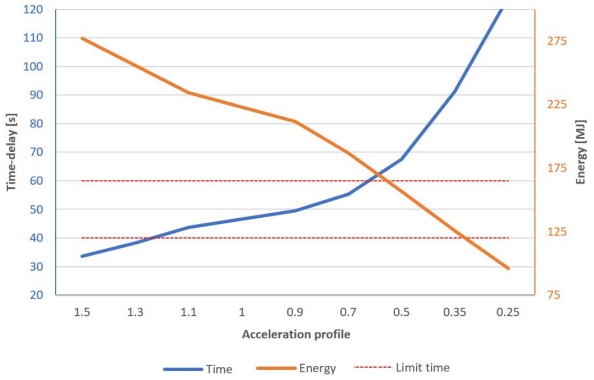

Figure 9.2: How taxi time and energy consumption change as a result of higher acceleration profiles when changed in the taxi performance model. The values at 1.0 acceleration represent the current system.

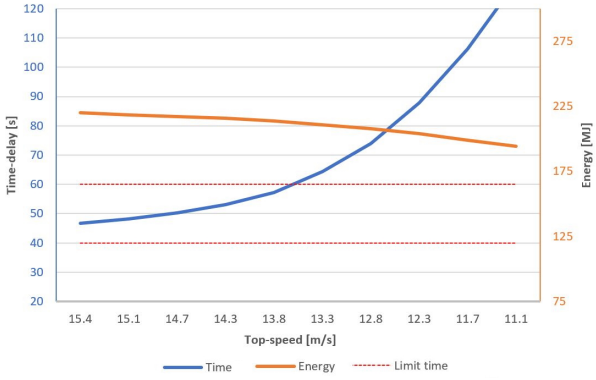

Figure 9.3: How taxi time and energy consumption change as a result of lower top-speed when changed in the taxi performance model. The curve at 15.4 m/s represents the current system.

9.4 RAMS Characteristics

To be able to access the operational performance of the RETS, the Reliability, Availability, Maintainability and Safety (RAMS) characteristics need to be evaluated. The Reliability is discussed in subsection 9.4.1, the Availability in subsection 9.4.2, with the Maintainability and Safety being discussed in sections 9.4.3 and 9.4.4 respectively.

9.4.1 Reliability

For the reliability of the RETS, it is assumed that the elements taken from the baseline towbarless tractor, which has been elaborated on in section 6.5, are reliable by their design. These elements have also proven themselves to be reliable during operational conditions.

One requirement focuses specifically on reliability. **[RETS-SH-TLREQ-04]**: RETS shall have a probability of catastrophic failure of less than 10^{-6} per year. However, at this stage of the design, the reliability cannot be obtained. This is due to a lack of information and detail on the different parts of the system. This will therefore be performed in future phases of the project. It is important to determine the reliability of each component and to combine the reliability accordingly depending on whether or not the system components are in series or in parallel. For systems in series, a single component failure would cause a system failure, whereas for systems in parallel, all components would need to fail for the entire system to fail. There are several ways to estimate the reliability of each component. The main method would be to use test data or estimates from manufacturers and suppliers of a certain component or of similar components. Naturally, testing the exact components or the system as a whole could be done but would be quite a lengthy process. Alternatively, certain companies also specialise in FMEDA (Failure modes, effects, and diagnostic analysis). These companies have access to large historical data on various types of components and can build statistical models to provide an analysis of the reliability of the system [119]. It has been decided at this stage of the project to focus on the safety critical aspects of the RETS .

9.4.1.1 Power Connection Failure

The power connection system, which has been elaborated on in sections 6.5.1.1 and 6.7.1, is based on proven design concepts. However, the combination of these concepts has not been used previously in the way described in sections 6.5.1.1 and 6.7.1. The combination of these concepts can lead to unexpected failures of the system, and hence, reduced reliability. However, the use of 2 separate systems to form the RETS does allow for the failure of the Power Connection System with minimal implications for the mission. In case of a failure in the Power Connection System, the external vehicle can still perform the taxi procedure, but with reduced performance.

[119] https://www.exida.com/Resources/Term/fmeda [Accessed 21 June 2020]

9.4.1.2 Drive Motor Failure

The full RETS consists of an External Vehicle and a Wheel-Based Engine system. Both elements of the RETS contain drive motors. The External Vehicle has four drive motors, as has been described in subsubsection 6.5.1.2 and the Wheel-Based Engine system has a single powered wheel on each MLG. This has been further elaborated on in section 6.6. The drive motors used in the external vehicle have proven themselves to be reliable in real-world situations. The motors (EMRAX268) selected for the Wheel-Based Engine have never been used in the way they are intended to be used, within RETS. However, these motors have received EASA certification for their use in aviation [120]. As the EMRAX268 has never been used to power the MLG wheels, its use can lead to unexpected failures, which in turn would decrease the reliability of the RETS. However, the use of two separate systems does allow for the failure of one or two of the drive motors on the MLG, as the external vehicle can also be used to tow the aircraft on its own, without the assistance of the Wheel-Based Engines. The system has also been designed for the whole MLG motor assembly to be removable, such that the system can be serviced externally. Hence, it can be said that the design has been made such that the reliability of the system has a minimal impact on airport operations.

9.4.1.3 Engine Heating System Failure

The Engine Heating System onboard the A321 is a system which increases the effectiveness of the RETS, as the Engine Heating allows for the main engines to be switched off during the taxi procedure. The Engine Heating System has been described in detail in subsection 4.6.2. A failure in this part of the RETS does not influence the mission of the RETS. However, it does increase the emission of the system as a whole, as the main engines need to be started earlier, to make sure that they have reached the operating parameters required for take-off. Even though a failure of the Engine Heating System does not influence the mission of the RETS, its chance of failure does reduce the reliability of the RETS.

9.4.1.4 Technology Readiness Level

In conclusion, it can be said that even though the individual components used on the RETS have a high technology readiness level (TRL), the combination of the components, within the RETS lowers the system TRL, because, a Wheel-Based Engine system has only been used previously by EGTS, which has mainly been used as a technology demonstrator [5]. The use of an external vehicle has a higher TRL, as this concept has already been proven, and certified, in the form of TaxiBot [61]. The combination of these two systems in RETS lowers the initial TRL of RETS. However, with more testing and detailed design, the TRL and the reliability of RETS will increase.

9.4.2 Availability

The availability is said to be the time in which the RETS is available. **[RETS-SH-TLREQ-05]** States that the system needs to have 95% availability. The main aspects which influence the system availability are maintenance, the weather, and the recharging time.

9.4.2.1 Maintenance

When maintenance needs to be performed, the RETS will not be available. To not impact the availability of the A321 to which it is attached, the Wheel-Based Engine System is removable. Hence, it can be serviced away from the aircraft. The maintenance procedures and impact on the RETS will be further discussed in subsection 9.4.3.

9.4.2.2 Weather

Another aspect which will seriously influence the availability of the RETS is the weather. This concerns **[RETS-F-GEN-03]**: RETS shall operate in most weather conditions. Under certain weather conditions, such as heavy snow, severe icing, and severe rain, the RETS may not be able to operate. However, the system has been designed to work in all weather condition in which normal engine based taxi, can be performed. The weather conditions mentioned can all cause low friction

[120] https://emrax.com/e-motors/emrax-268/ [accessed 18 June 2020]

coefficients, which could mean that the RETS will not have enough traction to operate as intended. In some cases, it may even be dangerous to try and operate RETS in such conditions.

9.4.2.3 Recharging Time

As has been described in subsection 5.4.7, the RETS has been designed to perform five taxi cycles to the Polderbaan (36L). After the five cycles, the system needs to be recharged. The RETS can perform 15 taxi cycles, on the conventional taxi route. As described in subsection 5.4.7, the recharging time of the batteries, is expected to be 40 min, when using a Tesla Supercharger. During this time, the system will not be available to perform its mission. During the same time, the external vehicle also needs to be refuelled. However, this is neglected in the recharging time estimation, as the battery recharging time is significantly longer than the time needed to refuel the external vehicle.

9.4.2.4 Concluding Remarks

In conclusion, it can be said that, even though aspects are present which influence the system availability, RETS, is deemed to meet the requirement, and hence, is available for at least 95% of the time.

9.4.3 Maintainability

To ensure a proper functioning system, the maintenance of the RETS must be well organised. Since the new taxi system is composed of a pushback vehicle and an onboard system, the focus of the maintenance is also different for the two systems.

9.4.3.1 Onboard System

As this part of the RETS is fixed to the aircraft itself, the maintenance routine of the onboard systems will preferably coincide with the maintenance intervals of the aircraft. This already starts with the pilot inspection of the aircraft before every flight. As the pilot also inspects the MLG, it will be little extra effort to also visually check the gears and its accompanying electric motor. In case an error has been spotted, it must be reported to the RETS control centre. They will decide if there will still be sufficient time to replace a component before take-off. If this is not the case, the aircraft will still be able to depart. This is due to the fact the the RETS will not restrict engine-based taxiing. Although this is not according to the mission statement as emissions will be higher than conventional flights, for the airline it will be important to reduce the chance of delays. The fact that engine-based taxiing is still possible is due to the fail-safe mechanism coupling the gears. This critical mechanism is still to be designed in a future design iteration as stated in subsubsection 6.6.3.1.

Besides the line maintenance, also the aircraft A-, B-, C- and D-checks could be used to check and maintain the on board components. Especially the gears should be inspected for wear and potential fatigue cracks. The electric motor, similar to a jet engine, could just be replaced with a serviced motor to save time. Cables are less easy to check, however, during B- and C-checks time will probably allow for the cables to be checked. The hangar maintenance checks could be performed by the same aircraft maintenance crew, however, they should be properly trained for the RETS.

9.4.3.2 Pushback Vehicle

The advantage of the pushback vehicle from a maintenance perspective is that the vehicle will always be at the airport, as opposed to the electric motor and its gears, which will be often airborne. This makes the maintainability of the pushback vehicles easier. The maintenance of the vehicles is represented by Figure 9.4 and can be divided into three main starting points. These three points represent the origin of a certain desire for maintenance.
First of all, the vehicle itself will be fitted with sensors and accompanying software to detect errors of the entire system. These errors also include maintenance checks and will pop up when a certain system is not behaving accordingly and potentially needs a maintenance check. Both during the active taxi operations and during idle time these errors might pop up. The error will then indicate

what system draws the sensors' attention together with an indication of the severity. If the detected error is not urgent and the taxi operations are not jeopardised, the vehicle will be checked after its current operation is finished.
In case the displayed error is critical, and thus requiring immediate repair or check ups, the current operation must be terminated. When the vehicle is performing a taxi operation, this means that the aircraft must be decoupled. The driver and/or pilot will then need to contact the airport authorities together with the RETS control centre to report the malfunction. In this way, the airport operation has the ability to adapt to a potential holding aircraft on a certain taxiway or other operational obstacle.
Besides the sensors inside and on the vehicle, data is also logged of other systems in the vehicle. This is less critical data, however, it might display smaller malfunctions that could potentially grow to a bigger problem or decrease the efficiency of the RETS. If the data shows a deficiency, a visual check will be recommended. Otherwise, during the routine maintenance after a certain number of cycles, this check must be performed.
If either of the three error messages is confirmed, the responsible maintenance department will set up a plan to repair or check the related system of the vehicle. In case of urgency, a technician must be sent to the pushback truck itself on the airport with a standard repair and maintenance kit. Bigger checks and maintenance will only be performed in a designated workshop. This could be the same workshop or maintenance facility where the maintenance of other aircraft servicing vehicles is currently performed.

9.4.3.3 Maintenance Requirements

The following list of requirements all fall under the maintenance category. A brief explanation of whether or not the requirement has been met or how it will be met in future phases of the project is given.

- **[RETS-SH-MTC-01]**: The failed component, in case of the RETS does not function properly, shall be found if the diagnosis procedure is followed correctly. (*Technical*).
  It is believed that using the procedures indicated in Figure 9.4, the failed component can be detected properly and the requirement can be satisfied. However, this requirement may need updating and further research once detailed parts are designed.
- **[RETS-SH-MTC-02]**: The maximum time required to replace a failed component when the replacement part is available shall not be more than <TBD> hours.
  This requirement needs to be updated after more research is done into aircraft and pushback truck maintenance. The requirement cannot be fulfilled at this point in the project as it requires detailed design of the system's components and additional knowledge on how each part can be replaced and how complex this process is.
- **[RETS-F-SAF-01]**: RETS shall operate for <TBD> cycles without a maintenance check.
  As shown in Figure 9.4, maintenance can be planned when errors occur during operations or when anomalies are detected in the data collected from the system. Routine maintenance will however be planned at a regular interval depending on the number of cycles the system has performed. This number will depend on the reliability of the system which is yet to be determined. The requirement cannot be fulfilled at this time.
- **[RETS-NF-MRO-01]** Inspection costs shall not exceed <TBD> EUR per inspection.
  The inspection cost will depend on the part that needs inspections and how complex it is to fully inspect it. This cannot be determined until later phases of the design. The requirement will also be fixed when more information is obtained on typical costs for aircraft and pushback truck inspections.
- **[RETS-NF-MRO-02]** Maintenance shall be able to be performed by at least an EASA Part 66 or equivalent technician.
  The detailed parts of the system have not been designed or modelled yet. As little information is known on the reliability and issues certain parts may have, it is difficult to plan maintenance in detail. Therefore it is not possible to say what will be require maintenance. However, it is believed that the complexity of the maintenance of the system will not be greater than that

of an aircraft and that Part 66 qualification should suffice.

- **[RETS-NF-MRO-03]** Maintenance training shall take a maximum of <TBD> days.
  The same reasoning applied for all three **[RETS-NF-MRO]** requirements. More research is required to fix this requirement and a more detailed design is necessary to fulfil it.
- **[RETS-NF-MRO-05]** An online support platform shall be available for the purchase of repair parts.
  Once again, at this phase of the project, it is not yet possible to have satisfied this requirement. However, it is believed that it can easily be fulfilled in later phases. Once a detail plan has been made on the parts that can be bought from suppliers or need to be manufactured and contracts have been signed, a website which includes the name, cost, part number, installation instructions and documentation can easily be created to help clients.

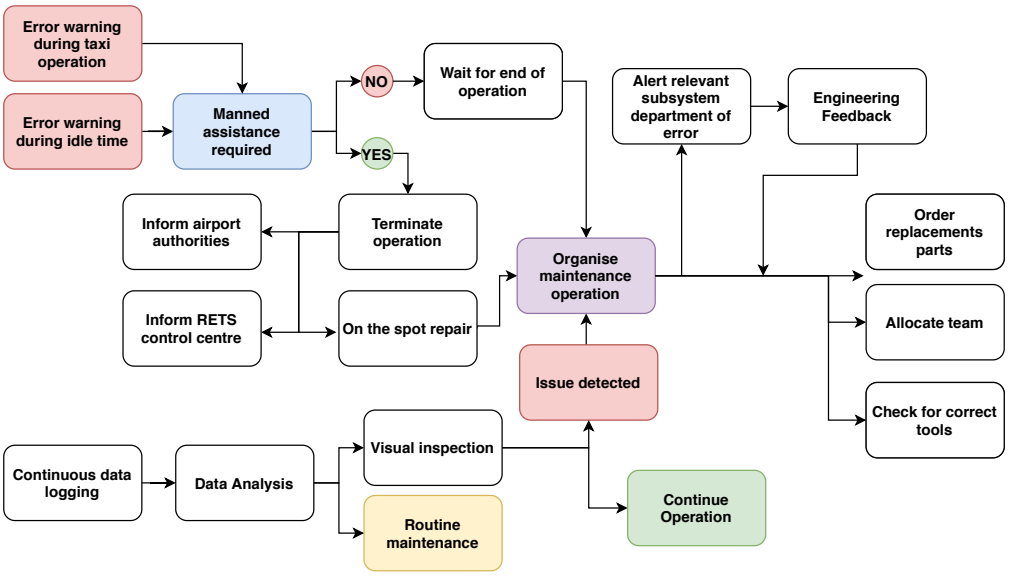

Figure 9.4: Maintenance flow chart for RETS pushback truck

9.4.4 Safety

To ensure safe operation of the RETS, the safety aspect needs to be considered. To ensure the safety of the Wheel-Based Engine components, these components have been designed, while taking CS25 into account (**[RETS-NF-REG-01]**). Hence, it can be said that the safety of the Wheel-Based Engine components has been insured. The Wheel-Based Engine also contains fail-safes designed to break in the case of over-stressing of the system. The safety features are discussed in section 6.6. Besides the Wheel-Based Engine components, the safety of the external vehicle also needs to be taken into account. The safety aspects which have been found, for the external vehicle are the emergency aircraft decoupling, emergency power decoupling, and the grounding of the RETS. These aspects have been discussed in more detail in subsection 6.7.3. For **[RETS-NF-REG-01]**: The parts of RETS placed on the aircraft shall be in compliance with CS25/FAR25, it is believed that the system up to this point has been designed to comply with the CS25/FAR25 certification. It will however require more research and time to check the detailed parts of the system for compliance. The requirement will therefore be fulfilled later in the project.

9.5 Technical Risk

In chapter 4 through 7, for every subsystem, specific technical risks have been identified. Part of these risks have already been listed in the midterm phase [1], however, new risks have also been identified. Besides the identification of new risks, the probability and the consequence of every risk has been estimated according to Table 4.1 and 4.2. The results of all identified risk probabilities and consequences up until now are shown in the pre-mitigation risk map, which can be seen in Figure 9.5.

Probability of occurrence \ Impact on the project	1	2	3	4	5
1					
2	C.6, C.9	C.8	O.3, P3, P4, P.5, P.7, S.5, S.9, C.3	P.2, S.3A, S.4, M.5, C.4	O.4, P.1, S.7, M.3, M.4
3		O.8, P.9, C.7	O.2, P.6, P.8, P.10, S.2, M.1, M.2, C.5	O.7, S.1, S.3B, S6, S.8, S.10, C.1, C.2	O.1
4			O.6		O.5
5					

Legend
- High risk
- Medium-to-high risk
- Low-to-medium risk
- Low risk

Figure 9.5: Pre-mitigation risk map

As can been seen, the highest risks have been identified for the operational aspects of the RETS. The structural and control/stability risks also show medium to high risks while the power/electrical risks only show low to medium risks. To lower the consequences and/or the probability of occurrence of the identified risks, a mitigation strategy has been determined for all risks as well. As stated per subsystem, some of the mitigation strategies have already been implemented during the subsystem design as this is a critical step in the design process. By designing with these mitigation strategies in mind, the final design will have a lower risk level. The post-mitigation risk levels can be found in Figure 9.6.

Probability of occurrence \ Impact on the project	1	2	3	4	5
1	C.6, C.9	P.9, C.3, C.5, C.8	O.2, P.1, P3, P.4, P.5, P.6, P.7, S.3A, S.4, S.5	P.2, S.1, M.5, C.4	O.1, O.4, S.7, M.3, M.4
2		O.2, O.8, P.8, S.9, C.2, C.7	P.10, S.2, S.10, M.1, M.2	O.7, S.3B, S.6, S.8	O.5
3			O.6, C.1		
4					
5					

Legend
- High risk
- Medium-to-high risk
- Low-to-medium risk
- Low risk

Figure 9.6: Post-mitigation risk map

As can be seen, by the difference of both tables, the majority of the risks can be decreased, to low and low-to-medium risks by the proposed mitigation strategy. However, for one risk, this could not be achieved. The risk of adverse effects on normal operations (**T.O.5**) will have a huge impact on the current taxi operations on the airports, which are highly undesirable as airlines and airports desire an efficient operation. If delays are caused, by RETS, this could result in extra costs for airlines. Other higher operational risks include insufficient engine pre-heating (**T.O.7**), not reaching simulated performance (**T.O.6**) and not reducing the total emissions (**T.O.4**).
Again in the post-mitigation, the power and electrical risks show a relatively low risk compared to the other three subsystems. The probable cause of this is the high ability to predict the electrical behaviour during the design where for other subsystems this is harder to do.
For the structural subsystem, the post-mitigated identified risks are slightly higher than the risks identified for power/electronics and control/stability. The highest risks deal with exceeding loads (**T.S.3B**), wheel brake cooling (**T.S.6**) and landing gear retraction (**T.S.7**).
Lastly, the risks of the control and stability subsystem could be mitigated, to a large extent as only half of the risks are low to medium while the remaining risks are all mitigated to low risks. The highest risks, to take into account during future design iterations are the stability reduction (**T.C.1**) and a sudden control input (**T.C.4**).

10 Future Outlook

This section will discuss the phases which will need to be performed in the post-DSE phase, to get the RETS into an operational state. Firstly, the Manufacturing, Assembly and Integration plan will be discussed in section 10.1. Secondly the Project Design & Development Logic, with all the phases which need to be performed, is elaborated on in section 10.2, and finally the expected time planning is shown in section 10.3.

10.1 Manufacturing, Assembly and Integration Plan

To be able to bring the system, that has been designed, into operation, a Manufacturing, Assembly and Integration (MAI) plan are necessary. The MAI plan can be seen in Figure 10.1. The MAI plan has been constructed such that, if followed correctly, the system can be assembled, from its constituent components. The MAI plan shown in Figure 10.1 is time ordered from left to right. On the left of the figure, the assembly process starts, and on the right side, the system is put into operational use. The manufacturing of the RETS starts with obtaining the needed materials and components. When the material has arrived, the manufacturing of the components can start. The different Sub-Assemblies can be assembled, from these components. The various Sub-Assemblies are then installed on the Towbarless Tractor (External Vehicle) and inside the aircraft. The installation of the system in the aircraft can be done. as a retrofit or as an OEM option. After the installation of RETS, an extensive system test needs to be performed, to make sure that the RETS will perform optimally in all conditions. When the RETS has passed the system tests, it can be deployed, into active service.

10.2 Project Design & Development Logic

To get the RETS, into active service the project will need to go through several phases. The phases which have been deemed necessary, are shown in Figure 10.3. The red boxes at the top of the figure, indicate the main project phases. These phases have been ordered chronologically, and have been expanded, using work packages. The Production of Prototypes has not been expaned, as it follows the same steps as the Production Phase. The work packages are indicating the basic tasks which have to be performed, within a project phase. In Figure 10.3, it can be seen that within every project phase, there is a Go/No Go element. This element has been added to each phase, to check if the design is still feasible, and continuation of the project is most likely going to result, in the successful completion of the project. A requirement which needs to be taken into account during the continuation of the project is **[RETS-SH-INV-03]**: The product development progress and risks shall be communicated monthly (Business)

10.3 Project Gantt Chart

Using the Project Design & Development Logic, shown in Figure 10.3, the Project Gantt Chart can be created. The Gantt Chart, in Table 10.1, shows the expected duration of the project to the delivery of the first system. A total development and production time of 7 years is being planned for, as it is expected that the certification is going to take two years. If the certification takes less time than expected, the whole project duration is reduced. Within Table 10.1 several colours can be seen. The lighter colours indicate subphases, and the darker colours indicate top-level phases.

10.4 Cost Breakdown Structure

A cost breakdown structure is a visualisation for the costs that are yet to come on the further phases. These are assumptions and the document will change in further design phases, but it can help when making cost estimates. Using this the requirement **[RETS-SH-INV-01]** can in the

future be checked. This requirement states that the system must be profitable for the developing party withing a certain amount of years. The cost breakdown structure for the RETS can be seen in Figure 10.2.

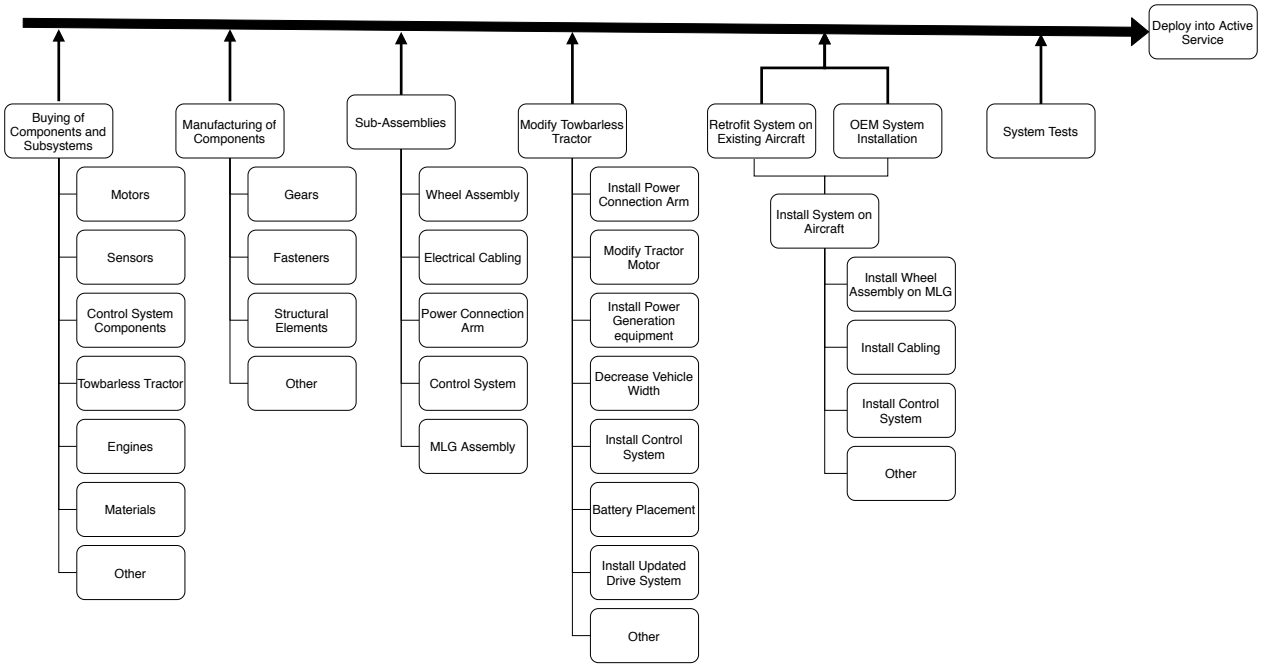

Figure 10.1: Manufacturing, Assembly and Integration Plan

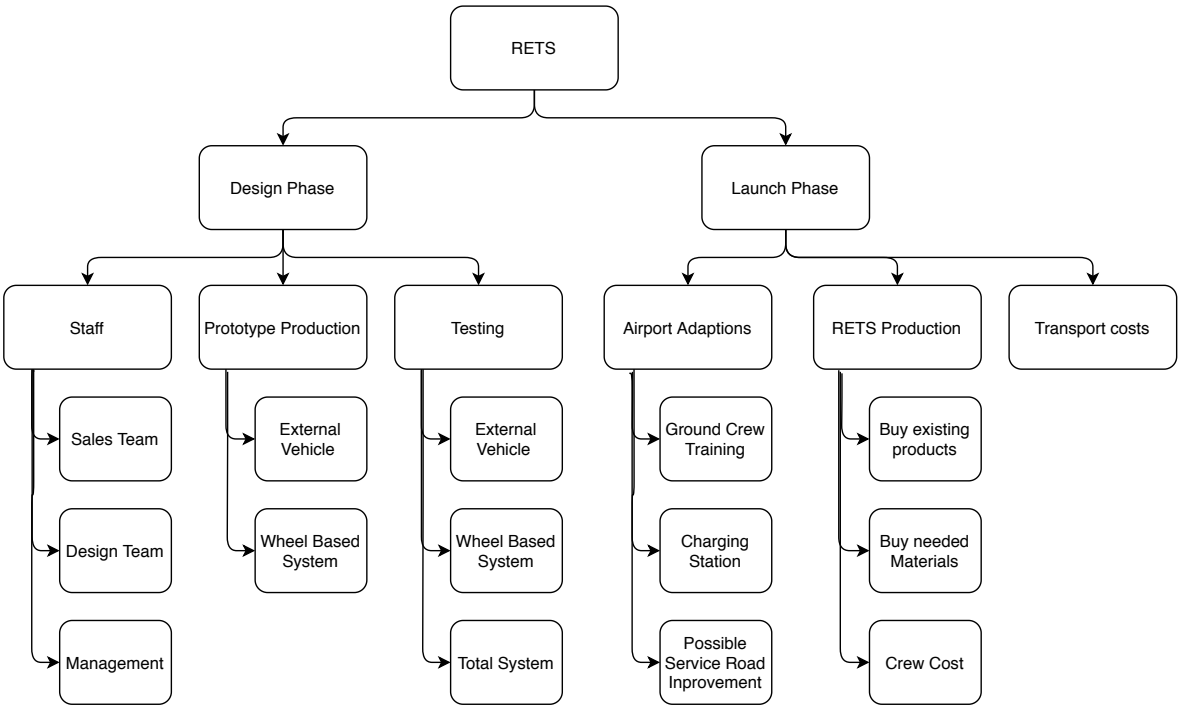

Figure 10.2: Cost Breakdown Structure

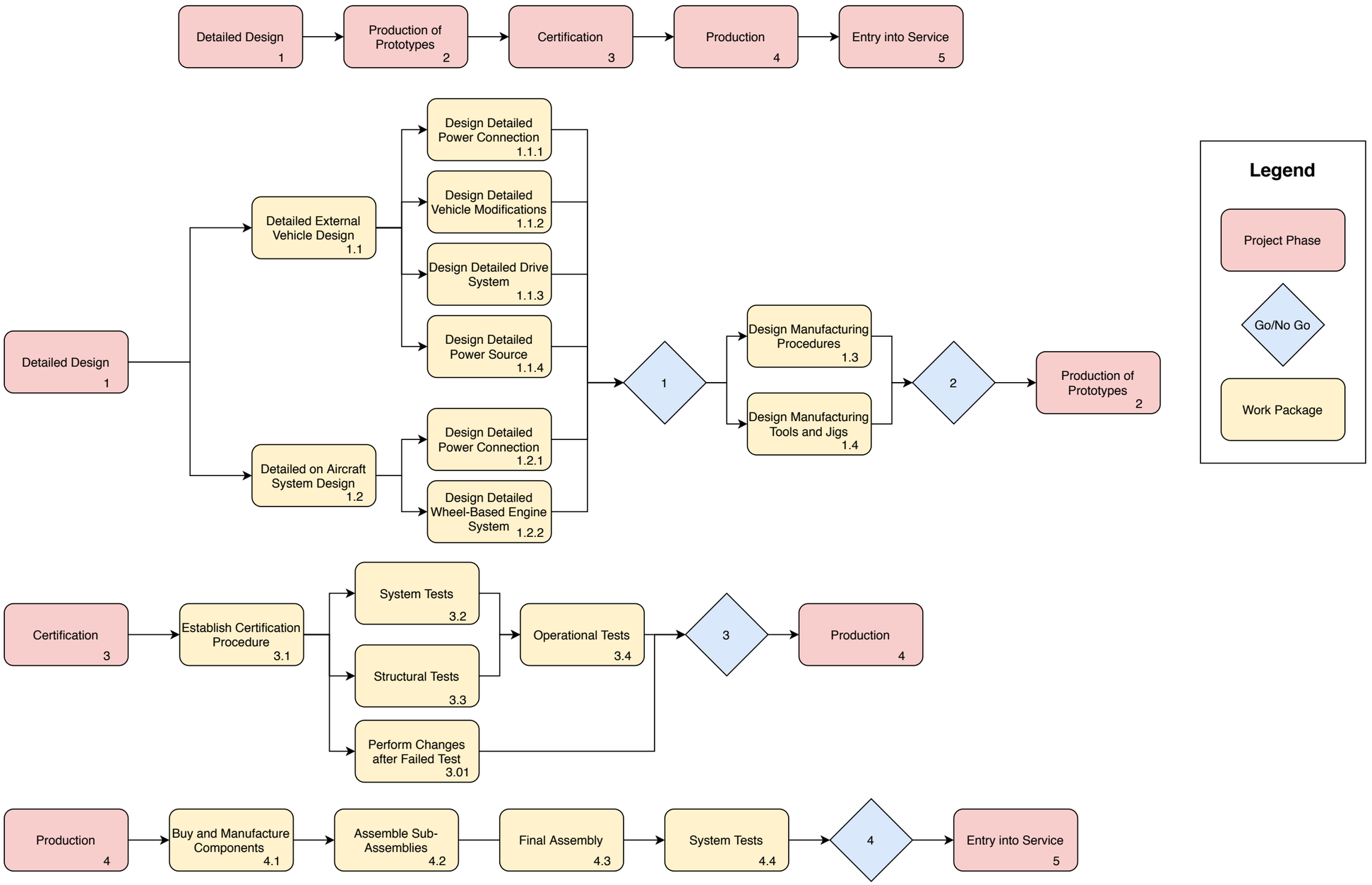

Figure 10.3: Project Design & Development Logic

Table 10.1: Project Gantt Chart

Development Phase	Timespan
1 Detailed Design	July 2020-July 2022
1.1 Detailed External Vehicle Design	July 2020-July 2021
1.1.1 Design Detailed Power Connection	July 2020-January 2021
1.1.2 Design Detailed Vehicle Modifications	July 2020-January 2021
1.1.3 Design Detailed Drive System	January 2021-July 2021
1.1.4 Design Detailed Power Source	January 2021-July 2021
1.2 Detailed on Aircraft System Design	July 2021-January 2022
1.2.1 Design Detailed Power Connection	July 2021-January 2022
1.2.2 Design Detailed Wheel-Based Engine System	July 2021-January 2022
1.3 Design Manufacturing Procedures	July 2022
1.4 Design Manufacturing Tools and Jigs	July 2022
2 Production of Prototypes	January 2023-July 2023
3 Certification	July 2021-January 2026
3.1 Establish Certification Procedure	July 2021 - January 2022
3.2 System Tests	January 2022-July 2025
3.3 Structural Tests	January 2022-July 2025
3.4 Operational Tests	January 2024-January 2026
3.0.1 Perform Changes after Failed Test	July 2024- January 2026
4 Production	January 2026-January 2027
4.1 Buy and Manufacture Components	January 2026
4.2 Assembly Sub-Assemblies	July 2026
4.3 Final Assembly	July 2026-January 2027
4.4 System Tests	January 2027
5 Entry into Service	July 2027

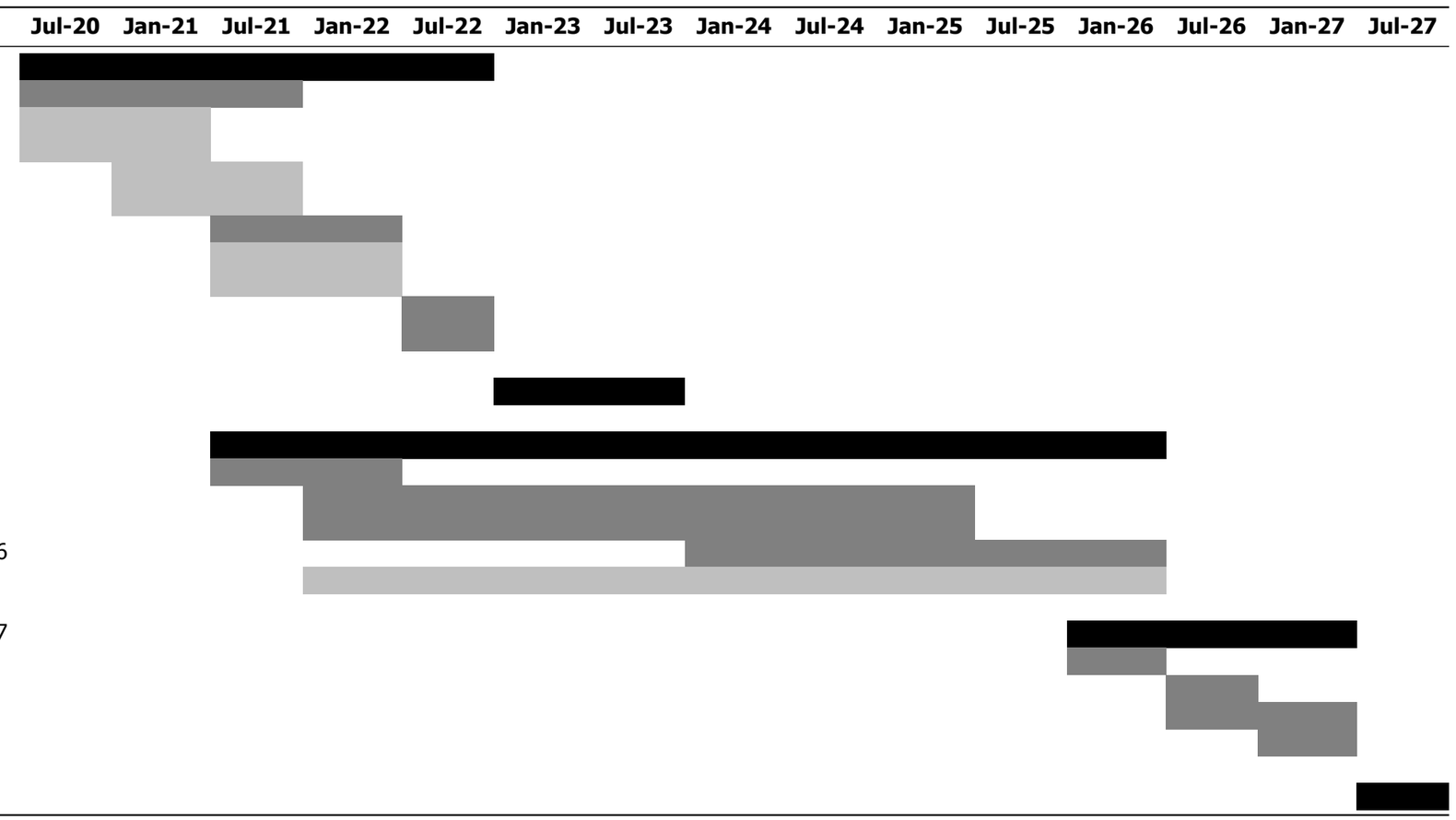

11 Conclusion & Recommendations

11.1 Conclusion

The goal of this project was to design a system which would allow for an aircraft to taxi with lower emissions than it currently does, and in doing so reduce its total emissions from gate to gate. Throughout the design process, and especially the midterm, the optimal solution was narrowed down to the final Reduced Emission Taxi System (RETS) design.

The RETS consists of an external vehicle as well as internal engines mounted at the main landing gear. With over 70% of the required force coming from the external vehicle, the system has been able to minimise weight on the aircraft without sacrificing performance. The combination of these systems also makes the RETS versatile. Operations are possible with only the internal motors, as well as with only the external vehicle.

Additionally, the RETS also meets all but one top level requirements set out by the main stakeholders thus far.

- **[RETS-SH-TLREQ-01]**: RETS taxi time is only, at most, 46.5 seconds slower.*(Performance)*
- **[RETS-SH-TLREQ-02]**: RETS does not lead to a reduction in aircraft payload. *(Performance)*
- **[RETS-SH-TLREQ-03]**: RETS only induces a 0.7% increase in operational empty weight of the aircraft. *(Performance)*
- **[RETS-SH-TLREQ-05]**: RETS is easily replaceable, operates in the same weather conditions as conventional taxi, and has reasonable charging times. Thus it is deemed to have an availability per system of at least 95% per taxi in and taxi out. *(Availability)*
- **[RETS-SH-TLREQ-06]**: RETS reduces total energy consumption from gate to gate with respect to engine based taxiing. *(Sustainability)*
- **[RETS-SH-TLREQ-07N]**: RETS predominantly uses recyclable materials.
- **[RETS-SH-TLREQ-08]**: RETS will prevent throttle input, and hence take-off, while the system is engaged rendering the system fail-safe. *(Safety)*
- **[RETS-SH-TLREQ-09]**: RETS has an operational cost of 82.68 USD per cycle, 33% lower than the upper limit. Thus, it will have a positive net present value in under five years based on average fuel prices before 2020.

The only top level requirement which has not yet been determined is the one regarding the probability of catastrophic failure. This requirement, along with other aspects to consider for the future, will be discussed in section 11.2.

Finally, RETS performs its main goal of reducing total, gate-to-gate emissions. Indeed, given the added internal weight of approximately 315 kg, the final emission reductions per mission profile will be at least 204 kg of fuel for 98 % of all A321 flights, and at least 240 kg of fuel for 70% of all A321 flights.

11.2 Recommendations

Although this report already addresses the most important design elements of the new RETS, not everything could be designed in the desired detail yet. Most importantly, an analysis on the probability of catastrophic failure of the RETS must still be performed to determine whether the **[RETS-SH-TLREQ-04]** top level requirement is indeed met. Furthermore, for all subsystems, it holds that further research is needed to come to a realistic final RETS. Especially the feasibility must be checked to see if the design is viable and worthwhile to take into a further design phase. A short overview of the most important elements to investigate in the next design iterations will be discussed for each subsystem.

For the operational aspects of the RETS, the most important elements to extend are the taxi simulations. Both the taxi time simulation and the fuel reduction simulation are now partially based on assumptions. In the next design iteration these assumptions should ideally be interchanged by realistic data, or modelled to specific routes. This will make sure less contingency is present in the taxi fuel calculations.

In the power and electronics subsystem there are three major aspects to investigate in the future. As the chosen engine, Emrax 268, is able to provide the desired torque, it will be its peak torque. According to the operations manual of the motor, peak torque can only be achieved for a couple of seconds. Further research must be done to check if this constraint is violated or a new bigger engine must be implemented in the design for a proper operation. Moreover, the cooling of the engine has also not been investigated yet. This is critical for the functioning of the motor and should therefore also be analysed in the future. Lastly, the possibility to charge the RETS batteries by means of the diesel engine of the pushback truck could be worthwhile for possible weight savings.

The structural subsystem contains two elements that must be investigated in the next design iteration. First of all, a (de-)coupling mechanism for the gears must be designed further to make sure the spring cylinder is integrated properly into the supporting structure. For the other major system of the RETS, the pushback truck, the lay-out must be investigated in further detail. In this design iteration only the general shape and outline have been established, however, a more detailed design must be made to make sure there is enough space for, for instance, the cooling system and the hydrostatic drive system. Also, the functioning of the robotic arm is subject to more detailed design. Besides the functioning, of the robotic arm, the exact placement of the power connection on the aircraft, will have to be investigated further, as it is a possibility to place the power connection inside the NLG bay. This location will allow for the removal of the power connection door and a more centred placing of the power connection. Finally, from a feasibility perspective, the stresses on the nose landing gear, due to the pulling force applied to it, need to be analysed in more detail to insure each individual load bearing component can sustain these loads and aren't subjected to excessive fatigue.

Lastly for the control and stability subsystem the steering is crucial. Although this element has already been covered quite extensively, in future design iterations it must be subject to real-life testing. This could be done with a simulation or a simplified prototype. Once this work mechanically, also pilots could be involved to test the controls of the RETS and provide feedback for improvements.

Bibliography

[1] N.J. van Amstel, S. de Boer, S. Brunia, W.G.E. Dekeyser, J.J.A. van 't Hooft, N.M. Jahjah, K.Y.T.Y. de Lange, M.N.X.Y. Pellé, G. Salem, and R.A. Vos. Short to Medium Range Aircraft with Zero Emission Taxi - AE3200 Design Synthesis Exercise: Midterm Report. (unpublished), 2020.

[2] N.J. van Amstel, S. de Boer, S. Brunia, W.G.E. Dekeyser, J.J.A. van 't Hooft, N.M. Jahjah, K.Y.T.Y. de Lange, M.N.X.Y. Pellé, G. Salem, and R.A. Vos. Short to Medium Range Aircraft with Zero Emission Taxi - AE3200 Design Synthesis Exercise: Project Plan. (unpublished), 2020.

[3] N.J. van Amstel, S. de Boer, S. Brunia, W.G.E. Dekeyser, J.J.A. van 't Hooft, N.M. Jahjah, K.Y.T.Y. de Lange, M.N.X.Y. Pellé, G. Salem, and R.A. Vos. Short to Medium Range Aircraft with Zero Emission Taxi - AE3200 Design Synthesis Exercise: Baseline Report. (unpublished), 2020.

[4] Ming Zhang, Qianwen Huang, Sihan Liu, and Huiying Li. Assessment Method of Fuel Consumption and Emissions of Aircraft during Taxiing on Airport Surface under Given Meteorological Conditions. *Sustainability*, 11(21):6110, 2019.

[5] Safran and Honeywell. Electric green taxiing system, June 2013.

[6] Paul Roling. A321 data set (includes flight distance, departure airport, arrival airport, and number of flights), 2018. Taken from Brighspace group files locker, posted on 09 June 2020 at 10:21 by Paul Roling.

[7] Louise Butcher. Lorry sizes and weights, 2009.

[8] S. M. L. Soepnel. Impact of Electric Taxi Systems on Airport Apron Operations and Gate Congestion at AAS. Master's thesis, TU Delft, 2015.

[9] P.J.A. Sillekens. Effect of EGTS on airport taxi movements at AAS. Master's thesis, TU Delft, 2015.

[10] David Foyle. Automation tools for enhancing ground-operation situation awareness and flow efficiency. 06 2020.

[11] *APS 3200 AUXILIARY POWER UNIT*. Hamilton Sundstrand Corporation, 2006.

[12] PhD Kamiar J. Karimi. Future Aircraft Power Systems- Integration Challenges.

[13] Airbus S.A.S. *AIRCRAFT CHARACTERISTICS AIRPORT AND MAINTENANCE PLANNING*. AIRBUS, 2018.

[14] International Aero Engines (IAE), LLC. TYPE-CERTIFICATE DATA SHEET No. IM.E.093, 2019. PW1100G type certificate.

[15] CFM International SA. TYPE-CERTIFICATE DATA SHEET No. E.110, 2019. LEAP-1A type certificate.

[16] HOBART. HOBART 3400 PCA, n.d. Brochure of company.

[17] ADELTE. Preconditioned Air Unit - ZEPHIR Inverter, n.d. Brochure of company.

[18] B.T.C. Zandbergen R. Vos, J.A. Melkert. *A/C Preliminary Sizing (class I weight estimation method)*. Faculty of Aerospace Engineering, Delft University of Technology, Delft, the Netherlands, 1 edition, 2018.

[19] Harshad Khadilkar and Hamsa Balakrishnan. Estimation of Aircraft Taxi-out Fuel Burn using Flight Data Recorder Archives. In *AIAA Guidance, Navigation, and Control Conference*, Guidance, Navigation, and Control and Co-located Conferences. American Institute of Aeronautics and Astronautics, August 2011. doi: 10.2514/6.2011-6383.

[20] Khánh Ngọc Đinh. Simulation of Taxiway System Maintenance to Optimize Operational Value at Schiphol Airport. Master's thesis, TU Delft, 2012.

[21] Jan Roskam. *Airplane Design*. Roskam Aviation and Engineering Corporation, 1985.

[22] Andrey Fomin. Pd-14 new-generation engine for mc-21. *Take-off*, page 20–21, Dec 2011.

[23] International Civil Aviation Organization. Operation of aircraft. *Annex 6 to the Convention on*

International Civil Aviation, Ninth Edition:4–9, July 2010.

[24] Antonio Filippone. *Advanced aircraft flight performance*, volume 34. Cambridge University Press, 2012.

[25] Yashovardhan S Chati and Hamsa Balakrishnan. Analysis of aircraft fuel burn and emissions in the landing and take off cycle using operational data. In *International Conference on Research in Air Transportation*, 2014.

[26] S Webb. Technical Data To Support FAA's Advisory Circular on Reducing Emissions from Commercial Aviations'. *US EPA*, 9, 1995.

[27] *TYPE-CERTIFICATE DATA SHEET for AIRBUS A318 – A319 – A320 – A321*. European Union Aviation Safety Agency (EASA), Dec 2015. Issue 45.

[28] Fabrizio Re. *Model-based Optimization, Control and Assessment of Electric Aircraft Taxi Systems*. PhD thesis, Technische Universität, Darmstadt, 2017.

[29] Ticiano Jordão. Analysis of fuel efficiency of largest european airlines in the context of climate change mitigation. *International Journal of Global Energy Issues*, 39:253, 01 2016. doi: 10.1504/IJGEI.2016.076348.

[30] Raffi Babikian, Stephen P Lukachko, and Ian A Waitz. The historical fuel efficiency characteristics of regional aircraft from technological, operational, and cost perspectives. *Journal of Air Transport Management*, 8(6):389–400, 2002.

[31] Giuseppe Graber. *Electric Mobility: Smart Transportation in Smart Cities*. PhD thesis, 05 2016.

[32] Inc. Aviation Supplies & Academics. *Aviation maintenance technician handbook*. Aviation Supplies & Academics, 2018.

[33] Federica Forte, Massimiliana Pietrantonio, Stefano Pucciarmati, Massimo Puzone, and Danilo Fontana. Lithium iron phosphate batteries recycling: An assessment of current status. *Critical Reviews in Environmental Science and Technology*, 0(0):1–28, 2020. doi: 10.1080/10643389.2020.1776053.

[34] Shigeru Tokuda, Sanae Horikawa, Kunio Negishi, Kenji Uesugi, and Hiroshi Hirukawa. Thermoplasticizing technology for the recycling of crosslinked polyethylene. *Furukawa Review*, 04 2003.

[35] Mohamed A. Elshaer, Allan Gale, and Chingchi Chen. Exploration of the impact of high voltage ground fault in an electric vehicle connected to earthing systems worldwide. In *SAE Technical Paper*. SAE International, 03 2017.

[36] MAN Engines. *OFF-ROAD: Diesel engines for agricultural and construction, environmental and special machinery*. MAN Truck Bus – a member of the MAN Group, 2020.

[37] EMRAX Innovative E-Motor. *Manual for EMRAX Motors / Generators v5.4* . EMRAX Innovative E-Motor, 2020.

[38] Dinko Mikulic. *Design Of Demining Machines*. Springer, 1 edition, 2013.

[39] C Iclodean, B Varga, N Burnete, D Cimerdean, and B Jurchiş. Comparison of different battery types for electric vehicles. *IOP Conference Series: Materials Science and Engineering*, 252: 012058, oct 2017. doi: 10.1088/1757-899x/252/1/012058.

[40] R.C. Hibbeler. *Mechanics of Materials: SI Edition*. Pearson Higher Education & Professional Group, 9 edition, 2013.

[41] A.P. Mouritz. *Introduction to Aerospace Materials*. Woodhead Publishing in Materials. Elsevier Science, 2012. ISBN 9780857095152.

[42] V Jeevanantham, P Vadivelu, and P Manigandan. Material based structural analysis of a typical landing gear. 2017.

[43] Bruce Boardman. Fatigue resistance of steels. *ASM International, Metals Handbook. Tenth Edition*, 1:673–688, 1990.

[44] GoodYear Aviation. Aircraft tire care and maintenance. page 51, 2004.

[45] M.; Henderson M.; Petersen H. ; Verzijden P. Cruijssen, H. J.; Ellenbroek and M. Visser. The European Robotic Arm: A High-performance Mechanism Finally on Its Way to Space. Baltimore, MD; United States, May 2014. "The 42nd Aerospace Mechanism Symposium"; p. 319-334; Financial Sponsor: NASA Goddard Space Flight Center; Greenbelt, MD, United States; NASA/CP-2014-217519.

[46] *Pump and Motor Sizing Guide*. Eaton, Heavy Duty Hydrostatic Transmissions, January 1998. No. 3-409.
[47] Cummins Inc. *Specification sheet: QSL9-G7*. Cummins Inc., 2019.
[48] Safran. Airbus a320ceo/neo - long life carbon brake, 2018. (Safran Landing Systems document).
[49] Ltd. Kohara Gear Industry Co. *The ABC's of Gears - Basic Guide - B*. Toshiharu Kohara, 2007.
[50] R Kuziak, Rudolf Kawalla, and Sebastian Waengler. Advanced high strength steels for automotive industry. *Archives of civil and mechanical engineering*, 8(2):103–117, 2008.
[51] Jeremiah Johnson, BK Reck, T Wang, and TE Graedel. The energy benefit of stainless steel recycling. *Energy policy*, 36(1):181–192, 2008.
[52] Dr. Fabrizio Oliviero. Ae3211-i systems engineering and aerospace design-design for ground operations. University Lecture, 2000.
[53] Norman S Currey. *Aircraft landing gear design: principles and practices*. American Institute of Aeronautics and Astronautics, 1988.
[54] Flight Operations Support. *FLIGHT CREW TRAINING MANUAL*. AIRBUS, 2008.
[55] S.Yang Z.Li, J.Li. The study on Differential Steering Control of In-wheel Motor Vehicle Based on Double Closed Loop System. *Elsevier*, 2018.
[56] Gregory Dudek and Michael Jenkin. *Computational Principles of Mobile Robotics*. Cambridge University Press, 2010.
[57] Federal Aviation Administrator. Aviation emissions, impacts and mitigation: A primer. *Office of Environment and Energy*, 2015.
[58] Statistics Norway (SSB). Emission factors used in the estimations of emissions from combustion, 2015.
[59] Dallas Fort Worth International Airport. Carbon Footprint, 2017.
[60] Charles Walker. Heathrow airport 2017 emission inventory, 2017.
[61] Jakub Hospodka. Electric taxiing – Taxibot system. *MAD - Magazine of Aviation Development*, 2(10):17–20, July 2014. ISSN 1805-7578. doi: 10.14311/MAD.2014.10.03. Number: 10.